

LOCKHEED MARTIN ENERGY RESEARCH LIBRARIES



3 4456 0515840 5

ORNL-4171  
Special

THE MOLECULAR ANATOMY OF CELLS AND TISSUES  
(The MAN Program)  
ANNUAL REPORT  
FOR PERIOD JULY 1, 1966, TO JUNE 30, 1967

OAK RIDGE NATIONAL LABORATORY  
CENTRAL RESEARCH LIBRARY  
DOCUMENT COLLECTION  
**LIBRARY LOAN COPY**

DO NOT TRANSFER TO ANOTHER PERSON

If you wish someone else to see this  
document, send in name with document  
and the library will arrange a loan.

UCN-7969  
13 2-67



**OAK RIDGE NATIONAL LABORATORY**  
operated by  
**UNION CARBIDE CORPORATION**  
for the  
**U.S. ATOMIC ENERGY COMMISSION**

LEGAL NOTICE

This report was prepared as an account of Government sponsored work. Neither the United States, nor the Commission, nor any person acting on behalf of the Commission:

- A. Makes any warranty or representation, expressed or implied, with respect to the accuracy, completeness, or usefulness of the information contained in this report, or that the use of any information, apparatus, method, or process disclosed in this report may not infringe privately owned rights; or
- B. Assumes any liabilities with respect to the use of, or for damages resulting from the use of any information, apparatus, method, or process disclosed in this report.

As used in the above, "person acting on behalf of the Commission" includes any employee or contractor of the Commission, or employee of such contractor, to the extent that such employee or contractor of the Commission, or employee of such contractor prepares, disseminates, or provides access to, any information pursuant to his employment or contract with the Commission, or his employment with such contractor.

Contract No. W-7405-eng-26

**BIOLOGY DIVISION**

**THE MOLECULAR ANATOMY OF CELLS AND TISSUES  
(The MAN Program)**

Cosponsored by the National Cancer Institute,  
The National Institute of General Medical Sciences,  
The National Institute of Allergy and Infectious Diseases,  
and the U.S. Atomic Energy Commission

**ANNUAL REPORT**

**For Period July 1, 1966, to June 30, 1967**

N. G. Anderson  
Program Coordinator

**NOTICE**

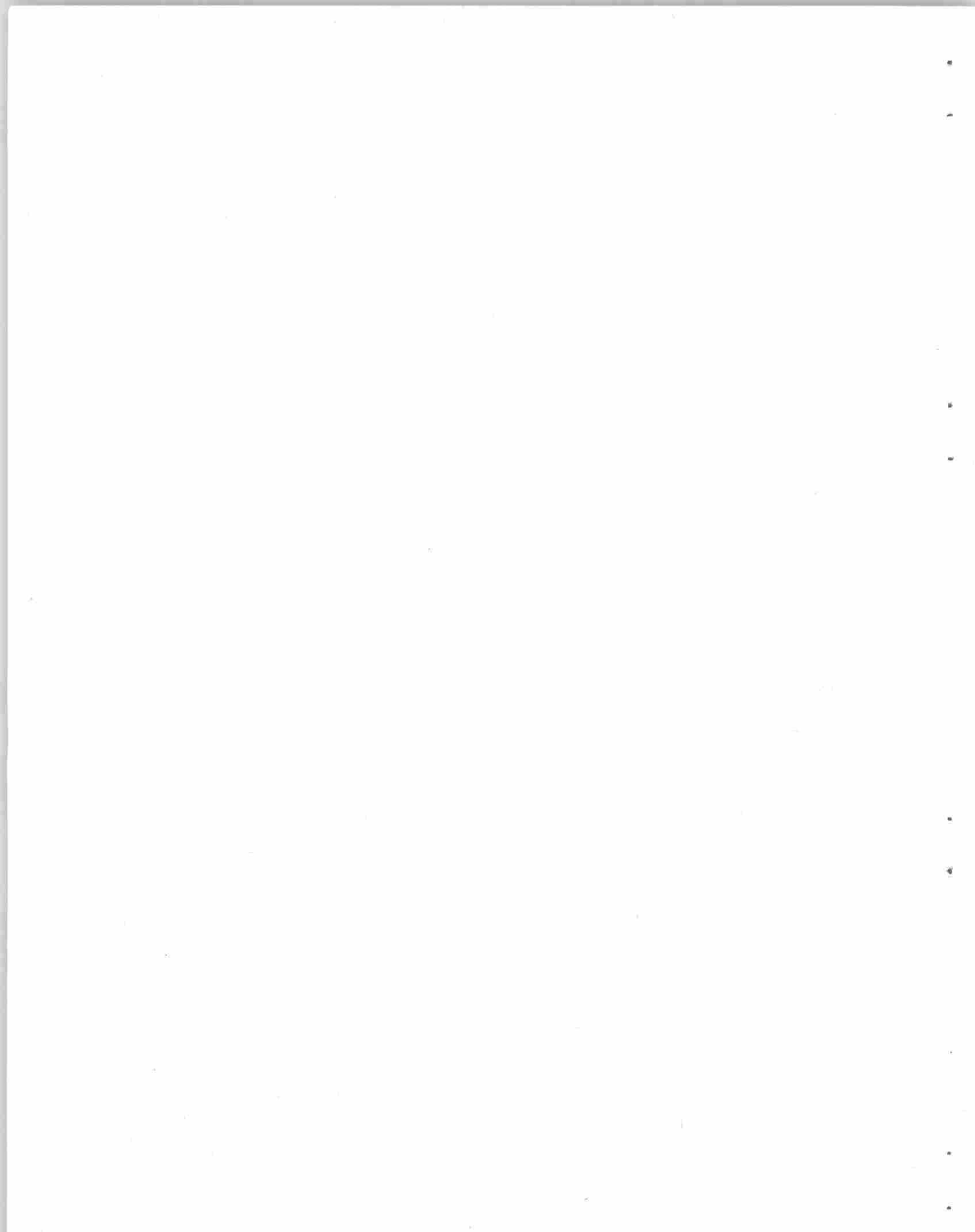
This document contains information of a preliminary nature and was prepared primarily for internal use. It is subject to revision or correction and, therefore, does not represent a final report. Quotations from, or reference to, this report must not be made in open literature without written permission from individual authors.

SEPTEMBER 1967

OAK RIDGE NATIONAL LABORATORY  
Oak Ridge, Tennessee  
operated by  
UNION CARBIDE CORPORATION  
for the  
U.S. ATOMIC ENERGY COMMISSION



3 4456 0515840 5



## Contents

ABSTRACT .....	v
1. INTRODUCTION .....	1
2. CENTRIFUGE DEVELOPMENT .....	3
A. Development of the K-II Continuous Flow Centrifuge .....	3
(1) Centrifuges for Vaccine Purification	
N. G. Anderson .....	3
(2) Design of the K-II Rotor	
R. F. Gibson, D. A. Waters and N. G. Anderson .....	4
(3) Basic Design Considerations	
D. A. Waters.....	5
(4) The K-II Drive System	
D. A. Waters, R. F. Gibson, and C. E. Nunley .....	11
(5) Seal Design and Testing	
R. F. Gibson and C. E. Nunley.....	11
(6) Crash Shield Design	
R. F. Gibson and E. F. Babelay .....	14
(7) The K-II Centrifuge Control System	
E. C. Denny .....	17
(8) Initial Destructive Test	
C. E. Nunley, R. F. Gibson, D. A. Waters,	
E. F. Babelay, and R. M. Schilling .....	19
(9) Problems of Titanium Rotor Development	
R. F. Gibson.....	24
B. Velocities and Shear Stress Distributions in Zonal Centrifuge Rotors	
H. W. Hsu .....	24
C. Multiple Gradient-Distributing Rotor (B-XXI)	
E. L. Candler, C. E. Nunley and N. G. Anderson .....	31
D. A Simple Gradient-Forming Apparatus	
N. G. Anderson and E. L. Rutenberg.....	35
E. Sedimentation Coefficients in Zonal Centrifuges	
B. S. Bishop and E. L. Rutenberg.....	38
F. Density Beads	
N. G. Anderson.....	43
3. CENTRIFUGAL SEPARATIONS.....	45
A. The Capacity of Zones in Density Gradient Centrifugation	
S. P. Spragg and C. T. Rankin, Jr. ....	45
B. Rate-Zonal Separation of Hamster Anti-Adenovirus 31 Tumor Antibodies	
E. L. Candler, N. G. Anderson, C. T. Rankin, W. L. Rasmussen,	
L. H. Elrod, and J. E. Norton .....	46
C. Purification of Treponema Pallidum by Zonal Centrifugation	
H. Russell, M. L. Thomas, V. W. Clark, Jr., G. B. Cline and	
N. G. Anderson.....	48

D. Adenovirus 31 Hamster Tumor Antigens: Differential Centrifugation of Tumor Homogenates N. G. Anderson, L. H. Elrod and E. L. Candler .....	57
E. Isolation of Rat Liver Cell Membranes by Combined Rate and Isopycnic Zonal Centrifugation N. G. Anderson, A. I. Lansing, I. Lieberman, C. T. Rankin, Jr., and H. Elrod.....	62
F. Improvement of Methods for Macroglobulin Isolation in B-XIV, XV, and XXVII Rotors C. T. Rankin, Jr., N. G. Anderson, and W. L. Rasmussen .....	65
G. Evaluation of Zonal Centrifuge Rotors for the Isolation of Serum Lipoproteins M. Heimberg.....	72
H. Lipid Class and Fatty Acid Composition of Rat Liver Cytoplasmic Membranes Isolated by Zonal Centrifugation R. C. Pfeleger, N. G. Anderson, and F. Snyder .....	76
I. Analytical Differential Centrifugation in Angle-Head Rotors N. G. Anderson .....	77
J. Zonal Separation of Human Macroglobulin in Warm Density Gradients G. B. Cline.....	84
K. A Method for Isolating Nuclei Using Sucrose-Deuterium Oxide Gradients L. H. Elrod and N. G. Anderson.....	86
4. PURIFICATION OF LARGE QUANTITIES OF INFLUENZA VIRUS .....	89
Purification of Large Quantities of Influenza Virus by Density Gradient Centrifugation C. B. Reimer, R. S. Baker, R. M. vanFrank, T. E. Newlin, N. G. Anderson, and G. B. Cline.....	89
5. ELECTROPHORETIC SEPARATIONS.....	101
Electrophoresis in Liquid Density Gradients Stabilized in a Centrifugal Field N. G. Anderson, A. Travaglini, and R. Jolley.....	101
6. CHROMATOGRAPHIC SEPARATIONS.....	105
Ultraviolet Absorbing Constituents of Urine C. D. Scott.....	105
7. AUTOMATED ANALYTICAL SYSTEMS .....	115
A. Measurement and Transfer of Small Fluid Volumes N. G. Anderson.....	116
B. An Improved Automated System for Total Protein Analysis L. H. Elrod.....	123
8. ELECTRON MICROSCOPY .....	125
A. Electron Phase Contrast Images of Myoglobin W. W. Harris, F. L. Ball, and N. G. Anderson .....	125
B. Particle Counting and Detection W. W. Harris and F. L. Ball .....	127
9. TUMOR IMMUNOLOGY .....	131
Tumor Immunology Studies .....	131

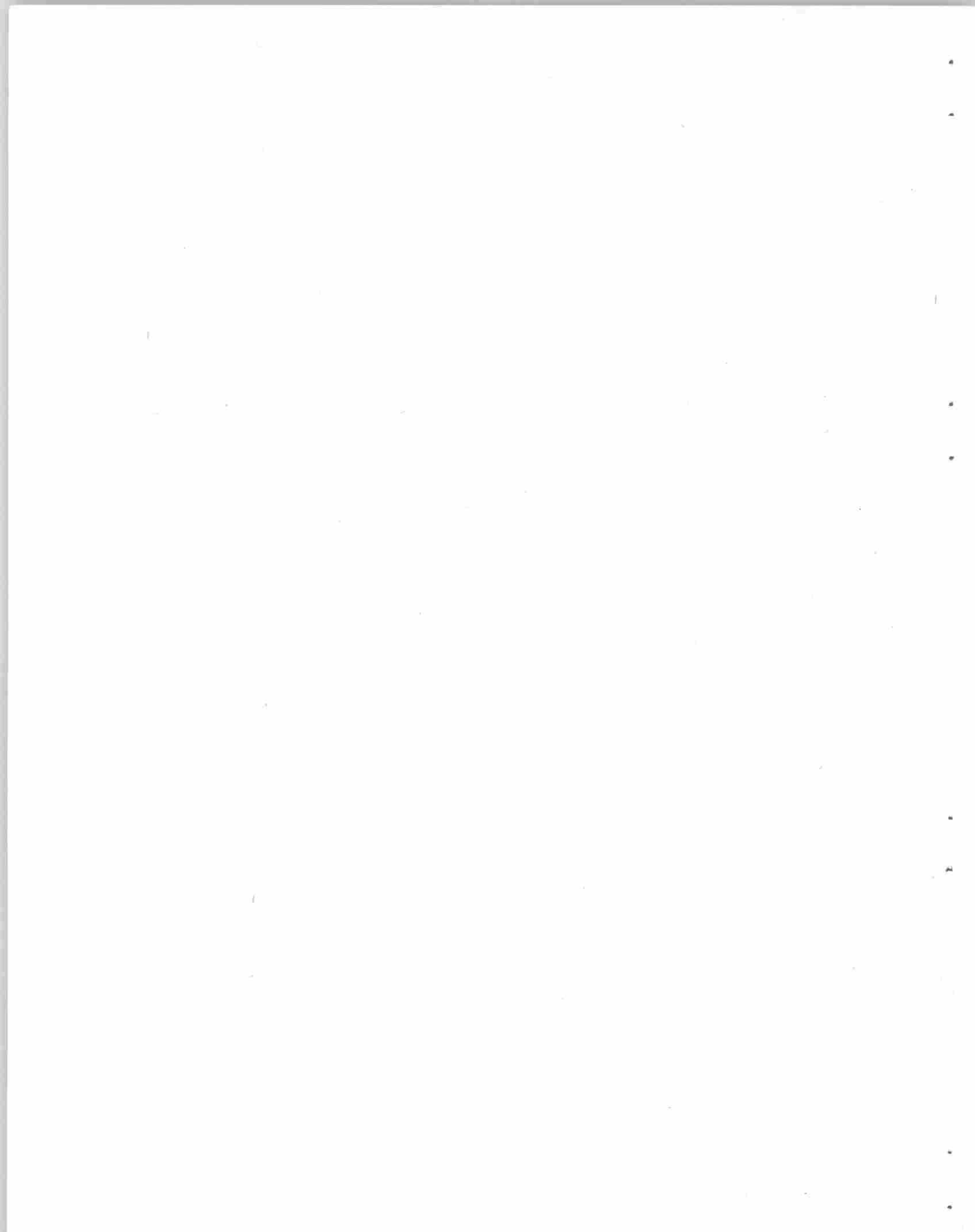
## Abstract

The Molecular Anatomy (MAN) Program is concerned with the development of separation and analysis methods applicable to the problem of fractionating human cells, and of describing their structure at the molecular level. During the period July 1, 1966, to June 30, 1967, research and development efforts have continued with emphasis on centrifugal separation methods. The K-IIA and K-IIB centrifuges have been completed and evaluated in vaccine purification at length. The rotor is a continuous-flow-with-banding type with single-pass fluid-line seals at each end. Large quantities of purified influenza virus have been prepared for mass field trials. Burst tests indicate additional developmental work should be done on the armor shield. Theoretical studies on the hydrodynamics of reorienting gradient rotors should allow the number of septa and the internal configuration of high-speed rotors of this type to be calculated. For s-p separations in which the isopycnic separation is accomplished in a gradient made of a slowly diffusing solute, a gradient-distributing rotor has been developed which allows 12 gradients to be made simultaneously in an angle-head rotor. A simple exponential gradient-forming device for use with the BXIV or BXV rotors has been completed. The computer program for calculating equivalent sedimentation coefficients has been updated and subroutines for data plotting included. Arrangements to produce density beads for isopycnic banding experiments have been completed and batches of the beads tested. Equations relating gradient capacity to gradient slope have been verified experimentally.

A variety of experimental studies are reported which include: separation of 7 and 18S hamster antibodies and the demonstration that antibodies to adenovirus 31 tumor antigens are in the 7S fraction, purification of quantities of *Treponema pallidum*, studies on the intracellular distribution of adenovirus 31 tumor

antigens, development of a method for isolating rat liver cell membranes by a combination of rate and isopycnic zonal centrifugation in the same rotor, exploration of the application of s-p techniques to human brain and brain tumor subcellular particles, improvements in methods for centrifugal separation of macroglobulins both at low temperature and at 30°C, evaluation of new titanium zonal rotors for human serum lipoprotein isolation, analysis of rat liver cell membrane lipids, and further exploration of gradient reorientation as applied to continuous-flow-with-banding rotors. Detailed information is presented on the application of the K-IIB centrifuge to the purification of five strains of influenza virus, using sucrose density gradients. A new technique for electrophoresis using a centrifugal field to stabilize the density gradient is presented. The use of an automated high-pressure liquid chromatographic system for the separation of ultraviolet absorbing constituents of human urine is continuing, together with the systematic analysis of the over 100 peaks observed. The problem of automating colorimetric analyses and enzyme assays has been approached by developing a new technique for accurately measuring and quantitatively transferring small fluid volumes. Improvements have been made in an automated system for total protein analysis.

New methods for supporting samples for high-resolution electron microscopy have been developed and applied to myoglobin. The electron micrographs obtained show structures resembling the myoglobin molecule as deduced from X-ray diffraction studies, thus raising difficult problems in image interpretation. Special centrifuge tubes for sedimenting particles on electron microscope grids have been developed and applied to the problem of virus counting below  $10^5$  particles per  $\text{cm}^3$ .



## 1. Introduction

N. G. Anderson

Each science, as it matures, is concerned with defining those basic units which in turn are definable by the next subjacent discipline. The boundary between chemistry and the biomedical sciences lies at the level of macromolecules. Since it is now generally accepted that the majority of human diseases are ultimately to be understood at the molecular level, we must conclude that the separation and cataloguing of the molecular constituents of human cells is a necessary groundwork for attempts to describe human pathological states in molecular terms. Such an enormous task is beyond the techniques now available. If it is ever to be done, a very considerable effort must be made to develop separation methods and analytical techniques which are applicable to the problem. We dare not ask whether separation systems are possible which will totally resolve cells. Rather, we conclude that all progress in this area would benefit from higher resolution methods, and that the ultimate objective justifies the time, energy, and costs involved.

Initially, we have been concerned with the solution of a limited number of theoretical and technical problems. These have centered chiefly around the centrifugal separation of cells and subcellular particles, and the development of automated systems for the separation and quantitation of low molecular weight compounds. Now we are concerned with the gradual development of an integrated program to produce and fractionate human cells, and with exploring the areas where major unsolved problems exist, and where gaps in our present program occur.

The first area for intensive investigation concerns the large-scale culture of human cells as a source material for fractionation studies. While many protein species (or antigens) may have been lost from cultured

cells as compared with the cell of origin, it is unlikely that the basic subcellular machinery of these cells has been altered. One would not expect the amino acid sequence of cytochrome *c* to have changed, for example. Cultured cells therefore appear to be a suitable source of human cell proteins. However, as specific proteins are isolated, parallel studies will be done on human tissues supplied by the NCI tissue procurement program. The development of automated cell culture systems will begin during the coming year and is a continuation of previous work done at Oak Ridge on cell synchronizers for use with sterile protozoan cell cultures.

Two of the most difficult areas which now concern us are subcellular particle disassembly and the fractionation of protein mixtures. The techniques required should ideally yield undenatured protein or nucleic acid molecules. In the disassembly of ribosomes this has thus far not been possible. Some success has been achieved in separating adenovirus T antigen from intracellular membranes. However, the methods available for solubilizing and fractionating membrane proteins are still far from ideal. The development of high resolution electrophoretic separation systems which can fractionate large volumes of material in a reasonably short time also remains to be done. Of all outstanding problems now under attack, this is probably the most difficult.

We must also consider the problems associated with making large numbers of analyses and enzyme assays. If presently available techniques are to be employed, then a prohibitively large investment in personnel and machines must be made. The alternate approach taken here is to ask what are the basic elements of the systems required and begin a research and devel-

opment program aimed at producing them. The result is the small volume measurement and transfer method described in a subsequent section.

From a broader viewpoint, the question of whether large defense-related, science-based research and development organizations can be usefully reoriented to solve basic biomedical problems is of increasing interest. The answer which appears to be developing is the following.

The development of new biophysical separations and analytical instrumentation can best occur when a small semiautonomous group is set up which can freely communicate with and, if necessary, employ diverse other groups in the surrounding laboratories. Either too close cooperation or cooperation through complex channels appears detrimental. There has not been a deep interest in developing new scientific tools among biologists with traditional training. The tendency is to instantly evaluate them solely on the basis of applicability to one or two specific problems now at hand. There is no room in such an environment for the embryogenesis of new ideas which do not stem directly from those which are completely familiar. This explains in part the simple fact that nearly all of the basic tools of modern biological research were developed abroad, where the yardstick of instant applicability does not appear to have been employed. Communication with the Biology Division is maintained but intimate involvement is avoided because of the oft-expressed aversion of traditional biologists for either engineering and for meaningful attempts to solve medical problems directly. In practice it is difficult to maintain morale except by partial isolation.

The problem of collaboration with specialist groups in Oak Ridge is twofold. First, it is important that a specialist maintain contact with, and competence in, his own field. To allow him to do this, the problems chosen for collaborative attack must be stated in terms which make sense to the specialist. The second problem concerns the definition of the problems. Considerable discussion and effort are required to be sure that both the biologists and the specialist understand precisely what the problem to be solved is. Once that is done, it is best to let the specialist seek his solutions in his own environment provided adequate communications are maintained.

This then leaves the problem of the maintenance of competence and relevance in the biological staff of the program. If the staff grows beyond a certain size, this could be done internally. However, many of the biological problems change rapidly as new approaches are evolved. A solution to this problem is to encourage visiting investigators to visit the laboratory to work on problems of mutual interest, and to arrange contracts with research groups in universities and in industry to jointly evaluate separation systems and techniques developed at Oak Ridge. This approach has been explored through contracts with six universities and two pharmaceutical firms and appears to be of great mutual benefit. Formal means for extending this contract mechanism must now be explored.

The MAN Program continues to evolve slowly and to approach the objective of developing the methods—experimental, organizational, contractual, and theoretical—necessary for the organization of a full scale attempt to write a molecular anatomy of human cells.

## 2. Centrifuge Development

The development of centrifugal separation systems has continued with emphasis on continuous flow devices which may be used in cascade to sequentially remove different particles from a fluid stream. The objectives are the purification of vaccine materials and the mass fractionation of cell and tissue particulates. A major part of the effort has gone into the development of the K-II centrifuge for large scale particle isolation. Also under development are low-speed continuous flow rotors for use with large particles such as whole cells and nuclei. Rotors for this purpose include B-XX and B-XXVIII.

### A. DEVELOPMENT OF THE K-II CONTINUOUS FLOW CENTRIFUGE

#### (1). Centrifuges for Vaccine Purification

N. G. Anderson

The suspensions from which viral vaccines are prepared contain a wide spectrum of particles ranging from whole cells, subcellular particles and debris, viruses, viral subunits, soluble proteins, nucleic acids, and low molecular weight substances, to insoluble precipitates which may be crystalline. These may be divided into four general classes:

- I. Immunoprotective antigens.
- II. Non-immunoprotective antigens.
- III. Non-antigenic macromolecular or particulate material.
- IV. Low molecular weight substances.

Class I may include intact virions, or viral subunits. Substances in class II are clearly undesirable. The immune system does not have limitless capacity to produce antibodies. The immunological potential

of an individual at a given instant may be expressed as:

$$N = \frac{M}{Q_m}$$

where  $M$  is the antibody mass, and  $Q_m$  is the average minimum antibody mass required for protection. The limiting number of different antigens against which protection may exist is  $N$ . The objection to the inclusion of miscellaneous antigens of Class II is first that the number  $N$  is reduced; secondly, allergic reactions occur which may sensitize the recipient to foods and environmental or his own antigens; and thirdly, the number of different viral antigens which may be combined to produce a multivalent vaccine is inversely proportional to the amount of Class II material present.

Substances of both Class II and III may act as adjuvants. The view that vaccines should not be purified because the non-immunoprotective mass may have a desirable adjuvant effect is untenable without experimental verification. It would appear desirable to control the composition and the quantity of adjuvants separately from the immunoprotective mass.

In class IV are included amino acids, vitamins, nucleotides, metabolites and salts which may be present in the culture fluids. These have rarely been a source of concern in vaccine preparation. In the finished vaccine additional substances may be present which are added to inactivate virus, to prevent bacterial growth, or to stabilize the antigens.

Two general approaches can be taken to vaccine purification. The first is a purely empirical one in which a variety of procedures are devised and applied sequentially and specific activity (activity per unit of mass, nitrogen, or protein) is followed. The problem is to know what purification could theoretically be achieved. Results are usually expressed in terms of the concentration and titer of the starting material,

i.e., as a 10-fold concentration or purification. It is evident that this does not indicate whether the final product is 100% or 0.01% pure. Expressions of enrichment relative only to the starting material are not satisfactory indications of purity.

The second approach to vaccine purification is to characterize biophysically all classes of particles present, using analytical techniques which have preparative counterparts. Purity may then be assessed by a number of different criteria which could include measurement of size, sedimentation rate, buoyant density, solubility, and surface charge. Nearly all the analytical tools required are now available. Not all of their preparative counterparts are developed to the point where they may be applied on a large scale, however.

It is one purpose of this program to examine the basic problems concerned with vaccine purification and to present the results of efforts to develop those techniques and large-scale separation systems which are not presently available.

Few fractionation methods are applicable to large volumes of very dilute antigen. The first problem, therefore, is to concentrate the antigen sufficiently so that a variety of fractionation methods may be used. The concentration methods which have been used include selective adsorption,<sup>1</sup> precipitation,<sup>2</sup> filtration,<sup>3</sup> concentration by phase separation,<sup>4</sup> or either batch or continuous-flow centrifugation.<sup>5-11</sup> Of these continuous-flow centrifugation has potentially the widest application. The disadvantages have been the small flow rate, bacteriological contamination, the batchwise recovery of a pellet of virus, and aggregation or inactivation during pelleting.

The combination of continuous-flow centrifugation with isopycnic banding allows virus particles to be concentrated, separated from particulate contaminants having different densities, and recovered in suspension—all in one operation.<sup>8-11</sup> A series of rotor core configurations in the B series of rotors developed at Oak Ridge (B-VIII, IX, XVI, and XXVI) were used to explore this technique with a number of different viruses. These rotors are useful for intermediate-scale vaccine purification. Sterility is difficult to maintain in the commercial versions of this instrument, and seal cross leakage between the inlet and outlet lines may present problems. Our attention was therefore directed toward the development of a production instrument with larger capacity, a simple drive mechanism, and with inlet and outlet seals on opposite ends of the rotor. The result is the K-II centrifuge prototype described here.

## (2). Design of the K-II Rotor

R. F. Gibson                      D. A. Waters  
N. G. Anderson

The requirements of the K-II centrifuge were based on the purification of influenza virus at a rate which would make the instrument commercially feasible.

This would mean that approximately 100 liters could be processed in an eight-hour day. This goal has not as yet been attained since the rotors are not being operated at designed speed.

The rotor was designed from data and criteria presented in the previous annual report.<sup>12</sup> The operating mode is continuous-flow-with-banding using a tapered core with six vanes. Pertinent data on the rotor is shown in Table 2.1.

The designs of earlier rotors such as the B-IX and B-XIV contributed greatly towards that of the K-II. Functionally, the K-II is a modified and lengthened B-IX type rotor with B-XIV type end caps. The pressure-vessel type end-cap design and the method of securing the end caps to the bowl with buttress threads is identical to that of the B-XIV and B-XV rotors. Reliability of this end-cap design was proved under extremely high stress conditions imposed during a destructive test (see section on destruction test). Except for the following differences the caps are identical: (a) the types of connections for top and bottom shafts are different, and (b) the bottom cap is fitted with two pins which lock the core against rotation inside the bowl. Two spanner-wrench notches in each end of the core fit the locking pins so that the tapered core is completely reversible. This means that the direction of sample fluid flow may be either up or down, depending on core orientation. Maxi-

**Table 2.1. Aluminum K-II Rotor**

Assembled Weight (empty)	52 lb
Total Volume with Core	3600 cc
Taper Volume	700 cc
Initial Operating Speed	28,000 rpm
Maximum g	53,400
Maximum Safe Speed	35,000 rpm
Maximum g	83,440
Inside Length	76.20 cm
Bowl Inside Radius	6.09 cm
Core Radius (large end)	4.94 cm
Core Radius (small end)	4.29 cm
Rotor Flexural Critical Speed	approx. 60,000 rpm

imum hoop stress (at the inside bowl wall) was calculated as a function of rotor speed for various densities of rotor fluid contents to determine the limitations on operating speed. As shown in Figure 2.1,

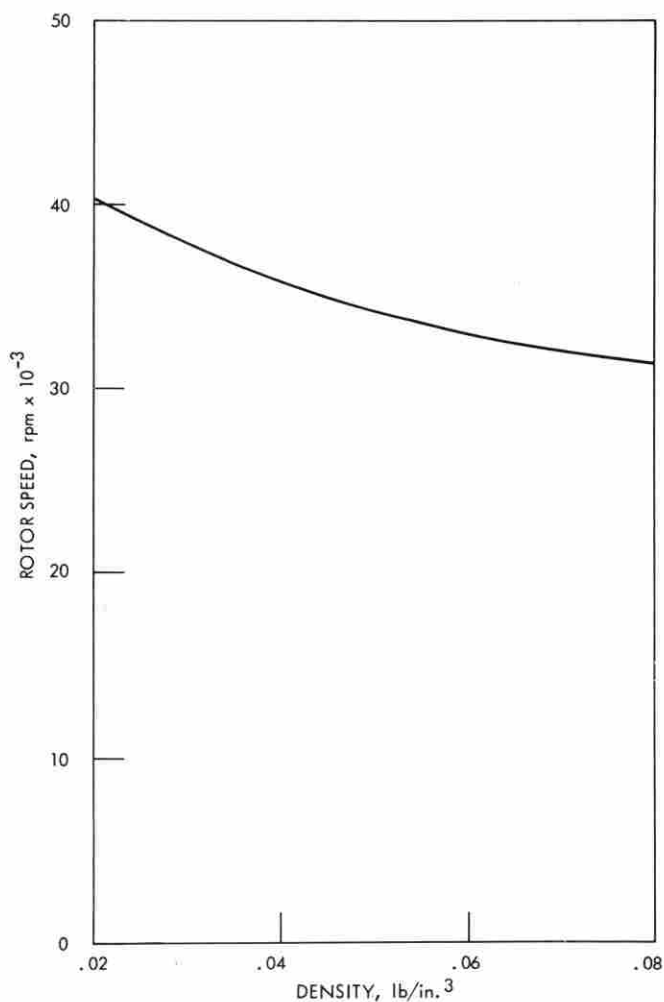


**Fig. 2.1** Maximum operating speed of the K-II aluminum centrifuge rotor as a function of the density of the fluid in the rotor. With liquid density gradients the density of the heavy end of the gradient is used rather than the average gradient density.

operating speed is limited by the density gradient used. The maximum safe operating speed will be 35,000 rpm with sucrose gradients, and overspeed devices will be set accordingly, once the crash shield problem is solved.

Since the core probably goes through its fundamental bending critical frequency at high rotor speeds,

six septa were used to give added radial support. The radial support should reduce harmful effects due to core vibration. Manifold plugs on each end cap serve to center and anchor the core inside the bowl. Sample fluid flowing through the rotor comes out through radial grooves in the end of the core, then flows up (or down) the tapered core periphery and back in through radial grooves on the other end. A clear plastic version of the K-II is being designed so that actual flow paths and other phenomena inside the spinning rotor may be studied using model particles.

### (3). Basic Design Considerations

D. A. Waters

The K-II rotor system was designed specifically to perform large-scale purification of influenza virus. At the onset it was conceived that this machine could be used for vaccine preparation at production capacities suitable for use by drug manufacturing companies. The primary consideration from the design standpoint then was to build the largest-capacity machine consistent with existing technology that would meet the requirements of the separation task. The specifications for the centrifuge system design from the biological standpoint are listed in Table 2.2. The design flow rate with 100% cleanout was initially set as a target, but in the process of optimizing other variables in the mechanical design of the system it became evident that this target flow rate would result in as large a machine as would be practical to use by drug firms at this time.

**Table 2.2** Design Requirements for the K-II Centrifuge.

Flow Rate	10 liters/hr
Sample Zone Viscosity	0.0152 poise
Virus Diameter	$8.2 \times 10^{-6}$ cm
Virus Density	1.193 gm/cm <sup>3</sup>
Sample Fluid Density	1.05 gm/cm <sup>3</sup>
Cleanout	100%

In addition to the target specifications listed in Table 2.2 there were several other considerations that influenced the centrifuge design, such as; (a) the rotor drive (compressed air or electrical power) should be

compatible with the facilities that are normally available at a vaccine manufacturing laboratory; (b) the seal design should be such that there would be absolutely no possibility of cross-leakage between the influent and effluent streams; (c) the weight of the rotor system should be limited in order to avoid the necessity of special handling equipment; and (d) if possible the system should be designed conservatively both to ensure the attainment of the target specifications, and to provide flexibility in the machine should an interest develop in large-scale production of "more difficult to separate" biological materials. The requirement that there be no possibility of cross-leakage between the influent and effluent streams imposed a limitation upon the selection of the type of centrifuge drive. The only positive method to ensure against the possibility of cross-leakage is to completely separate the seals by placing them at opposite ends of the rotor. This also implies that one fluid passage must go through the centrifuge drive itself. A turbine drive was selected because of its simplicity and the fact that a central fluid passage within the drive could easily be arranged. The turbine drive has the added advantage that it will not heat the fluid within the flow passage as much as might be expected from an electrical drive. The weight of the rotor was arbitrarily limited to 70 lbs to satisfy the requirement that peripheral handling equipment be kept to a minimum. Design curves for the constant effective length as a function of sample zone radius and speed can be determined for the parameters listed in Table 1 by the relation

$$L_e = \frac{18Q}{\omega^2 D^2 A_s} \int_{r_c}^{r_s} \frac{\mu(r)}{\rho - \rho_1(r)} \frac{dr}{r}$$

Where

- $r_s$  = Outside radius of sample zone (cm)
- $r_c$  = Core radius (cm)
- $D$  = Diameter of virus (cm)
- $\mu(r)$  = Viscosity of Sample (poise)
- $\rho$  = Density of virus (gm/cm<sup>3</sup>)
- $\rho_1(r)$  = Density of sample zone (gm/cm<sup>3</sup>)
- $Q$  = Flow rate (Cm<sup>3</sup>/sec)
- $A_s$  = Annular cross sectional area of sample zone (cm<sup>2</sup>)
- $\omega_e$  = Speed (Radians/sec)
- $L_e$  = Effective (separative) rotor length (cm)

It can be assumed with negligible error that the density and viscosity of the sample will not vary radially in the rotor if the residence time within the rotor

is short. With this assumption the relationship for the effective separative rotor length becomes:

$$L_e = \frac{18Q\mu}{V_s^2 D^2 (\rho - \rho^1)} \cdot \left[ \frac{\text{Ln}(K)}{1 + (1/K)^2} \right]$$

Where;

$V_s$  = Sample zone peripheral velocity (cm/sec)

$K = r_s/r_c$

The ratio  $K$  should be kept as close as practical to unity in order to minimize the effective length required to do the separation task at a given value of sample peripheral velocity. The physical implications of this are that the residence time of the virus particle within the sample zone will be minimum if the annular area of the zone is minimized. Values of  $L_e$  as a function of  $V_s$  and  $K$  are shown in Figure 2.2. For design purposes a value of  $K$  equal to 0.9 was used

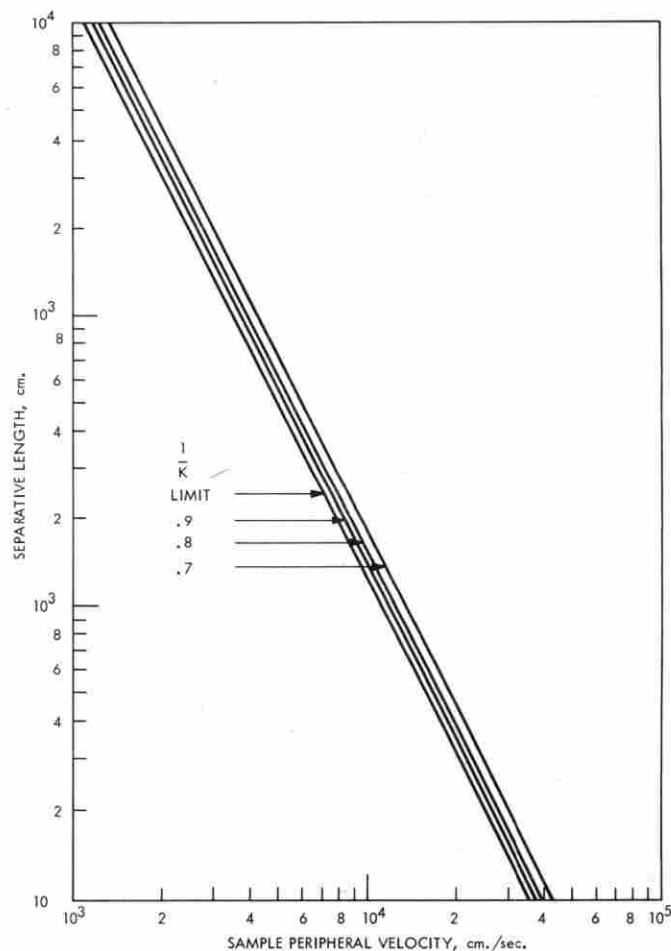


Fig. 2.2 Separative length required as a function of sample peripheral velocity.

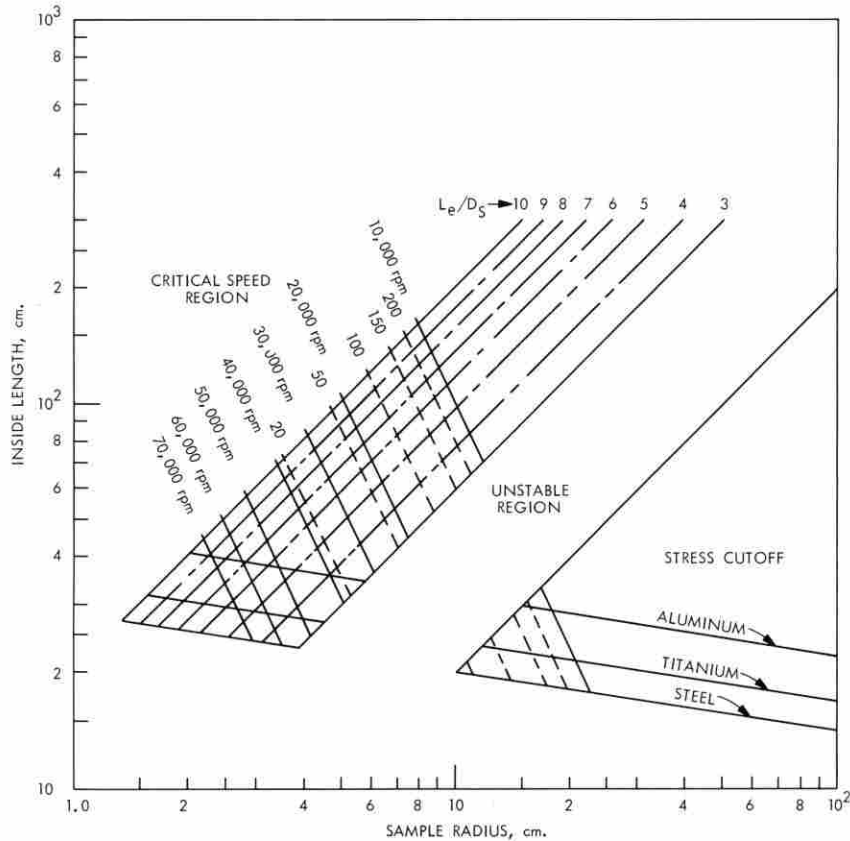


Fig. 2.3 Length, speed, sample zone radius, and weight of rotor required for 100% cleanout of influenza virus at 10 liters/hr. flow rate.

in the remaining calculations. The values of  $L_e$  as a function of  $r_s$  and rotor speed in rpm are shown in the composite design curves in Figure 2.3.

The rotor stress, its flexural critical speed, its stability, and its weight all impose physical limitations upon the allowable diameter and length of the rotor. These parameters can be considered separately in determining the allowable limits of the rotor design.

The stress in a filled liquid centrifuge rotor, where the wall thickness has been optimized for minimum stress is given by:

$$\sigma_t = V_\rho^2 \left\{ (\delta + \rho) + [(3 + \mu)\delta\rho]^{1/2} \right\} \dots$$

Where

- $\sigma_t$  = the tensile hoop stress at optimum wall thickness.
- $V_\rho$  = the rotor peripheral speed (inside).
- $\delta$  = metal density.
- $\rho$  = fluid density.
- $a$  = inside rotor radius.
- $b$  = outside rotor radius.

The optimum rotor wall thickness is:

$$t = a \left( \left\{ 1 + \left[ \frac{4\rho}{(3 + \mu)\delta} \right]^{1/2} \right\}^{1/2} - 1 \right) \dots$$

The stress cut off shown in Figure 2.3 was determined for 7075-T6 aluminum, 6Al-4V Titanium and maraging steel rotors with the inside radius of the rotor assumed to be  $1.25 r_s$ .

The rotor must operate below its rotor flexural critical speed in order to limit the amplitude and balance requirements to a level suitable for mass production of the rotor. A maximum value of  $L_e/2r_s$  or  $L_e/D_s$  of 10 was determined to be the suitable limiting value.

The rotor stability can be enhanced by designing a machine wherein the ratio of the polar moment of inertia to the transverse moment of inertia lies in the region;

$$\frac{I_\rho}{I_t} \geq 1.2, \quad \frac{I_\rho}{I_t} \leq \frac{1}{4}$$

This does not imply that a rotor cannot be operated

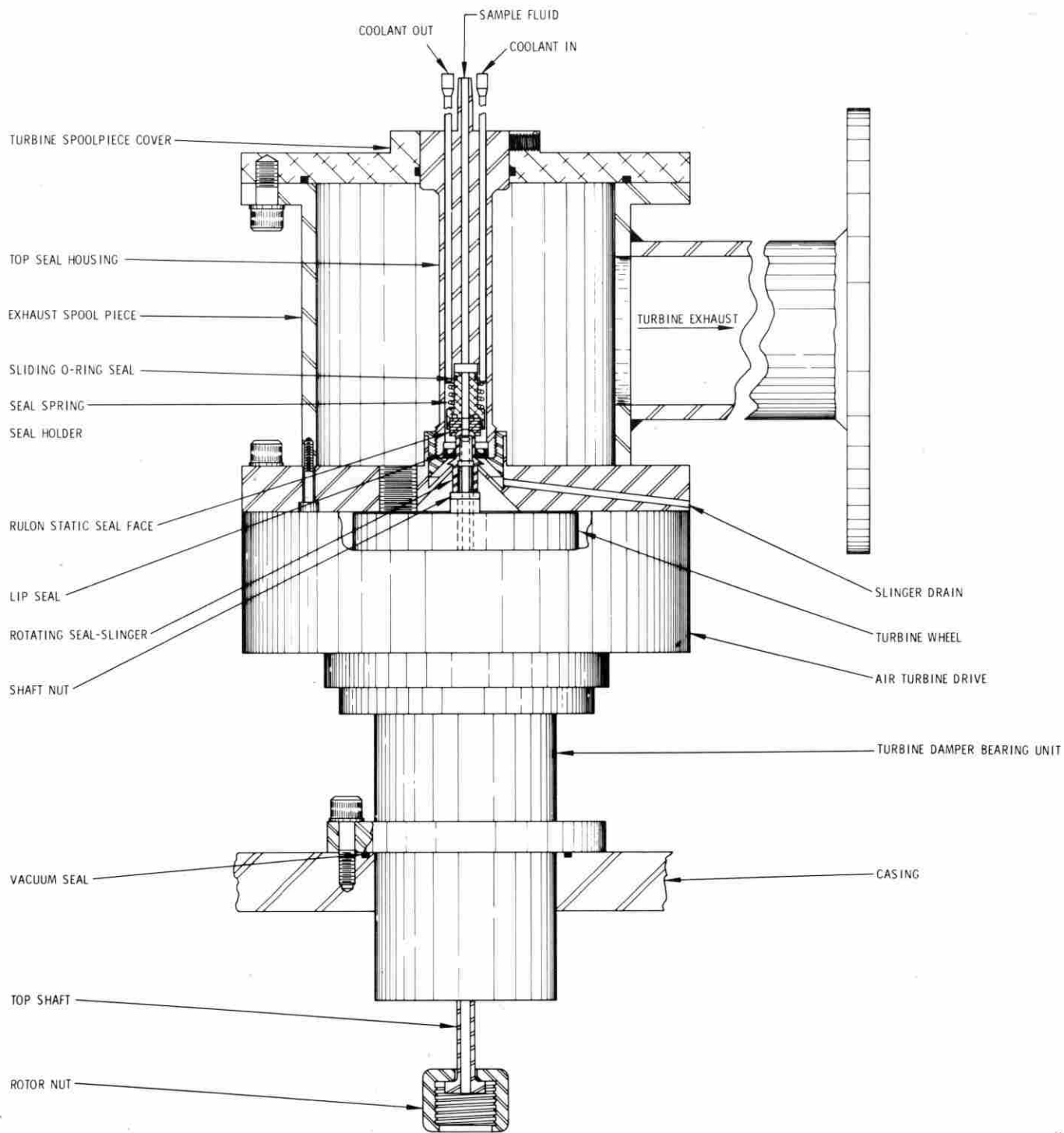


Fig. 2.4 Diagrammatic presentation of upper part of K-II centrifuge.

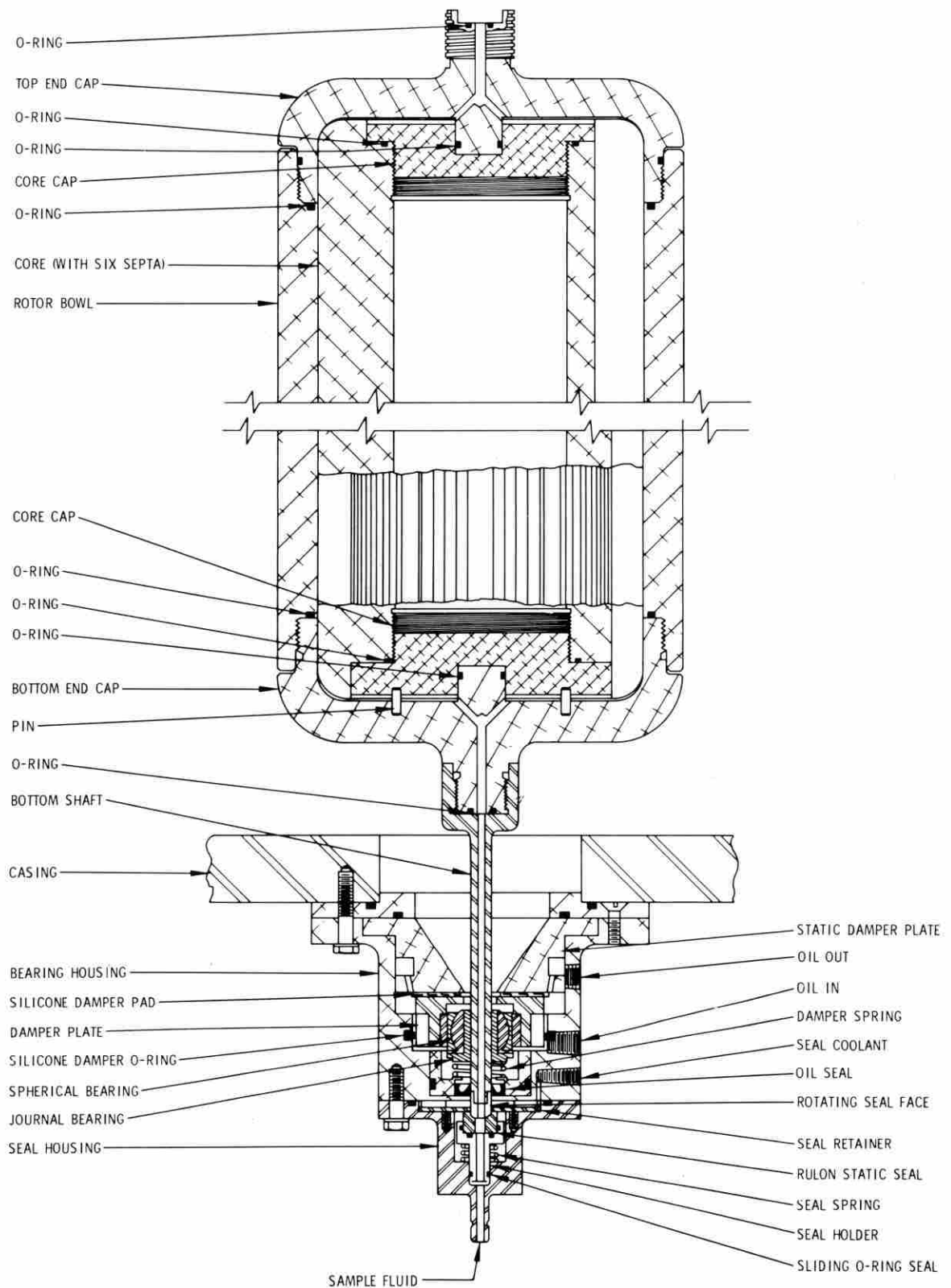


Fig. 2.5 Diagrammatic presentation of lower part of K-II centrifuge.

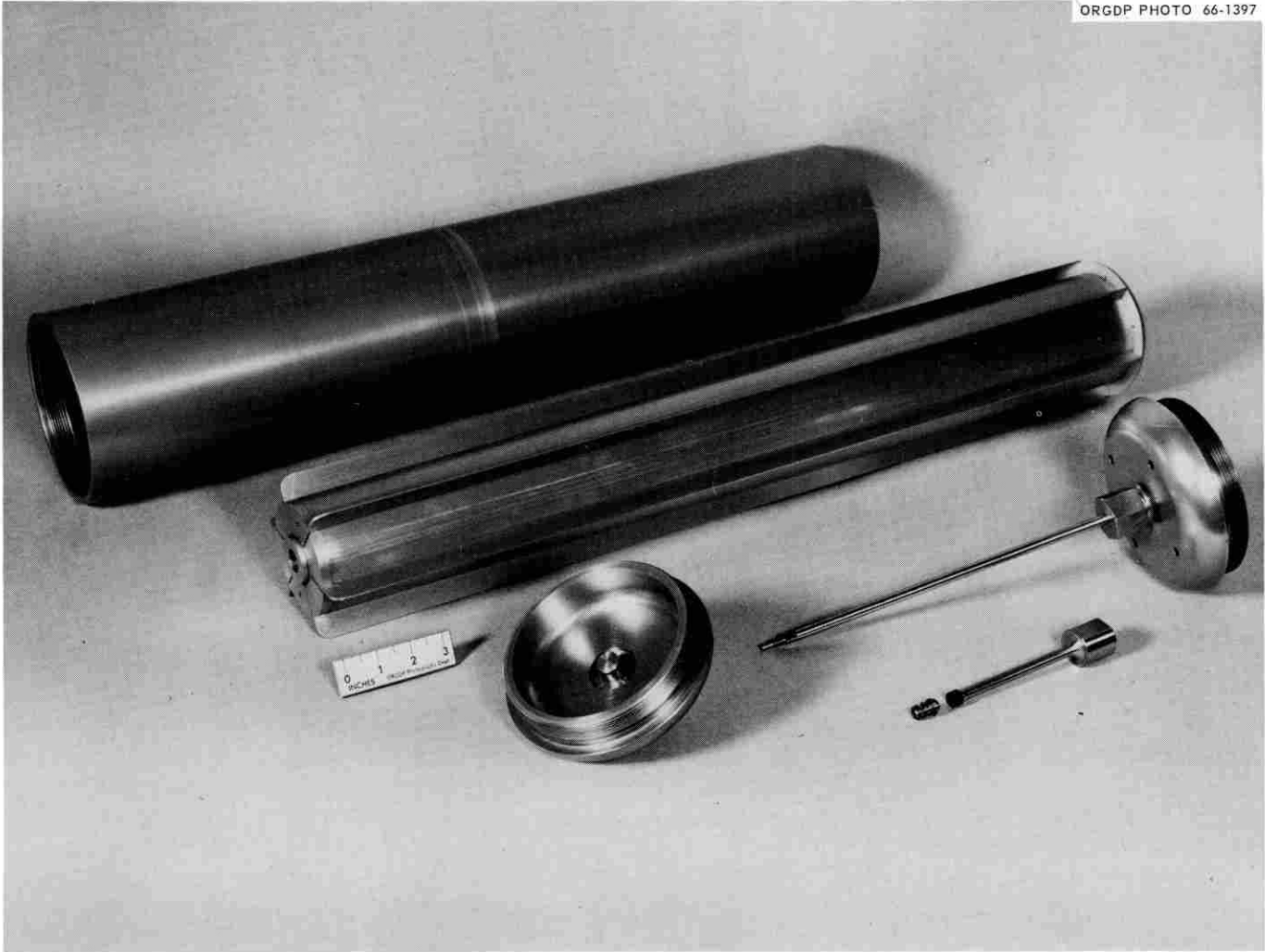


Fig. 2.6 Disassembled K-II centrifuge rotor. Tubular centrifuge bowl is shown above six vaned rotor core. Upper end cap and shaft shown at lower right above lower (short) shaft. Lower end cap shown in center.

within the unstable region shown in Figure 2.3, but merely indicates that it would be more difficult to design suspensions to attenuate the whirl frequencies of the rotor within this region.

Finally the rotor weight can be approximated by the formula

$$\text{Weight} = \delta\pi(1.69r_s^2 + 1.67r_s t)L_e + 0.94r_s^3$$

Where

$\delta$  = rotor material effective density (including fluid)

$L$  = rotor thickness

$r_s$  = sample zone radius

$L_e$  = rotor effective length.

At values of  $L_e/D_s$  above 4 this reduces to

$$\text{Weight} \approx 2.18\pi r_s^2 L_e$$

The design region for the rotor system with all mechanical factors considered as well as the biological requirements lies in the region bounded by

$$3 \leq L_e/D_s \leq 10$$

and

$$20,000 \leq \text{rpm} \leq 40,000$$

where the limit of 20,000 rpm is determined by the maximum allowable rotor weight and the 40,000 rpm is the present upper limit of proven reliable seal design. All disk-type rotors where  $I_\rho/I_t \geq 1$  are eliminated by either the rotor stress or the rotor weight.

The actual K-II rotor ( $L_e/D_s \approx 8$ ) was designed in the upper half of this region for two reasons; (a) the  $L_e/D_s$  was made as large as possible to reduce the shafting requirements to, and the damping requirements

of, the suspension systems, but (b) the  $L_e/D_s$  was limited to a value below 10, and  $r_s$  was limited to 4.94 cm to allow overspeed operation above the initial speed of 26,500 rpm to 35,000 rpm without encountering any problems due to either the rotor flexural critical speed or due to overstress in the rotor.

**Stability.**—As mentioned in the design section, the rotor stability was enhanced as much as possible within the restrictions imposed by the separation task. This choice was in part dictated by the desire to use simple, quick disconnect locking devices to hold the shafts to the rotor. In other words, if an  $L_e/D_s$  of three or four were chosen much stiffer shafts would be required to couple the rotor to the suspension and damping systems in order to attenuate the natural whirl frequencies of the rotor; the use of stiff shafting would preclude the possibility of using a nut locking device for the shaft. Since the natural stability of the rotor was in a sense maximized, relatively flexible shafting could be used which would allow operation of a more unbalanced rotor without causing runout at the seals (since at operating speed the dampers would be essentially “seismic”). In actual operation no stability problems whatsoever have been encountered.

The K-II rotor is shown diagrammatically in Figures 2.4 and 2.5 and disassembled in Figure 2.6.

#### (4). The K-II Drive System

D. A. Waters                      R. F. Gibson  
C. E. Nunley

Selection of an air turbine as the optimum drive system for the machine has been previously discussed. The particular turbine chosen was a Barbour-Stockwell Co. Model 2501, 4-in. vertical turbine. This turbine used the diameter shaft needed for the rotor, had the peak of its horsepower curve in the range of anticipated operating speed and had a maximum safe operating speed of 60,000 rpm. Air consumption at 27,000 rpm under normal rotor operating conditions has been measured at ~80 scfm at ~25 psi inlet pressure. At 35,000 rpm air consumption will probably be in the range of 90–100 scfm.

From deceleration rates, the power required to spin the full rotor at 27,000 rpm was computed to be ~1 hp. It may be of interest to note here that the machine uses four journal bearings and two ball bearings. Three of the journal bearings are located in the turbine damper unit, one is used in the lower damper bearing, and the two ball bearings are used to mount the turbine wheel. One modification made on the

turbine damper unit was to mount the bronze bearings inside spherical bearings so that misalignment could be more easily accommodated. The hollow drive spindle is easily installed and is supported by a nut on the top of the turbine wheel.

Lubrication of the turbine wheel ball bearings comes from an air mist lubricator on the turbine control manifold. The turbine damper bearing unit is filled with oil which is recirculated by the same oil pump that lubricates the lower damper bearing. Safety features built into the lubrication system and turbine control are described later.

A modification of the turbine exhaust spoolpiece was required to accept the top seal mounting flange. Exhaust air from the turbine which normally goes straight up through the spoolpiece, was routed out the side of the spoolpiece so that the top seal would be more accessible.

A magnetic pickup unit furnished with the turbine is connected into the centrifuge control panel speed indicator and overspeed circuitry.

Due to the extremely high pitched noise level created by the turbine, the use of a muffler was necessary to protect operators. To prevent an aerosol oil mist from filling the room, piping of exhaust air outside was found to be desirable.

#### (5). Seal Design and Testing

R. F. Gibson                      C. E. Nunley

One of the features that sets the K-II apart from previously-developed zonal centrifuges is the use of rotating seals on both ends of the rotor system. Two identical single-path seals are used; one is mounted on top of the turbine drive and the other is mounted under the lower damper bearing. With this straight-through design, the sample fluid flowing through the rotating system enters and leaves at approximately the same radius; therefore there is no “pumping effect” to limit the direction of flow. Neglecting the effects of core orientation (since the core is reversible), there is little or no difference in the inlet pressure required to pump through the rotor from either end. It is evident that fluids are subjected to less shearing action with the straight-through seal than with the previously developed two-path seals.

During the initial stages of development, several seal configurations were tested. The first seal was a rounded convex static seal face spring-loaded against a concave Rulon face on the end of a rotating shaft. This design was modified a number of times but still

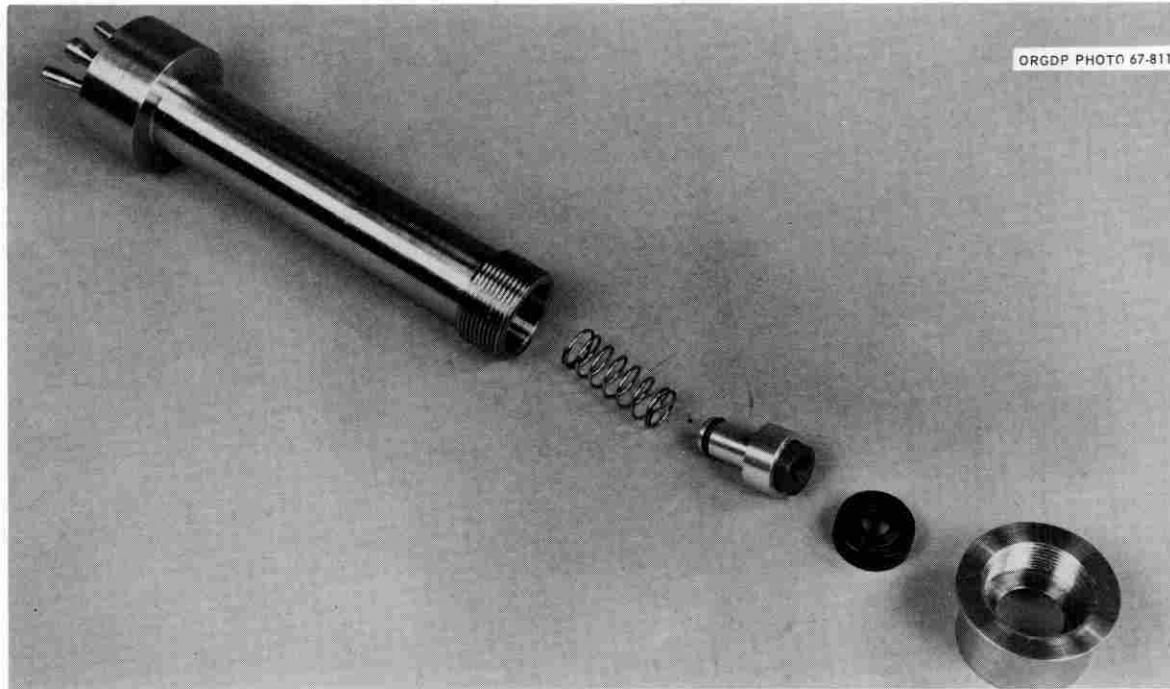


Fig. 2.7 Upper seal assembly for K-II centrifuge system.

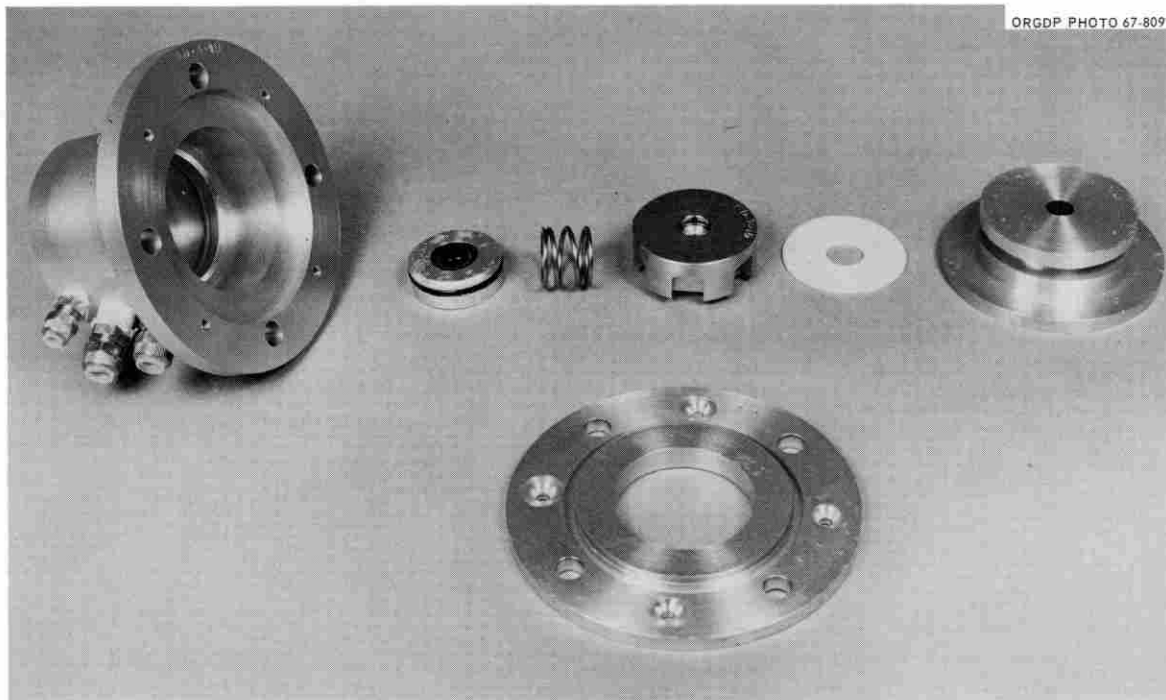


Fig. 2.8 Bottom damper bearing for K-II centrifuge system.

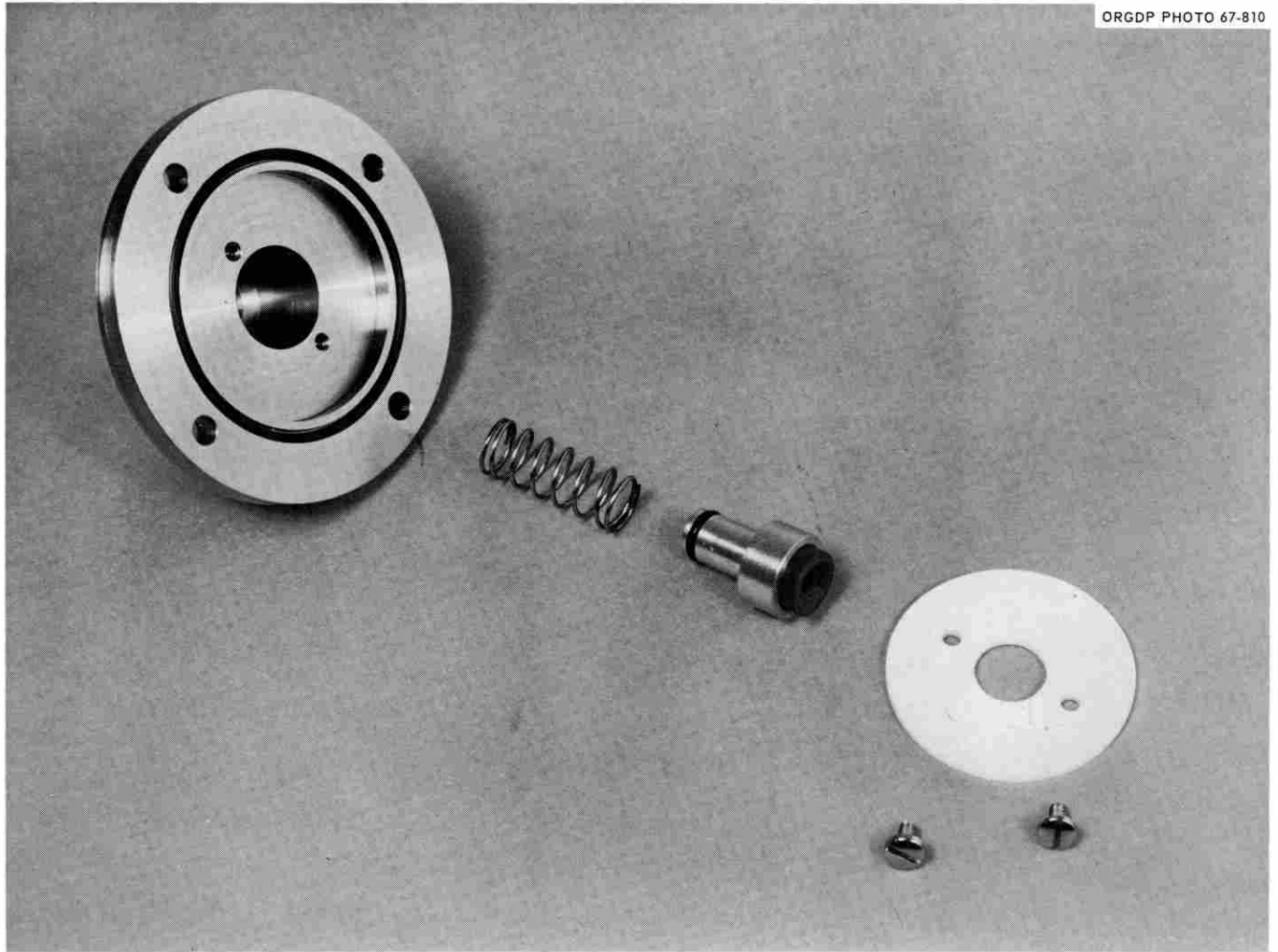


Fig. 2.9 Lower seal assembly for K-II centrifuge system.

proved to be too susceptible to vibration and separation of the seal faces at high speed. The upper seal performed more reliably since its rotating part was mounted directly on top of the turbine drive rotor (the rotor being mounted rigidly on ball bearings). Due to the nature of the suspension, very little rotor vibration was transmitted to the seal and only the runout of the dynamic seal face itself was a problem. The rotary seal face on the bottom seal had a more flexible suspension in the bottom damper bearing. In addition, rotor runout and precessional motion was transmitted by the bottom shaft to the seal face. It was noted that the conical Rulon seal face had to be machined perfectly concentric and aligned with the shaft and that the loading spring had to be replaced

with soft rubber washers to prevent the onset of separation. After considerable testing and modification it was decided that this design was unreliable. A much more reliable design was found by reversing the seal faces so that a conical concave Rulon static seal face was spring-loaded against the rounded convex end of the rotary member. Testing showed that this seal did not require precision alignment and vibration damping as the previously described seal did. Another improvement was the prevention of sticking by minimizing the squeeze on the sliding O-ring seal between the seal holder and its housing.

The fluid which is circulated around the seal carries away much of the heat generated by friction and also catches any material that might leak past the seal faces.

During centrifugation of hazardous material, a disinfectant may be used as the coolant, providing a better secondary seal. Tap water has been used as the coolant in most of the runs thus far. A slinger-catcher unit is used on the upper seal to prevent leakage of coolant into the turbine if a leak past the lip seal should occur.

The upper seal now in use is shown in Figure 2.7. The bottom damper bearing is shown in Figure 2.8, and the lower seal assembly in Figure 2.9. As of this writing, at least 1000 hours of accumulated run time has been recorded using these seals and reliability has been generally good. Wear characteristics have been acceptable even with the somewhat gritty sample solutions used during evaluation. Seal life will be greatly improved by heat-treating (hardening) the rotating seal faces. Although nearly all of the seal

reliability data has been accumulated at 27,000 rpm, it is believed that the seals will perform satisfactorily at the maximum safe rotor speed of 35,000 rpm.

### (6). Crash Shield Design

R. F. Gibson

E. F. Babelay

The design of a safe rotor chamber or crash shield has turned out to be one of the most perplexing problems of the K-II machine development. Two casing designs (K-IIA and K-IIB) have been used but high-speed rotor burst tests have pointed out weaknesses in both types. A partial cylinder with a hinged, flat door has been the basic design thus far. The second design differed from the first in the manner of latching the door shut (Figures 2.10-2.12). Although the problem

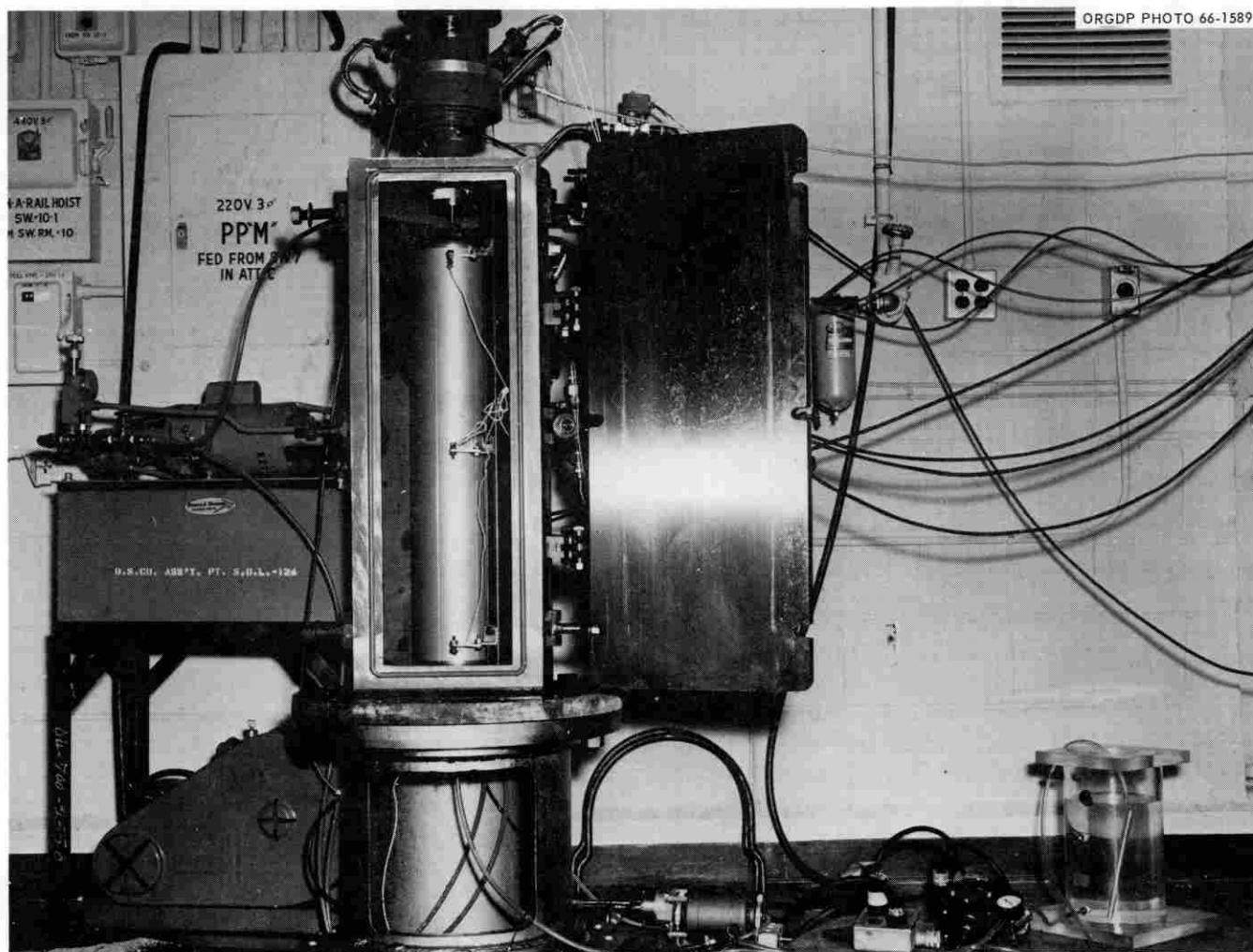


Fig. 2.10 K-IIA shield arranged as a test stand for initial burst tests.

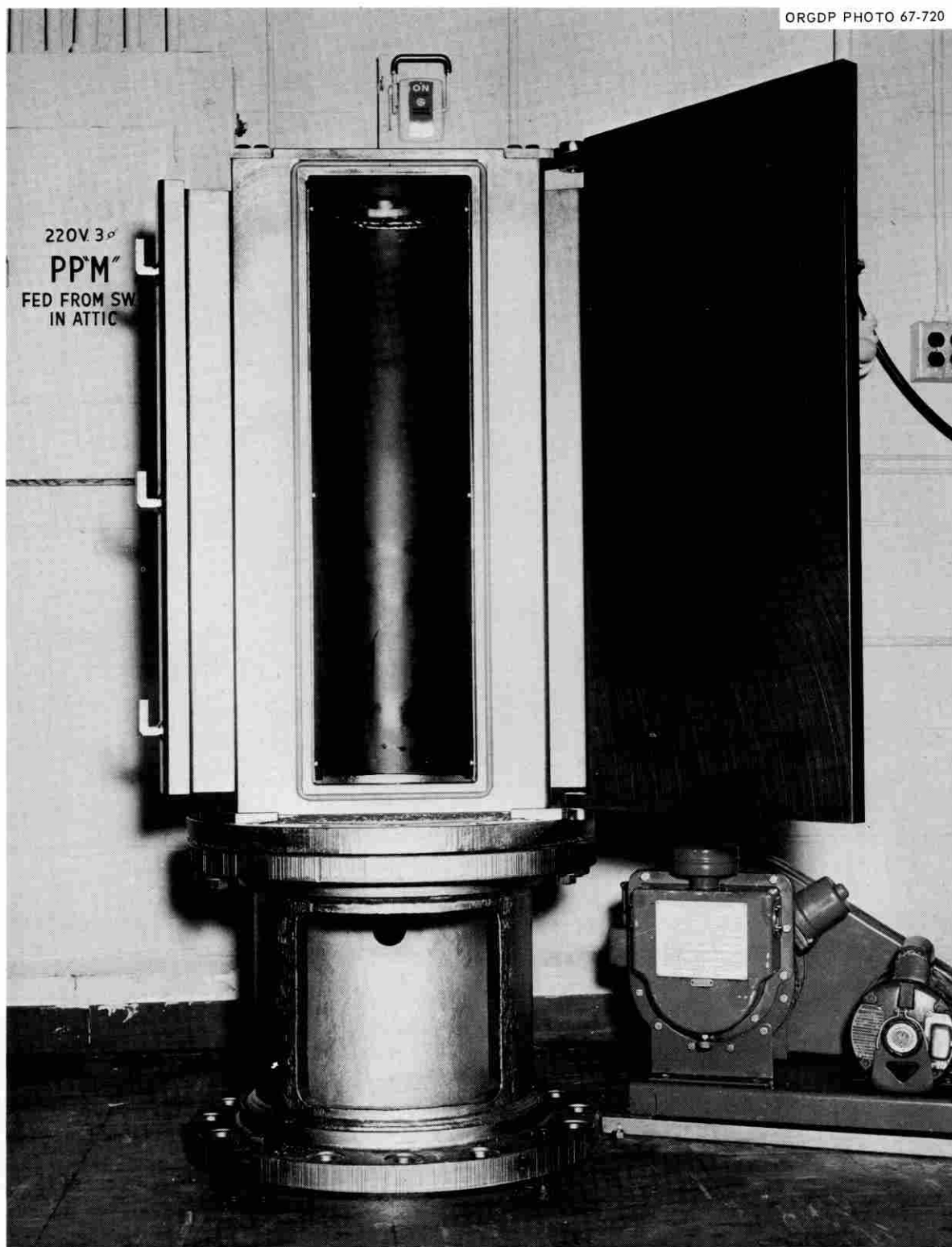


Fig. 2.11 K-IIB armor shield showing clamping arrangements for securing door.

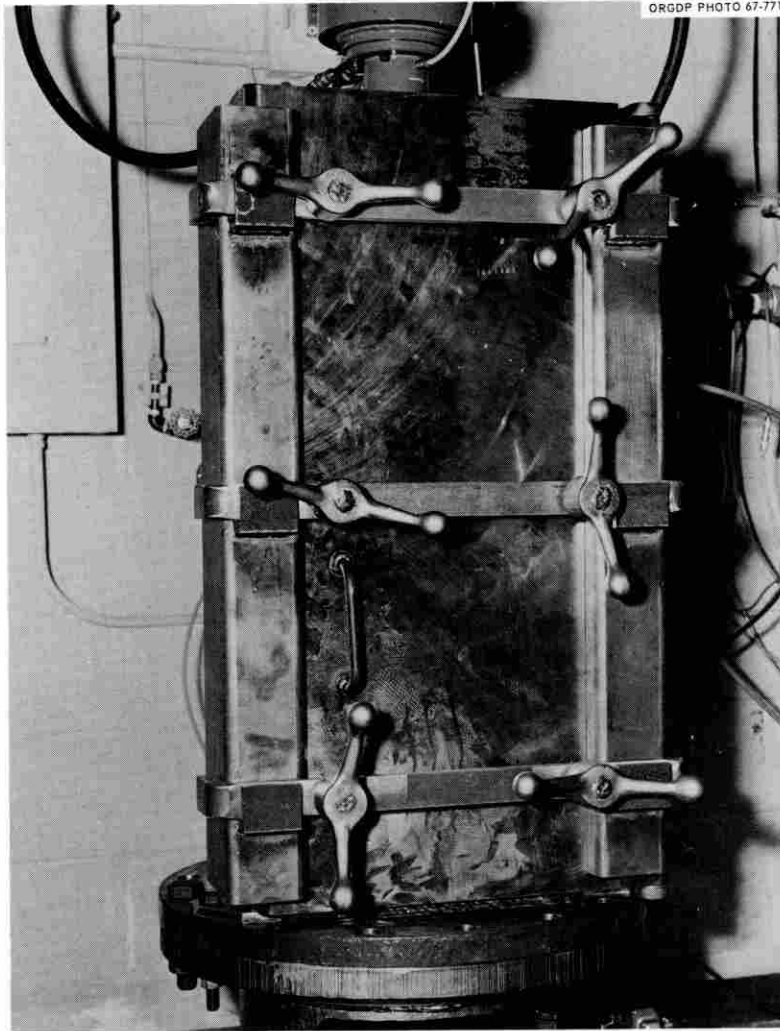


Fig. 2.12 K-IIB centrifuge closed ready for operation.

of holding the door shut under impact has apparently been solved, the selection of armor plate material itself has come under scrutiny as a result of the burst tests.

To gain a better understanding of design criteria and materials specification for armor, considerable research has been done on the subject. Many pertinent technical reports have been studied and discussions were held with personnel at the U.S. Army Materials and Mechanics Research Center, Watertown, Mass.

It appears that the typical mechanical properties of materials (especially ductility as measured by percent elongation and the area under a tensile test diagram) are of little value in determining the impact toughness. Such properties might be used if one was certain that

the material had the desired microstructure (one where brittle fracture would be unlikely to initiate under given impact). One type of test that can be useful is the impact test of specimens at low temperatures ( $\sim -120^{\circ}\text{F}$ ). It has been found that the effect of very high impact velocities may be simulated by a standard Charpy test carried out at low temperatures.<sup>13</sup> The notion of a critical impact velocity also appears to be of interest.<sup>14</sup> No clear-cut theoretical approach has been found for problems similar to this and the experience of experts in this field is apparently the best source of design data.

There is no doubt that a cylindrical casing would be safer and cheaper to make than the partial cylinder with a door, but other factors have been considered

also. The turbine-rotor system would have to be lifted out the end of a cylindrical casing, which would require the disconnection of air lines, fluid lines, a tachometer lead and the muffler. A fork lift or chain hoist and plenty of head room would be required because of the weight and length of the assembly. A door-type casing could be installed in many locations which could not handle a cylindrical casing. Several other designs which have been considered also tend to require special installation sites.

### (7). The K-II Centrifuge Control System

E. C. Denny

Due to the high energy levels contained within the rotating system it is of utmost importance to consider

the safety of both personnel and equipment. Since energy increases directly as the square of the rotational speed it is important to control and contain this speed within bounded limits. Thus the majority of features of the control system itself are aimed at providing the necessary safety in a simple but effective manner.

Features of the control system will be described in detail with appropriate comments regarding reasons for its incorporation. This description covers only the safety features of control and does not include details of mechanical design for safety not directly related to control itself.

The control system consists of a main panel containing relays, switches, pressure regulator, vacuum gage, and electronic circuitry, and an air manifold containing manual valves, solenoid valves, control valve, critical flow orifice, an oil mist lubricator, and appropriate

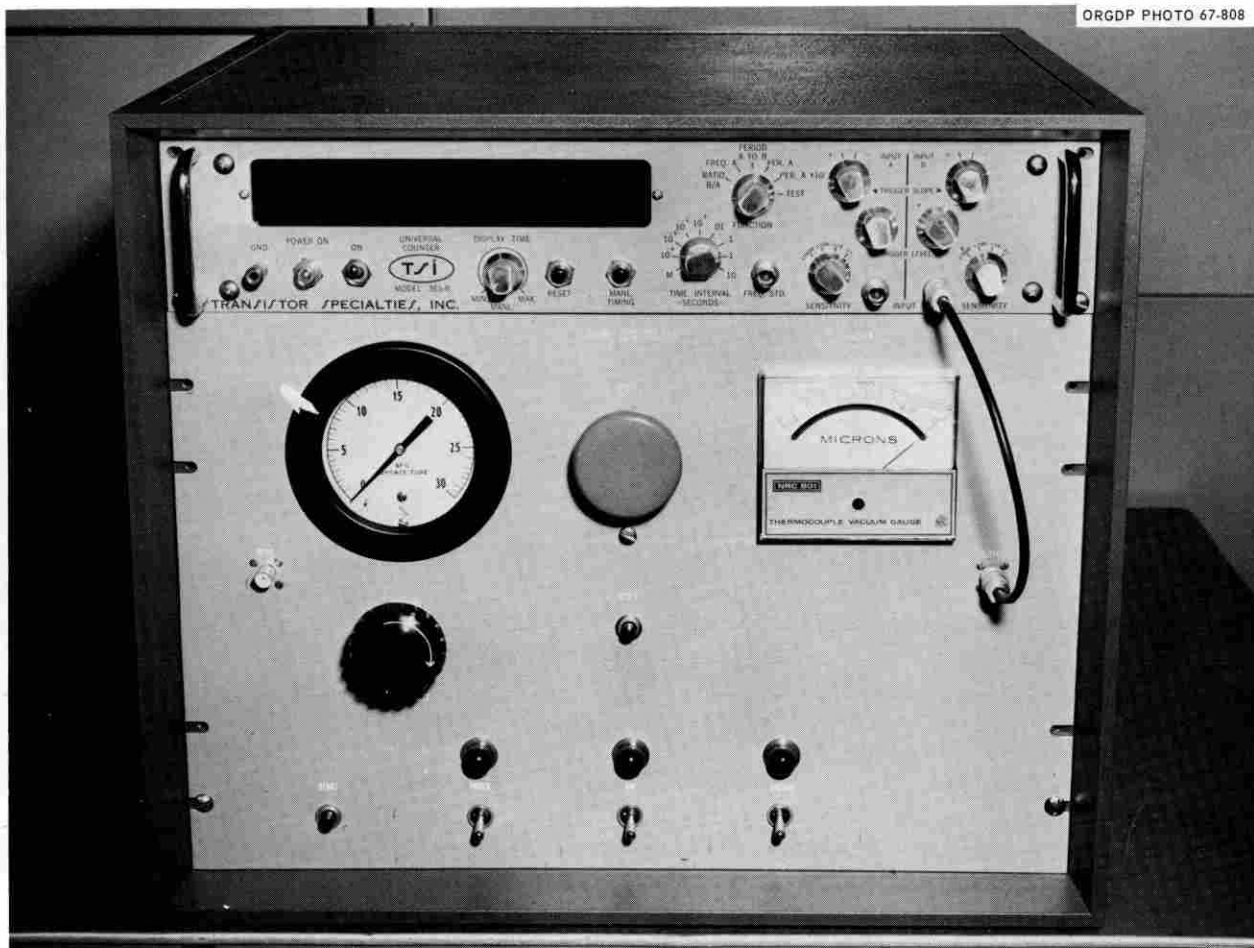


Fig. 2.13 Control panel for K-II centrifuge.

ate pressure taps and quick disconnect couplings. Air flow to the turbine is effected by manipulation of the solenoid valves and the control valve from the panel which may be located remotely from the centrifuge. Speed is registered on a digital readout device. A photograph of the control panel and digital readout device is shown in Figure 2.13 and the manifold is shown in Figure 2.14.

A manual valve on the air manifold admits air pressure to the main air solenoid and the brake solenoid. At the same time air is admitted to the oil mist system to insure that the turbine is not operated without adequate lubrication. When the power switch on the

panel is actuated the oil pump supplying oil to the rotor bearings is energized. Thus the rotor cannot be run without adequate lubrication.

Redundancy is provided between the air switch and the start switch. Each must be activated before the main air solenoid can be operated. However, these switches serve two separate purposes. The air switch provides a means of manually controlling the air to the turbine if it is desired to allow the system to coast, or to make adjustments, etc., without shutting down the lubrication system. The start button allows reactivation of the air supply in the event of an over-speed cut out.

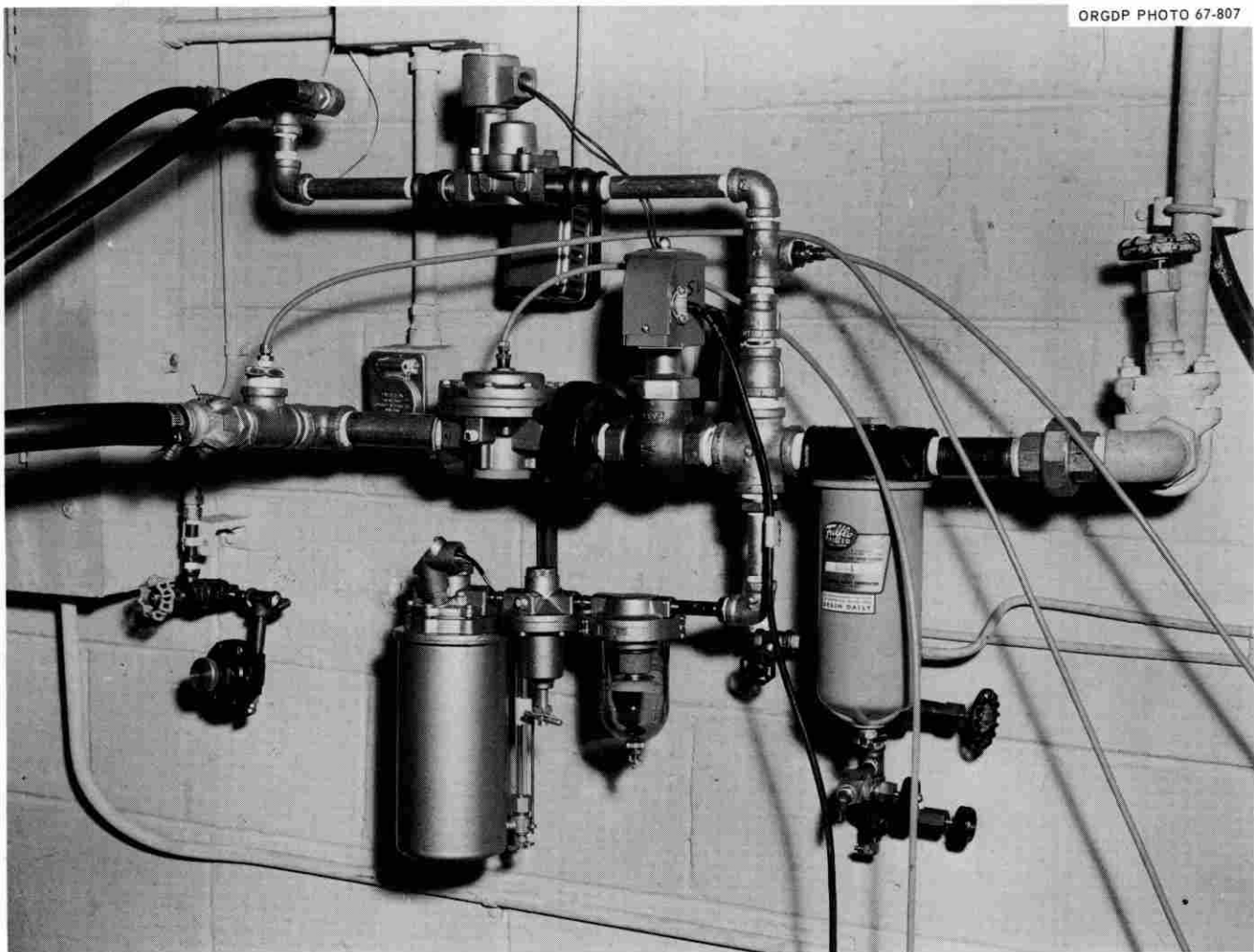


Fig. 2.14 Air control valves and filter system for K-IIB centrifuge.

Speed is controlled by adjusting pneumatic pressure to a control valve. This is effected through the throttle (pressure regulator) and pressure indicator. The pressure regulator is an internal feedback type such that output pressure is maintained constant regardless of changes in upstream pressure. The control valve is a self-balancing type maintaining constant flow for a given control setting. Due to the large moment of inertia with consequent slow response time on the rotor it has been found unnecessary to provide automatic control of speed under normal operating conditions. The pressure indicator is useful as an accelerometer or as a rough speed indicator. Speed may be controlled reliably during either acceleration or deceleration. If it is desired to program the system this can be done quite readily by gearing the throttle to an electric motor driven from a timing or controlled unit.

Three methods are available for deceleration. These are: (a) coasting—by shutting off the air switch and allowing the system to decelerate due to bearing friction, etc. (b) controlled deceleration—readjusting throttle setting for lower speeds, usually for slower deceleration than would be obtained by coasting, and (c) emergency stop—by cutting off the air supply to the turbine and applying air to the brake. This is activated by depressing the "STOP" button. The system may be restarted after depressing the stop button by depressing the reset button and then "start." Thus one is enabled to make rather rapid decelerations in the event of emergencies but may restart without coming to a full halt or cutting off lubrication.

Three main safety features remain and are somewhat independent of the controls thus far mentioned. An electronic circuit automatically cuts the turbine air off in the event the system exceeds a preselected speed. This prevents operation of the rotor at a speed exceeding safe design, thus providing a "circuit-breaker" for speed. The system may be restarted after the speed has again dropped to the safe operating level.

Provision is made on the air manifold for insertion of a critical flow orifice in installations where air pressure may be exceptionally high or fluctuates excessively. This limits the upper speed attainable to a safe level.

The final safety provision is a throw-out pin on the rotor. This pin breaks at excessive speed allowing an arm to extend. The whirling arm will break an electrical circuit cutting off air to the turbine. In this case the system must be shut down for pin replacement and circuit repair.

Provision is made on the control panel for activation of the vacuum solenoid and the monitoring of system pressure. These circuits are independent of the speed control.

Square wave signals are available for digital counting of speed. These signals are derived from the electronic overspeed circuit and a proximity pickup in the turbine. A conventional counter is used for speed register. All circuitry is solid-state. Conventional operational amplifiers are used for low maintenance and ready replacement. Relays are plug-in type units and the solenoids have replaceable coils and plungers.

#### (8). Initial Destructive Tests

C. E. Nunley                      R. F. Gibson  
E. F. Babelay                    D. A. Waters  
R. M. Schilling

In an attempt to prove that the rotor chamber would contain the huge amounts of impact energy created by a high-speed rotor failure, a remotely controlled burst test was conducted in the K-IIA shield. Two grooves were machined 180° apart on the outside periphery of a standard K-II rotor bowl so that the bowl would pull apart in two halves at about 45,000 rpm. The rotor was filled with sucrose and water to give the added stress created by a rotating mass of fluid inside the rotor. The test stand is shown in Figure 2.10.

On the initial run the rotor was driven to approximately 46,000 rpm and appeared to be quite near the rupture point when it suddenly began whirling at large amplitudes (~30 mils). The precession mode was identified as the same 25 cps translational whirl that had been observed at lower speeds with improper damping. Several probable reasons have been given for the onset of whirl in this case including (a) the increasing ellipticity of the bowl due to the two halves trying to pull apart, (b) the rotor was beginning to accelerate into its flexural critical speed. Enough of the rotational energy of the system was dissipated by the large amplitude whirl that it could be driven no further with the available air supply. Surprisingly, the rotor decelerated and the whirl gradually disappeared without shaft breakage.

For the next attempt the depth of the radial grooves was increased in hopes that the rotor would burst before the onset of whirl. Again the rotor was filled with sucrose and water and accelerated while stability and growth were checked with proximity probes. This

time the rotor was driven to about 45,000 rpm where the whirl suddenly appeared again and caused deceleration without failure. Since this was the second time the bowl had been stressed *past* yield strength, it was feared that if the next attempt failed the bowl would be too elliptical and unbalanced to run again. The groove depth was then increased to 66% of the wall thickness and a heavier cesium chloride gradient was used in the rotor. Rotor failure finally occurred at about 17,000 rpm and the remains of the rotor are shown in Figure 2.15. Neglecting stress concentration around the bottom of the groove, the average stress across the section between the inside bowl wall and the

bottom of the groove was calculated to be about 32,000 psi. Since the ultimate strength of the aluminum bowl material was about 81,000 psi a stress concentration factor of at least 2.5 was required to cause failure. It is known that deep grooves perpendicular to the direction of tension produce high stress concentration around the bottom of the grooves. By extrapolation of data taken on grooved bar specimens,<sup>15</sup> a stress intensity factor of approximately 2.5 was calculated.

The K-IIA casing showed no evidence of penetration or cracking although the door latch bolts were loosened by the impact. Steel washers behind the latch-bolt nuts were extruded by the impact, leaving the

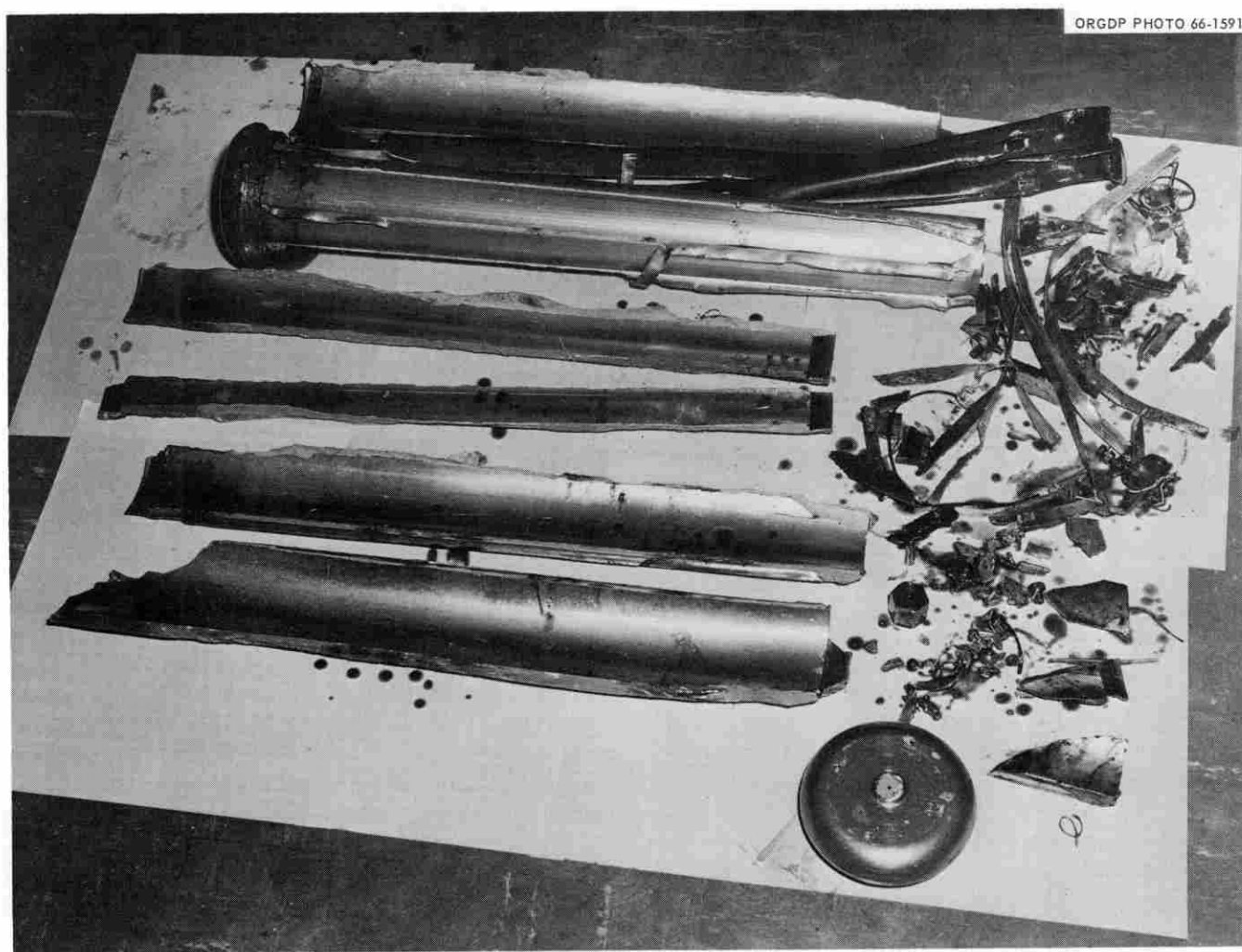


Fig. 2.15 Fragments of K-II rotor recovered after initial burst test.

bolts free to swing away. At this point it was decided that better ways of latching the door should be investigated.

Although the rotor failed to burst at the desired energy level, a great deal was learned about the inherent safety of the rotor system at runaway speeds. The design of future burst rotors will no doubt be more successful as a result of this experience.

The K-IIB casing was designed to provide better door closure and less chance of shrapnel development in case of rotor failure at high speed. It was tested using a specially-designed burst rotor. In designing the burst rotor, the primary concern was to build a

stable rotor with about *two* times the energy per unit length of the K-II bowl at 40,000 rpm. The rotor developed was a hollow aluminum cylinder, 6-in. long by 8-in. O.D. and 6-in. I.D., which is shown in Figure 2.16. It was grooved along the length at 180° to facilitate failure in two halves. It was constructed of brass and was threaded into the center of the rotor to prevent the rotor from growing away from the drive disc. The burst rotor was designed to burst at 30,000 rpm and contain 176,000 ft lb of energy at failure.

The rotor was supported at the top of the casing by the turbine shaft and the brass drive disc. Actual burst-speed of the rotor (the last printing on the electronic

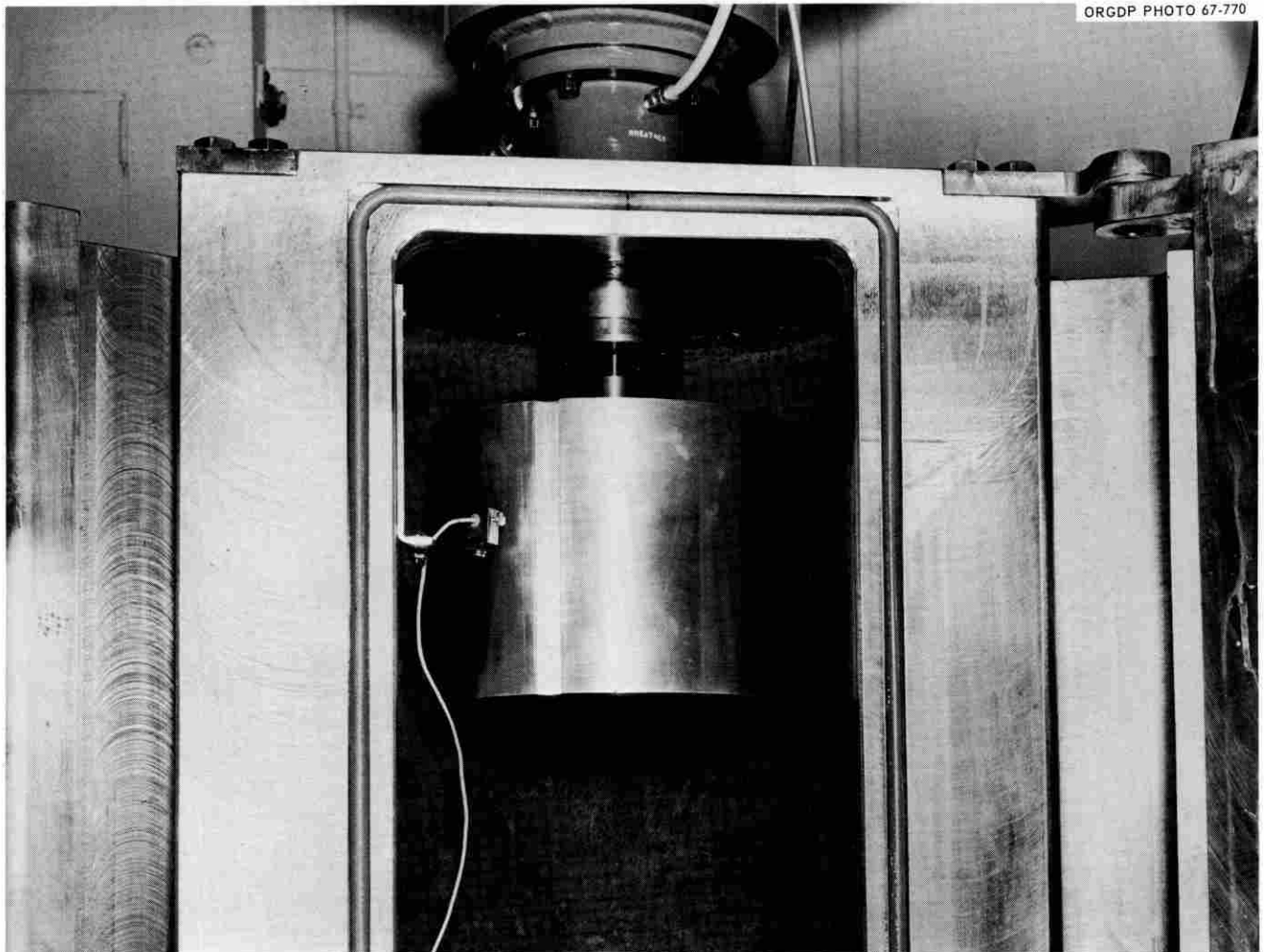


Fig. 2.16 Rotor simulator for burst tests in K-IIB centrifuge.

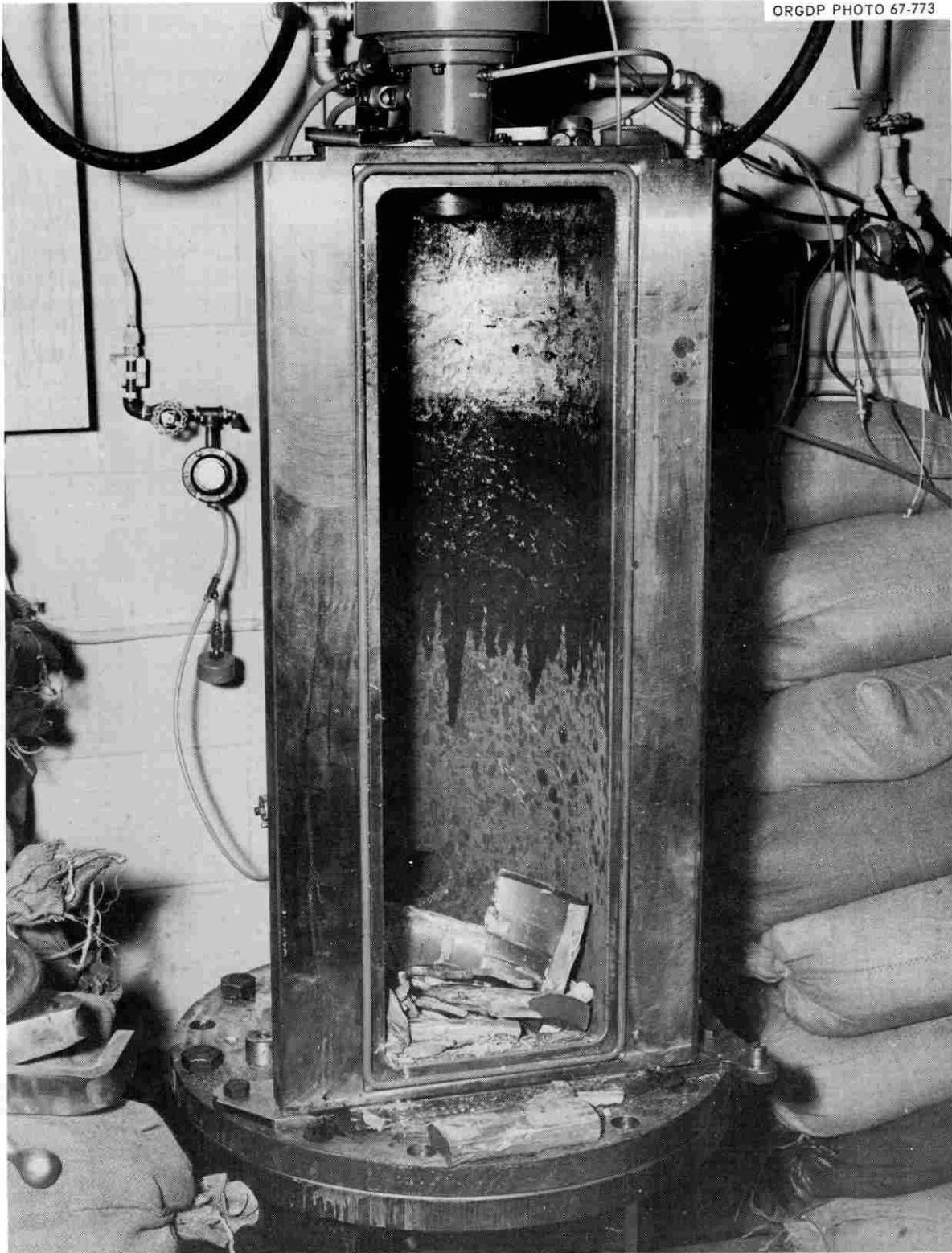


Fig. 2.17 Simulator rotor fragments after burst in K-IIB centrifuge.

counter) was 30,900 rpm. Energy contained in the rotor at this speed was 185,000 ft lb, which is 44% of the energy of the entire K-II bowl at 40,000 rpm. Energy per unit length ratio to the K-II bowl at 40,000 rpm was 2.15, however. A single probe mounted at the center of the rotor (see Figure 2.16) indicated the average growth. Total growth just before burst was 0.017-in., 0.010-in. growth was detected from 25,900 rpm to burst. Figure 2.17 shows the remains of the rotor in the bottom of the casing. Examination of the parts indicated that failure was at the grooves as expected.

The casing being tested was damaged by the impact. The door was bowed slightly and small fragments of

aluminum were found on the flange outside the O-ring gasket. The ends of the top safety bar failed when the door bowed, but the door remained closed. The 14-in.-diam schedule 160 steel pipe was cracked in the area of impact (Figure 2.18); and the top plate of the casing was pulled away from the weld above the impact area.

With full realization of the severity of this test, a study is being made to provide a stronger casing for the K-II centrifuge. Existing casings will probably be fitted with an energy-absorbing liner while research on high strength materials for use in the K-IIC casing continues.

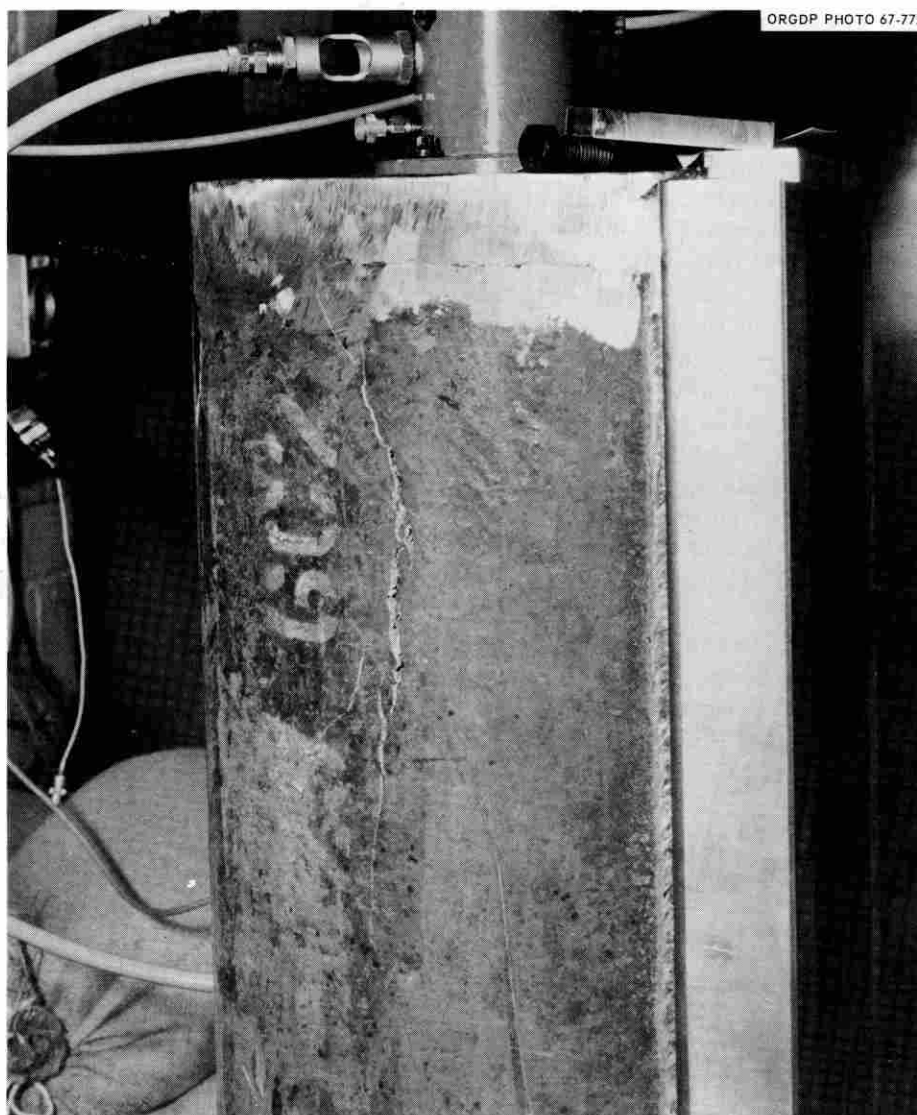


Fig. 2.18 Crack in armor casing of K-IIB centrifuge after rotor simulator burst tests.

## (9). Problems of Titanium Rotor Development

R. F. Gibson

The problem of safely containing an exploding rotor at high speeds will be compounded when K-type titanium rotors are built. Not only will the titanium rotors be capable of operating at higher energy levels (at least 100% higher than that of aluminum K-II), but the heavier titanium material will be more capable of armor penetration. Obviously, it is desirable to have one casing design that will handle both aluminum and titanium rotors. Whether this is feasible or not remains to be seen.

The ratio  $\sqrt{E/\rho}$ , where  $E$  is the modulus of elasticity and  $\rho$  is the density, is almost the same for the aluminum and titanium materials under consideration. The rotor flexural critical speed of a titanium version of the present rotor would therefore be about the same as that of the aluminum rotor. Although the titanium rotor would have different dimensions, the critical speed and stress considerations would probably limit operating speed to about 40,000 rpm.

Since a titanium K-type rotor would weigh at least 80 lbs, handling would have to be done with a special lifting device. The aluminum K-II is probably about as much as one operator can safely handle manually.

Although the turbine drive would have more than enough power, there is a possibility that the shaft spring rates and available damping in the present machine may not handle the heavier titanium rotor. If heavier shafting is needed, then the turbine drive would require modification to accept a larger diameter shaft.

To the centrifuge user the advantages of titanium rotors are many. Among them are higher g-fields, good corrosion resistance, and use of steam sterilization.

## REFERENCES

- <sup>1</sup>J. B. Robinson, R. J. Douglas, I. Grinyer, and E. H. Garrard, *Can. J. Microbiol.* **6**, 565-572 (1960).
- <sup>2</sup>R. L. Steere, *Adv. in Virus Research* **6**, 3-73 (1959).
- <sup>3</sup>P. Oxelfelt, *Virology* **30**, 740-741 (1966).
- <sup>4</sup>L. Philipson, P. A. Albertsson, and G. Frick, *Virology* **11**, 553-571 (1960).
- <sup>5</sup>N. G. Anderson, *Nature (London)* **199**, 1166-1168 (1963).
- <sup>6</sup>E. E. Jensen, F. L. Dunn, and R. Q. Robinson, *Prog. in Medical Virology* **1**, 165-209 (1957).
- <sup>7</sup>V. Dostal, *Prog. in Medical Virology* **4**, 259-303 (1962).
- <sup>8</sup>N. G. Anderson, C. L. Burger, and H. P. Barringer, *Fed. Proc.* **23**, 140 (1964).

<sup>9</sup>N. G. Anderson, H. P. Barringer, J. S. Amburgey, Jr., G. B. Cline, C. E. Nunley, and A. S. Berman, *Natl. Cancer Inst. Monograph* **21**, 199-216 (1966).

<sup>10</sup>G. B. Cline, H. Coates, N. G. Anderson, R. M. Chanock, and W. W. Harris, *J. Bact.* in press. (1967).

<sup>11</sup>G. B. Cline, C. E. Nunley, and N. G. Anderson, *Nature* **212**, 478-489 (1966).

<sup>12</sup>The Molecular Anatomy of Cells and Tissues. Annual Report for the period July 1, 1965 to June 30, 1966. ORNL 3978 Special. (N. G. Anderson, Ed.).

<sup>13</sup>F. Poberil, *Metal Progress*, **56**, 58 (July, 1949).

<sup>14</sup>T. Von Karman, and P. Duwez, *J. of Appl. Phys.* **21**, 987 (Oct. 1950).

<sup>15</sup>A. J. Durelli, and R. H. Jacobson, *Proc. SESA*, **8**, 163 (1951).

## B. VELOCITIES AND SHEAR STRESS DISTRIBUTIONS IN ZONAL CENTRIFUGE ROTORS

H. W. Hsu

The objective of the following work was the quantitative evaluation of velocities and shear stress distributions in zonal centrifuge rotor operations. An adequate knowledge of various velocity components in zonal centrifuge rotors will facilitate their use for the mass separation of new biomaterials. An adequate knowledge of shear stress distributions in the rotors will serve as a guide for controlling the rotors' acceleration to their maximum speed in order to prevent damage to biomaterials being separated.

We consider a centrifuge, a cylindrical container of radius  $R$ , filled with a fluid of linear density gradient, whose density increases with increasing distance  $r$  from the axis. The cylindrical container is to rotate about its own axis at an angular velocity  $\Omega_i$ . When the cylinder is rotating at steady state, the fluid in the container moves as the elements of a rigid body.<sup>1</sup> Thus there is no shear stress existent within the fluid. The shear will be generated only during the acceleration or deceleration periods. The transient behavior of the fluid in a cylindrical container rotating about its own axis was studied using the equations of motion.

### Formulation of Problem

The system is described most easily in cylindrical coordinates. At steady state it is known that  $V_z = V_r = 0$  and that  $V_\theta$  is a function of radius,  $r$ , alone. In the transient case, accelerating the rotor's angular velocity from  $\Omega_i$  to  $\Omega_f$ ,  $V_r$  and  $V_z$  are also negligible compared to the order of magnitude of  $V_\theta$ . Thus the motion can

be adequately represented by the tangential-component equation alone. This is given by<sup>1</sup>

$$\frac{\partial V_\theta}{\partial t} = \nu_0 (1 + \epsilon r) \cdot \frac{\partial}{\partial r} \left( \frac{1}{r} [r V_\theta] \right) \quad (1)$$

The initial and boundary conditions for this case are:

$$V_\theta(0, r) = 0$$

$$V_\theta(\Delta t, R) = \Delta \Omega R (1 - e^{-a \Delta t}) \quad (2-b)$$

$$V_\theta(\Delta t, 0) = 0 \quad (2-c)$$

where  $a$  is the time constant in the equation expressing the control of the rotor's acceleration or deceleration.

### Solution to Problem

Equations (1) and (2) can be rewritten with reduced variables. These are

$$\frac{\partial V_\theta}{\partial \tau} = \frac{1}{\zeta} \frac{\partial V_\theta}{\partial \zeta} - \frac{V_\theta}{\zeta^2} + \frac{\partial^2 V_\theta}{\partial \zeta^2} + \lambda \left[ \frac{\partial V_\theta}{\partial \zeta} - \frac{V_\theta}{\zeta} + \zeta \frac{\partial^2 V_\theta}{\partial \zeta^2} \right] \quad (3)$$

$$V_\theta(0, \zeta) = 0 \quad (4-a)$$

$$V_\theta(\Delta \tau, 1) = \Delta \Omega R (1 - e^{-\alpha/\nu_0 \Delta \tau}) \quad (4-b)$$

$$V_\theta(\Delta \tau, 0) = 0 \quad (4-c)$$

where

$$\tau = \frac{\nu_0 t}{R^2}, \quad \zeta = \frac{r}{R}, \quad \epsilon R = \lambda, \quad \alpha = a R^2 \quad (5-a, b, c, d)$$

Equation (3) is to be solved by the method of separation of variables.<sup>2</sup> If it is assumed that

$$V_\theta = T(\tau)Z(\zeta) \quad (6)$$

One will obtain the following two ordinary differential equations

$$\frac{dT}{d\tau} = -b^2 T \quad (7)$$

$$(1 + \lambda \zeta) \frac{d^2 Z}{d\zeta^2} + \frac{(1 + \lambda \zeta)}{\zeta} \frac{dZ}{d\zeta} - \left( \frac{1 + \lambda \zeta + b^2 \zeta}{\zeta^2} \right) Z = 0 \quad (8)$$

where  $b^2$  is a constant or constants (eigenvalues). Equation (7) can be easily integrated to give the following solution

$$T = B e^{-b^2 \tau} \quad (9)$$

Equation (8) is solved by the method of Frobenius.<sup>3</sup> If one assumes that the solution is to be the form of following power series

$$Z = \sum_{j=0}^{\infty} A_j \zeta^{m+j} \quad (10)$$

then, substituting Equation (10) into Equation (8), one obtains

$$A_0(m^2 - 1)\zeta^{m-2} + [A_1\{(m+1)^2 - 1\} + A_0\lambda(m^2 - 1)]\zeta^{m-1} + \sum_{j=0}^{\infty} [A_{j+2}\{(m+j+2)^2 - 1\} + A_{j+1}\lambda\{(m+j+1)^2 - 1\} - A_j b^2]\zeta^{m+j} = 0 \quad (11)$$

In order to satisfy Equation (11), the following conditions must hold

$$A_0(m^2 - 1) = 0 \quad (12-a)$$

$$A_1\{(m+1)^2 - 1\} + A_0\lambda(m^2 - 1) = 0 \quad (12-b)$$

$$A_{j+2}\{(m+j+2)^2 - 1\} + A_{j+1}\lambda\{(m+j+1)^2 - 1\} - A_j b^2 = 0 \quad (12-c)$$

Inspection of Equation (12-a) shows that the coefficient  $A_0$  is the lowest coefficient in the summation and hence not zero, therefore from Equation (12-a) one obtains

$$m = \pm 1 \quad (13)$$

Then, from Equations (12-b) and (13),

$$A_1 = 0 \quad (14)$$

With  $m = 1$  and Equation (12-c) as a recurrence equation, one obtains

$$A_2 = \frac{b^2}{3^2 - 1} A_0 \quad (15-a)$$

$$A_3 = -\frac{A_2 \lambda (3^2 - 1)}{4^2 - 1} = -\frac{b^2 \lambda}{4^2 - 1} A_0 \quad (15-b)$$

$$A_4 = \frac{1}{5^2 - 1} [A_2 b^2 - A_3 \lambda (4^2 - 1)] = \frac{A_0 b^2}{5^2 - 1} \left( \frac{b^2}{3^2 - 1} + \lambda^2 \right) \quad (15-c)$$

$$A_5 = -\frac{A_0 b^2 \lambda}{6^2 - 1} \left( \frac{b^2}{4^2 - 1} + \frac{b^2}{3^2 - 1} + \lambda^2 \right) \quad (15-d)$$

$$A_6 = \frac{A_0 b^2}{7^2 - 1} \left[ \frac{b^2}{5^2 - 1} \left( \frac{b^2}{3^2 - 1} + \lambda^2 \right) + \left( \frac{b^2}{4^2 - 1} + \frac{b^2}{3^2 - 1} + \lambda^2 \right) \lambda^2 \right] \quad (15-e)$$

$$A_7 = -\frac{A_0 b^2 \lambda}{8^2 - 1} \left[ \frac{b^2}{6^2 - 1} \left( \frac{b^2}{4^2 - 1} + \frac{b^2}{3^2 - 1} + \lambda^2 \right) + \frac{b^2}{5^2 - 1} \left( \frac{b^2}{3^2 - 1} + \lambda^2 \right) + \left( \frac{b^2}{4^2 - 1} + \frac{b^2}{3^2 - 1} + \lambda^2 \right) \lambda^2 \right] \quad (15-f)$$



The Z-equation is in a divergent series after the fourth term. Thus, in order to have a finite value of Z, the series has to be terminated after some finite number of terms. In order to have  $A_{j+5} = 0$  at some finite  $j$ , there must exist the eigenvalues  $b_j^2$  such that

$$b_j^2 = \frac{A_{j+4}}{A_{j+3}} \lambda [(j+4)^2 - 1] \quad (21)$$

From Equation (21) the first few eigenvalues are as follows:

$$\begin{aligned} b_0^2 &= -8.0000\lambda^2 \\ b_1^2 &= -5.2174\lambda^2 \\ b_2^2 &= -4.2857\lambda^2 \\ b_3^2 &= -3.8182\lambda^2 \\ b_4^2 &= -3.5368\lambda^2 \\ b_5^2 &= -3.3488\lambda^2 \\ b_6^2 &= -3.2143\lambda^2 \end{aligned} \quad (22)$$

With the eigenvalues, the Z-equation should be written as follows:

$$Z = A \cdot \zeta \left[ 1 + \frac{b_0^2}{3^2 - 1} \zeta^2 - \frac{b_0^2 \lambda}{4^2 - 1} \zeta^3 + \frac{b_0^2}{5^2 - 1} \left( \frac{b_1^2}{3^2 - 1} + \lambda^2 \right) \zeta^4 - \frac{b_0^2 \lambda}{6^2 - 1} \left( \frac{b_2^2}{4^2 - 1} + \frac{b_1^2}{3^2 - 1} + \lambda^2 \right) \zeta^5 + \frac{b_0^2}{7^2 - 1} \left[ \frac{b_3^2}{5^2 - 1} \left( \frac{b_1^2}{3^2 - 1} + \lambda^2 \right) + \left( \frac{b_2^2}{4^2 - 1} + \frac{b_1^2}{3^2 - 1} + \lambda^2 \right) \lambda^2 \right] \zeta^6 - \frac{b_0^2 \lambda}{8^2 - 1} \left[ \frac{b_4^2}{6^2 - 1} \left( \frac{b_2^2}{4^2 - 1} + \frac{b_1^2}{3^2 - 1} + \lambda^2 \right) + \frac{b_3^2}{5^2 - 1} \left( \frac{b_1^2}{3^2 - 1} + \lambda^2 \right) + \left( \frac{b_2^2}{4^2 - 1} + \frac{b_1^2}{3^2 - 1} + \lambda^2 \right) \lambda^2 \right] \zeta^7 + \frac{b_0^2}{9^2 - 1} \left[ \frac{b_5^2}{7^2 - 1} \left\{ \frac{b_3^2}{5^2 - 1} \left( \frac{b_1^2}{3^2 - 1} + \lambda^2 \right) + \left( \frac{b_2^2}{4^2 - 1} + \frac{b_1^2}{3^2 - 1} + \lambda^2 \right) \lambda^2 \right\} + \left\{ \frac{b_4^2}{6^2 - 1} \left( \frac{b_2^2}{4^2 - 1} + \frac{b_1^2}{3^2 - 1} + \lambda^2 \right) \right\} \right]$$

$$\left[ + \frac{b_3^2}{5^2 - 1} \left( \frac{b_1^2}{3^2 - 1} + \lambda^2 \right) + \left( \frac{b_2^2}{4^2 - 1} + \frac{b_1^2}{3^2 - 1} + \lambda^2 \right) \lambda^2 \right] \zeta^8 + \dots \quad (23)$$

After simplification Equation (23) becomes:

$$Z = A \cdot \zeta \left[ 1 - \lambda^2 \zeta^2 + 0.53333\lambda^3 \zeta^3 - 0.1160\lambda^4 \zeta^4 + 0.0142\lambda^5 \zeta^5 - 0.0011\lambda^6 \zeta^6 + 0.00006\lambda^7 \zeta^7 - 0.00003\lambda^8 \zeta^8 + \dots \right] \quad (24)$$

Then, the tangential-component velocity,  $V_\theta$ , becomes

$$V_\theta = A \cdot \zeta \left[ e^{-b_0^2 \Delta \tau} - (\lambda^2 \zeta^2 - 0.53333\lambda^3 \zeta^3) e^{-b_1^2 \Delta \tau} - 0.1160\lambda^4 \zeta^4 e^{-b_2^2 \Delta \tau} + 0.0142\lambda^5 \zeta^5 \cdot e^{-b_3^2 \Delta \tau} - 0.0011\lambda^6 \zeta^6 \cdot e^{-b_4^2 \Delta \tau} + 0.00006\lambda^7 \zeta^7 e^{-b_5^2 \Delta \tau} - 0.00003\lambda^8 \zeta^8 e^{-b_6^2 \Delta \tau} + \dots \right] \quad (25)$$

The constant  $A$  in Equation (25) is determined from the boundary condition, Equation (4-b). Then the tangential-component velocity becomes

$$V_\theta = \Delta \Omega R (1 - e^{-\alpha/v_0 \Delta \tau}) \cdot \zeta \cdot \left[ 1 - (\lambda^2 \zeta^2 - 0.53333\lambda^3 \zeta^3) e^{(b_0^2 - b_1^2) \Delta \tau} - 0.1160\lambda^4 \zeta^4 e^{(b_0^2 - b_2^2) \Delta \tau} + 0.0142\lambda^5 \zeta^5 e^{(b_0^2 - b_3^2) \Delta \tau} - 0.0011\lambda^6 \zeta^6 e^{(b_0^2 - b_4^2) \Delta \tau} + 0.00006\lambda^7 \zeta^7 e^{(b_0^2 - b_5^2) \Delta \tau} - 0.00003\lambda^8 \zeta^8 e^{(b_0^2 - b_6^2) \Delta \tau} + \dots \right] \times \left[ 1 - (\lambda^2 - 0.53333\lambda^3) e^{(b_0^2 - b_2^2) \Delta \tau} - 0.1160\lambda^4 e^{(b_0^2 - b_2^2) \Delta \tau} + 0.0142\lambda^5 e^{(b_0^2 - b_3^2) \Delta \tau} - 0.0011\lambda^6 e^{(b_0^2 - b_3^2) \Delta \tau} + 0.00006\lambda^7 e^{(b_0^2 - b_3^2) \Delta \tau} - 0.00003\lambda^8 e^{(b_0^2 - b_3^2) \Delta \tau} + \dots \right] - 1 \quad (25-a)$$

The radial velocity,  $V_r$ , is related to the tangential-component velocity,  $V_\theta$ , by the sedimentation coefficient,  $s$ , in such a manner that

$$V_r = V_\theta \cdot s \quad (26)$$

therefore an expression for the radial velocity can be written as

$$V_r = \Delta \Omega R (1 - e^{-\alpha/v_0 \Delta \tau}) \cdot s \cdot \zeta \cdot \left[ 1 - (\lambda^2 \zeta^2 - 0.53333\lambda^3 \zeta^3) e^{(b_0^2 - b_2^2) \Delta \tau} - 0.1160\lambda^4 \zeta^4 e^{(b_0^2 - b_2^2) \Delta \tau} + 0.0142\lambda^5 \zeta^5 e^{(b_0^2 - b_3^2) \Delta \tau} \right]$$

$$\left[ \begin{array}{l} -0.0011\lambda^6 \zeta^6 e^{(b_0^2 - b_3^2)\Delta\tau} + 0.00006\lambda^7 \zeta^7 e^{(b_0^2 - b_3^2)\Delta\tau} \\ -0.0003\lambda^8 \zeta^8 e^{(b_0^2 - b_3^2)\Delta\tau} + \dots \end{array} \right] \quad (26-a)$$

$$\left[ \begin{array}{l} 1 - (\lambda^2 - 0.5333\lambda^3) e^{(b_0^2 - b_2^2)\Delta\tau} - 0.1160\lambda^4 e^{(b_0^2 - b_2^2)\Delta\tau} - 1 \\ + 0.0142\lambda^5 e^{(b_0^2 - b_2^2)\Delta\tau} - 0.0011\lambda^6 e^{(b_0^2 - b_2^2)\Delta\tau} \\ + 0.00006\lambda^7 e^{(b_0^2 - b_2^2)\Delta\tau} - 0.00003\lambda^8 e^{(b_0^2 - b_2^2)\Delta\tau} \\ + \dots \end{array} \right]$$

### Shear Stress Distributions

The shear stress distributions  $\tau_{r\theta}(r)$  and  $\tau_{rr}(r)$  now may be obtained by the velocity distributions. The tangential shear stress distribution,  $\tau_{r\theta}(\zeta)$  is given as<sup>1</sup>

$$\begin{aligned} \tau_{r\theta} = \tau_{\theta r} &= -\mu \left[ r \frac{\partial}{\partial r} \left( \frac{V_{\theta}}{r} \right) \right] \\ &= -\frac{\mu_0}{R} (1 + \delta\zeta) \cdot \zeta \frac{\partial}{\partial \zeta} \left( \frac{V_{\theta}}{\zeta} \right) \end{aligned} \quad (27)$$

After differentiation the reduced tangential shear stress distribution may be expressed as follows

$$\frac{\tau_{r\theta}}{\Delta\Omega\mu_0} = (1 + \delta\zeta)(1 - e^{-\alpha/\nu_0\Delta\tau}) \cdot \left[ \begin{array}{l} (2\lambda^2\zeta^2 - 1.5999\lambda^3\zeta^3) e^{-2.7826\lambda^2\Delta\tau} \\ - 0.4640\lambda^4\zeta^4 e^{-3.7143\lambda^2\Delta\tau} \\ - 0.0710\lambda^5\zeta^5 e^{-4.1818\lambda^2\Delta\tau} \\ + 0.0066\lambda^6\zeta^6 e^{-4.4632\lambda^2\Delta\tau} \\ - 0.000042\lambda^7\zeta^7 e^{-4.6512\lambda^2\Delta\tau} \\ + 0.00024\lambda^8\zeta^8 e^{-4.7857\lambda^2\Delta\tau} \\ + \dots \end{array} \right] \quad (28)$$

$$\left[ \begin{array}{l} 1 - (\lambda^2 - 0.5333\lambda^3) e^{-2.7826\lambda^2\Delta\tau} - 1 \\ - 0.1160\lambda^4 e^{-3.7143\lambda^2\Delta\tau} \\ + 0.0142\lambda^5 e^{-4.1818\lambda^2\Delta\tau} \\ - 0.0011\lambda^6 e^{-4.4632\lambda^2\Delta\tau} \\ + 0.00006\lambda^7 e^{-4.6512\lambda^2\Delta\tau} \\ - 0.00003\lambda^8 e^{-4.7857\lambda^2\Delta\tau} \\ + \dots \end{array} \right]$$

In a similar manner, the radial shear stress distribution,  $\tau_{rr}(r)$  may be obtained. It is given by<sup>1</sup>

$$\tau_{rr} = -\mu \left[ 2 \frac{\partial V_r}{\partial r} \right] = \frac{-\mu_0(1 + \delta\zeta)}{R} \cdot 2 \frac{\partial V_r}{\partial \zeta} \quad (29)$$

Finally the reduced radial stress distribution is

$$\frac{\tau_{rr}}{2\Delta\Omega\mu_0 s} = (1 + \delta\zeta)(1 - e^{-\alpha/\nu_0\Delta\tau}) \left[ \begin{array}{l} 1 - (3\lambda^2\zeta^2 - 2.1332\lambda^3\zeta^3) e^{-2.7826\lambda^2\Delta\tau} \\ - 0.5800\lambda^4\zeta^4 e^{-3.7143\lambda^2\Delta\tau} \\ + 0.0852\lambda^5\zeta^5 e^{-4.1818\lambda^2\Delta\tau} \\ - 0.0077\lambda^6\zeta^6 e^{-4.1818\lambda^2\Delta\tau} \\ + 0.00048\lambda^7\zeta^7 e^{-4.4632\lambda^2\Delta\tau} \\ - 0.00027\lambda^8\zeta^8 e^{-4.7857\lambda^2\Delta\tau} + \dots \end{array} \right] - 1 \quad (29-a)$$

Typical tangential-component velocity profiles and shear stress distributions in B-XIV zonal centrifuge rotors with a fluid of linear density gradient are illustrated in Figures 2.19 and 2.20 for the sucrose density gradient changing from 10% to 30% in the direction of increasing distance from its own axis. For this case  $\lambda = 1.45$  and  $\delta = 1.66$ , and no septa is present.

### REFERENCES

- <sup>1</sup>R. B. Bird, W. E. Stewart, and E. N. Lightfoot, *Transport Phenomena*, McGraw-Hill Book Co., pp. 84-89, 96-98 (1960).
- <sup>2</sup>H. Margenau, and G. M. Murphy, *The Mathematics of Physics and Chemistry*, Van Nostrand, pp. 59-68 (1955).
- <sup>3</sup>C. R. Wylie, Jr., *Advanced Engineering Mathematics*, McGraw-Hill Book Co., pp. 251-255 (1951).

### Nomenclature

- $a$  time constant
- $A_j$  coefficients of power series
- $b^2$  characteristic constants (eigenvalues)
- $B$  constant
- $m$  characteristic values in the indicial equation
- $r$  radius variable
- $R$  radius
- $s$  sedimentation coefficient
- $t$  time
- $T$  function of  $t$  or  $\tau$
- $V_r$  radial velocity component
- $V_{\theta}$  tangential velocity component

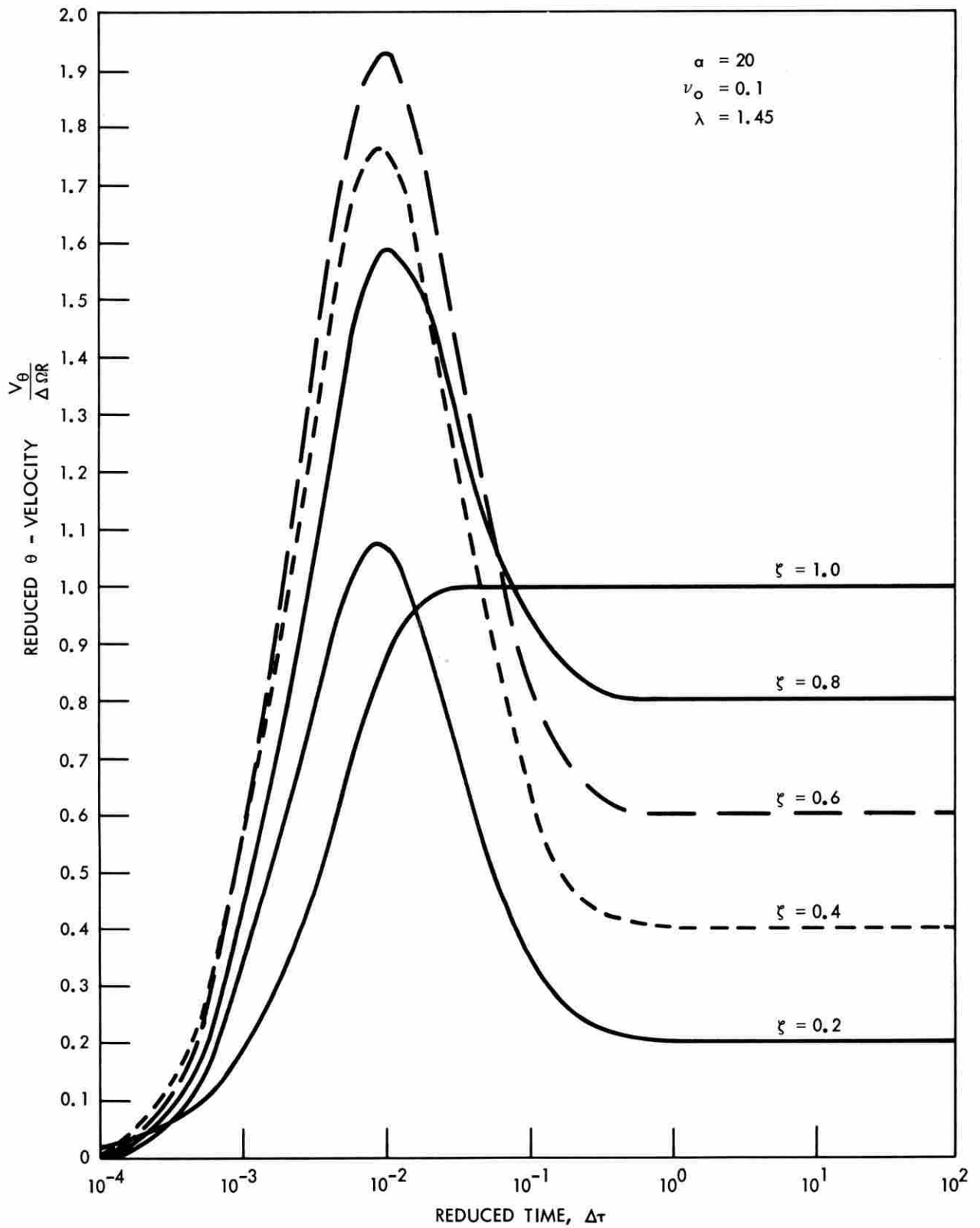


Fig. 2.19 The tangential-component velocity distribution in a centrifuge rotor.

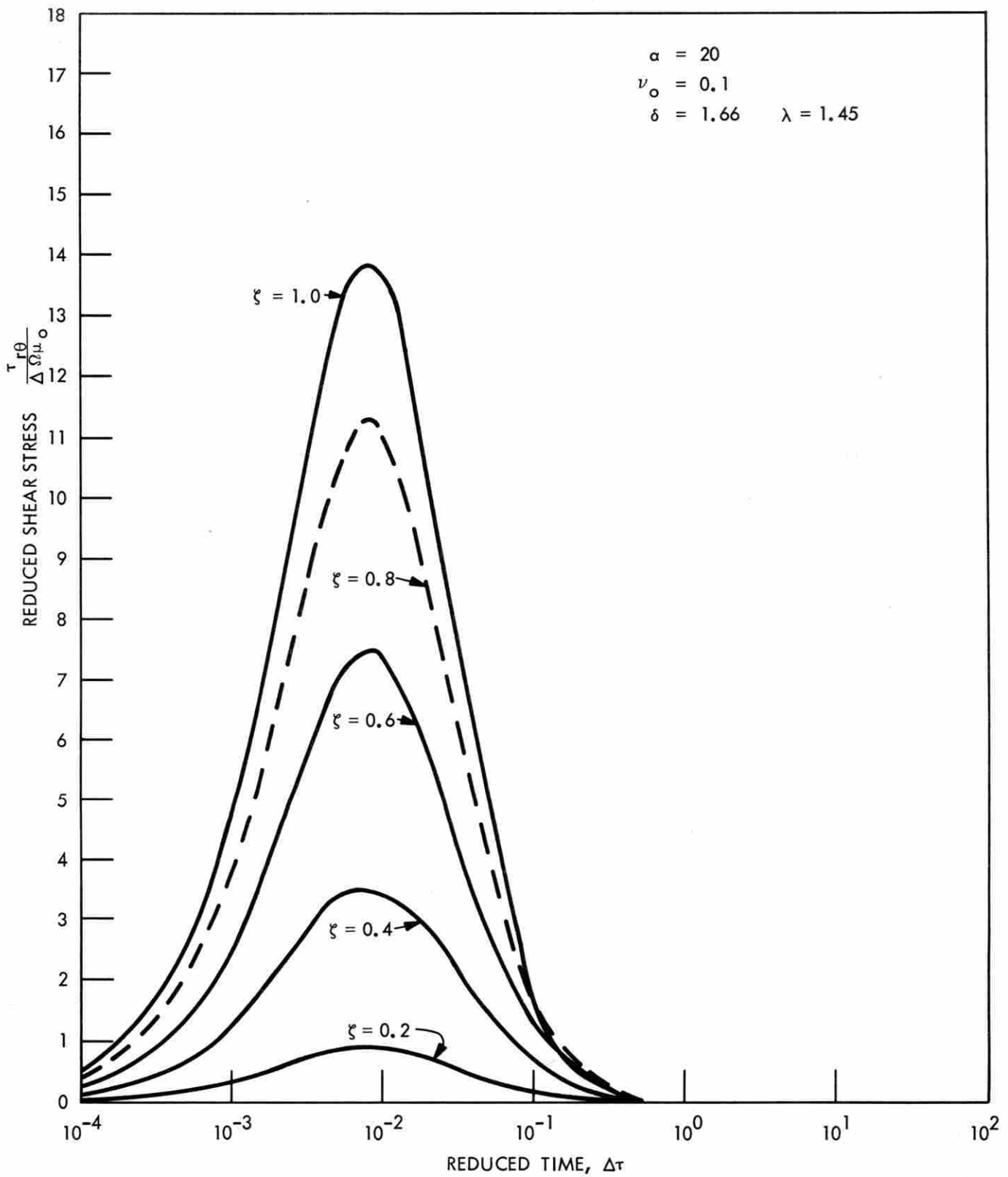


Fig. 2.20 The tangential shear stress distribution in a centrifuge rotor.

$V_z$	axial velocity component
$Z$	function of radius variable
$\alpha$	constant defined in Equation (5-d)
$\rho$	density
$\mu$	dynamic viscosity
$\nu$	kinematic viscosity $\nu = \mu/\rho$
$\tau$	reduced time $\tau = \nu t/R^2$
$\zeta$	reduced radius variable $\zeta = r/R$
$\Omega$	angular velocity
$\tau_{ij}$	shear stress tensor
$\epsilon$	characteristic constant for kinematic viscosity variation
$\lambda$	characteristic constant for kinematic viscosity variation in rotor $\lambda = \epsilon R$
$\delta$	characteristic constant for dynamic viscosity variation in rotor

#### Subscripts

0	quantity evaluated at reference condition
1, 2, 3,	indices of the coefficient
$r$	radius direction
$\theta$	angular direction
$j$	summation index

### C. MULTIPLE GRADIENT-DISTRIBUTING ROTOR (B-XXI)

E. L. Candler                      C. E. Nunley  
N. G. Anderson

The use of angle-head centrifuges for high-speed isopycnic banding of nucleic acids,<sup>1,2</sup> viruses,<sup>1,3</sup> and subcellular components including microsomes and glycogen<sup>3,4</sup> offers the possibility of banding as many as 12 samples in one rotor. With rapidly diffusing materials such as cesium chloride, relatively steep gradients may be formed in a short time by diffusion.<sup>3</sup> However, if slowly diffusing substances such as sucrose, potassium citrate or tartrate, dextran or serum albumin are to be used, or if very shallow gradients are required, then simple diffusion between two layers may require a prohibitively long period of time.

In previous studies,<sup>5</sup> a distributor head was used to distribute one gradient evenly among several swinging-bucket tubes during rotation. In this study we describe a distributor rotor (designated B-XXI) which apportions a single liquid gradient uniformly among 12 Oak Ridge No. 30 polycarbonate tubes (6) during rotation at 2000 rpm. The technique is useful

when a particle suspension or homogenate is to be subdivided on the basis of sedimentation rate into a number of fractions, each one of which is to be further fractionated by isopycnic zonal centrifugation by the so-called "s- $\rho$ " method.<sup>3</sup>

#### Principle of Operation

A liquid stream flowing into a spinning cup will be evenly divided between a series of equally-spaced apertures as it flows out of the cup under centrifugal force. By connecting the apertures to a series of angle-head centrifuge tubes, a single density gradient may be *apportioned* equally among them.

The gradient distributor rotor consists of a standard Beckman No. 30 preparative angle-head rotor with the distributor head securely attached by the radiation handle. The central gradient-receiving annular groove connects through 12 evenly-spaced delivery spouts into the openings of the polycarbonate tubes (Figure 2.21).

The tubes are loaded while the rotor is spinning at 2000 rpm in a Model L preparative ultracentrifuge. The gradient (150–300 ml) is introduced as a continuous stream, beginning with the densest portion of the gradient, in a period of 5 min or less. The gradient may be made previously by any one of a variety of methods and stored in a vertical cylinder drained through the bottom. The entire assembly is shown in Figure 2.22 with the nozzle of the gradient feed line properly positioned in the gradient-receiving ring of the B-XXI proportioning rotor.

#### Results

To test the uniformity of the gradient distribution, three separate density gradient solutions—cesium chloride, potassium citrate, and sucrose—were used. Each had a total volume of 240 ml. A 5-ml overlay of a dilute rat-liver homogenate was added by hand to the 20-ml gradient in each tube. These were spun at 24,000 rpm in a preparative ultracentrifuge for 1 hr or less. If the gradient solutions had distributed equally among 12 tubes of each set, the subcellular particles should band in the same position in all the tubes of each set. At the end of centrifugation, each set of 12 tubes was photographed in a special banding camera.<sup>6</sup>

As shown in Figure 2.23, the even alignment of the rat-liver bands indicates the reproducibility of the gradient in sets of tubes. In Figure 2.23A, the cesium chloride density gradient extended from 1.10 to 1.82

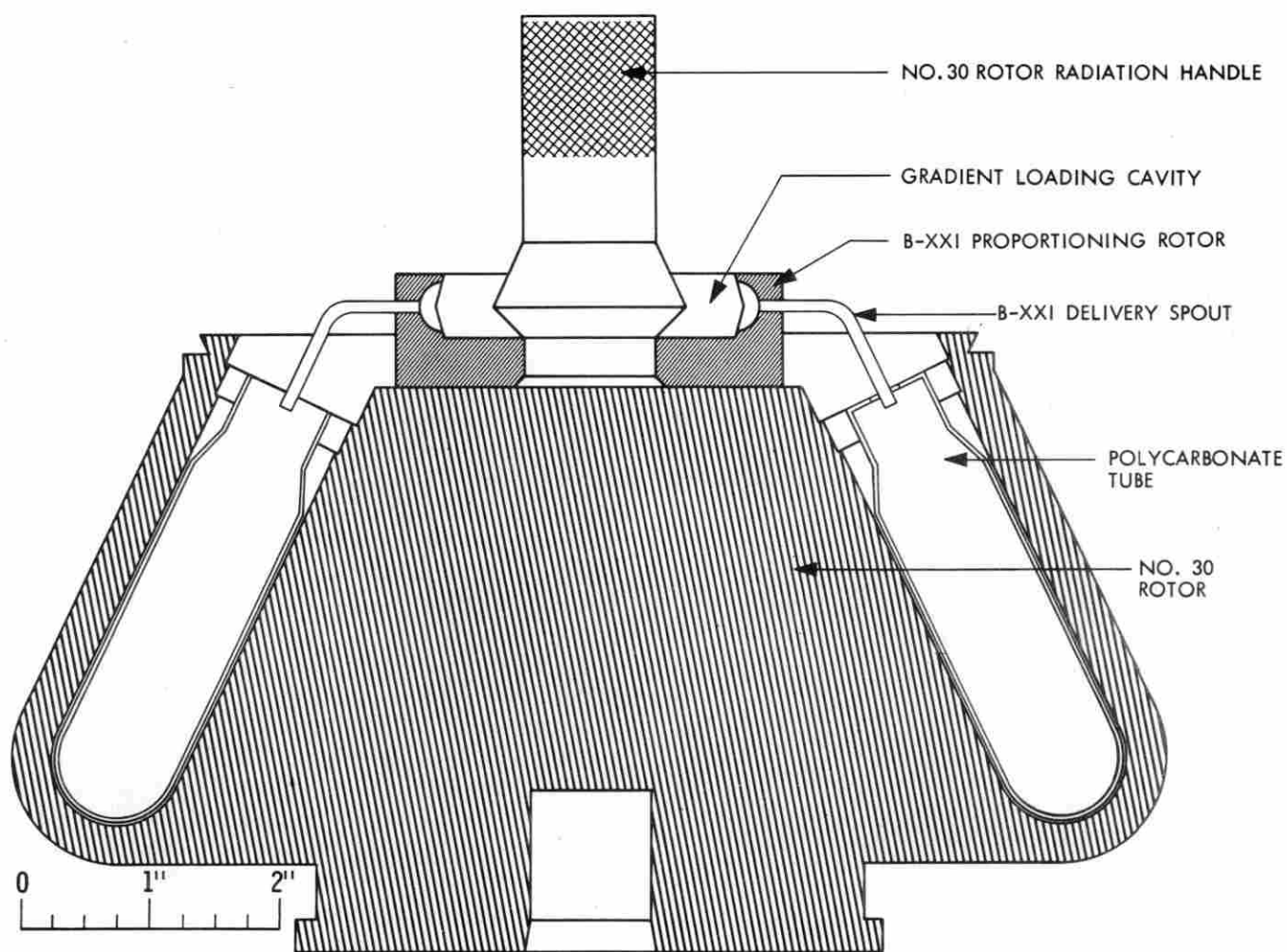


Fig. 2.21 Multiple gradient-distributing assembly. The diagram shows the combination of the B-XXI proportioning rotor and a standard Beckman No. 30 preparative angle-head rotor. The gradient solution is fed into the gradient loading cavity in the B-XXI rotor where it is distributed to the tubes in the No. 30 rotor through the delivery spouts by centrifugal force. To scale.

gm/ml. After 30 min at 24,000 rpm, two distinct bands are observed, the lower being glycogen<sup>4</sup> at density 1.62, the upper being largely cell membranes and mitochondria. Figure 2.23B depicts the banding pattern of the rat liver centrifuged in 1 hr in a potassium citrate gradient which ranged in density from 1.10 to 1.51 gm/ml. Figure 2.23C shows the alignment of the particulate bands in a sucrose gradient. The tubes were centrifuged for 1 hr, and the density of the gradient in this instance extended from 1.13 to 1.26 gm/ml. The potassium citrate gradient and the sucrose gradient were not sufficiently dense to allow glycogen to band.

#### Discussion

The even alignment of the rat-liver bands in the three sets of tubes demonstrates that the gradient distributor rotor is capable of distributing a gradient solution equally among 12 tubes. The banding pattern of the rat liver in these tubes is not the same pattern that would be observed had the tubes been centrifuged longer. The centrifugation time was purposely kept short to show that the gradients were produced by even distribution of the gradient material and not by simple diffusion.

The greatest advantage of the gradient-distributing rotor is that gradients can be prepared in a very short

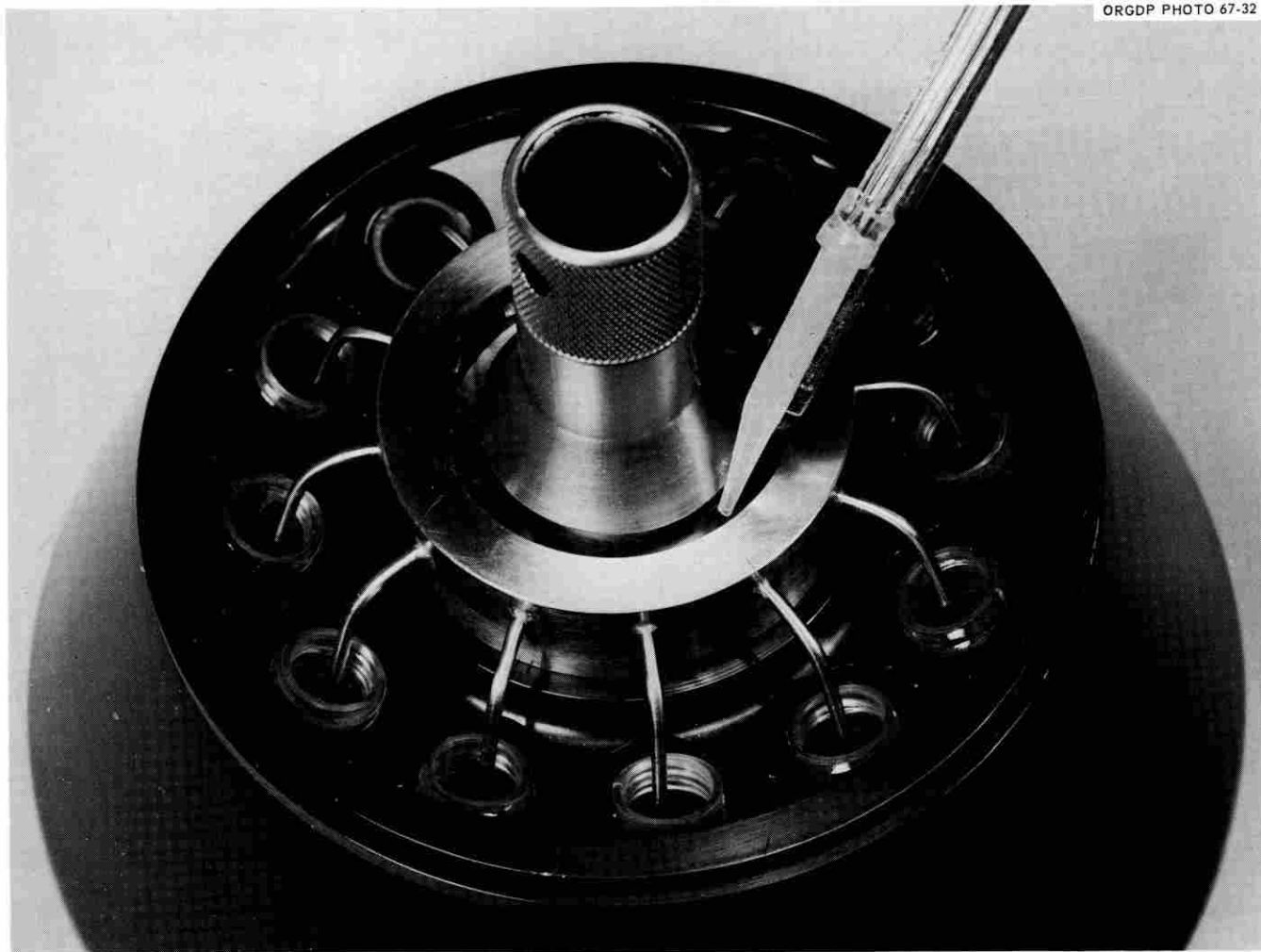


Fig. 2.22 The gradient-distributing assembly with the gradient feed line in position.

time. Gradients of the three different solutions used for this study were prepared in less than 30 min, or about 10 min for each set of 12 tubes.

If the gradient solution is fed to the distributor rotor properly, there should be less than 1 ml variation in the volumes of the gradient in any two tubes in the rotor. Good distribution of the gradient solution can be achieved only if the gradient solution is fed to the rotor in an uninterrupted stream which has a constant flow rate. Any sudden change in the flow rate of the gradient solution during loading will cause a few tubes to be overloaded. The rotational speed of the rotor during loading is also very important for equal distribution. At speeds below 2000 rpm

the No. 30 rotor is unstable, and unequal gradient distribution occurs.

In the  $s\text{-}\rho$  technique, subcellular particles are separated first on the basis of sedimentation rate in a zonal centrifuge. Each of the recovered fractions is then banded isopycally in angle-head rotors. In previous studies, relatively steep diffusion-formed gradients were used. The B-XXI distributor head now allows shallow gradients to be made in which a much higher resolution separation of endoplasmic reticulum fragments, cell membranes, and viruses is possible. Experimental studies with this system will be described elsewhere.

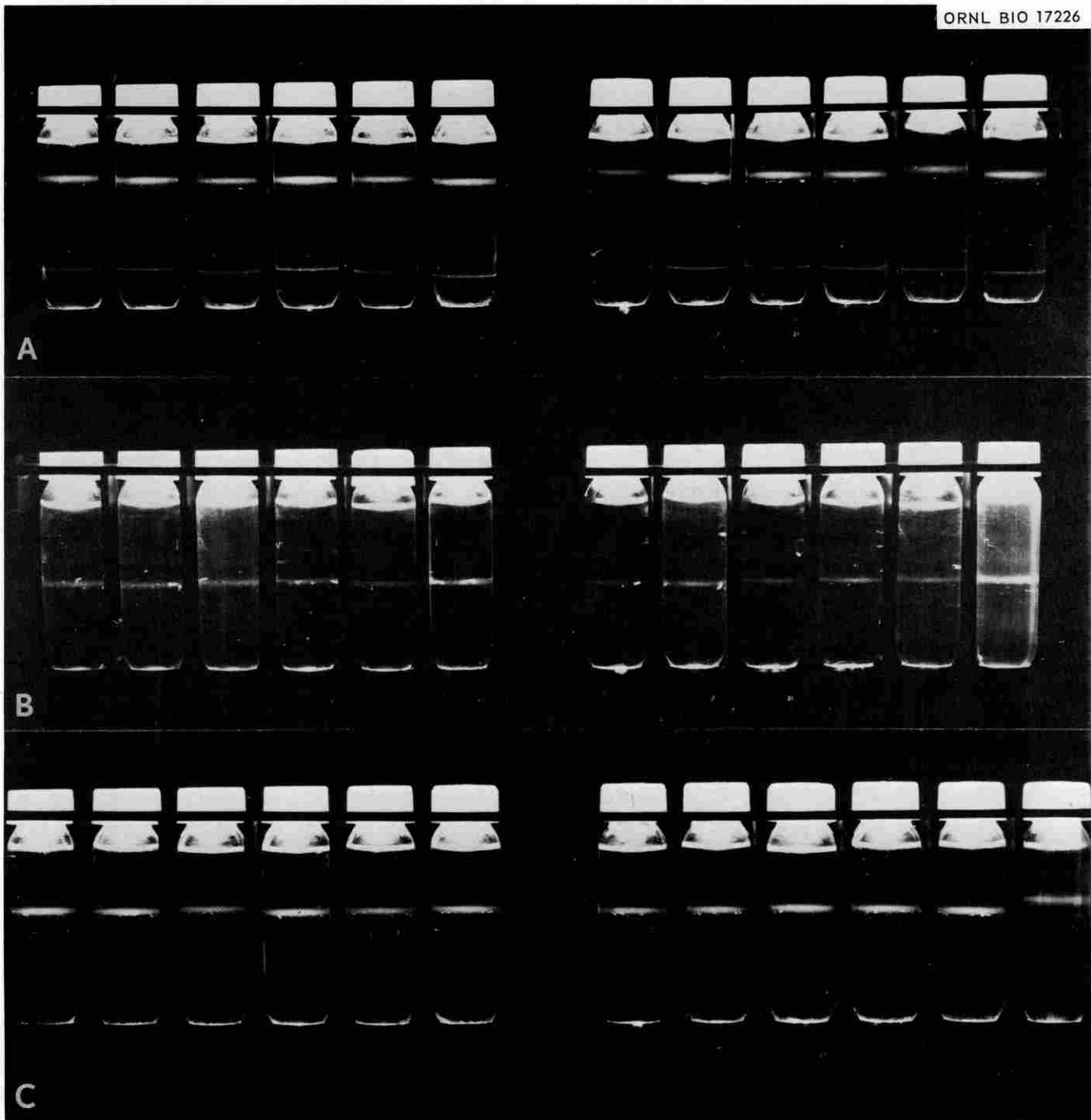


Fig. 2.23 Rat liver banded in gradients prepared with the gradient-distributing device. The bands were photographed by scattered light. The even alignment of the bands in each set of tubes serves to indicate the reproducibility of the gradients. (A) Rat liver banded in a cesium chloride gradient; (B) Rat liver banded in a potassium citrate gradient; (C) Rat liver banded in a sucrose gradient.

#### Summary

Identical liquid density gradients required for  $s\text{-}\rho$  separations have been prepared in 12 angle-head

rotor tubes in less than 10 min by a spinning distributor rotor. The technique is especially useful for the preparation of gradients with materials that would

take too long to establish gradients by simple diffusion, such as sucrose or potassium citrate.

#### REFERENCES

- <sup>1</sup>W. D. Fisher, G. B. Cline, and N. G. Anderson, *Anal. Biochem.* **9**, 477 (1964).
- <sup>2</sup>W. G. Flamm, H. E. Bond, and H. E. Burr, *Biochim. Biophys. Acta* **129**, 310 (1966).
- <sup>3</sup>N. G. Anderson, W. W. Harris, A. A. Barber, C. T. Rankin, Jr., and E. L. Candler, (N. G. Anderson, ed.), *J. Natl. Cancer Inst. Monograph* **21**, 253 (1966).
- <sup>4</sup>A. A. Barber, W. W. Harris, and N. G. Anderson, (N. G. Anderson, ed.), *J. Natl. Cancer Inst. Monograph* **21**, 285 (1966).
- <sup>5</sup>J. F. Albright, and N. G. Anderson, *Exptl. Cell. Res.* **15**, 217 (1958).
- <sup>6</sup>N. Cho, H. P. Barringer, J. W. Amburgey, G. B. Cline, N. G. Anderson, L. L. McCauley, R. H. Stevens, and W. M. Swartout, (N. G. Anderson, ed.), *J. Natl. Cancer Inst. Monograph* **21**, 485 (1966).

#### D. A SIMPLE GRADIENT-FORMING APPARATUS

N. G. Anderson                      E. Rutenberg

For rate-zonal centrifugation in zonal centrifuge rotors, smooth gradients of large volume are required. In most instances the shape of the gradient in the rotor should be convex, i.e., the rate of change of concentration should decrease with radius.<sup>1</sup> This follows from the following: (a) the capacity of a gradient increases as the difference between the particle and the solvent density decreases; therefore, to obtain identical particle capacity at all levels, the steepness of the gradient may be decreased at higher densities. (b) Greatest particle capacity is required just below the sample zone to support the particle population before it becomes widely spread throughout the gradient. (c) Radial dilution and diffusion combine to diminish the particle concentration in a zone as it sediments, thus diminishing the steepness of the gradient required to support it. In addition, since the gradients are spun in sector-shaped compartments, the gradient must be convex in a concentration vs volume plot even when the gradient is to be linear-with-radius in the rotor.

These considerations suggest that a simple exponential gradient-making device that uses a constant-volume mixing chamber could be adapted to zonal centrifuge rotor loading.

##### Construction of Gradient Device

A convex gradient may be made by introducing a dense solution into a constant volume mixer which initially contains a dilute solution corresponding to

the light end of the gradient, and by withdrawing a stream from the mixing chamber continuously. The concentration of the stream withdrawn at any given time<sup>2-4</sup> is given by the equation:

$$C_t = C_2 - (C_2 - C_1)e^{-v_t/v_1}$$

where  $C_t$  is the concentration at time  $t$ ,  $C_2$  is the concentration of the denser solution,  $C_1$  is the concentration of the light solution originally in the mixer,  $v_1$  = the volume of the mixer, and  $v_t$  = the volume withdrawn to time  $t$ . If the mixer concentration is taken to be zero, and the concentration of the dense solution is set equal to one, then the equation reduces to

$$C_t = 1 - \frac{1}{e^{v_t/v_1}}$$

and  $C_t$  is in terms of the fraction of the denser fluid found in the lighter. This equation assumes that the contents of the mixer are homogeneous and that the rate of mixing is rapid relative to the rate of fluid withdrawal. When viscous sucrose solutions are being used, considerable energy must be expended to satisfy this requirement, and magnetic mixers or propeller stirrers have not been found adequate.

A small centrifugal pump<sup>3</sup> connected to a conical reservoir by very large tubing as shown in Figure 2.24 has therefore been used.

The mixing flask was constructed from a heavy-walled suction flask with one-half-inch openings to the pump. Dense solution is introduced into the line leading from the flask to the pump. Initial mixing therefore occurs in the impeller chamber of the pump. The fluid then flows rapidly back to the mixing chamber through a tangentially-attached tube to produce maximum spinning of the mixing chamber contents. Any unmixed dense solution tends to be centrifuged to the lower peripheral portion of the flask where it would mix with the incoming stream. Outflow is from a point at the vertex of the mixing chamber cone to insure that only fluid equal in density to, or very slightly lighter than the bulk of the fluid is removed. In addition, air bubbles may be removed initially through the delivery (to rotor) line. Mixing in the chamber should be so fast that a tiny air bubble will be drawn out to form a very fine line extending almost the full length of the flask.

##### Performance

The theoretical curves for mixers of various sizes are shown in Figure 2.25. It is evident that nearly linear gradients can be produced if only the very first

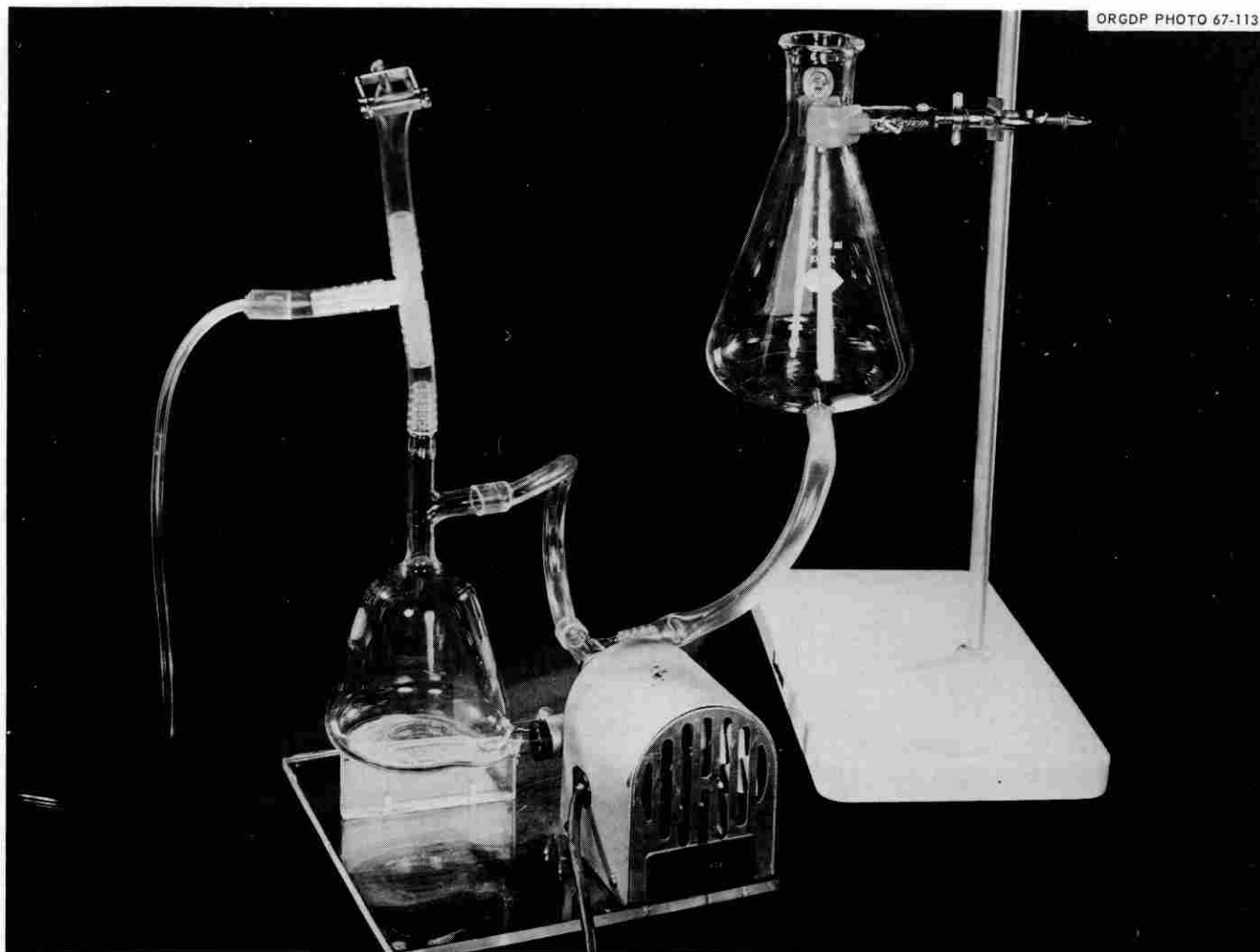


Fig. 2.24 Gradient mixer with (A) mixing chamber, (B) centrifugal pump, and (C) reservoir for dense gradient solution. Initially, the mixing chamber and the centrifugal pump are filled with the solution used for the light end of the gradient. As fluid is removed through line leading to rotor, an equal volume of dense fluid flows into the gradient mixer.

portion of the gradient is used. Note that the volume of the mixer includes the volume of solution in the conical reservoir, in the pump, and in the lines connecting the two. A number of mixers were tested by measuring the sucrose concentration as delivered by the pump, and as recovered from a B-XV zonal rotor.<sup>5</sup> Theoretical and experimental curves obtained are shown in Figure 2.26 for a 668 ml mixer. Only very small departures from the predicted curves were seen when gradients prepared from 20% and 60% (w/w) sucrose were used. Higher concentrations will require the use of heavier pumps than have been used

here. When the sample volume plus the overlay equals 200 ml, 1460 ml remain for the gradient in the B-XV rotor.<sup>5</sup> By using a 668-ml gradient mixer, the fraction of the dense solution in the less dense when the rotor was full would be 0.89. Thus, if the gradient were constructed from 20% and 60% sucrose, the gradient in the rotor would actually extend from 20% to 55.6% (w/w) sucrose. If necessary a dense underlay can be used to make the very end of the gradient steeper.

#### Shape of Gradient in Rotor

The relationship between volume and radius in a

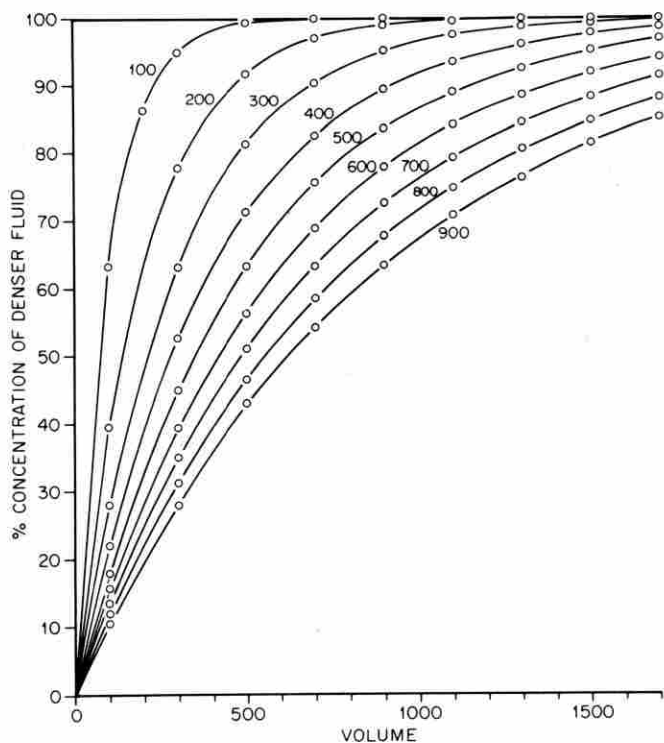


Fig. 2.25 Calculated plots showing gradients produced by mixers having different total volumes. Concentration is given as percent of heavier solution in the lighter one. Volume is in ml.

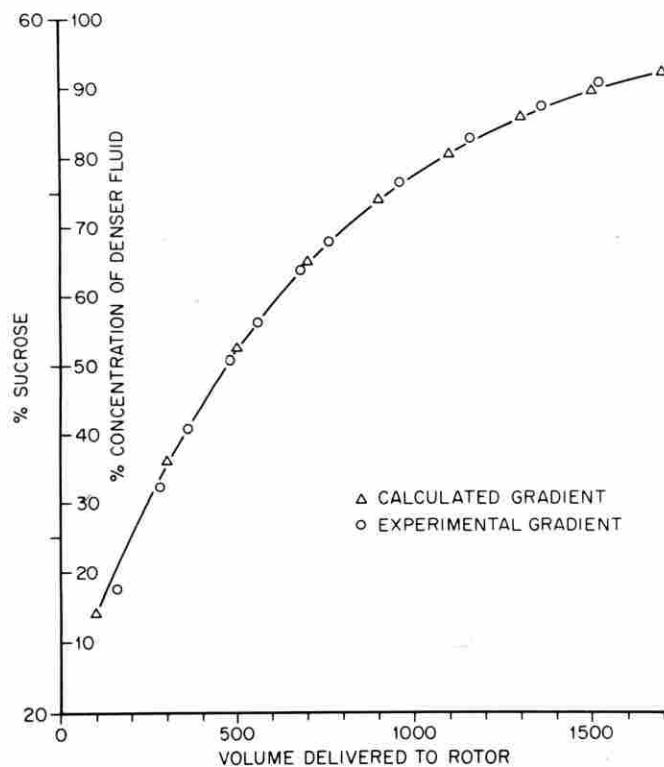


Fig. 2.26 Theoretical and experimental plots for a mixer having a total volume of 668 ml. Volume is in ml.

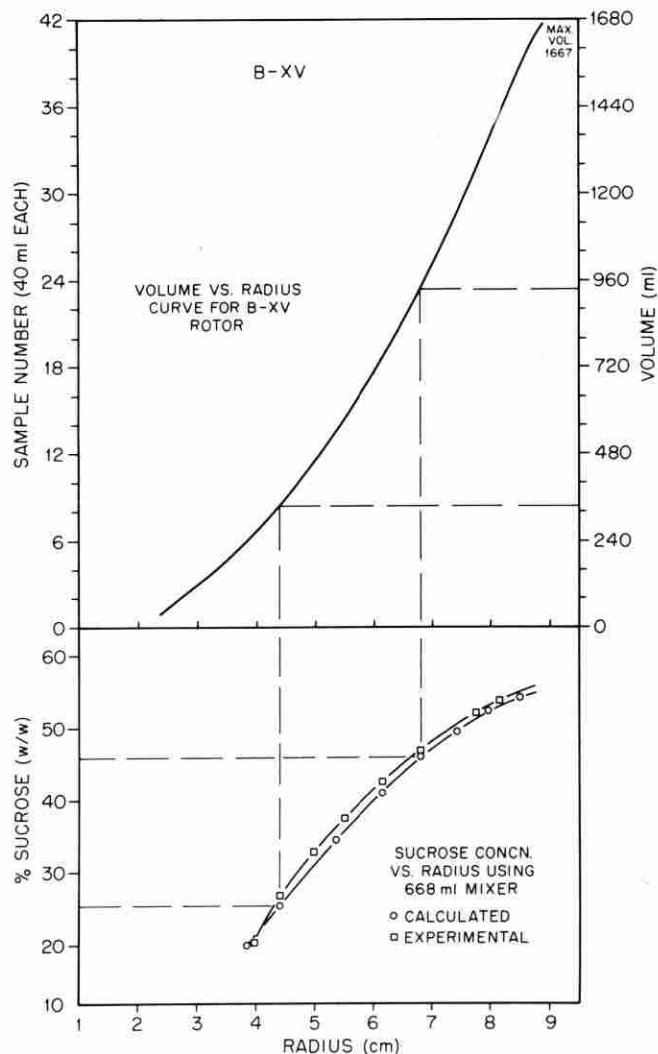


Fig. 2.27 Method for plotting shape of gradient in rotor. Upper plot relates volume to radius in B-XV rotor. Data on concentration vs. volume for a gradient mixer are plotted in the lower part of the figure as follows: The radius for a particular volume is found by locating the volume on the upper right-hand scale and then drawing a horizontal line to intersect the rotor volume-vs.-radius curve. A vertical line is dropped from this intersection to intersect a horizontal line indicating the sucrose concentration at that volume (or radius). In this experiment the gradient was formed from 20 and 60% (w/w) sucrose.

zonal rotor is a complex one since the chambers are only approximately sector-shaped due to the shape of the vanes attached to the core, and the curvature of the chambers near the edge. A plot of volume as a function of radius for the B-XV rotor is shown in Figure 2.27 (upper curve). In the lower portion of the diagram, the curve relating radius to concentration for a 668-ml mixer is given. The vertical and

horizontal lines allow concentration to be related to rotor radius in a simple graphical manner. The plot given assumes a 40-ml sample and a 200-ml overlay. An actual experimental plot is also included which was made by loading the B-XV rotor at 2500 rpm, inserting an overlay of distilled water, and then recovering the gradient by displacement. Good agreement between the theoretical and experimental plots was obtained.

Very little pressure is required to load B-XV zonal rotors, provided flow into the rotor is started at about 1000 rpm. Near the end of the loading period, additional pressure may be required. This may be produced by either raising the reservoir for dense sucrose or by using low pressure air to pressurize the reservoir.

## REFERENCES

- <sup>1</sup>N. G. Anderson, *J. Natl. Cancer Inst. Monograph* **21**, 9 (1966).
- <sup>2</sup>R. M. Bock, and N. Ling, *Anal. Chem.* **26**, 1543 (1954).
- <sup>3</sup>H. Svensson, *Sci. Tools* **5**, 37 (1958).
- <sup>4</sup>H. Busch, R. B. Hurlbert, and V. R. Potter, *J. Biol. Chem.* **196**, 717 (1952).
- <sup>5</sup>N. G. Anderson, and D. A. Waters, *Federation Proc.* **25**, 421 (1966).

## E. SEDIMENTATION COEFFICIENTS IN ZONAL CENTRIFUGES

Barbara S. Bishop

Elizabeth L. Rutenburg

The Zonal Centrifuge process for separating biological particles by centrifugation of a suspending medium and a biological sample results in the separated particles being recovered in sample tubes which represent equal fractional parts of the original volume. It is of interest to calculate a Sedimentation Coefficient which indicates the distance an ideal particle has travelled in the given suspending medium for a definite period of time. Since the manual calculations are laborious, a computer program, using the FORTRAN IV programming language, has been developed to calculate the sedimentation coefficients of particles of a given size and density at 20°C in water for each fractional part recovered. The program has undergone a number of revisions, and has been presented in outline form in previous reports. The program described here includes the most recent modifications. We use the following equation:

$$S_{i,20,w}^* = \frac{\rho_p - \rho_{20,w}}{\omega^2 t \eta_{20,w}} \sum_{R_s}^{R_i} \frac{\eta_{T,m,f_i}}{(\rho_p) - (\rho_{T,m,f_i})(R_i + R_{i-1})/2} (R_i - R_{i-1})$$

where:

- $S_{i,20,w}^*$  = Ideal sedimentation coefficient at 20°C in water in Svedberg units for a given fraction.  
 $\rho_p$  = Assumed particle density.  
 $\rho_{20,w}$  = Density of water at 20°C.  
 $\omega$  =  $2\pi \text{rpm}/60$  (rpm is the operating speed of the rotor in revolutions per minute).  
 $t$  = Time in seconds of effective centrifugation.  
 $\eta_{20,w}$  = Viscosity of water at 20°C.  
 $\eta_{T,m,f_i}$  = Viscosity of suspending medium ( $m$ ) at the temperature ( $T$ ) for a given fraction ( $f_i$ ).  
 $\rho_{T,m,f_i}$  = Density of suspending medium ( $m$ ) at temperature ( $T$ ) for a given fraction ( $f_i$ ).  
 $R_i$  = Radius at end of given fraction.  
 $R_{i-1}$  = Radius at beginning of given fraction.

The derivation of the above equation may be found in the article entitled "Digital Computation of Sedimentation Coefficients in Zonal Centrifuges" in *National Cancer Institute Monograph No. 21*, page 175.

At present, the program contains the equations for calculating the viscosity and density for only one suspending medium, sucrose; however, provisions have been made to add eight other media when the viscosity and density equations are available. The sucrose equations were developed from standard viscosity and density tables by Dr. E. J. Barber of the Technical Division of the Oak Ridge Gaseous Diffusion Plant.

The radii are calculated from the center of the rotor, thus, the term  $R_i - R_{i-1}$  calculates a torodial section of the rotor for the fractional part,  $f_i$ . The term  $(R_i + R_{i-1})/2$  is included to calculate the radius for the center of each fraction. The volumes for the various rotors are calculated using the incremental cut, or fractional volume, entered as part of the input data. Since the configuration differs for each rotor, the radius calculations differ for each rotor. The equations for the B-II, B-IV, B-XIV, B-XV and C-III rotors are included in the program.

The  $\omega^2 t$  term is obtained from an automatic integrator as an average value for the centrifuge run and includes the acceleration and deceleration time and time at speed.

In one mode of operation the entire contents of the rotor is collected in sample tubes of equal volume. In a second mode of operation, only part of the rotor effluent is collected, the rest being diverted at a known and constant rate to an automated analytical system for either chemical or enzymatic analysis. In the second case, the time required to fill each fraction collector

tube (cut) is recorded and entered as part of the input data to the program.

### Data Input

The data required for one centrifuge run is entered with an identification card as the first data card and a variable number of cut cards, each of which contains the sucrose concentration and cut time, if applicable, for each fraction or cut.

Identification Card		
Card Col.	Fortran Format	Date Description
1-4	I4	Run number (numeric right adjusted)
5-8	I4	Experiment number (numeric right adjusted)
9-14	A6	Month
15-16	I2	Day
17-18	I2	Year (last two digits)
19-24	A6	Rotor identification (alphanumeric)
25-26	I2	Rotor Code (numeric)
27-29	I3	Temperature, °C
30-33	F4.3	Auxiliary pump rate (ml/min)
34-43	F10.4	$\omega^2 t \times 10^{-6}$ (centrifuge force)
44-47	F4.1	Overlay volume (ml)
48-51	F4.1	Cut volume (ml)
52-54	F3.0	Sample volume (ml)
55	I1	Density code (homogeneous - 1 heterogeneous - 2)
56-58	F3.0	Line volume (ml)
59-62	F4.3	Assumed particle density No. 1
63-66	F4.3	Assumed particle density No. 2
67-70	F4.3	Assumed particle density No. 3
71-74	F4.3	Assumed particle density No. 4
75	I1	Solution code (sucrose, 1)
76	I1	Plot number 1 control
77	I1	Plot number 2 control

\*For plotting purposes the densities should be entered in ascending order.

The rotor codes in the above list are used to identify the various rotors for radius calculations and are listed as following:

Rotor Code	Rotor
1	B-II
2	B-IV
3	C-III
4	B-XIV
5	B-XV

The plot controls in columns 76 and 77 are used only if an automatic plotting system is available. The controls are set to a positive value (usually 1) if plots are desired. Plot number 1 plots  $S_{i,20,w}^*$  versus tube or cut number for each assumed particle density. Plot number 2 plots the assumed particle density versus cut or tube number for an extrapolated even value of  $S_{i,20,w}^*$ .

### Cut Cards

Card Col.	Fortran Format	Data Description
1-8	F8.0	Cut time (if needed)
9-16	F8.0	Cut sucrose concentration (percentile)
17-77	61X	Blank
78-80	I3	Cut number

A maximum of 100 cut cards may be used for one centrifuge run. If more than 100 cards are entered as data, the program will process the first 100 cards and ignore the remainder of the data.

### Trailer Cards

A cut number of 998 following the last cut card signals the end of one centrifuge run and a cut number of 999 following the last 998 card signals the end of the computer run.

### Program Arrangement

The program is arranged with a main program and ten subroutines or functions identified as: ZONCEN (main program), CALCR, RADLQ, VISDEN, TERPOL, COMPUT, OUTPUT, SEDEVN, FUNCTION R, NEWPLT AND PLTSED.

The main program reads the data input cards for one centrifuge run and accomplishes some error-checking as the cards are read. The data are then checked to see if a homogenous or a heterogenous sample was used. If a homogenous sample was used the sample mass center volume is taken to be half of the usable sample volume; however, if a heterogenous sample was used the sample mass center volume is approximately one third of the sample volume.

Subroutine CALCR is called to calculate the accumulative incremental rotor volumes, using the cut volume. The incremental radii are then calculated from the incremental rotor volumes. A separate set of constants are used to calculate the radii for each rotor configuration. For rotors C-III, B-XIV and B-XV a generalized set of equations, given in function RADLQ and function R, is used to calculate the radii. The derivation of these equations is included in ORNL special report

No. 3978. Separate rotor equations given in Appendix A, are used to calculate the radii for rotors B-II and B-IV.

When the rotor volumes and radii are calculated, the main program searches the rotor volume array to locate the tube containing the sample mass center volume (designated as S tube). The radius for the sample mass center is calculated and the tube number, volume and radius for the sample mass center is printed.

The subroutine VISDEN is called to calculate the viscosity and density of sucrose for each tube using the equations developed by Dr. E. J. Barber as shown in Appendix A. The subroutine TERPOL is called immediately following to calculate the average concentration, density and viscosity for S tube.

The subroutine COMPUT is called for each particle density entered on the identification card and  $S_{i,20,w}^*$  values are calculated. The values calculated by subroutine COMPUT are printed by subroutine OUTPUT.

The subroutine SVEDEVN calculates an even sedimentation coefficient value that most nearly corresponds to the center of each tube and extrapolates the exact fractional tube value for the calculated even value for the last particle density entered on the identification card. The fractional values for the other particle densities given on the identification card are extrapolated for the same even value of sedimentation coefficient. The three point extrapolation equation:

$$Y = \frac{Y1(X - X2)(X - X3)}{(X1 - X2)(X1 - X3)} + \frac{Y2(X - X1)(X - X3)}{(X2 - X1)(X2 - X3)} + \frac{Y3(X - X1)(X - X2)}{(X3 - X1)(X3 - X2)}$$

was used to extrapolate the fractional tube values ( $Y$ ) for an even sedimentation value ( $X$ ). The results are printed in tabular form and the subroutine PLTSED presents the same information in a family of plots if the PLTSED (Plot control number 1) control on the identification card is set to some positive value.

The subroutine NEWPLT plots the originally calculated values for sedimentation coefficient versus tube number for each particle density entered on the identification card. Both the PLTSED and NEWPLT subroutines require an auxiliary binary package to output a tape that is acceptable to the automatic plotter.

When all calculations, output and plots are complete for one centrifuge run, the program returns to read

another identification card until the trailer 999 card is encountered.

### Program Output

The output from the program is in the form of printed lists on  $14 \times 11$  paper and optional plots. The incremental radii and sample mass center variables are printed first. The values of  $S_{i,20,w}^*$  calculated by subroutine SEDEVN are presented in tabular form. If any of the error messages given in Appendix C are encountered during the processing of the data, they are printed and, depending on the severity of the error, the calculations may be terminated for the set of data being processed. When all the data has been processed the message:

\_\_\_\_\_ LOGICAL RUNS COMPLETED IN THIS JOB  
is printed.

A glossary of most of the FORTRAN names used in the program is presented in Appendix B.

## APPENDIX A

### Rotor Equations

Rotor B-II

$$R = 8.273 V^2 - 74.506V - 102.082$$

where:

$$R = \text{radius, cm}$$

$$V = \text{volume, ml}$$

Rotor B-IV

$$R = \sqrt{0.0018061V + 0.032082} + 0.16567$$

where:

$$R = \text{radius, in inches when } 2.468 \text{ cm} \leq R \leq 5.077 \text{ cm}$$

$$V = \text{volume, in ml when } 181.9 \text{ ml} \leq V \leq 1683 \text{ ml}$$

The computer program converts the above value of  $R$  to cm before the radii are printed.

Note: The limitations on B-XIV rotor are:

$$R = \text{radius, cm when } 2.357 \text{ cm} \leq R \leq 6.665 \text{ cm}$$

$$V = \text{volume, ml when } 30.4 \text{ ml} \leq V \leq 640.3 \text{ ml}$$

The limitations on B-XV rotor are:

$$R = \text{radius, cm when } 2.39 \text{ cm} \leq R \leq 8.89 \text{ cm}$$

$$V = \text{volume, ml when } 44.2 \text{ ml} \leq V \leq 1667.2 \text{ ml}$$

**Equations Derived by Dr. E. J. Barber**

**Density Equations for Sucrose. —**

Range

0 to 30°C 0 to 75 weight percent sucrose

$$\rho_{T,m} = (B_1 + B_2T + B_3T^2) + (B_4 + B_5T + B_6T^2)Y + (B_7 + B_8T + B_9T^2)Y^2$$

where:

$\rho_{T,m}$  = density of a sucrose solution

$T$  = temperature, °C

$Y$  = weight fraction sucrose

and  $B_i$ 's are constants

Constant	Value
$B_1$	1.0003698
$B_2$	$3.9680504 \times 10^{-5}$
$B_3$	$-5.8513271 \times 10^{-6}$
$B_4$	0.38982371
$B_5$	$-1.0578919 \times 10^{-3}$
$B_6$	$1.2392833 \times 10^{-5}$
$B_7$	0.17097594
$B_8$	$4.7530081 \times 10^{-4}$
$B_9$	$-8.9239737 \times 10^{-6}$

Range

30 to 60°C 0 to 70 weight percent sucrose

$$\rho_{T,m} = \frac{ym_1 + (1-y)m_2}{y(C_1 + C_2T + C_3T^2) + (1-y)(A_1 + A_2T + A_3T^2)}$$

where:

$$y = \frac{Y/m_1}{Y/m_1 + (1-Y)/m_2}$$

$y$  = mole fraction of sucrose

$Y$  = weight fraction sucrose

Constants	Value
$A_1$	18.027525
$A_2$	$4.8318329 \times 10^{-4}$
$A_3$	$7.7830857 \times 10^{-5}$
$m_1$	342.30
$m_2$	18.032
$C_1$	212.57059
$C_2$	0.13371672
$C_3$	$-2.9276449 \times 10^{-4}$

**Viscosity Equations for Sucrose. —**

Range

0 to 80°C 0 to 75 weight percent sucrose

$$\log \eta_{T,m} = A + \frac{B}{T + C}$$

where:

$$C = G_1 - G_2 \left[ 1 + \left( \frac{y}{G_3} \right)^2 \right]^{1/2}$$

Constant	Value
$G_1$	146.06635
$G_2$	25.251728
$G_3$	0.070674842

and

$$A = D_0 + D_1y + D_2y^2 + D_3y^3 + \dots + D_ny^n$$

Constant	Value (weight percent)	
	0-48	48-75
$D_0$	1.5018327	-1.0803314
$D_1$	9.4112153	$-2.0003484 \times 10^1$
$D_2$	$-1.1435741 \times 10^3$	$4.6066898 \times 10^2$
$D_3$	$1.0504137 \times 10^5$	$-5.9517023 \times 10^3$
$D_4$	$-4.6927102 \times 10^6$	$3.5627216 \times 10^4$
$D_5$	$1.0323349 \times 10^8$	$-7.8542145 \times 10^4$
$D_6$	$-1.1028981 \times 10^9$	
$D_7$	$4.5921911 \times 10^9$	

$$B = D_0 + D_1y + D_2y^2 + D_3y^3 + \dots + D_ny^n$$

Constant	Value (weight percent)	
	0-48	48-75
$D_0$	$2.1169907 \times 10^2$	$1.3975568 \times 10^2$
$D_1$	$1.6077073 \times 10^3$	$6.6747329 \times 10^3$
$D_2$	$1.6911611 \times 10^5$	$-7.8716105 \times 10^4$
$D_3$	$-1.4184371 \times 10^7$	$9.0967578 \times 10^5$
$D_4$	$6.0654775 \times 10^8$	$-5.5380830 \times 10^6$
$D_5$	$-1.2985834 \times 10^{10}$	$1.2451219 \times 10^7$
$D_6$	$1.3532907 \times 10^{11}$	
$D_7$	$-5.4970416 \times 10^{11}$	

**APPENDIX B**

**Glossary of Fortran Names**

**Names in Common**

AA, BB, CC	Constants used in radius calculations.
CENTRI	$\omega^2 t$ (centrifugal force).
CONC	Sucrose concentration of each cut.
CUTTIM	Cut time.

CUTVOL	Volume of each cut.
DENFR1	Assumed particle densities.
DENFR2	
DENFR3	
DENFR4	
DENSIT	Temporary storage area for one particle density.
DENTUB	Density of sucrose for each cut.
ICPL	Control for plot number 2.
IQUANT	The number of cuts being processed for one centrifuge run starting with S tube.
IROTOR	Rotor identification (alphanumeric).
ISAMCD	Density code.
JRTRCD	Rotor code identification (numeric).
KHEAT	Temperature of run °C.
LTUBES	Logical number of S TUBE.
MM	Switch for program flow control.
MONTH,	Current date.
IDAY, IYR	
NN	Number of particle densities being processed.
NUMEXP	Experiment run.
NUMRUN	Run number.
OVLAY	Overlay volume.
PMPRAT	Pump rate of auxiliary analytical device.
RADIUS	Incremental radii representing end of a cut.
RTRVOL	Rotor volume for each cut.
SAMVOL	Sample volume.
SEDCOE	$S_{i,20,w}^*$ for each cut.
SEDMAX	Maximum sedimentation coefficient.
SEDVAL	Extrapolated even values of sedimentation coefficient.
TUBFRC	Fractional tube values representing center of sample (located in S tube).
TUBVAL	Fractional values of tube numbers corresponding to even sedimentation coefficients.
VISC	Viscosity of sucrose for each cut.
VOLLIN	Volume of solution in lines (charging or withdrawing).

#### Main Program (ZONCEN)

GRAD	Constant for calculation gradient of sample mass.
ITEM	Number of cut cards read.
LOGRUN	Number of logical runs completed.

LSOLCD	Solution code (sucrose, 1).
SMCVOL	Sample mass center volume.

#### Subroutine CALCR

CUTNOW	Cut being processed.
SIDVOL	Volume used in auxiliary device.

#### Function RADLQ

BS	Ordinate of septa intersection—half of base—inches.
HC	Height of chamber—inches.
RS	Radius of chamber—inches.
SN	Number of septa in rotor.
TS	Septa tip half thickness—inches.
VL	Volume of liquid—cm <sup>3</sup> .

#### Subroutine VISDEN

AM2, Constants used by Dr. Barber in calculating density of sucrose. AD0, AD1, AD2, AD3, AD4, AD5, AD6, AD7, BD0, BD1, BD2, BD3, BD4, BD5, BD6, BD7, Constants used by Dr. Barber in calculating viscosity of sucrose.

#### Subroutine TERPOL

FAC	Interpolated values for volume, concentration, density and viscosity of S tube.
SZMCON	
SZMDEN	
SZMVIS	
SZMVOL	

#### Subroutine COMPUT

COFDEN	Intermediate steps in calculating $S_{i,20,w}^*$
CURFAC	
FACDEN	
FACNUM	
FACSUM	
RAD	

#### Subroutine SEDEVN

S	Calculated even value of $S_{i,20,w}^*$ .
X1, X2, X3	Known values in $S_{i,20,w}^*$ array.
Y1, Y2, Y3	Known values in tube array.

#### Subroutines NEWPLT and PLTSED

LEGEND	Entry points in binary package used to write plot tape.
NEWPIC	
PAXIS	
PLOTLN	
PLOTPT	

## APPENDIX C

### Error Messages

CUT NUMBER ERROR, TUBE \_\_\_\_\_ RUN \_\_\_\_\_  
JOB TERMINATED

RUN \_\_\_\_\_ NUMBER OF SAMPLES EXCEEDS  
100. CALCULATIONS COMPLETED FOR 100  
TUBES.

SAMPLE GRADIENT CODE ERROR RUN \_\_\_\_\_  
NO CALCULATIONS.

RUN \_\_\_\_\_ SAMPLE MASS CENTER. VOLUME  
EXCEEDS ROTOR CAPACITY.

RUN \_\_\_\_\_ ERROR IN ROTOR CONSTANTS.  
NO CALCULATIONS.

DENSITY OF CELL SOLUTION NOT SUPPLIED  
FOR RUN \_\_\_\_\_.

ROTOR VOLUME EXCEEDS CAPACITY.

EXCESS CONCENTRATION DATA, RUN \_\_\_\_\_  
ERROR IN RADIUS OR VOLUME TABLES  
RUN \_\_\_\_\_.

RESULTS FOR RUN \_\_\_\_\_ ARE INVALID. THE  
SOLUTION CODE IS ERRONEOUS.

THE TEMPERATURE FOR RUN \_\_\_\_\_ EXCEEDS  
EQUATION LIMIT.

CUT \_\_\_\_\_ RUN \_\_\_\_\_ CONCENTRATION EX-  
CEEDS PERMISSIBLE MAXIMUM.

DENSITY DIFFERENCE OR RADIUS EQUAL  
ZERO FOR DENSITY \_\_\_\_\_ CALCULATIONS  
TERMINATED FOR THIS DENSITY.

### F. DENSITY INDICATOR BEADS

N. G. Anderson

The  $s-\rho$  system previously described used plastic density beads to indicate density levels in liquid den-

sity gradients.<sup>1,2</sup> These did not indicate density in an even series, and were not available in densities to match the major virus classes. We have now arranged production of beads which are color coded and have the desired characteristics. The even series<sup>3</sup> and the virus and membrane series<sup>4</sup> are listed in Table 2.3. These now make identification of density levels routine.

### REFERENCES

<sup>1</sup>N. G. Anderson, W. W. Harris, A. A. Barber, C. T. Rankin, Jr., and E. L. Candler, *Natl. Cancer Inst. Monograph* **21**, 253-284 (1966).

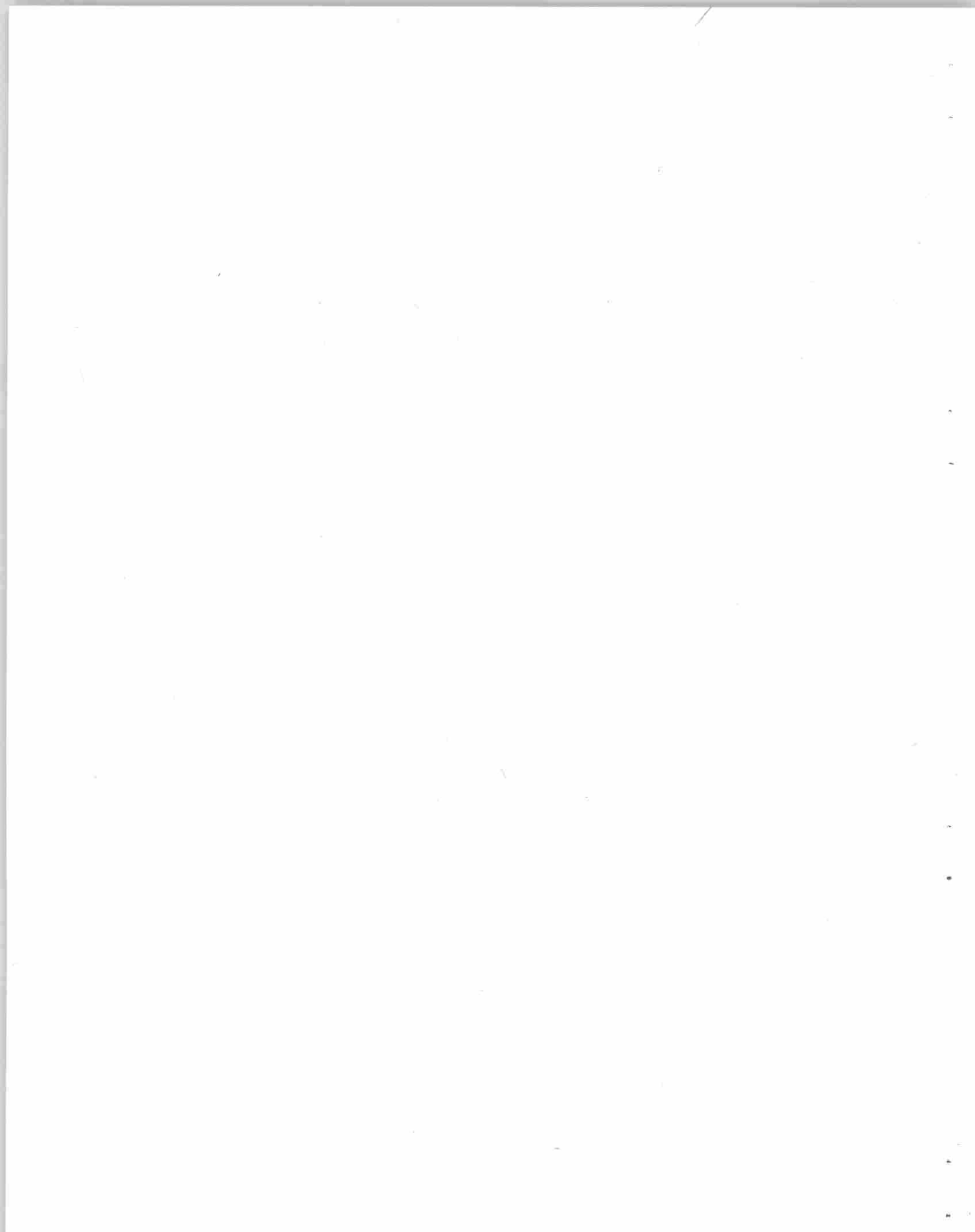
<sup>2</sup>N. Cho, H. P. Barringer, J. W. Amburgey, C. B. Cline, N. G. Anderson, L. L. McCauley, R. H. Stevens, and W. M. Swartout, *ibid.* 485-502 (1966).

<sup>3</sup>Available from Spinco Division of Beckman Instruments, Palo Alto, California.

<sup>4</sup>Available as Micule Density Markers from Microsphere, 931 Commercial St., Palo Alto, California.

**Table 2.3. Densities and Colors of Density Marking Beads Densities in gm/cc  $\pm 0.0025$**

Even Series	
Density	Color
1.10	dark green
1.20	dark blue
1.30	red
1.40	black
1.50	yellow green
1.60	orange
Virus and Membrane Series	
1.16	blue
1.18	green
1.22	orange-grey
1.29	red
1.33	rust
1.43	black
1.70	green



### 3. Centrifugal Separations

#### A. THE CAPACITY OF ZONES IN DENSITY GRADIENT CENTRIFUGATION

S. P. Spragg<sup>1</sup>

C. T. Rankin, Jr.

A recurrent problem in using zonal rotors for separating biological particles and macromolecules is the choice of experimental gradients to give maximum resolution of the components in the starting mixture. The diffusion potential for these large molecules is small; hence, the major factors affecting the width of the separated zones are radial dilution, the buoyant density of the zone and the density and viscosity gradients of the supporting medium. Svensson *et al.*<sup>2</sup> first developed a model for describing the effect of these factors on the mass of material that could be supported on a gradient and remain stable. This has been expanded by Berman<sup>3</sup> to show the effect of sedimentation on this mass. In view of the practical implications from these models it is important to consider how well they apply to conditions occurring during an experiment with a zonal rotor.

#### Experimental Conditions

Homogeneous samples of T3 phage were prepared<sup>4</sup> and used as the experimental particle. A sucrose gradient (5% to 12%, increasing linearly with radius) was loaded into a B-XIV zonal rotor rotating at approximately 3000 rpm (Anderson *et al.*<sup>5</sup>) and the density of the gradient adjacent to the core measured. The density of a 4 ml sample of T3 phage suspension was adjusted to be 0.001 g/ml less than this and then loaded into the rotor. This was followed by the sucrose overlay, similarly adjusted so the density was 0.001 g/ml less than the sample. The rotor was immediately unloaded following the normal procedure<sup>5</sup> and both the light absorption at 260 m $\mu$  and density of the issuing solution were measured. Tests were made for a Gaussian shape of the zone and the mass of T3

phage in the zone estimated by summation of the absorption curve following conversion to mass with the appropriate factor.

#### Results

A series of phage samples were tested on different gradients and the results are given in Table 3.1. It was found possible to reach 85% of the theoretical load as calculated from the Svensson-Berman model<sup>2,3</sup> and the zones still had a Gaussian shape. Overloading the gradient produced an asymmetrical shape. Since the model is based on a triangular shape for the zone a test was made for the percentage loading based on this shape and this showed that a practical gradient could be loaded to greater than 60% of the theoretical.

Following from these tests it was possible to predict zonal widths at different positions in the rotor. Comparing these with experimental cases showed that the zones were wider than calculated. However, it was interesting to find that some asymmetrical shapes of the zones, which were associated with discrete changes in the supporting gradient, could be qualitatively predicted by the model.

**Table 3.1. A Comparison Between the Calculated and Added T3 Phage on Sucrose Gradients**

Experimental Parameters						
Amount added (mgm)	Calc. $M_{\max}^a$ (mgms)	$\bar{r}$ (cms)	$d\rho_m/dr$ ( $g/cm^4$ ) $\times 10^3$	$r$ (cm)	Added Calcu- lated <sup>a</sup>	Test for Gaussian Peak
16.8	20.2	2.72	2.78	0.23	0.83	— <sup>b</sup>
8.5	10.0	2.73	5.68	0.12	0.85	+
21.8	59.5	2.58	57.1	0.09	0.37	+

<sup>a</sup>The calculated values were obtained using the experimental parameters quoted.

<sup>b</sup>The  $M_{\max}$  using  $\Delta r = 0.1$  cm was 4.5 mg, and for  $\Delta r = 0.15$  cm was 11.0 mg, giving between 373% and 153% overload.

The present results are different from those obtained by Brakke<sup>6</sup> using gradients formed in tubes by layering a series of sucrose solutions in a centrifuge tube and allowing them to diffuse before layering the virus on top. These zones were always asymmetrical after centrifuging the tubes. At present it is not possible to reconcile the two sets of results although it may be an expression of the differences between the two techniques.

## REFERENCES AND NOTES

<sup>1</sup>On study leave from the Department of Chemistry, The University, Birmingham, England.

<sup>2</sup>H. Svensson, L. Hagdahl and K. D. Lerner, *Science Tools*, **4**, 1 (1957).

<sup>3</sup>A. Berman, *J. Natl. Cancer Inst. Monograph*, **21**, 41 (1966).

<sup>4</sup>G. B. Cline, C. E. Nunley and N. G. Anderson, *Nature*, **212**, 487-489 (1966).

<sup>5</sup>N. G. Anderson, D. A. Waters, G. B. Cline, and C. E. Nunley, *Fed. Proc.*, **25**, 421 (1966).

<sup>6</sup>M. K. Brakke, *Arch. Biochem. Biophys.*, **107**, 388 (1964).

## B. RATE-ZONAL SEPARATION OF HAMSTER ANTI-ADENOVIRUS 31 TUMOR ANTIBODIES

E. L. Candler	W. L. Rasmussen
N. G. Anderson	L. H. Elrod
C. T. Rankin	J. E. Norton

Heubner *et al.*<sup>1</sup> have shown that the anti-virion complement-fixing antibodies in human serum resulting from adenovirus 31 infection were found exclusively in the 7S fraction. It was also shown that the complement-fixing antibodies to the nonvirion tumor and "T" antigens in the sera of hamsters bearing adenovirus 12 tumors were located in the 7S- $\gamma$  globulin fraction. The analytical separations of the serum components in this study were achieved in sucrose density gradients with low capacity swinging-bucket rotors. While this separation technique is perfectly suited for small samples, it does not provide a means of isolating the serum proteins in quantities large enough for thorough analysis.

The present communication reports the fractionation of sera from hamsters bearing transplanted adenovirus 31 tumors by ultracentrifugation in a B-XV zonal rotor.<sup>2,3</sup>

### Materials and Methods

A pool of antisera was prepared by bleeding hamsters bearing transplanted adenovirus 31 tumors for 6 wks. The tumors were implanted into weanling

hamsters by injecting 0.2 ml of a 20% tumor cell suspension (tumor weight/volume) in Tyrodes solution into each shoulder. During the 6 wks, the tumor size was kept below 3 cm in diameter by frequent excision. The serum from these tumor bearing animals was decomplemented and checked for its specificity for the non-virion adenovirus 31 tumor antigens.

The tumor antigen was prepared from a homogenate of frozen adenovirus 31 tumors in 8.5% sucrose and 0.05M Tris base by differential centrifugation. The homogenate was centrifuged in a Beckman No. 30 rotor at 30,000 rpm for 30 min. The supernatant fluid was collected and centrifuged again in a Beckman No. 50 rotor at 50,000 rpm overnight. The pellets were collected and homogenized by hand in veronal buffer. This solution was used as the tumor antigen preparation.

The B-XV zonal rotor was loaded so that it contained an overlay of 700 ml of Miller-Golder buffer (pH 7.3), 20 ml of antisera, 500 ml 10 to 23% sucrose in buffer, and 450 ml of 23% sucrose in buffer. Separation of the antisera was obtained by centrifugation until  $\int_0^t \omega^2 dt = 43.6 \times 10^{10}$  (approximately 16.5 hours at 26,000 rpm). The contents of the rotor were recovered by displacement in forty-two 40-ml fractions while a continuous recording of absorbancy at 260 m $\mu$  was made by a flow cell equipped Beckman DU spectrophotometer. Each zonal fraction (excluding the overlay volume, fractions 1-18) was divided and prepared for complement fixation tests, total protein determinations, and sedimentation measurements.

All complement fixation titrations were done by the LBCF (Laboratory Branch Complement Fixation) micro technique.<sup>4</sup> The titers given in this report are the greatest dilutions of the zonal fractions (fractions of antisera) showing 30% (3+) or less hemolysis with specific antigen diluted to 1:40 (4 units). Total protein determinations were made by a modified Lowry method in a Technicon Auto Analyzer<sup>5</sup> and reported as milligrams protein per milliliter. Sedimentation measurements of the zonal fractions were made in a Beckman Model E Analytical Ultracentrifuge by use of an An-D rotor. Data were evaluated by the use of a computer program.<sup>6</sup> The macroglobulin zonal fractions were concentrated five times by pressure ultrafiltration in order that more accurate determinations could be made of their sedimentation values.

### Results

The separation of the hamster antisera in the B-XV rotor into two distinct peaks is shown in Figure 3.1.

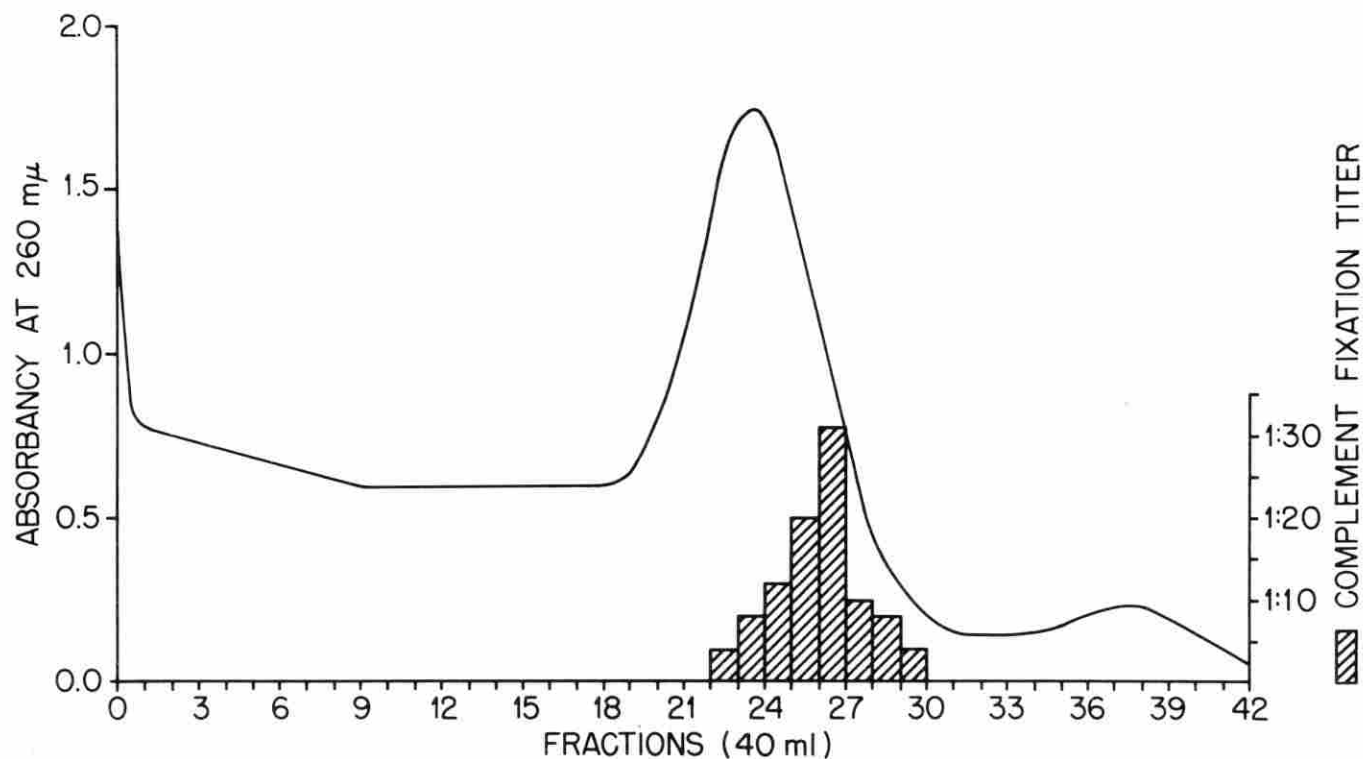


Fig. 3.1 Separation of hamster antiserum in a B-XV zonal rotor. Upper curve, absorbancy at 260 m ; lower bar graph, complement fixation activity of the fractionated antisera.

The first peak (fractions 19–31) is a mixture of 4S and 7S proteins with the greatest concentration of 7S proteins being in the last half of this peak. The second peak (fractions 34–42) is 18.5S macroglobulins exclusively. The location of the complement-fixing antibodies in the B-XV gradient is illustrated by bar graph in the same figure. It can be seen that the peak of complement-fixing activity is in fraction 27, which corresponds with position of the greatest concentration of 7S proteins. Titration of the macroglobulin peak did not exhibit the presence of any complement-fixing antibody. Since the amount of total protein in the macroglobulin fractions was lower than those of the first peak (Figure 3.2), the macroglobulin fraction containing the most protein was concentrated and tested for antibody titer. No titer could be obtained with this macroglobulin isolate, even though the amount of protein after concentration was nearly twice as great as the fraction in the first peak demonstrating the highest titer.

### Discussion

The results of this study indicate that the non-virion complement-fixing antibodies to the adenovirus 31 tumor antigens are in the 7S fraction of the hamster antiserum. It has also been shown that the 18.5S macroglobulins in the sera of the hamsters bearing adenovirus 31 tumors for 6 wks do not demonstrate antibody titer to these tumor antigens. These findings agree with Heubner's observations on the adenovirus anti-virion complement-fixing antibodies in man and the non-virion complement-fixing antibodies to adenovirus 12 tumor antigens in hamster.

While the zonal centrifuge technic employed in this study is most useful for extracting pure macroglobulins, it does not make possible the separation of the more slowly sedimenting proteins in a pure state. Acrylamide gel disc electrophoresis<sup>7</sup> of fraction 27, which gave the highest antibody titer, indicates the existence of at least eight distinct components.

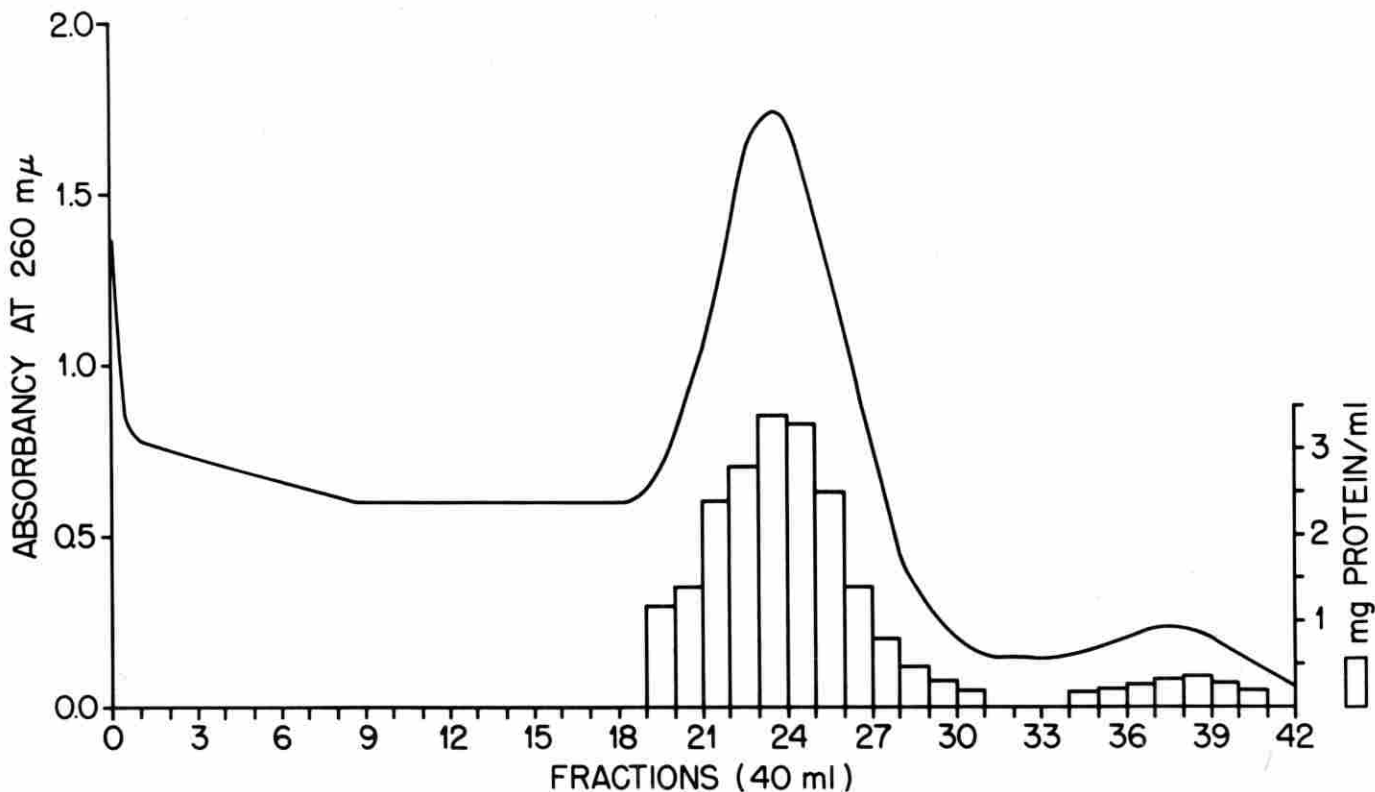


Fig. 3.2 Separation of hamster antiserum in B-XV zonal rotor. Protein concentrations of the zonal fractions of antisera represented by bar graph. Compare with Figure 3.1.

## REFERENCES

- <sup>1</sup>A. C. Hollingshead, T. C. Alford, H. C. Turner, and R. J. Heubner, *Nature* **211**, 423-424 (1966).
- <sup>2</sup>N. G. Anderson, D. A. Waters, G. B. Cline, and C. E. Nunley, *Federation Proc.* **25**, 421 (1966).
- <sup>3</sup>N. G. Anderson, *Science J.* **3**, 35-41 (1967).
- <sup>4</sup>Helen L. Casey, *P. H. Monograph* **74**, (1965).
- <sup>5</sup>L. H. Elrod and N. G. Anderson, "Improved Automated System for Total Protein Analysis," this publication.
- <sup>6</sup>Rhodes Trautman, *Brookhaven Natl. Lab.* 990 (T-420), 1966.
- <sup>7</sup>Leonard Ornstein, *Annals of the N. Y. Acad. Sci.* **121**, 321-349 (1964).

## C. PURIFICATION OF *TREPONEMA PALLIDUM* BY ZONAL CENTRIFUGATION

H. Russell<sup>1</sup>            M. L. Thomas<sup>1</sup>  
 V. W. Clark, Jr.<sup>1</sup>    G. B. Cline  
 N. G. Anderson

We are interested in isolating the agents which cause venereal disease to (a) determine their physical and

chemical properties, (b) purify specific antigenic components for both research and diagnostic purposes, and to (c) explore the possibility of producing effective vaccines.

Cultivation of *T. pallidum*, the causative agent of syphilis, can only be done *in vivo*. While a number of reports have appeared claiming to grow the organism *in vitro*, it now appears that they were adventitious spirochetes which often contaminate primary lesions. Purification of *T. pallidum* must therefore involve its extraction from the tissue in which it is grown. Since the organism may be considered as an infectious sub-cellular (or intercellular) particle, techniques for cell fractionation should be applicable to its purification. Rather little work has been done previously on the zonal centrifugation of testicular tissue such as is generally used for *T. pallidum* production.<sup>2</sup> In the experiments described here we have been interested in determining whether the centrifugal systems already developed can be adapted to this problem or whether new systems are required.

Orienting studies were done with Reiter's treponeme, a noninfectious spirochete which may be grown *in vitro*.

### Experimental Studies

*Treponema pallidum*-infected testes from 36 rabbits were minced in mortars with scissors, transferred to Erlenmeyer flasks and agitated with 3600 ml of phosphate buffered saline, Bacto Hemagglutination Buffer No. 0512, pH 7.2 on a rotating shaker platform. The supernatant was siphoned off and centrifuged at 300X g for 10 min. The remaining minced tissue was re-extracted in 3600-ml buffered saline three times.

Organisms in an aliquot of the combined extract were counted by four experienced individuals. Based on the averages of these counts, the estimated yield from 36 rabbits was  $250-300 \times 10^9$  organisms in 13.5 liters, or  $18.3-22.2 \times 10^6$  per ml. The extract was free of contaminating bacteria as demonstrated by lack of growth on human blood agar plates, trypticase soy broth, thioglycollate broth and Sabouraud's agar slants.

The treponeme suspension was stored at 5°C overnight and transported to Oak Ridge, Tennessee by automobile the following day. The temperature of the suspension was maintained at 5°-10°C during transportation.

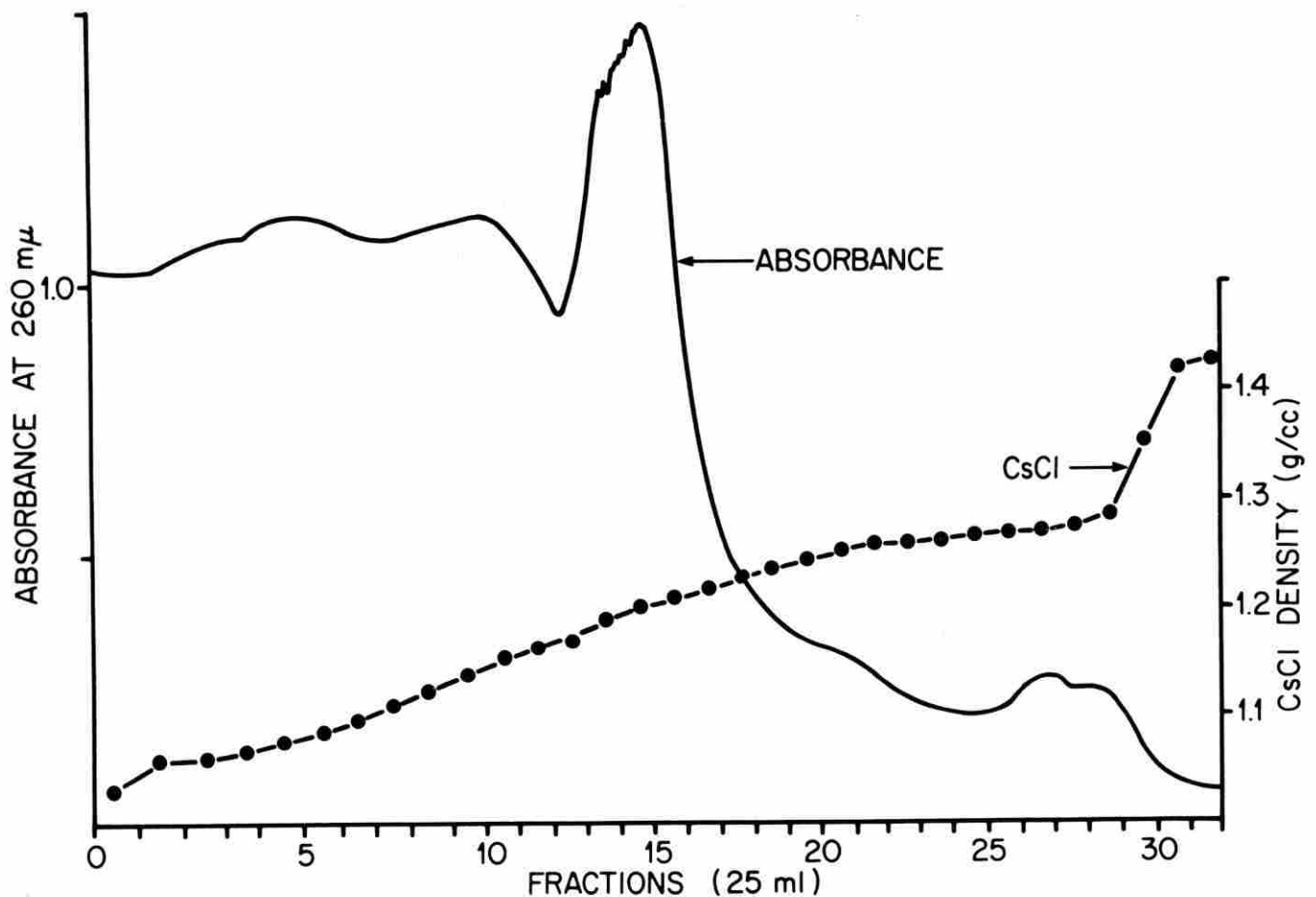


Fig. 3.3 is an absorbance profile of the density gradient as detected during unloading the rotor at 0 rpm. The left portion of the chart represents the portion of the gradient of lowest density next to the rotor core with density increasing with rotor radius. The cesium chloride gradient was made by pumping 450 ml CsCl into a buffer-filled B-XXVI rotor at rest. The rotor was accelerated from 0 rpm to 3,000 rpm over a 40 min period and then accelerated to 20,000 rpm at a maximal rate. The *T. pallidum* solution was pumped through the rotor at a flow rate of 5.88 liters per hr. 13.5 liters were passed through the rotor after completion of flow through, the rotor speed was increased to 35,000 rpm for 30 mins to further band the particles. The rotor was unloaded at rest by displacement of the gradient with density 1.45 CsCl.

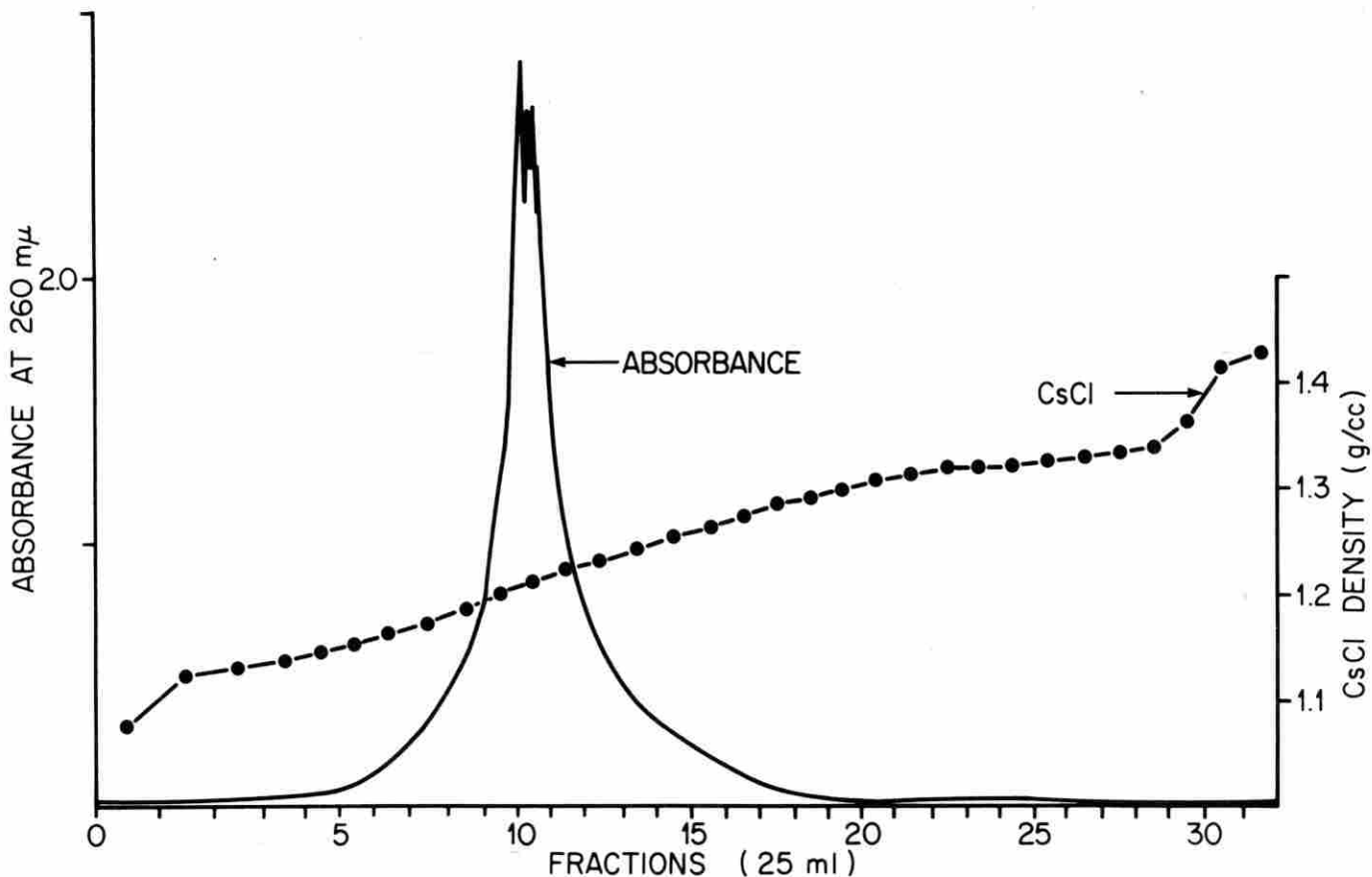


Fig. 3.4 was obtained in the same manner as in Fig. 3.3. The flow through rate was 4.0 liters per hr at a rotor speed of 15,000 rpm. The banding period was 30 mins at 24,000 rpm. The center of the *Treponema* peak is banded isopycally at density 1.215. A total of 4.35 liters of *Treponema* suspension was passed through the rotor.

#### Purification of *Treponema pallidum* Suspension. —

The starting sample (*treponeme* suspension), containing many aggregates, was centrifuged through the B-XXVI rotor system<sup>3</sup> (CsCl gradient) at 20,000 rpm with a flow speed of 5.88 liters per hr. The gradient profiles for experiments ZU-136-139 are shown in Figures 3.3-3.6. All samples, including effluent, were subjected to darkfield examination. Crude counts of number of organisms, and observation concerning the relative amounts of debris in each sample were recorded (Tables 3.2 and 3.3).

Fractions 13-32 from Run ZU-136 were combined, diluted to 4.35 liters with phosphate buffered saline and recentrifuged (ZU-137). A stringy sediment which was sticking to the vanes of the rotor after completion of the run and other large masses which were floating in the "piston" were split into two equal volumes (2

Table 3.2. Nitrogen Content of Zonal Centrifuge Fractions from ZU-136

Fraction Number	$\mu\text{g N/ml}$
1	73
2	98
3	103
4	106
5	94
6	82
7	63
8	46
9	36
10	40.5
11	24
12	23.5

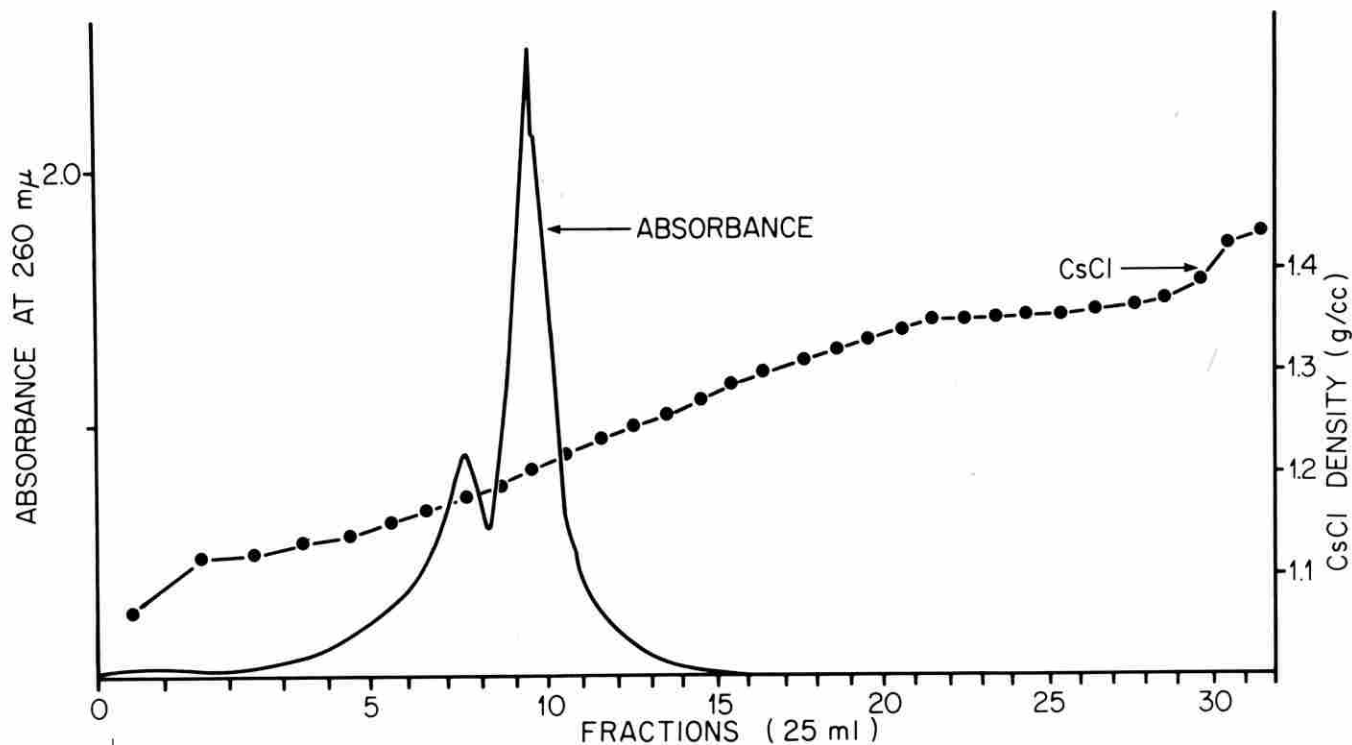


Fig. 3.5 and Fig. 3.6 were obtained under the same experimental conditions as outlined in Figure 3.4. Only 2 liters of *Treponema* suspension were used in each of these experiments.

liters each) and run as ZU-138 and ZU-139. Tables 3.4 and 3.5 show the results of particle counts of these two experiments. With the exception of organism enumeration, all other data were obtained from fractions of Run ZU-137 which appeared to be more debris-free than the other two. Purification was followed in the electron microscope (Figure 3.7).

**Fractions from ZU-136.**—Fractions 1–12 were not combined to be re-centrifuged; therefore, a nitrogen determination<sup>4</sup> was performed on each. The organisms were not subjected to detailed enumeration, but it is estimated that none of the fractions contained more than  $3 \times 10^6$  organisms, and some fractions contained even less. The results are shown in Table 3.2. It can be concluded from the nitrogen content of the fractions in Table 3.2 that a large amount of protein was removed from the starting sample. The nitrogen peak is higher than the most concentrated *T. pallidum* peak in Run ZU-137, shown in Table 3.3. Darkfield photomicrographs taken during purification are shown in Figure 3.8.

**Immuno Gel Diffusion**<sup>5</sup>.—Purified fractions of treponeme suspensions were reacted against goat anti-rabbit testicular homogenate, goat anti-rabbit whole serum, and goat anti-rabbit globulin in a gel diffusion test. Starting treponeme suspension, normal rabbit testicular homogenate, and ZU-136 effluent were run as controls. A precipitin line formed between all of the antisera and controls but none was observed between antisera and purified fractions. It appears that all soluble components from the rabbit tissue capable of detection in the gel diffusion system were absent in the purified fractions.

**Electron Micrographs**<sup>6</sup>.—The micrographs were made from aliquots of the starting sample (Figure 5a) and from fractions 11 and 12 (Figures 5b and 5c) of ZU-317.

**Darkfield Photomicrographs.**—The photomicrographs are shown for the starting sample (Figure 6a) fraction 1 of ZU-136 (Figure 6b) (showing isolated debris clumps and small particles), and fraction 12 of ZU-136 (Figure 6c) showing purified *T. pallidum*.

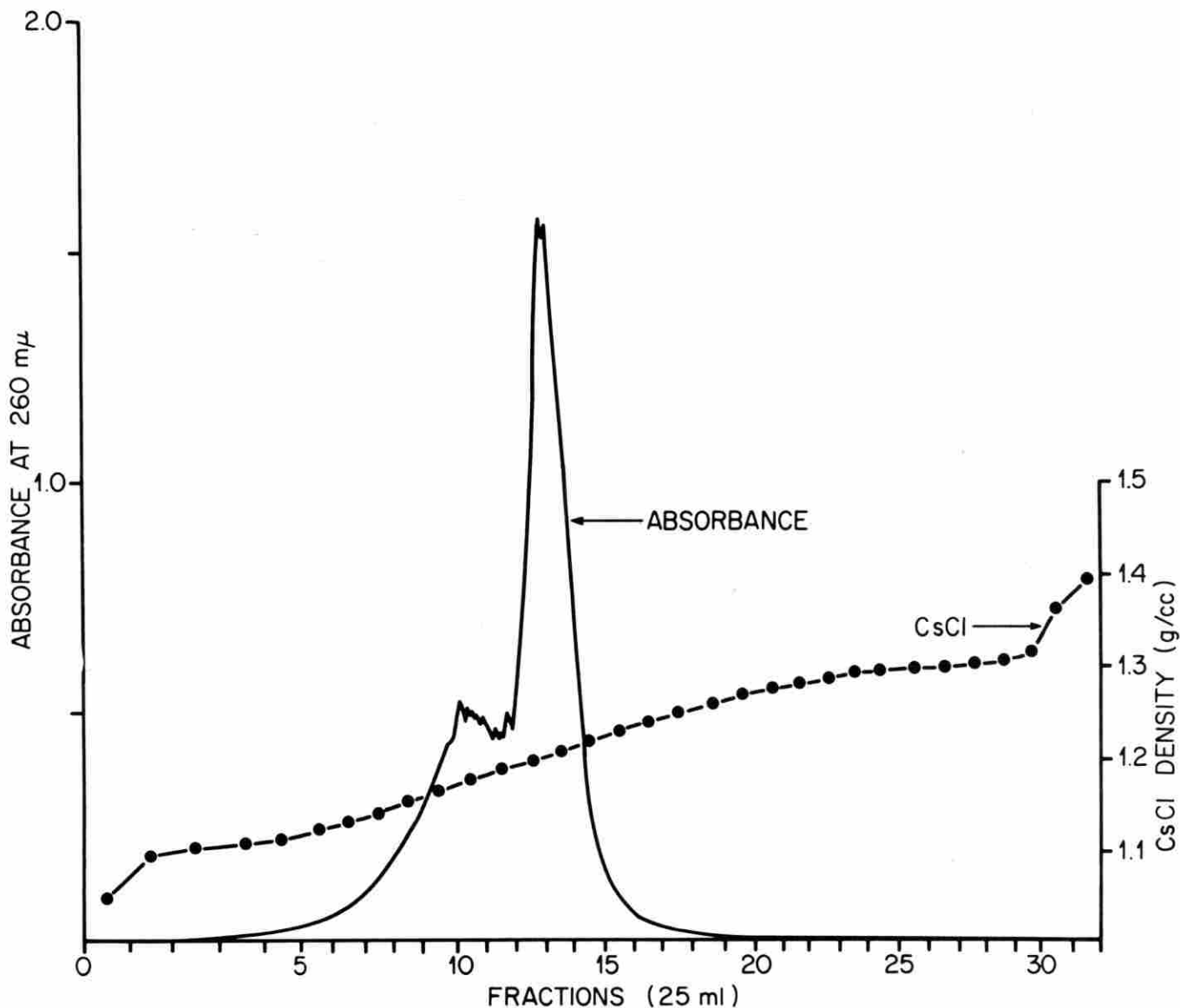


Fig. 3.6 Experimental conditions as outlined for Fig. 3.5.

**Assessment of Purity.**—The evaluation of an isolation method depends on having a method for determining how pure the final preparation is. This requires that we have an assay or analysis which can be related to the number of organisms present. Total protein, total nitrogen, or dry weight per organism would answer the purpose. For treponemes which may be grown *in vitro* and hence obtained in pure form the data can be obtained quite simply. The Reiter treponeme has been found to have a dry weight of  $8 \times 10^{-13}$  grams.<sup>7</sup> However, it is much larger than *T. pallidum*

and the results, therefore, cannot be applied to the latter organism.

An alternate approach is to attempt to calculate the mass of *T. pallidum* from light and electron microscopic data, realizing that the results are only crude approximations since the extent of shrinkage and deformation during specimen preparation for the electron microscope are difficult to measure. The volume is approximated by the formula:

$$V = \pi r^2 L \sqrt{1 + 4\pi R^2 P^2}$$

Table 3.3. Analysis of Fractions From ZU-137

Fraction Number	Treponemes × 10 <sup>6</sup> /ml <sup>a</sup>	μg N/ml	Debris (1-4+)	Nitrogen Present per Treponema (gm × 10 <sup>12</sup> )
1	0.8	—	2+	—
2	1.7	2.0	2+	1.8
3	0.9	—	2+	—
4	1.1	2.75	2-3+	2.5
5	3.4	—	2-3+	—
6	2.3	2.0	2+	0.87
7	4.3	—	2+	—
8	8.7	3.5	3+	0.40
9	33.8	6	2+	0.178
10	284	12.25	+	0.0431
11	820	34	+	0.0415
12	345	16.25	+	0.0471
13	67	6	+	0.0896
14	29	3.5	+	0.121
15	30	3.9	+	0.13
16	13.8	2.0	+	0.145
17	10	3.25	+	0.325
18	10	3.25	+	0.328
19	7.5	—	+	—
20	3.3	3.25	+	0.985
21	4.4	—	++	—
22	6.8	3.25	+	0.478
23	6.5	—	+	—
24	42.0	5.0	+	0.119
25	13.0	—	+	—
26	3.3	1.63	+	0.494
27	7.3	—	+	—
28	3.6	1.61	+	0.447
29	2.3	—	+	—
30	4.4	3.25	+	0.739
31	4.3	—	+	—
32	1.9	4.25	+	2.24

<sup>a</sup>Counting procedure: See C. Artley, and J. W. Clark, Jr., *Applied Microbiol.* (in press). Percent yield, based on 250 × 10<sup>9</sup> treponemes in starting suspension, was 17.76%. The organism suspensions seem to be relatively debris-free, especially those in fractions 10-32.

where:

$V$  = total volume

$r$  = radius of spirochete filament (0.065μ)

$L$  = average length of spirochete (10.5μ)

$R$  = radius of coil (0.17μ)

$P$  = number of loops in spiral per unit length (0.87/μ)

Table 3.4. Description of Fractions from ZU-138

Fraction Number	Treponemes × 10 <sup>6</sup> ml <sup>†</sup>	Debris (1-4+)
1	2.0	—
2	3.0	—
3	3.8	—
4	5.5	Clumps of <i>T. p.</i> fragments
5	28.0	" " " " "
6	23.0	—
7	53.0	Few clumps
8	75.0	2+
9	141.0	2+
10	644.0	3+
11	513.0	2+
12	109.0	—
13	57.0	—
14	23.0	—
15	13.0	—
16	14.0	—
17	23.0	—
18	5.0	—
19	5.0	Small clumps of <i>T. p.</i>
20	4.0	Large clumps of <i>T. p.</i>
21	6.0	—
22	3.0	—
23	3.0	Large clumps of <i>T. p.</i>
24	4.0	—
25	2.0	—
26	1.0	—
27	1.0	—
28	1.0	—
29	1.0	—
30	3.0	Small clumps of <i>T. p.</i>
31	1.0	—
32	1.0	—

<sup>†</sup>Percent yield, based on 250 × 10<sup>9</sup> treponemes in starting sample, was 17.71%.

Data is taken from Swain,<sup>6</sup> and the volume is calculated to be 1.92 × 10<sup>-13</sup> cm<sup>3</sup> (Freeman and Doak, unpublished studies). If the dry weight were 25% of wet weight, and the density were close to one, then one organism would have a dry mass of 5 × 10<sup>-14</sup> gms. Christiansen<sup>8</sup> has calculated the dry weight to be twice this value, or 10 × 10<sup>-14</sup> gms per organism. The starting material used here contained 2.5-3.0 × 10<sup>11</sup> organ-

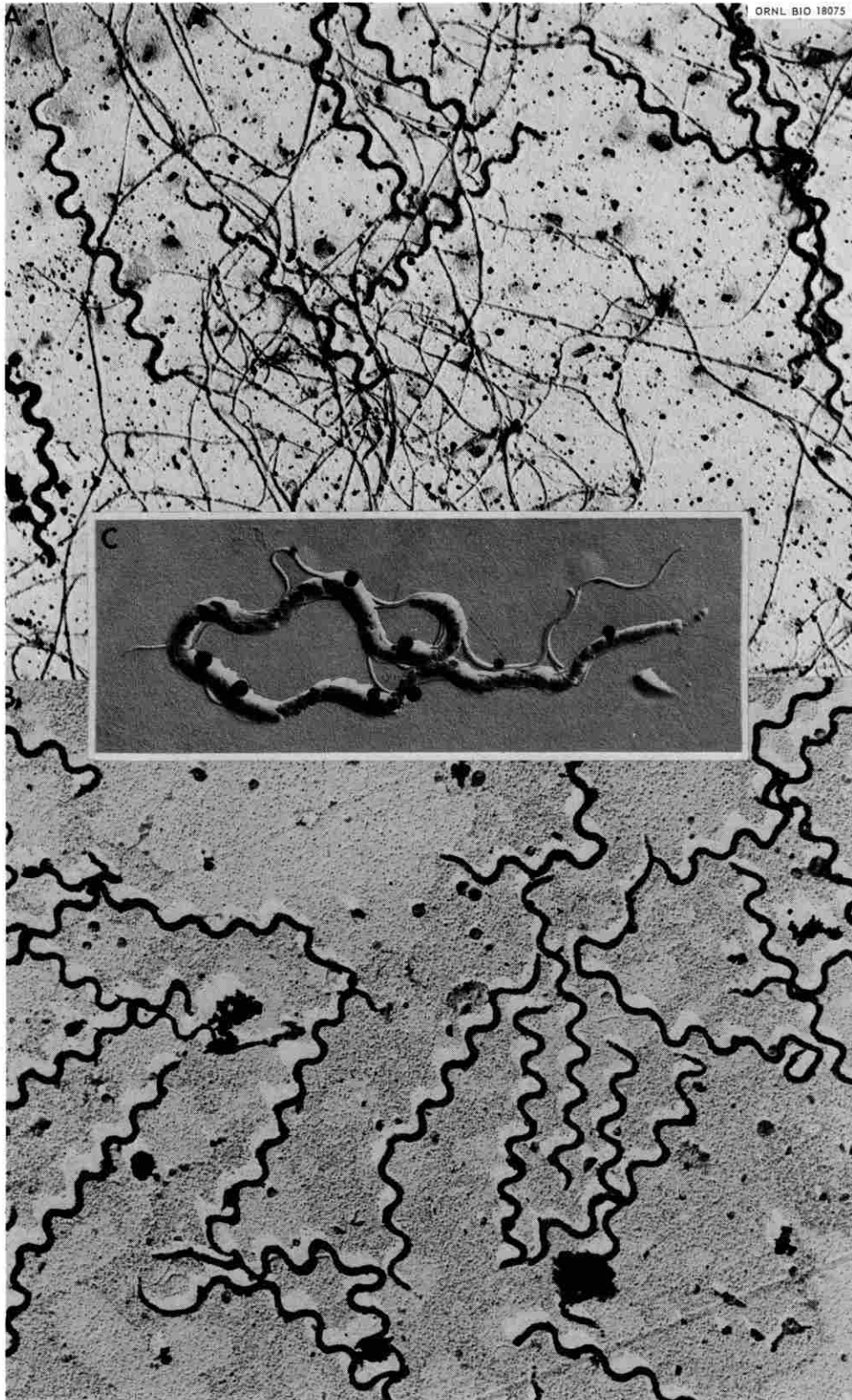


Fig. 3.7 (a) Electron micrograph of starting sample of *T. pallidum* extract for zonal centrifuge run number ZU 137. 13,750X (b) Micrograph of *T. pallidum* in fraction 11, ZU 137. 13,750X (c) Micrograph of *T. pallidum* in fraction 12, ZU 137. 28,750X.

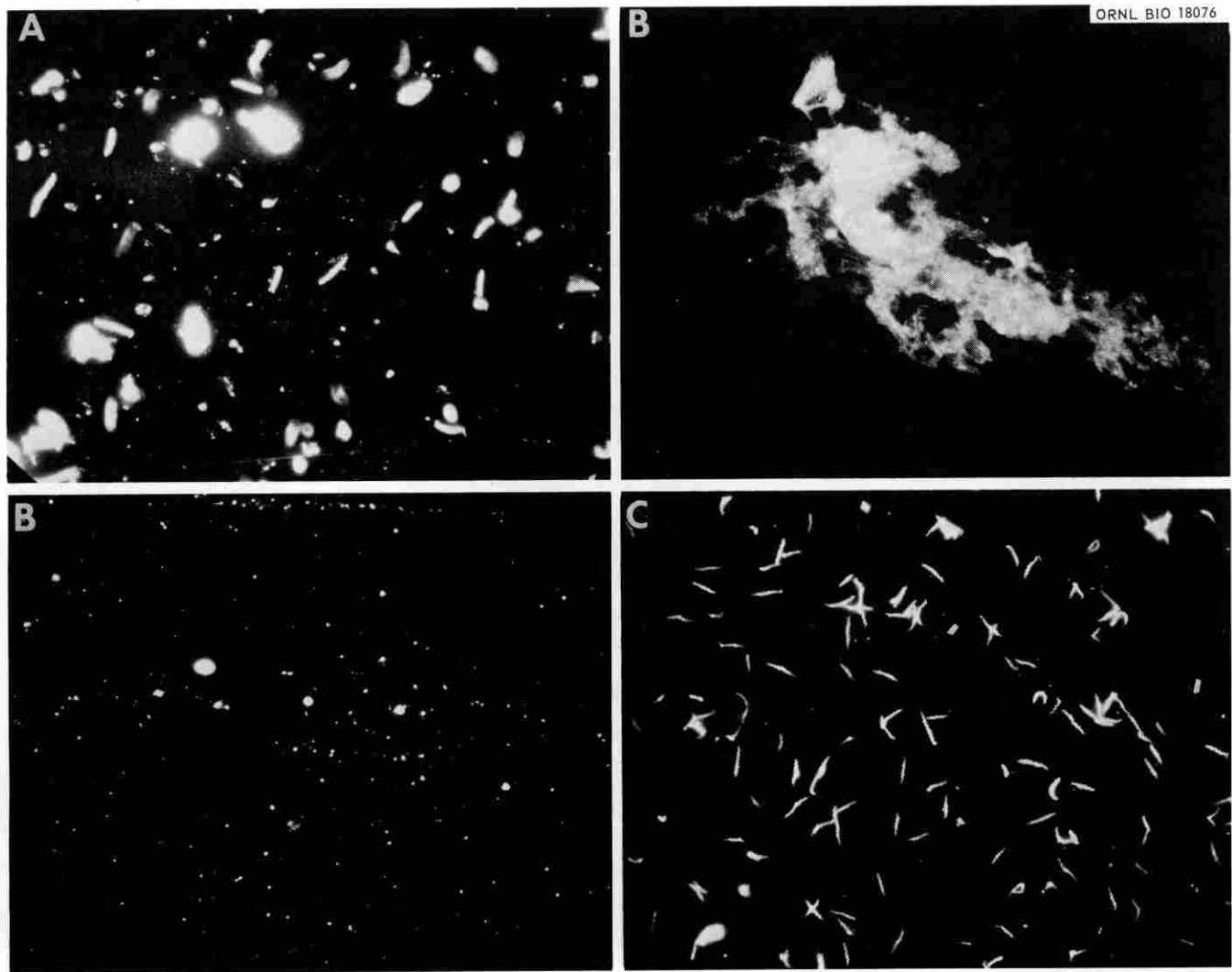


Fig. 3.8 (a) Dark field light micrograph of *T. pallidum* extract before purification in zonal centrifuge (ZU 136) (b) Debris found in fraction 1, zonal centrifuge run number ZU 136 (c) Purified *T. pallidum* from fraction 12 zonal centrifuge run number ZU 136.

**Table 3.5. Description of Fractions from ZU-139**

Fraction Number	Treponemes × 10 <sup>6</sup> ml <sup>†</sup>	Debris (1 - 4+)
1	0.4	-
2	0.6	-
3	0.6	<i>T. p.</i> clumps
4	0.7	-
5	2.2	-
6	5.5	Small clumps of <i>T. p.</i>
7	4.4	" " " " "
8	6.4	" " " " "
9	4.3	-
10	17.0	Few small <i>T. p.</i> clumps
11	28.0	2+
12	115.0	3+
13	150.0	3+
14	202.0	-
15	99.0	-
16	11.8	-
17	10.1	-
18	4.4	-
19	3.0	-
20	1.4	-
21	0.8	-
22	0.8	-
23	0.8	-
24	1.2	-
25	0.7	-
26	0.49	-
27	0.39	-
28	0.5	-
29	0.4	-
30	0.3	-
31	0.2	-
32	0.9	-

<sup>†</sup> Percent yield, based on  $250 \times 10^6$  treponemes in starting sample, was 1.74%. Note that it is rather difficult to determine if some clumps are treponemes or tissue debris.

isms and therefore the total dry mass of treponemes is calculated to be between 12.5-30 mg depending on the values chosen.

From Table 3.3 it is seen that the purest preparation contained  $4.15 \times 10^{-14}$  gms of nitrogen per organism counted. Assuming all nitrogen to be protein nitrogen, this would mean  $26 \times 10^{-14}$  gms of dry protein per organism counted, i.e., the protein mass was 2.5-5

times the calculated treponema mass. This degree of purity has not been previously reported. It does not, however, indicate the limits of purification which could be achieved in zonal centrifuges.

It should be noted that calculations of *T. pallidum* volume have been made from data obtained from dried specimens in the electron microscope and using estimates of percent dry weight obtained from organisms. The calculated dry weight per organism may therefore be in error by a factor of two or even more. For this reason, analytical data on extensively purified *T. pallidum* are urgently required.

In previous studies using differential centrifugation, the final product has been estimated to contain at the most 2-3% of *T. pallidum*.<sup>8</sup>

The effect of the procedures used here on the morphology and composition of *T. pallidum* require further study. The high osmotic pressure of the gradient material used may damage the organisms by osmotic shock when it is removed by dialysis. Studies on the effect of 0.3 osmolal solutions on the related Reiter treponeme showed that sphere formation occurred rapidly in glycerol, very slowly in sucrose, and not at all in lactose, maltose, and a variety of salt solutions.<sup>9</sup> In studies on the effect of various ions on *T. pallidum*, large concentrations of cesium ions could partially replace potassium ions; however neither rubidium nor cesium could replace sodium as tested by maintenance of motility.<sup>10</sup> These two findings are in agreement with the lack of gross morphological damage observed in these studies. A brief report of the purification of this organism by isopycnic centrifugation in potassium citrate has appeared.<sup>7</sup> No analytical data, electron micrographs, or information on the banding density of the organism were presented.

From these preliminary studies it would appear that zonal centrifuges are useful for the purification of the causal agent of syphilis. The low yields may be due in part to the long delays which transportation from Atlanta to Oak Ridge entailed. To facilitate more rapid fractionation arrangements have been made to do the centrifugation at the National Communicable Disease Center in Atlanta. In addition, cascaded systems for the preclarification of testis extracts on a continuous-flow basis, and continuous tissue extractors are being designed.

#### REFERENCES AND NOTES

<sup>1</sup> Veneral Disease Research Laboratory, National Communicable Disease Center, Atlanta, Georgia.

<sup>2</sup>A. A. Barber, C. T. Rankin, Jr., and N. G. Anderson, *J. Natl. Cancer Inst. Monograph* **21**, 333-344.

<sup>3</sup>G. B. Cline, J. N. Brantley, and J. Gerin, "Reorienting Density Gradients in Continuous Sample Flow Rotors." (In Preparation)

<sup>4</sup>Koch and McMeekin, *J. Am. Chem. Soc.*, **46**, 2066 (1924).

<sup>5</sup>O. Ouchterlony, *Acta Path. Microbiol. Scand.*, **25**, 186 (1948).

<sup>6</sup>R. H. A. Swain, *J. Path. Bact.*, **69**, 117-128 (1955).

<sup>7</sup>A. Gelperin, *Am. J. Syph. Gonorr. and Ven. Dis.*, **33**, 101 (1949).

<sup>8</sup>A. H. Christiansen, *Acta Path. et Microbiol. Scand.*, **61**, 141-149 (1964).

<sup>9</sup>P. H. Hardy, and E. E. Nell, *J. Bact.*, **82**, 967-978 (1961).

<sup>10</sup>G. O. Doak, L. D. Freedman, and J. W. Clark, Jr., *J. Bact.*, **78**, 703-708.

#### D. ADENOVIRUS 31 HAMSTER TUMOR ANTIGENS: DIFFERENTIAL CENTRIFUGATION OF TUMOR HOMOGENATES

N. G. Anderson  
E. L. Candler

L. H. Elrod

Antigens have been demonstrated in a variety of virally-induced tumors and in virally transformed tissue culture cells which react with serum from a tumor bearing host.<sup>1-6</sup> How many different antigens are involved in these reactions is not known, although it appears that more than one may be present. Nor is it known how the antigens affect the structure and function of the tumor cell. The first step in a tissue protein isolation procedure is generally the centrifugal isolation of the subcellular organelle having the highest specific activity. In fluorescent antibody studies SV40 T antigen<sup>7</sup> and adenovirus tumor antigens are observed to be concentrated in the nucleus. The localization observed in isolated cell fractions may or may not reflect the localization in the intact cell<sup>8</sup> depending on the lability of the site linkage in the cell, and the degree to which the isolation conditions resemble those existing in the living cell.

The centrifugal fractionation of frozen and of fresh adenovirus 31 hamster tumors has been examined using two techniques. The first is an adaptation of preparative angle head centrifugation which allows information on sedimentation rates to be obtained under the experimental conditions used for preparative work,<sup>9</sup> and the centrifugation time required for sedimentation of a biological activity to be determined. The data obtained allow large-scale initial fractionation methods to be designed. The results suggest that antigenic activity is associated with a wide spectrum of particles having sedimentation coefficients which may extend as low as 10S.

Zonal centrifugation of tumor homogenates, as presented in a subsequent study, allows a higher resolution separation of subcellular particles to be achieved. However in a given experiment separation over only a limited range of sedimentation coefficients is possible. In addition, even with very large zonal rotors, the amount of material which may be fractionated is limited. For preparative work therefore differential centrifugation is often a necessary first step.<sup>9</sup>

#### Experimental Studies

**Tumors.**—A transplantable adenovirus 31 hamster tumor free of detectable infectious virus was obtained from Dr. Ray Gilden of Flow Laboratories. Finely minced tumor tissue was injected subcutaneously into the scapular region of weanling hamsters (either bred at Oak Ridge or purchased from Lakeview Farms). Tumors were harvested when approximately 1-2 cm in diameter.

**Antisera.**—Animals from which tumors had been removed two or three times were bled, the blood allowed to clot, and the sera pooled and frozen.

**Titration.**—Titrations were carried out using the Microteter system and four units of complement.<sup>10</sup> The titers were read by comparison with a series of standards. Control titrations with normal hamster sera or with saline were used to determine the level of anticomplement activity.

**Protein Analysis.**—Total protein was determined by a modified Folin-biuret method using the Technicon Autoanalyzer.

**Homogenization.**—Tumors were homogenized in 8.5% sucrose to give a final concentration of 5% tissue w/v. Both Potter Elvehjem and Sorvall Omnimixer homogenizers were employed.

**Centrifugation.**—All centrifugal steps were carried out in a Spinco No. 50 titanium rotor using polycarbonate centrifuge tubes<sup>11</sup> at 5°C. The numerical value of the integral of  $w^2t$  was determined electronically<sup>12</sup> or, for long runs where acceleration and deceleration can be neglected, by calculation from the odometer readings.<sup>9</sup> The technique for recovering the supernatant has been previously described<sup>9</sup> and consists in carefully removing the upper 7 ml from a 9-ml sample after revolving the tubes 180° in position. The remaining 2 ml was considered as the "pellet volume." The results are plotted as activity vs. the log of the integral of  $w^2t$ . On such a scale a homogeneous substance with a sedimentation coefficient of 8S gives a curve such as is shown in Figure 3.9. The intersection of this

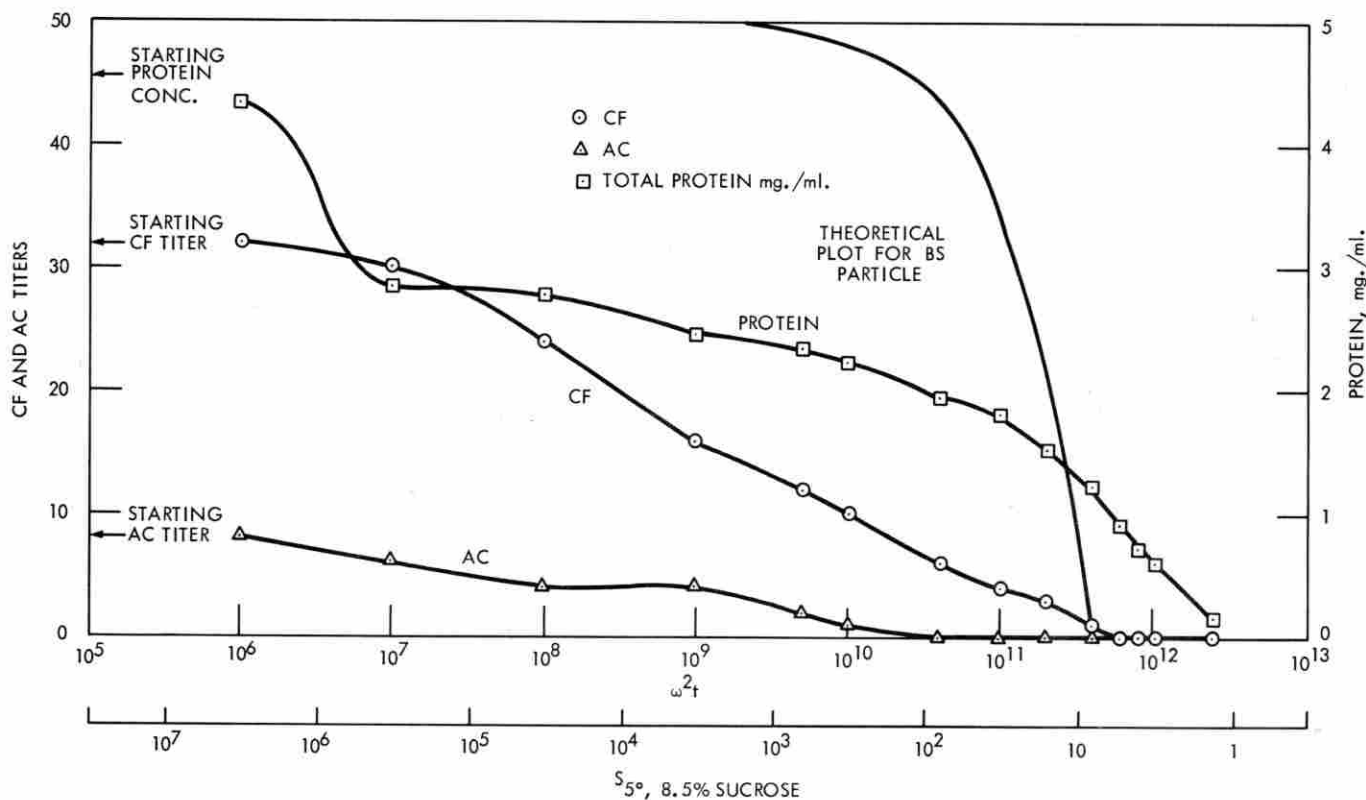


Fig. 3.9 Decrease in total protein, tumor antigen (CF titer against tumor bearing host serum), and anticomplement titer of a fresh adenovirus 31 hamster tumor homogenate as a function of the integral of  $w^2t$ . Theoretical sedimentation of an 8S particle is also shown.

curve with the base line indicates complete removal of the protein or activity from the supernatant. The sedimentation coefficients corresponding to particles completely removed by a given centrifugation step may also be calculated and are indicated below the baseline.

The radius of the meniscus during rotation before and after withdrawal of the 7-ml supernatant sample were 4.88 cm and 6.8 cm respectively. For sedimentation at 1 g a lucite block was drilled to hold tubes inclined at  $26^\circ$  from the horizontal to allow sedimentation to occur at rest in a position geometrically comparable to that occurring during rotation.

### Results

The results obtained with frozen tissue is shown in Figure 3.9, and with fresh tissue in Figure 3.10. The tissue was homogenized using 50 strokes of a Pyrex homogenizer with a teflon pestle. Calculated sedi-

mentation coefficients (corrected to  $20^\circ\text{C}$  and water) are also indicated.

Since no nuclei were observed in supernatants in tubes centrifuged until  $w^2t = 10^7$ , antigen sedimented by this treatment may be considered to be largely nuclear. The amount of antigen sedimenting under these conditions was highly variable, ranging from approximately one third to only a few percent. The difference between the fresh and frozen samples shown in Figures 3.9 and 3.10 was not consistently seen, and the reason for this variability is unknown. The remainder of the sedimentation curve was slightly sigmoidal, sometimes exhibiting a plateau in the region  $w^2t = 10^7 - 10^9$ . The curve then sloped down, reaching the baseline in such a manner as to suggest a very broad distribution of sedimentation coefficients. The distribution suggests that the smallest particles bearing activity have sedimentation coefficients in 8.5% sucrose at  $5^\circ\text{C}$  of approximately 5–8S. For reference, a theoretical plot of the sedimentation of a particle

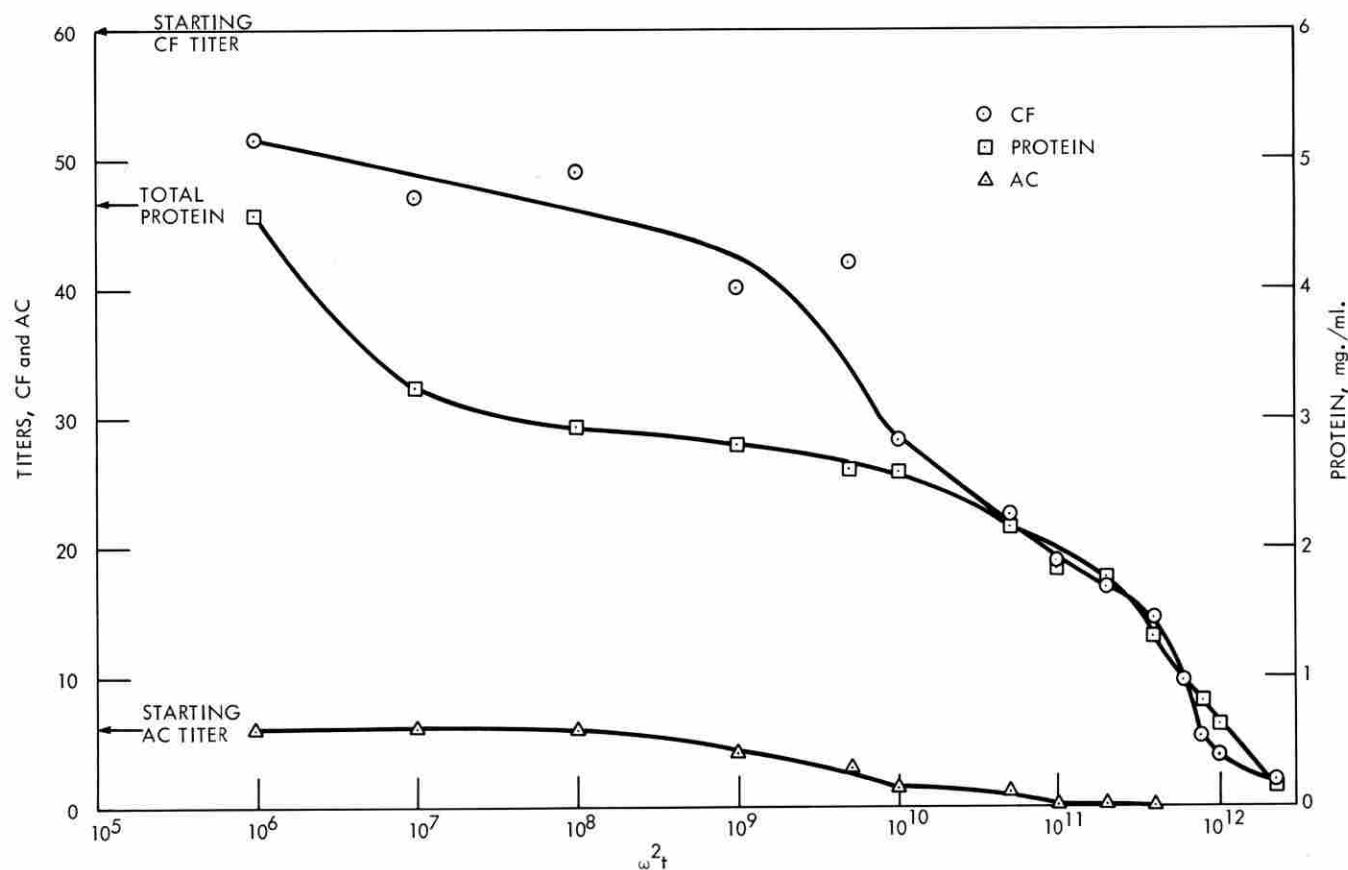


Fig. 3.10 Sedimentation of protein, tumor antigen, and anticomplement in frozen, thawed, and homogenized adenovirus 31 tumor as a function of the integral of  $w^2t$ .

species having a sedimentation coefficient of 8S under these conditions is shown in Figure 3.10 for reference. Some purification of antigen is achieved by discarding the low-speed sediment, however this is not true with all preparations.

Additional experiments were performed using a high-speed mixer in combination with repeated freezing and thawing to determine whether more activity would be observed in smaller particles. A 5% w/v homogenate in 8.5% sucrose was prepared by blending in a Servall Omnimixer two minutes, and alternately slow-freezing, thawing, and blending for two minute periods a total of three times. The homogenate was strained through four layers of cheesecloth before use. The results obtained are shown in Figure 3.11. This treatment appears to release antigen from larger particles including nuclei, but it does not break the particles down to a small homogeneous population.

Differential centrifugation under carefully controlled conditions does not offer promise as a method for purifying adenovirus T antigen. However, it does provide a very simple method of concentrating the activity using high-speed titanium-rotor centrifugation. All the activity is sedimented in 10 hrs at 50,000 rpm, while 80–95% is sedimented in 4 hrs at this speed.

The results show that the antigen is distributed in the homogenate in particles having a very wide spectrum of sedimentation coefficients, possibly extending to 8S or below. It is suggested that the antigen is widely distributed in membranous fragments, and that only a small fraction is in a soluble form.

For future studies it is important to develop a very simple technique for determining whether the antigen has been solubilized. If the free antigen has a sedimentation coefficient of 8S in sucrose at 5°C, then

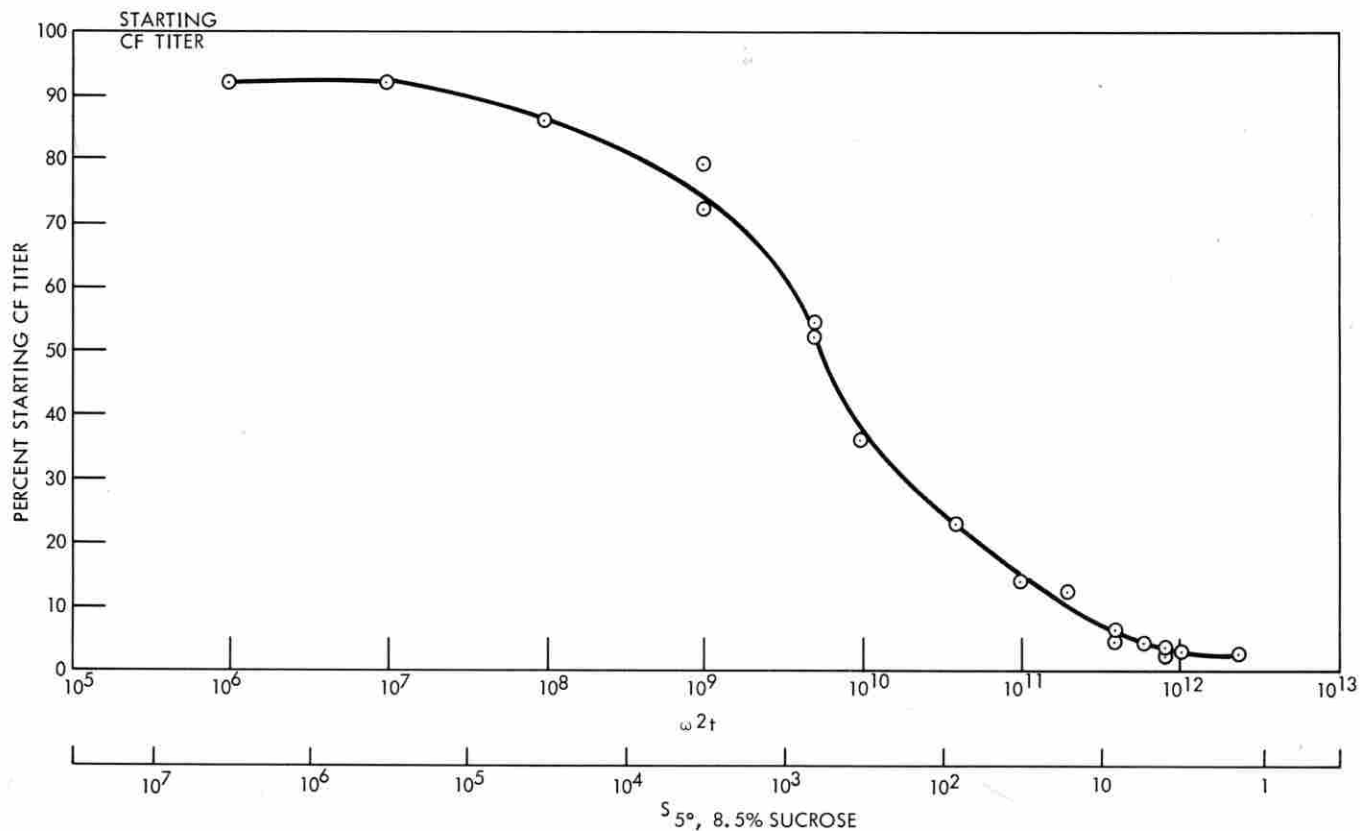


Fig. 3.11 Decrease in supernatant CF titer in repeatedly frozen and thawed adenovirus 31 tumor homogenate as a function of integral of  $w^2t$ .

70% of the activity will remain in the supernatant volume when  $w^2t = 10^{11}$  (1 hr at 50,000 rpm) under the conditions of the experiments described. In the experiments performed to date the percent of complement fixing activity in the supernatant has varied from approximately 2 to 30% of the starting activity.

These studies suggest that the antigen is not confined to a particle having a single sedimentation coefficient. Additional studies in the zonal ultracentrifuge are required to confirm this conclusion.

#### Orienting Studies on The Soluble Phase

Initially soluble extracts of small hamster adenovirus 31 tumors were prepared using the following scheme.

A 20% (w/w) homogenate was prepared in an 0.05 M potassium phosphate buffer at pH 8.2 using frozen tissue. Homogenization was done for three 1-min periods, with 1 min cooling periods interspersed, in

a small Servall stainless steel homogenizer packed in ice. The homogenizer was centrifuged 1 hr at 30,000 rpm in Spinco No. 30 rotors. The supernatant was carefully recovered and frozen until used. The soluble antigen contained an average of 12.7 mg of protein/ml.

#### Isoelectric Precipitation

A fraction of soluble phase proteins are precipitated isoelectrically in the region of pH 5.0.<sup>13</sup> In the first experiment, a 1-ml aliquot of the adenovirus 31 soluble phase was added to 9 ml of a series of cold 0.1 M sodium acetate buffers of varying pH, mixed and centrifuged for 1 hr at 2°C at 2,000 rpm in the International Equipment Co. PR-2 centrifuge using the No. 253 head. In a second experiment 2-ml aliquots of extract and 8 ml of buffer were mixed and allowed to stand 10 mins before centrifugation for 30 mins at 2000 rpm. The supernatants were removed for pH determinations. The tubes were in-

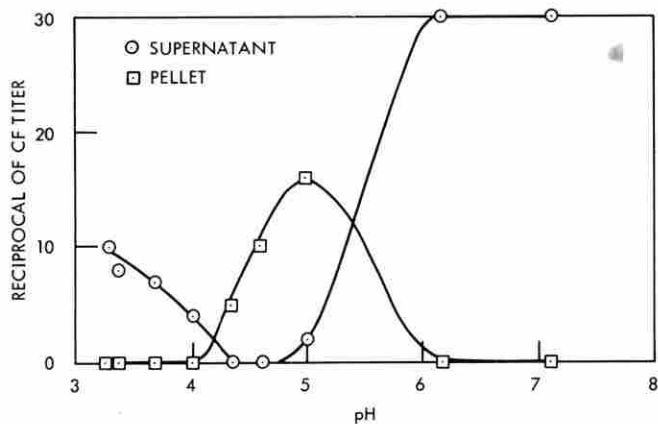


Fig. 3.12 Adenovirus 31 tumor antigen titers in supernatants and pellets as a function of pH.

verted over absorbant paper in the cold and allowed to drain. The pellets from the first experiment were then taken up to 10 ml with 0.1 ionic strength pH 7.5 Miller-Golder buffer and used for protein determinations using the Folin-biuret technique in the Autoanalyzer. In the second experiment the pellets were suspended in VBD. The results are shown in Figures 3.12 and 3.13. Maximum precipitation was

observed at pH 4.5 in both experiments. The re-suspended pellets from the second experiment were assayed for compliment fixing antigen using serum from tumor-bearing animals. The results are included in Figure 3.13. In this experiment only 50% of the antigen was recovered in the isoelectric precipitate at pH 4.97.

These experiments were repeated using the same conditions described in experiment two above. In this instance both the CF titers for the dialyzed supernatant and the resuspended pellet are recorded. It appears that some activity is lost by exposure to pH 3-4. Again half of the activity disappeared in the precipitation at pH 5.0.

#### Ultrafiltration Experiments

Adenovirus T antigens from tissue culture cells have been reported to have a relatively low molecular weight. Since cellophane dialysis tubes under pressure may pass molecules of relatively large size<sup>14</sup> it was of interest to determine whether any compliment-fixing activity would appear in a pressure ultra filtrate. Stretched cellophane has been reported to pass ovalbumin (mol. wt 45,000).<sup>14</sup> A sample of an adeno-

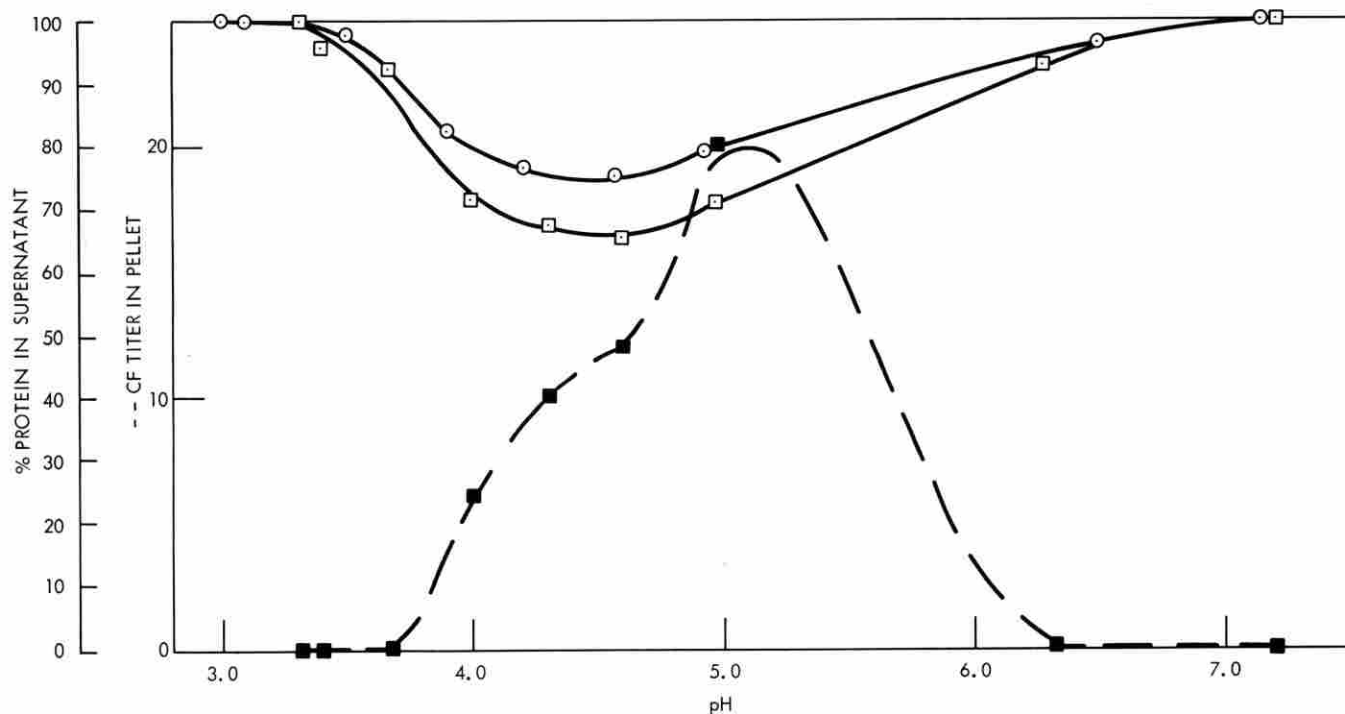


Fig. 3.13 Protein content of adenovirus 31 hamster tumor extract as a function of pH (solid lines, two experiments), and tumor antigen CF titer from one of the experiments (dashed line).

virus 31 tumor extract was filtered under 15 lbs nitrogen pressure overnight in the cold. 160 ml of clear faintly yellow dialysate was obtained. The retentate was made up to 190 ml and  $\mu = 0.1$ , pH 7.5 buffer. As measured by the Folin-Biuret reaction 5.96% of the original protein appeared in the dialysate, of this 17.1% was precipitable by 90% ethanol. All of the CF activity was found in the retentate, no trace of activity being found in the filtrate. Similar results were obtained with an SV40 hamster tumor extract.

## REFERENCES

- <sup>1</sup>P. H. Black, W. P. Rowe, H. C. Turner, and R. J. Huebner. *Proc. Natl. Acad. Sci.* **50**, 1148-1156 (1963).
- <sup>2</sup>R. J. Huebner, W. P. Rowe, H. C. Turner, and W. T. Lane. *Proc. Natl. Acad. Sci. U.S.* **50**, 379-389 (1963).
- <sup>3</sup>Z. Gilead, and H. S. Ginsberg, *J. Bact.* **90**, 120-125 (1965).
- <sup>4</sup>M. D. Hoggan, W. P. Rowe, P. H. Black, and R. J. Huebner. *Proc. Natl. Acad. Sci.* **53**, 12-19 (1965).
- <sup>5</sup>R. J. Huebner, *Perspectives in Virology V.* (Morres Pollard, Ed.) Academic Press, New York. (In Press).
- <sup>6</sup>K. Schell, W. T. Lane, M. J. Casey, and R. J. Huebner, *Proc. Natl. Acad. Sci. U.S.* **55**, 81-83 (1966).
- <sup>7</sup>F. Rapp, J. S. Butel, and J. L. Melnick, *Proc. Soc. Exp. Biol. Med.* **116**, 1131-1135 (1964).
- <sup>8</sup>N. G. Anderson, *Physical Techniques in Biological Research*, Vol. III. *Cells and Tissues.* (G. Oster and A. W. Pollister, Eds.) Academic Press, New York, pp. 299-352 (1956).
- <sup>9</sup>N. G. Anderson, *Anal. Biochem.* in press. (1967).
- <sup>10</sup>John Sever, Personal communication.
- <sup>11</sup>N. Cho, H. P. Barringer, J. W. Amburgey, G. B. Cline, N. G. Anderson, L. L. McCauley, R. H. Stevens, and W. M. Swartout, *J. Natl. Canc. Inst. Monograph* **21**, 485-502 (1966).
- <sup>12</sup>N. G. Anderson, H. P. Barringer, E. F. Babelay, C. E. Nunley, M. J. Bartkus, W. D. Fisher, and C. T. Rankin, Jr., *J. Natl. Canc. Inst. Monograph* **21**, 137-164 (1966).
- <sup>13</sup>N. G. Anderson, *Exptl. Cell Research* **11**, 186-196 (1956).
- <sup>14</sup>L. C. Craig, and T. P. King, *Methods of Biochemical Analysis* **10**, 175-199 (1962).

### E. ISOLATION OF RAT LIVER CELL MEMBRANES BY COMBINED RATE AND ISOPYCNIC ZONAL CENTRIFUGATION

N. G. Anderson                      I. Lieberman  
A. I. Lansing                        C. T. Rankin, Jr.  
H. Elrod

Cell membrane rich fractions from rat liver and other sources have been isolated by a combination of centrifugal methods which depend on sedimentation rate and on isopycnic separations.<sup>1-15</sup> As the pH of the homogenizing medium is raised from pH 5.8 to 7.8,

the efficiency of homogenization under controlled conditions increases, and the amount of cytoplasm attached to cell membranes decreases.<sup>16</sup> In rat-liver homogenates prepared in slightly alkaline hypotonic solutions, a large number of cell membrane fragments may be produced by gentle homogenization which have sufficient size to sediment more rapidly than mitochondria. The initial centrifugal procedures which have been used separate membranes and nuclei from the majority of lysosomes and mitochondria on a rate basis first using swinging-bucket or angle-head rotors. This step may be repeated several times. To separate the membranes from nuclei the preparation is then banded isopycnicly in a sucrose gradient. The yields vary and are reported to be quite low, i.e., most of the membranes are lost in the isolation process. The major source of loss appears to be in the initial differential centrifugation steps since this separation would not be expected to be quantitative even if the sedimentation coefficients of mitochondria and cell membranes did not overlap. Since smaller membrane fragments do overlap the sedimentation coefficient spectrum of mitochondria the low yield observed would be expected.

Using the A-XII low-speed zonal centrifuge rotor<sup>17</sup> it has recently been shown that liver-cell membranes could be sedimented as a band which occupied a position intermediate between nuclei and mitochondria,<sup>11</sup> confirming the view that cell membrane fragments tend, for the most part, to sediment faster than mitochondria.

Since most of the separation methods described depend on rate sedimentation followed by isopycnic banding, it appeared of interest to explore the possibility of achieving both a high-resolution-rate zonal separation and an isopycnic separation sequentially in the same rotor. The B-XV titanium zonal rotor recently described<sup>18</sup> has a capacity of 1666 ml, and can be adapted to both rate zonal and isopycnic zonal separations.

### Basis of Separations

Both mitochondria and cell membrane fractions are heterogeneous with respect to their sedimentation properties. However the mean sedimentation coefficients appear to differ widely. The degree of overlap is unknown, however, and may depend on the method of homogenate preparation, i.e., on whether the membranes in the initial homogenate are broken down into

large or small fragments. If a clean separation of cell membranes from mitochondria, lysosomes, microbodies and endoplasmic reticulum fragments can be made in a zonal centrifuge rotor, then the centripetal portion of the gradient may be removed and replaced with a particle-free solution. The rotor may then be spun for a prolonged period of time to band the membranes sharply at their isopycnic points. Nuclei and nuclear fragments would be centrifuged to the rotor wall since their banding density exceeds the density of the centrifugal end of the sucrose gradient.

### Rate Zonal Separation of Mitochondria and Membranes

**Preparation of homogenates.**— Fresh unperfused rat liver from male Sprague-Dawley rats was diced with a scissors in cold 0.001 M  $\text{NaH}_2\text{CO}_3$  adjusted to pH 7.6 with NaOH, and homogenized in a loose-fitting Dounce-type homogenizer. Fifteen even strokes were

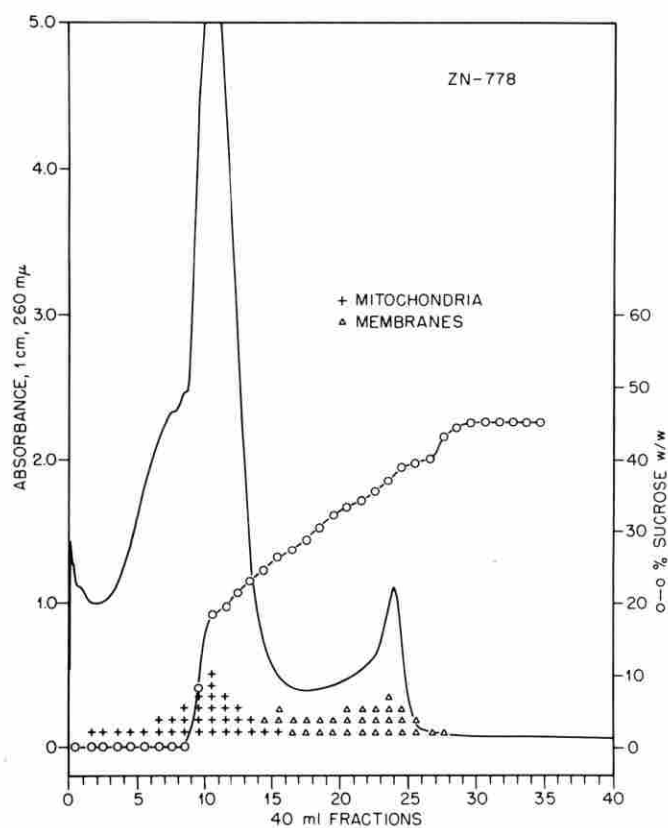


Fig. 3.14 Rate zonal separation of rat liver cell membranes in a sucrose gradient in the BXV titanium rotor. Relative quantities of mitochondria (+) and membranes ( $\Delta$ ) in recovered fractions as judged by phase contrast microscopy.

used with each liver sample. The homogenate was diluted to a final volume of 30-ml-per-gram of liver and centrifuged for 15 min at 27,000 spin at 0°C in an International Equipment Company PR-2 centrifuge using 250 ml Pyrex tubes in the No. 259 head. The supernatant was removed by gentle suction and discarded. The pellet was resuspended in 200 ml of 0.001 M bicarbonate buffer and used as the sample suspension for zonal centrifugation.

**Zonal Centrifugation.**— A B-XV titanium zonal rotor was operated in a modified Spinco Model L centrifuge equipped with the temperature sensing and controlling device and  $\int w^2 dt$  integrator previously described.<sup>19</sup> Gradients were formed in a Spinco Model 131 gradient pump or in an exponential mixer designed for use with zonal rotors.<sup>20</sup> Rotor effluents were collected in either 40- or 10-ml fractions. Sucrose concentrations were determined refractometrically. Absorbance of the effluent stream was measured as previously described.<sup>19</sup> Equivalent sedimentation co-

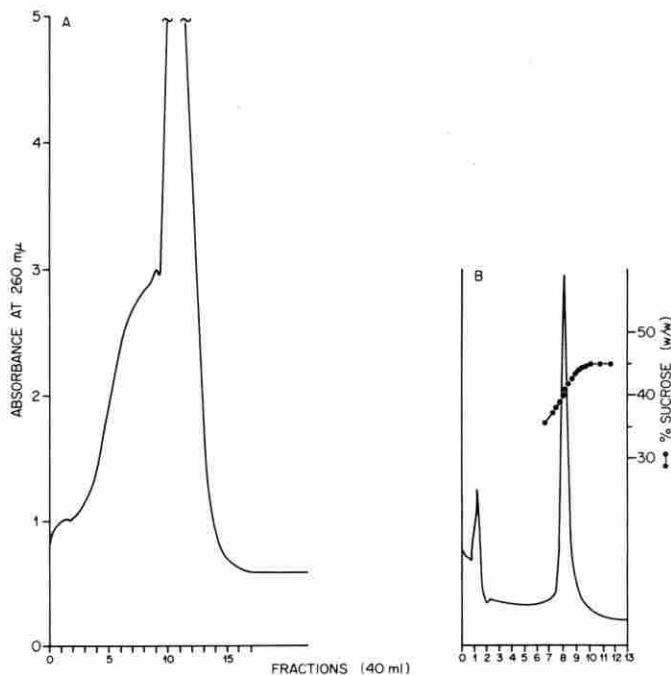


Fig. 3.15 Two-stage separation of rat liver cell membranes. A. Overlay, sample layer, and part of gradient recovered after short rate zonal centrifugation.

Overlay: 50 ml 0.001 M  $\text{NaHCO}_3$ .

Sample: 200 ml resuspended crude membrane fraction.

Gradient: 500 ml 19–35% sucrose (w/w).

Cushion: 45% sucrose (w/w).

Centrifugation:  $2.11 \times 10^8 W^2t$ .

B. Banded cell membranes after centrifuging until  $w^2t = 6 \times 10^9$ . Membranes banded sharply at 40.8% sucrose (w/w).

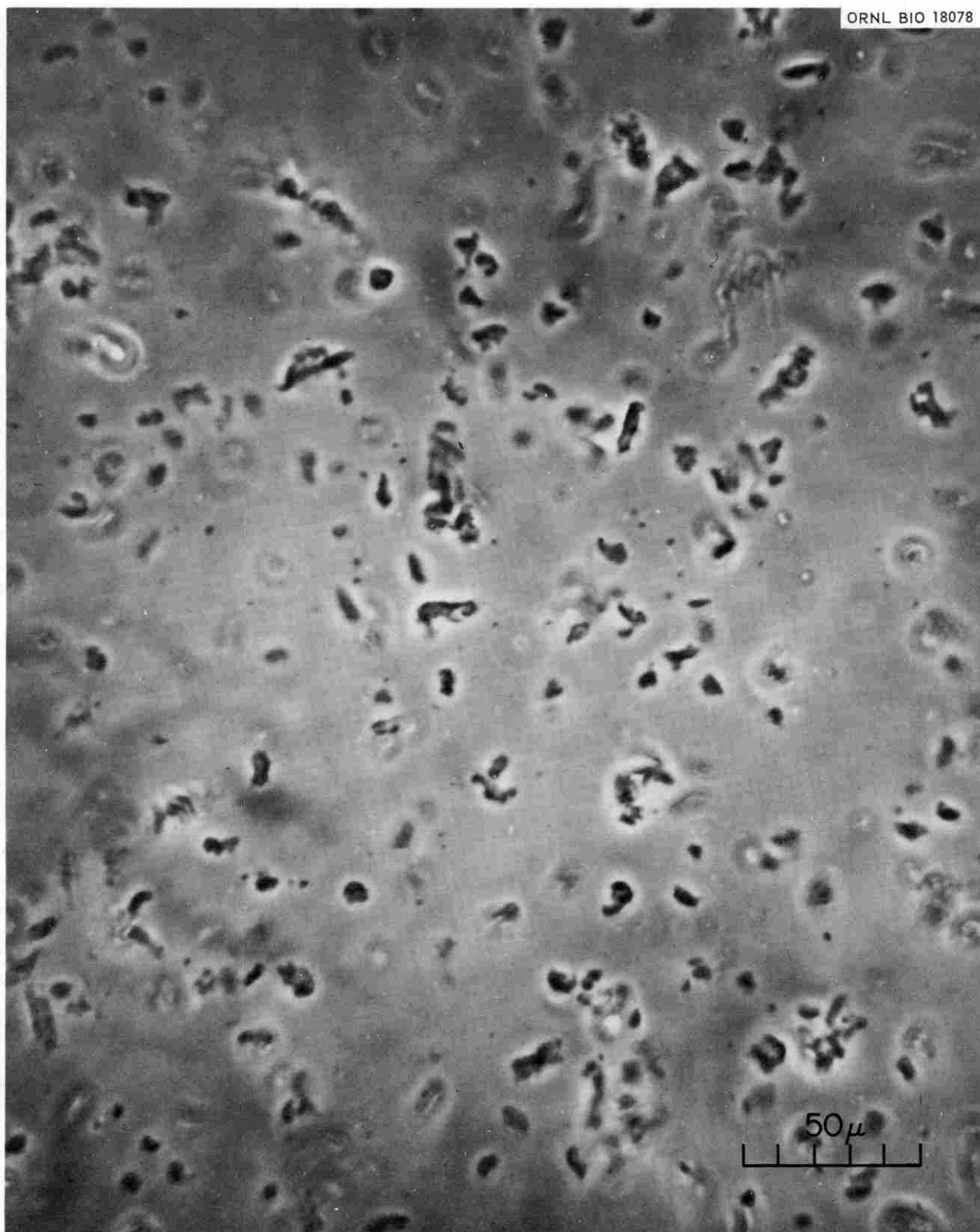


Fig. 3.16 Phase contrast micrograph of cell membranes isolated in the BXV titanium rotor by the method described in the text. (ZU 768 Fraction 15).

efficients were determined using a computer program which incorporated equations for determining the density and viscosity of sucrose solutions at the temperature used for the experiment.

**Calculation of Sedimentation Coefficients.**—Sedimentation coefficients were approximated from the initial preparative centrifugation steps. Microscopic examination of the supernatant after centrifugation in the No. 259 International showed that not all of the membranes were sedimented after 15 min at 2700 rpm. Using maximum and minimum radii of 23 and 13 cm and the equation

$$s = \frac{1}{\omega^2 t} \ln \frac{R^{\max}}{R^{\min}}$$

a membrane that traversed the length of the tube would have a sedimentation coefficient of  $7.9 \times 10^4 S$  at  $5^\circ$  in the medium used.

This value is greater than that calculated for mitochondria.<sup>21</sup> In addition it should be noted that mitochondria in a hypotonic media are swollen and would sediment more slowly than intact mitochondria in a more physiological suspending medium.

**Experimental Studies.**—A series of twenty-six experiments were performed to develop the method and to provide membrane preparations for lipid analyses. The first problem was to determine the centrifugation procedure for sedimenting membranes away from mitochondria, and the volume of fluid including overlay, sample layer, and the light end of the gradient to be removed in the initial step.

A membrane suspension (190 ml) was layered over a sucrose gradient (19–35% w/w sucrose, 500 ml) and followed by an overlay (200 ml of .001 M NaHCO<sub>3</sub>), and centrifuged at 5000 rpm until  $\omega^2 t = 2 \times 10^8$ . The rotor was then unloaded and the relative amounts of mitochondria (visible granules) and cell membranes then scored by phase contrast microscopy. The results are shown in Figure 3.14. It was concluded that by unloading the first 750 ml (18 $\frac{3}{4}$ –40 ml fractions) the bulk of the soluble, microsomal, and mitochondrial mass would be separated from the membranes. This procedure was found to be reproducible with liver preparations. An example is shown in Figure 3.15.

After removal of the centripetal 750 ml the rotor was accelerated to 20,000 rpm and run until  $\omega^2 t = 3.5 \times 10^9$  at unloading. The membrane fragments were found to be sharply banded at an average of 41.04% (w/w) sucrose. (Experimental values were 40.2, 40.8, 40.8, 41.2, 40.8, 41.9, and 41.6). Observation of the banded membranes in the phase contrast micro-

scope revealed that very few visible granules were present (Figure 3.16). Electron microscopy confirmed the high purity of the preparation.

## REFERENCES

- <sup>1</sup>D. M. Neville, Jr., *J. Biophys. Biochem. Cytol.* **8**, 413–422 (1960)
- <sup>2</sup>T. Kono, and S. P. Colowick, *Arch. Biochem. Biophys.* **93**, 520–533 (1961).
- <sup>3</sup>E. Tria, and O. Barnabei, *Nature* **197**, 598–599 (1963).
- <sup>4</sup>C. H. O'Neill, *Exp. Cell Res.* **35**, 477–496 (1964).
- <sup>5</sup>P. Emmelot, C. J. Boss, E. Benedetti, and Ph. Rümke, *Biochem. Biophys. Acta* **90**, 126–145 (1964).
- <sup>6</sup>S. Razin, H. J. Morowitz, and T. M. Terry, *Proc. Natl. Acad. Sci. U.S.A.* **54**, 219–225 (1965).
- <sup>7</sup>M. Tackeuchi, and H. Terayama, *Exp. Cell Res.* **40**, 32–44 (1965).
- <sup>8</sup>V. P. Skipski, M. Barclay, F. M. Archibald, O. Terebus-Kekish, E. S. Reichman, and J. J. Good, *Life Sciences* **4**, 1673–1680 (1965).
- <sup>9</sup>V. Kamat, and D. F. H. Wallach, *Science* **148**, 1343–1345 (1965).
- <sup>10</sup>A. I. Lansing, and W. K. Zollinger, *Biol. Bull.* **129**, 411 (1965).
- <sup>11</sup>A. A. El-Aaser, J. T. R. Fitzsimons, R. H. Hinton, E. Reid, E. Klucis, and P. Alexander, *Biochem. Biophys. Acta* **127**, 553–556 (1966).
- <sup>12</sup>L. Warren, M. C. Glick, and M. K. Nass, *The Specificity of Cell Surfaces*. (B. D. Davis and L. Warren, Eds.) Prentice-Hall, Englewood Cliffs, N. Y., pp. 109–127 (1967).
- <sup>13</sup>C. S. Song, and O. Bodansky, *J. Biol. Chem.* **242**, 694–699 (1967).
- <sup>14</sup>L. Warren, M. C. Glick, and M. K. Nass, *J. Cel. Physiol.* **68**, 269–288 (1966).
- <sup>15</sup>I. Lieberman, A. I. Lansing, and W. E. Lynch, *J. Biol. Chem.* **242**, 736–739 (1966).
- <sup>16</sup>N. G. Anderson, *Exp. Cell Res.* **8**, 91–100 (1955).
- <sup>17</sup>N. G. Anderson, H. P. Barringer, N. Cho, C. E. Nunley, E. F. Babelay, R. E. Canning, and C. T. Rankin, Jr., *Natl. Cancer Inst. Monograph* **21**, 113–136 (1966).
- <sup>18</sup>N. G. Anderson, D. A. Waters, W. D. Fisher, C. E. Nunley, L. H. Elrod, and C. T. Rankin, Jr., *Anal. Biochem.*, in press (1967).
- <sup>19</sup>N. G. Anderson, H. P. Barringer, E. F. Babelay, C. E. Nunley, M. J. Bartkus, W. D. Fisher, and C. T. Rankin, Jr. (N. G. Anderson, Ed.), *J. Natl. Cancer Inst. Monograph* **21**, 137–164 (1966).
- <sup>20</sup>N. G. Anderson, and E. Rutenberg, *Analytical Techniques for Cell Fractions. VII. A simple gradient forming apparatus* (1967), *Anal. Biochem.*, in press.
- <sup>21</sup>N. G. Anderson, *Science* **154**, 103–112 (1966).

## F. IMPROVEMENT OF METHODS FOR MACROGLOBULIN ISOLATION IN B-XIV, B-XV, AND B-XXVII ROTORS

C. T. Rankin, Jr.                      N. G. Anderson  
W. L. Rasmussen

Macroglobulins including immunoglobulins,  $\alpha_2$  globulins, and abnormal macroglobulins are associated with several pathological conditions. Recently, centrifugally-isolated mouse and rat macroglobulins have been shown to reduce mortality in mice when injected

after irradiation, and to markedly increase spleen colony formation in irradiated mice injected with isologous bone marrow.<sup>1</sup> If these observations are to be extended to man, much larger amounts of macroglobulin will be required than are presently available. Our attention has therefore been directed to the problem of increasing the yield of macroglobulins in zonal centrifuge rotors using the B-XIV and XV rotors previously described,<sup>2</sup> and the B-XXVII modification described here.

### Experimental Studies

To achieve a separation of macroglobulin from human plasma in the B-XV titanium zonal centrifuge rotor, the starting zone must be moved well out into the rotor. This places the sample in a higher centrifugal field, reducing the time for separating particles with low sedimentation rates and minimizing diffusion.

To insure purity of the macroglobulin, a clear zone must occur between the 7S gamma globulin and the macroglobulin. If the amount of plasma to be fractionated is increased, the recovery zone is correspondingly widened. This width increase is acceptable until the trailing edge of the macroglobulin zone overlaps with the 7S zone or the leading edge reaches the rotor wall.

The method for separating macroglobulin in the titanium B-XV rotor<sup>3</sup> was found to be effective for sample volumes of approximately 25 mls when human plasma was used as starting sample. To achieve a separation in 17 hr or  $4.250 \times 10^{11} w^2t$ , an overlay of 700 mls was required to start the sample zone at the correct radius. 700 mls of overlay plus 25 mls of plasma displaced enough of the 1000 ml linear with volume gradient (10% to 22% w/w% sucrose dissolved in Miller-Golder buffer pH 7.5  $\mu$ 0.2) (ref. 4) to leave in the rotor a gradient 10-20% with no cushion. (Gradi-

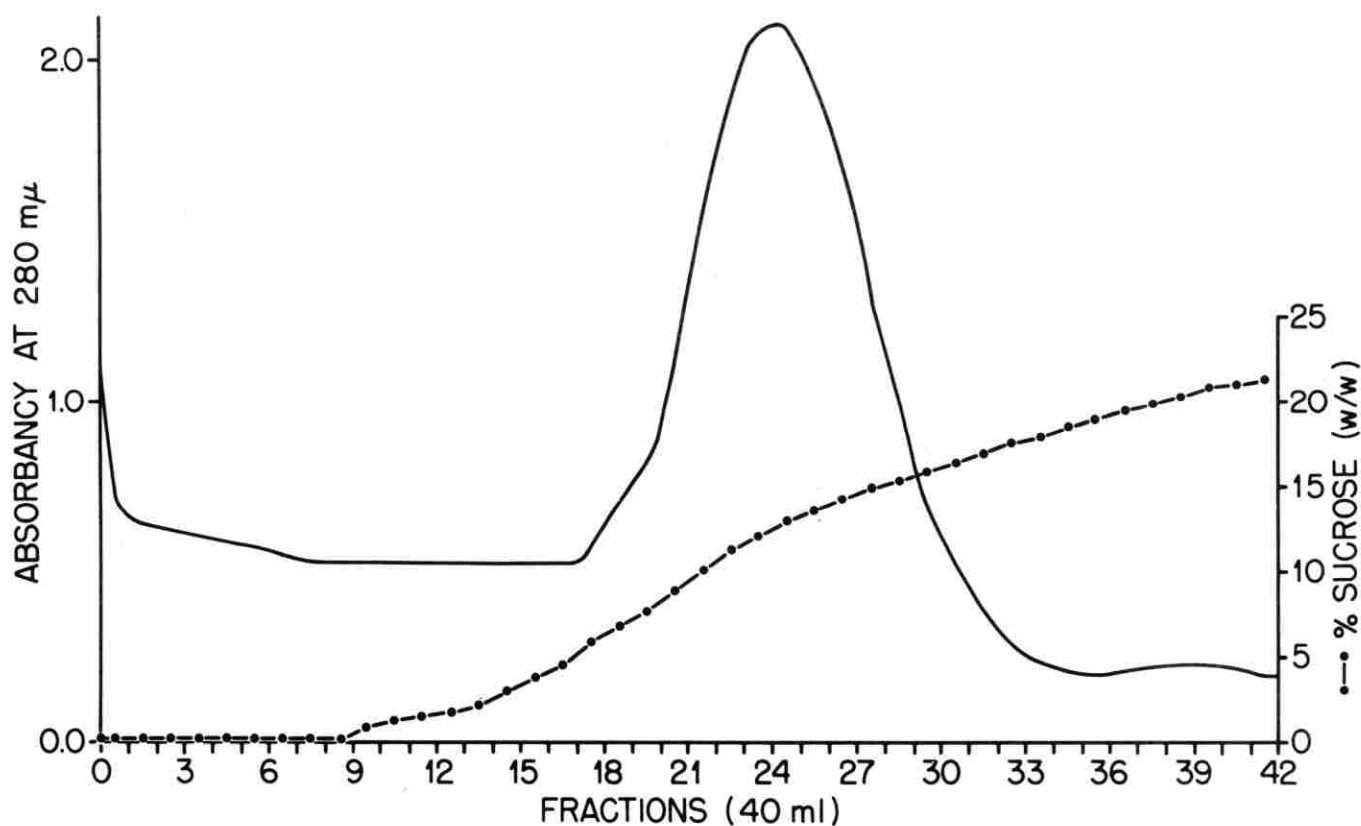


Fig. 3.17 Rate zonal separation of human plasma macroglobulin in the BXV titanium rotor.  
 Sample volume: 25 ml undiluted plasma.  
 Gradient: 1 liter, 10-22% sucrose containing 0.2 ionic strength Miller-Golder buffer, pH 7.5.  
 Overlay: 700 ml Miller-Golder buffer.  
 Centrifugation:  $w^2t = 4.26 \times 10^{11}$ , 5°C.

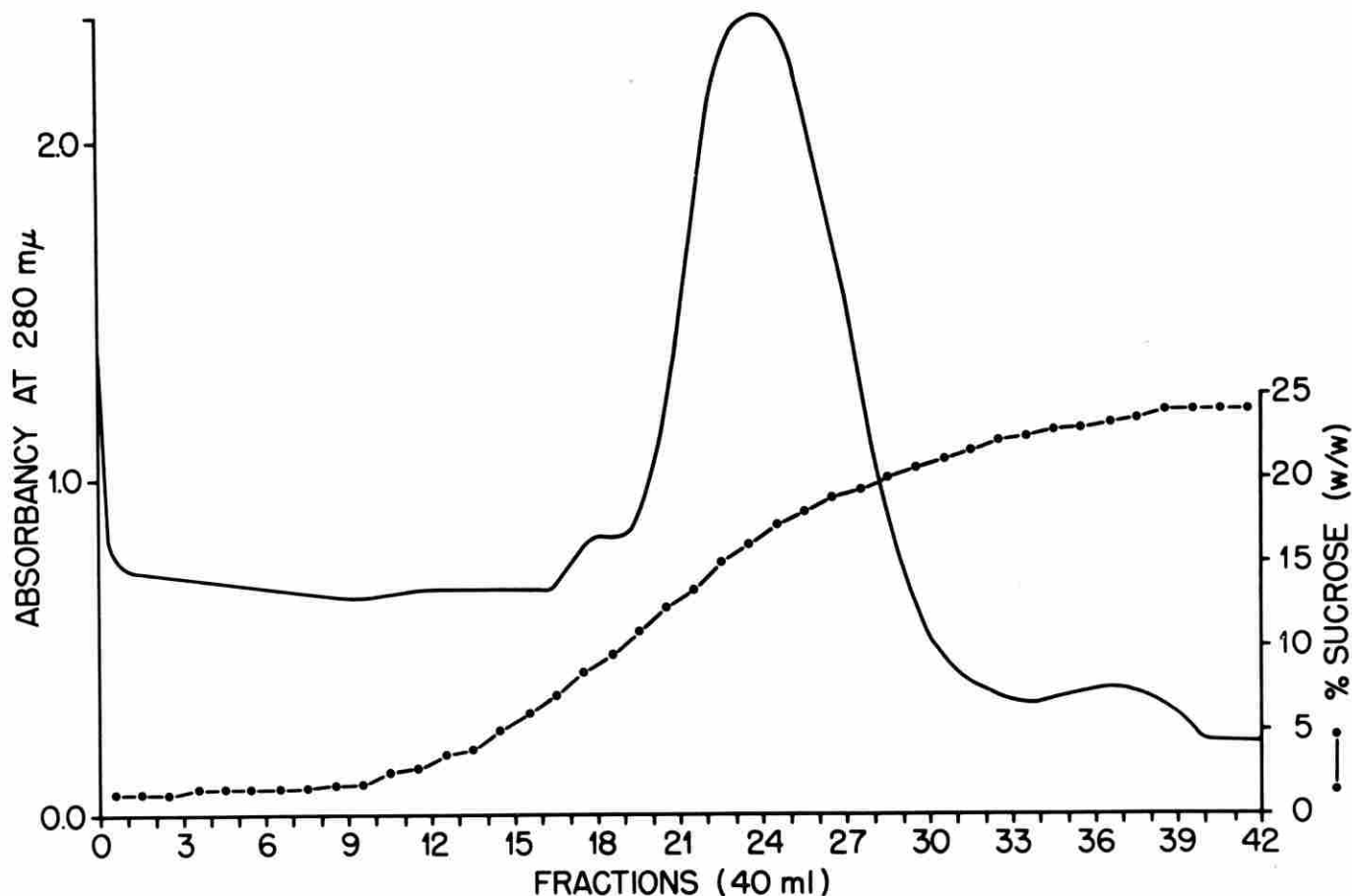


Fig. 3.18 Rate zonal separation of human plasma macroglobulin in the BXV titanium rotor. Sample volume: 25 ml undiluted plasma. Gradient: 500 ml, 10–23.5% sucrose w/w, containing 0.2 ionic strength Miller-Golder buffer. Overlay: 700 ml Miller-Golder buffer. Centrifugation:  $w^2t = 4.28 \times 10^{11}$ , 5°C.

ent pump Model 131 obtained from Spinco Division of Beckman Instruments, Inc.) This method placed severe limitations on the radial distance available for the macroglobulin fraction between the overlapping 7S  $\gamma$  globulin and the rotor wall (Figure 3.17, ZU-877).

To increase the volume of plasma that could be used as a starting sample, this zone must either be widened or the capacity of the gradient increased. Increasing the gradient capacity seemed more desirable since the macroglobulin could then be recovered in a smaller volume. To do this the gradient was changed to 500-ml linear with volume, extending from 10% to 23.5% w/w sucrose dissolved in Miller-Golder buffer pH 7.5  $\mu = 0.2$ .<sup>4</sup> This steeper gradient, while increasing the carrying capacity,<sup>5,6</sup> also allowed the entire

gradient plus 440 mls of a 23.5% sucrose cushion to remain in the rotor when 700 mls of overlay and a 25 ml sample was used (Figure 3.18, ZU-876). The 440-ml cushion also made it possible to increase plasma volume and still maintain the entire gradient in the rotor. The starting plasma volume was now increased by 10 to 20 mls per run until 100 mls was used as starting sample. When the sample volume exceeded 70 mls the overlap of 7S and macroglobulin zone made the separation unacceptable. By redesigning gradients and adjusting run time we have not been able to improve on the separation. 70 mls of human plasma as a starting sample therefore appears to be the upper-limit for separating macroglobulin in the titanium B-XV rotor with these run conditions (Figure 3.19,

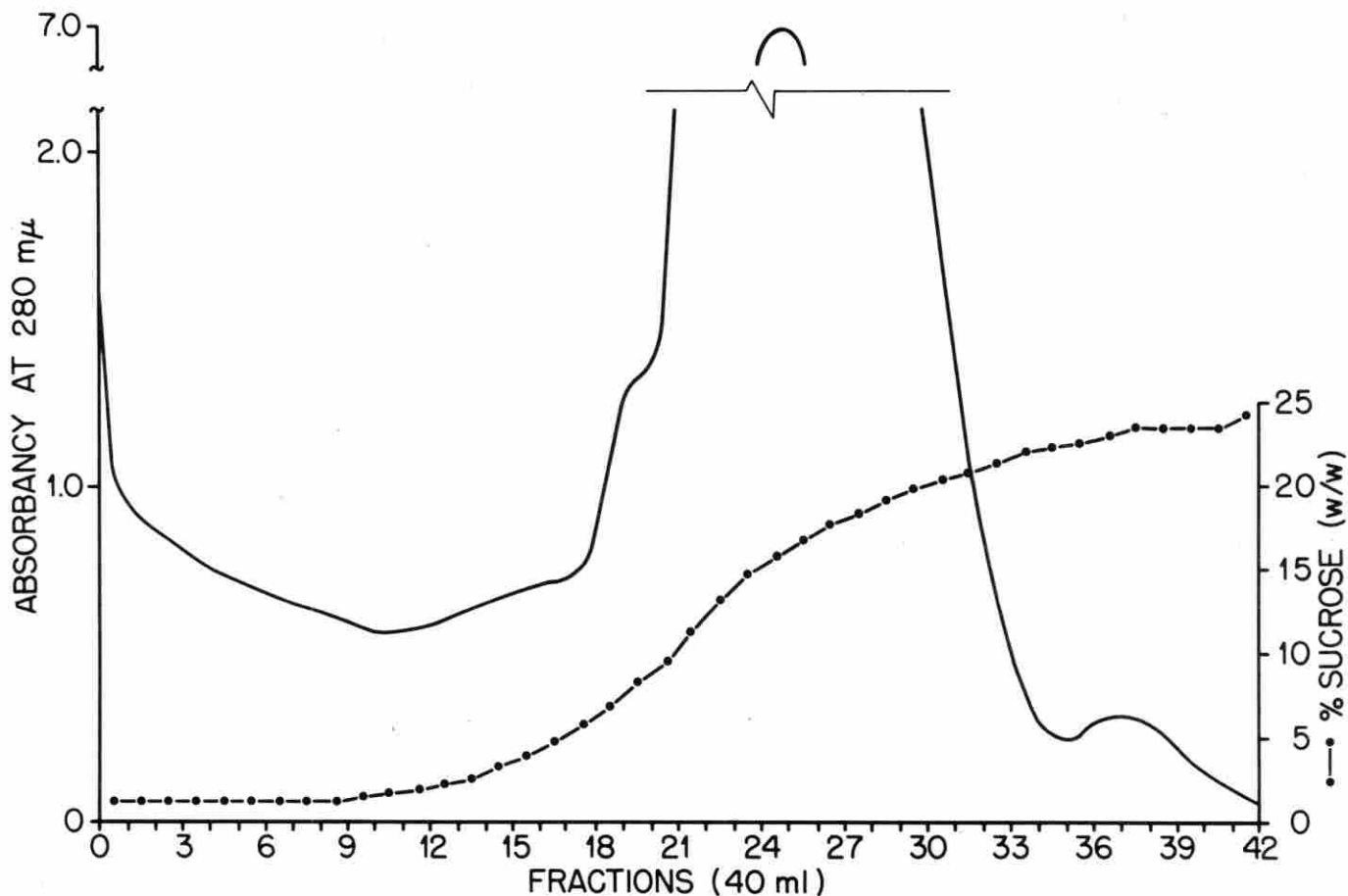


Fig. 3.19 Rate zonal separation of human plasma macroglobulin in the BXV titanium zonal rotor.  
 Sample volume: 70 ml undiluted plasma.  
 Gradient: 500 ml, 10–23.5% sucrose w/w with 0.2 ionic strength Miller-Golder buffer.  
 Overlay: 700 ml Miller-Golder buffer.  
 Centrifugation:  $w^2t = 4.52 \times 10^{11}$ , 5°C.

ZU-879). A composite sample of fractions 36–42 was examined in the Analytical Ultracentrifuge (Figure 3.20). It shows that the peak marked “M” in Figure 3.19 is pure macroglobulin. With identical run conditions, the titanium B-XV rotor has been used to separate macroglobulin from calf, rat, hamster, and mouse serum with comparable results.

The titanium B-XIV zonal centrifuge rotor<sup>2</sup> has been used to separate macroglobulin from human plasma samples of only five ml. (140 ml overlay; 500 ml, linear with radius gradient, extending from 10% to 25% sucrose; run to  $5.70 \times 10^{11} w^2t$ .)

The B-XIV and B-XV can therefore be used to recover macroglobulin from starting samples of 5 to 70 ml of plasma. The macroglobulin fractions are not

contaminated with 7S particles (Figure 3.20) and recovery is about 94%.

Since the peak (“M” in Figure 3.19) represents only 67.2 mg of recovered macroglobulin, the problem of efficient preconcentration was attacked. Macroglobulins from different species vary in their response to pelleting in a preparative ultracentrifuge. Macroglobulin from mouse, for example, does not resuspend to give a centrifugally homogeneous solution. The effect of sedimentation on human macroglobulin in the Beckman No. 30 rotor was therefore examined.

400 mls of human plasma was placed in No. 30 polycarbonate blow molded tubes<sup>7</sup> and spun in the Beckman No. 30 rotor for 19 hr at 28,500 rpm. The supernatant was removed to the round bottom of the

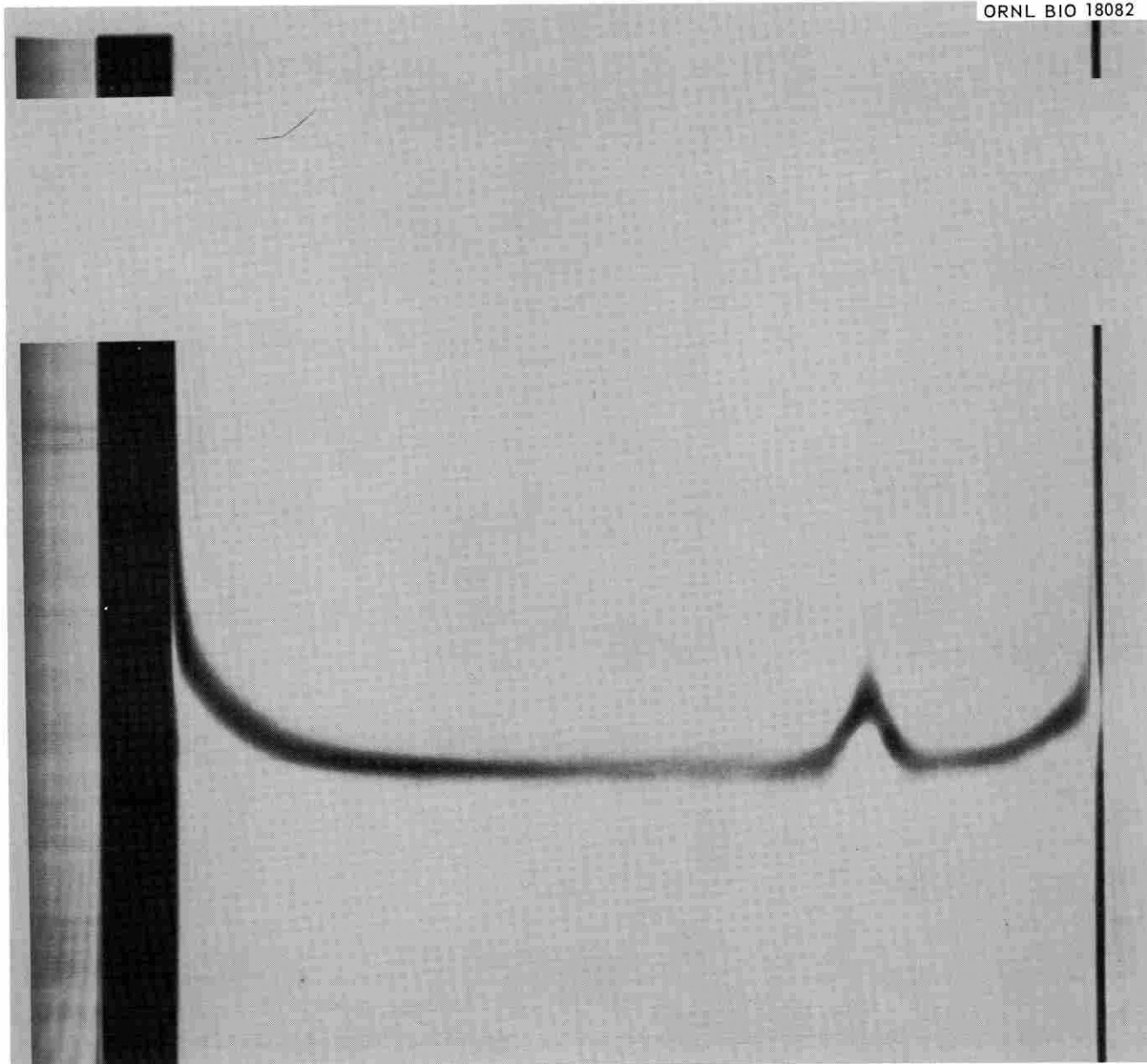


Fig. 3.20 Analytical ultracentrifuge diagram of human plasma macroglobulin, fractions 36-42 from ZU 879 (Figure 3).  $S = 18.56 \pm .07$ . Concentration = 0.239 mgm/ml.

tube. The remaining supernatant and the pellet was resuspended in Miller-Golder buffer pH 7.5  $\mu = 0.2$  (ref. 4) to which methiolate 1:10,000 had been added. A small amount of albumin and gamma globulin contamination is seen in the resuspended macroglobulin as shown in Figure 3.21.

The problem of pelleting large amounts of macroglobulin in a zonal rotor was therefore examined. The B-XIV rotor was modified as shown in Figure 3.22. (This modification is designated B-XXVII.) The edge lines through the septa were opened to the chamber at a point 0.5 cm from the inner rotor wall and the

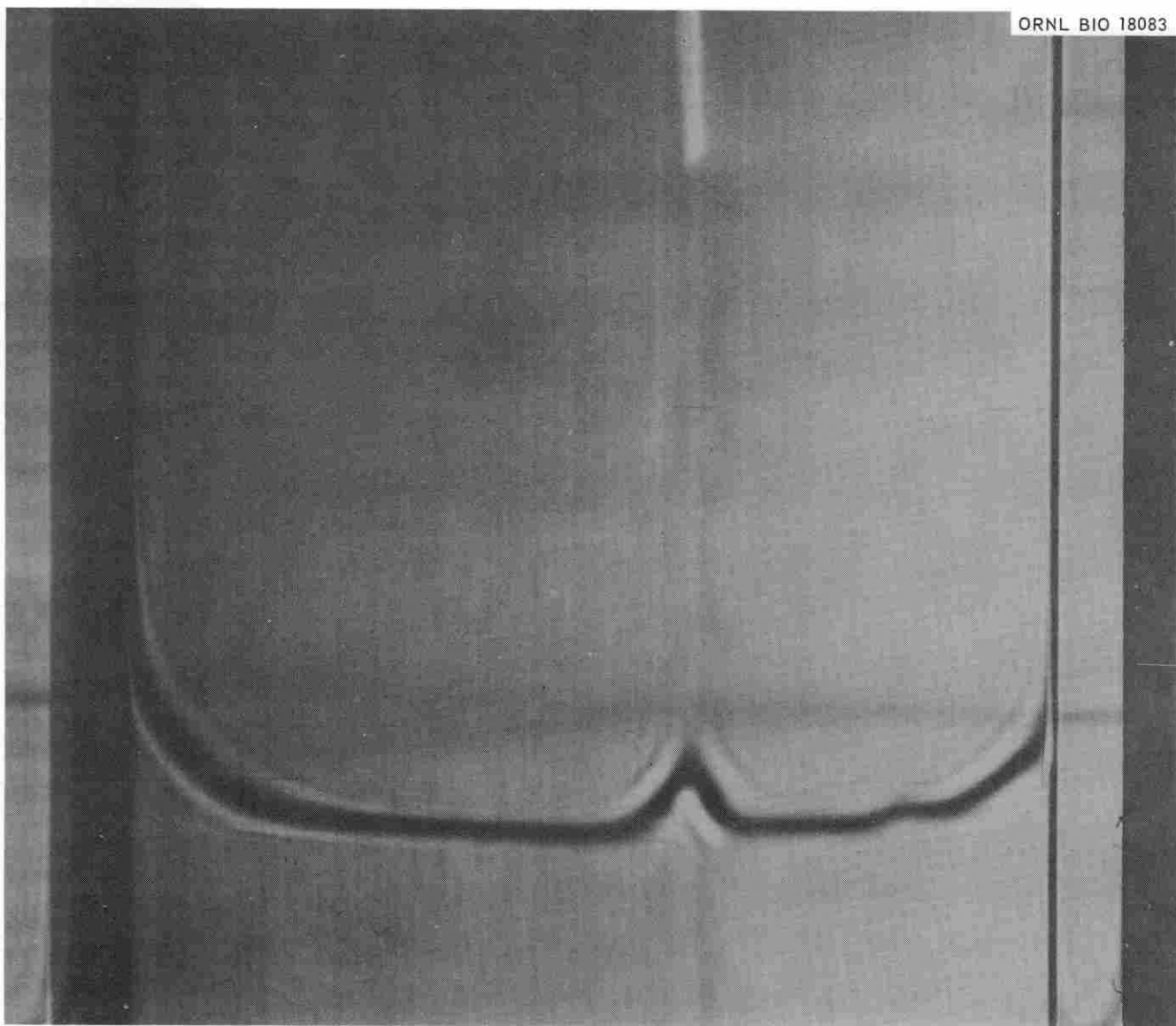


Fig. 3.21 Analytical ultracentrifuge diagram of pelleted human plasma macroglobulin.  $S = 17.52 \pm 0.02$ . Concentration = 0.625 mg/ml.

section of the edge line remaining between these cross openings and the wall was filled with an epoxy resin. The objective was to allow the contents of the rotor to be forced out by air pressure introduced to the rotor center without disturbing the pelleted protein. The volume remaining in the rotor is 100 ml. It would thus be possible to pellet sequentially several batches of macroglobulin without disassembling the

rotor. Using the equation (refs. 8, 9):

$$S = \frac{1}{-2w^2t} \ln \left[ \frac{R_1^2}{R_2^2} + \frac{C_t}{C_0} \left( 1 - \frac{R_1^2}{R_2^2} \right) \right]$$

with values of  $R_1 = 2.665$  cms and  $R_2 = 6.100$  cms, and 8.96S for macroglobulin in undiluted plasma; the value obtained for  $w^2t$  is  $9.240 \times 10^{11}$ . This should move 100% of the macroglobulin past the crossover

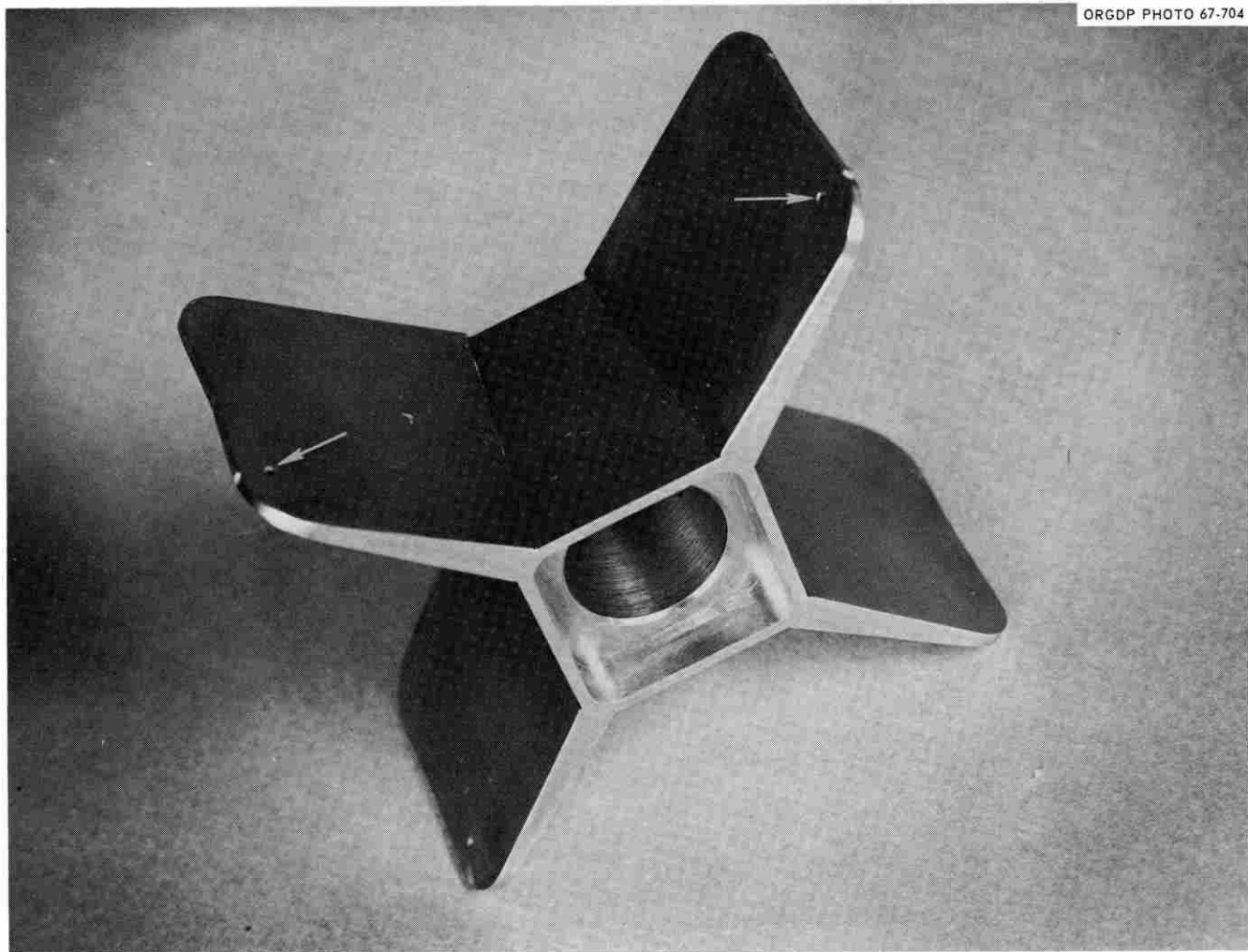


Fig. 3.22 View from below of core BXVII showing cross holes in edge lines in septa (see arrows). The rotor was used to sediment macroglobulin to the rotor wall, supernatant plasma inboard of the cross holes was displaced out of the rotor with a light buffer.

holes in the edge line and allow it to remain in the rotor as a pellet on the rotor wall or as part of the 100-ml retained volume.

To evaluate the B-XXVII zonal centrifuge rotor, it was loaded with 603 ml of human plasma and 40 ml of overlay (Miller-Golder buffer, pH 7.5,  $\mu = 0.2$ ) was added to make  $R_1 = 2.665$  cms. The rotor was run at 25,000 rpm to  $9.2498 \times 10^{11} w^2t$ . The speed was reduced to 3000 rpm and 10 psig of air pressure was introduced to the center of the rotor. Contents of the rotor, inboard of the crossover holes in the edge line, were displaced and collected. When examined in the analytical ultracentrifuge, the supernatant contained no macroglobulin. Miller-Golder buffer (pH 7.5,

$\mu 0.2$ ) = 1:10,000 merthiolate was added to the 100 ml retained in the rotor and the pellet was resuspended, this total volume was reduced to 70 ml by pressure dialysis. 86.3% of the macroglobulin in the starting volume was found to have been sedimented and resuspended. A similar run was made which produced 90 ml of resuspended macroglobulin.

This 160 ml of resuspended human macroglobulin was used as starting samples to determine the maximum production of centrifugally homogenous macroglobulin with the B-XV and B-XXVII zonal centrifuge rotor combination. Using the same gradient and run conditions as for plasma, we introduced samples of 7 mls to 25 mls of the resuspended macroglobulin.

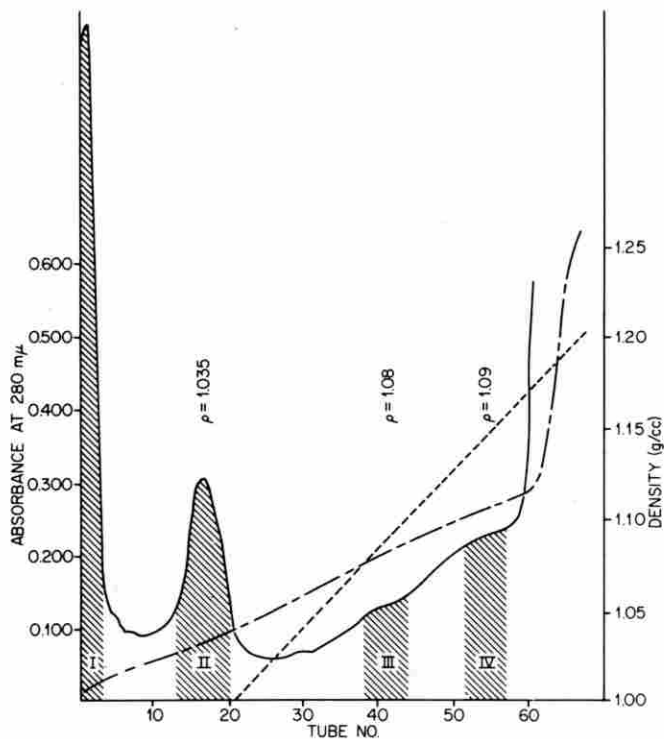


Fig. 3.23 Isopycnic separation of human serum lipoproteins in a sucrose-KBr gradient. The ratio of sucrose to KBr was 2:1 by weight. The ratio of cholesterol esters to cholesterol in the various fractions is given in Table 3.6.

When the macroglobulin content of the sample approximated the macroglobulin content of 70 mls of plasma, the overlap with 7S  $\gamma$  globulin made the separation unacceptable. Increasing the run time to 20 hr or  $5.00 \times 10^{11}$  allowed the leading edge of the sedimenting macroglobulin to reach the rotor wall without a complete separation from the 7S  $\gamma$  globulin. By decreasing the overlay from 700 mls to 600 mls and adding 100 mls of 23.5% w/w sucrose cushion and running to  $5.0 \times 10^{11}$   $w^2t$  we could prevent the macroglobulin from sedimenting to the rotor wall. This also improved the separation between globulin and macroglobulin. By adjusting the overlay volume and redesigning gradients, while keeping the run time less than 22 hr, we were not successful in isolating pure macroglobulin from pre-concentrated human macroglobulin when the sample contained appreciably more than the 70-90 mg in 70 ml of concentrate.

The theoretical capacity of the gradient in the region where the macroglobulin was recovered was calculated to be 98.6 mg.<sup>10</sup> We have succeeded in these experi-

ments in achieving approximately 80% of the theoretical capacity.

Gradients of higher carrying capacity could be used to increase the amount of macroglobulin that can be isolated in the B-XV zonal centrifuge rotor. This would require sucrose of higher concentration and viscosity to increase the gradient slope and correspondingly longer run times or higher-speed rotors. We did not pursue this possibility because we were interested in the highest macroglobulin production with the most economical use of time and present hardware. Our conclusion is that the gradient described with 70 mls of plasma as the sample run to  $4.25 \times 10^{11}$   $w^2t$  represents the optimum method for isolating pure human macroglobulin with our present equipment.

## REFERENCES

- <sup>1</sup> M. G. Hanna, Jr., P. Nettesheim, W. D. Fisher, Leona Peters, and Mary W. Francis, "A Serum Macroglobulin: Survival and Recovery Effect in Irradiated Mice," submitted to *Science*.
- <sup>2</sup> N. G. Anderson, D. A. Waters, W. D. Fisher, G. B. Cline, C. E. Nunley, L. H. Elrod, and C. T. Rankin, Jr., *Anal. Biochem.* In press.
- <sup>3</sup> *Ibid.*
- <sup>4</sup> G. L. Miller, and R. H. Golder, *Arch. Biochem.* **29**, 420 (1950).
- <sup>5</sup> A. Berman, *J. Natl. Cancer Inst. Monograph* **21**, 41 (1966).
- <sup>6</sup> S. P. Spragg, and C. T. Rankin, Jr., *Biochem. Biophys. Acta.* In press.
- <sup>7</sup> N. Cho, H. P. Barringer, J. W. Amburgey, G. B. Cline, N. G. Anderson, L. L. McCauley, R. H. Stevens, and W. M. Swartout, *J. Natl. Cancer Inst. Monograph* **21**, 485 (1966).
- <sup>8</sup> S. P. Colowick and N. O. Kaplan, *Methods in Enzymology* Vol. IV, p. 63, (1957).
- <sup>9</sup> Rodes Trautman, Brookhaven Natl. Lab. 990 (T-420), 1966.
- <sup>10</sup> Calculated from Berman's formula by Dr. Hsien-Wen Hsu, University of Tennessee.

## G. EVALUATION OF ZONAL CENTRIFUGE ROTORS FOR THE ISOLATION OF SERUM LIPOPROTEINS<sup>1</sup>

M. Heimberg

The methods which are employed currently for the preparative isolation of the serum lipoproteins by ultracentrifugation require that the various lipoprotein classes be separated by a sequential series of adjustments of solvent density (with salts such as KBr, NaCl, CsCl<sub>2</sub>), and by the flotation of the lipoproteins through these salt gradients by repeated centrifugations in angle head rotors. The fractions obtained by these procedures are classes of lipoproteins having densities between finite limits (e.g., 1.063-1.210). To obtain

all the lipoprotein classes from human serum would require four centrifugations (20 hrs, 106,000 g for each). We have evaluated the use of BXV-aluminum and titanium zonal rotors and the B-XIV titanium rotor for the purpose of isolation of lipoproteins from human serum, and have isolated the VLDL<sup>2</sup> and LDL lipoproteins classes from serum after a single 20–24 hr centrifugation.

#### BXV-Aluminum Rotor

Serum (ca. 25 ml, adjusted to density 1.300 with solid KBr), from normal adult human males was introduced into the BXV-Al rotor, after the density gradient had been established (NaCl, KBr, H<sub>2</sub>O; range 1.000–1.300). Centrifugation was carried out for 20–24 hrs at 20,000 rpm. The fractions collected from the rotor were monitored by ultraviolet absorption at 280m $\mu$ . The peaks monitored by UV absorption were identical with those discerned by chemical measurement of total protein or lipid content. A complete separation of VLDL and LDL lipoproteins from the serum proteins was obtained. The HDL could not be separated and the serum proteins (remainder) tended to diffuse throughout the outer third of the rotor volume. This rotor is suitable for the isolation of the VLDL and LDL from serum simultaneously and in preparative amounts, but cannot be used for the isolation of the HDL.

#### BXV-Titanium Rotor

Experiments were carried out with this rotor identical to those described with the BXV-Al except that the rotor velocity was maintained at 25–27,000 rpm. The gravitational force generated at this angular velocity approximates 60,000 g. Good separation of VLDL and LDL from human serum was obtained with the Ti rotor as with the Al rotor. At best, only partial separation of the HDL was observed. The HDL is the most difficult of the lipoprotein fractions to separate by conventional techniques; it requires 20–24 hrs of centrifugation at 105,000 g. The results obtained with the BXV-Ti rotor are tantalizing since the HDL peaks (280 m $\mu$ ) can be seen but are very poorly separated from the bulk of the serum proteins. If one does lipid analyses, however, one can see peaks of lipid appearing in the area of the expected HDL.

In these experiments, the gradients were constructed of a solution of NaCl:KBr in the density range 1.000–1.300. This particular gradient may have been

distorted by apparently large rates of diffusion of the salts. The diffusion of salt may have disturbed the distribution of the serum proteins in the gradient sufficiently to obscure the HDL. This appeared to be reasonable since the residual serum proteins were distributed throughout 1/3 of the rotor volume. Experiments were therefore carried out in order to obtain a more stable gradient. Sucrose-KBr 2:1, w/w) was found to be suitable for this purpose. However, even with this more stable gradient, and with less diffusion, the HDL could not be separated in this rotor when it was operated at the recommended maximum velocity (27,000 rpm) (Figure 3.23 to 3.25). Using the B-XV-Ti rotor, it could be demonstrated (Figure 3.26) that the  $\beta$ -lipoprotein of human serum could be isolated from serum by zonal ultracentrifugation (fraction with peak at d 1.04) and could then be recentrifuged and recovered at the same density. The lipids of the serum follow the lipoprotein peaks and are isolated, therefore, by this procedure. Analytical data from fractions shown in Figure 3.23 are given in Table 3.6.

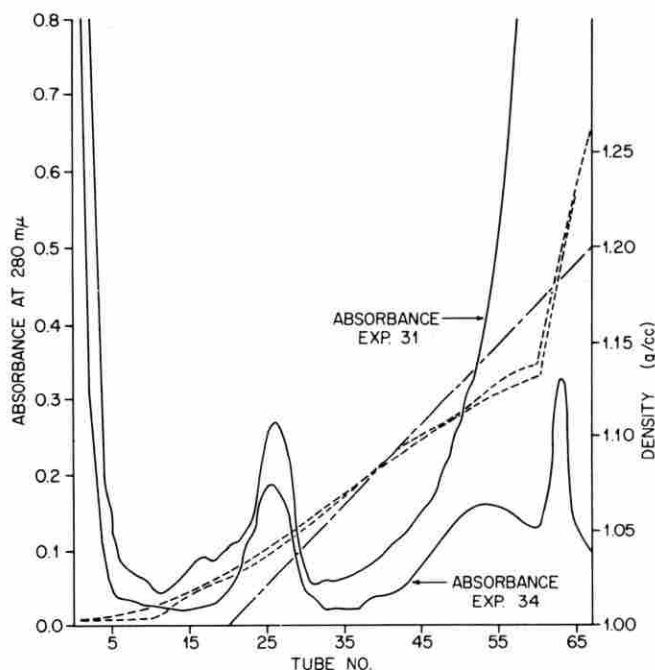


Fig. 3.24 Separation of human serum lipoproteins in a sucrose-KBr gradient. Human serum does not show a complete separation of HDL from the mass of serum proteins. When a preparation of lipoproteins prepared to contain particles having densities less than serum lipoproteins was run (lower curve) then the position of the HDL is clearly seen.

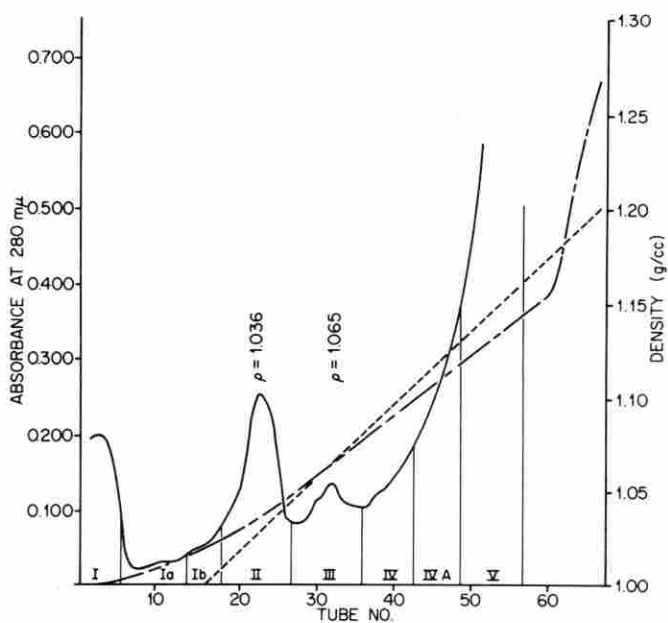


Fig. 3.25 Separation of human serum lipoproteins in the BXV titanium rotor using a sucrose gradient containing 0.7% KBr. The cholesterol and phospholipid contents of portions of the recovered gradient were also determined.

It is apparent that a zonal rotor which can deliver considerably more gravitational force than the B-XV-Ti rotor will be required for the complete separation of all of the classes of lipoproteins from serum in one run. The B-XIV-Ti rotor may be practical for the isolation of HDL, since it can generate about 100,000 g. If other rotors can be developed, capable of even greater maximum force than the BXIV-Ti rotor, they would, undoubtedly, be most useful in the lipid-lipoprotein field.

#### B-XIV-Ti Rotor

This rotor has not been in our possession for a sufficiently long period of time to allow us to evaluate the rotor completely. It can deliver a maximum force of about 105,000 g and is most promising for the isolation of the serum lipoproteins. The KBr-NaCl gradients which were used with the BXV rotor are unstable in the B-XIV at higher velocities. In order to obtain a linear gradient, it was necessary to use sucrose-KBr mixtures. The increased viscosity of the sucrose solutions maintains a more stable density gradient than can solutions of KBr-NaCl alone. We have, unfortunately, been beset with additional problems of loss of solvent by evaporation from the rotor in vac-

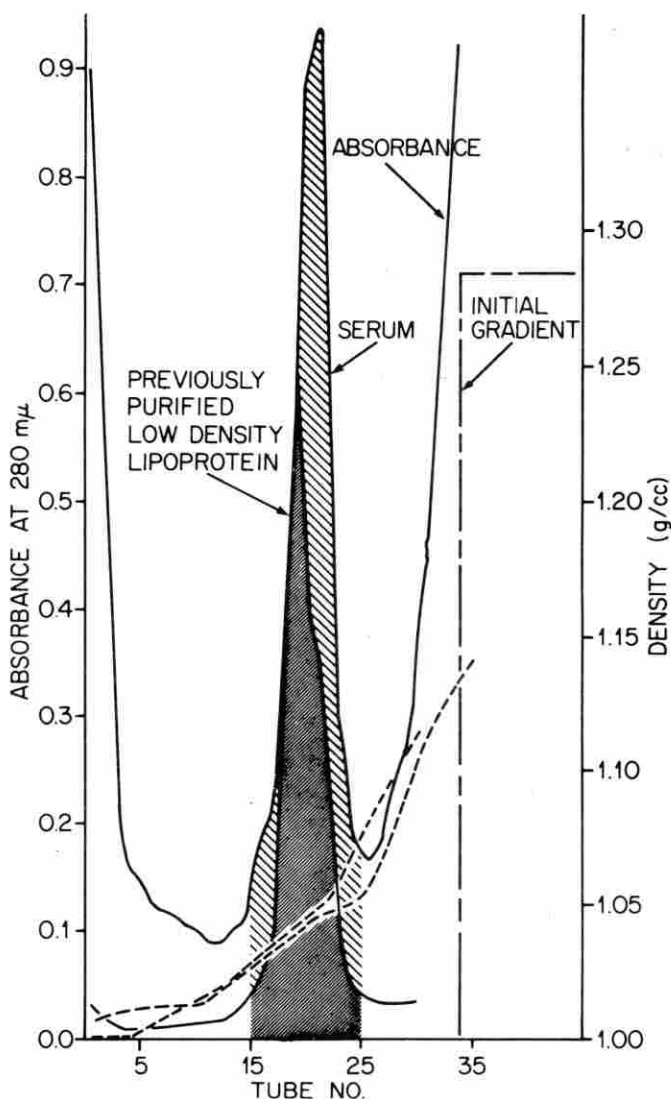


Fig. 3.26 Isolation of human serum  $\beta$  lipoprotein (LDL) in the BXV titanium rotor. The gradient was formed by diffusion using a single sucrose solution (2:1 sucrose to KBr by weight) having a density of 1.283 gm/cc. Total cholesterol and total phospholipids were determined in combined fractions 15-25. Expressed as  $\mu$  moles per ml of original serum, for the lipoprotein separated from whole serum the concentration of total cholesterol was 2.27, and phospholipid .691. For the previously purified LDL the values were 2.22 and .628 respectively.

uum during the course of a 48-hr-long centrifugation. We expect these problems to be corrected shortly. We have had the opportunity to carry out very few acceptable centrifugations with the B-XIV-Ti rotor, but have obtained excellent separation of VLDL and LDL from serum, and have also observed two distinct HDL peaks (Figure 3.27).

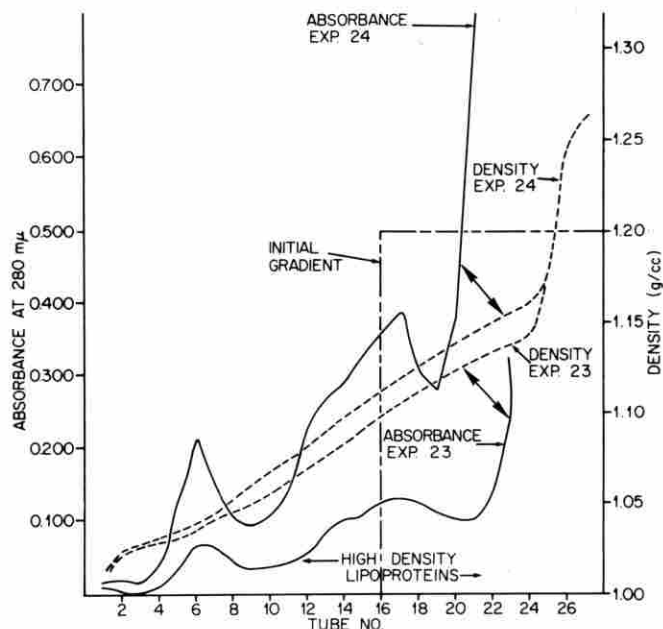


Fig. 3.27 Partial separation of high density lipoproteins in two separate runs using unfractionated human serum in the titanium BXIV rotor run 48 hrs at 37,000 rpm. The gradient was prepared from sucrose-KBr in the ratio of 2:1 w/w.

#### Significance of this Research

The methods which are being developed in this laboratory for the isolation of the serum lipoproteins by zonal ultracentrifugation have a high potential for success and offer a number of advantages over the procedures now in use. We have indicated already how zonal ultracentrifugation can reduce the time and labor required for the isolation of serum lipoproteins. The lipoproteins obtained may, furthermore, be more homogenous, since they will all be exposed to identical conditions of temperature, time, ionic composition, and centrifugal force. Using the methods described here, we can obtain a graphic record of the distribution of lipoprotein peaks in normal human serum; furthermore, we may readily determine any alterations of this pattern with age, sex, and diet. From this pattern, we may obtain quantitative information of the lipid and protein composition of each peak, and also learn the solution density (specific gravity) at which each peak appears. This method, however, is more than analytical, and offers more than a picture of the distribution of lipoproteins in serum; it is a preparative method, and, we believe, therefore, will now permit large-scale separation of lipoproteins from serum with relative ease. This

Table 3.6. Analysis of Fractions Separated in Experiment Shown in Figure 3.23

Fraction	Molar Ratio of Cholesterol Esters To Cholesterol	Percent Total Serum Cholesterol
I	1.88	6.2
II	2.51	31.4
III	2.42	2.0
IV	3.00	2.3
Serum	2.56	100

preparative method will be most useful in the study of lipid metabolism and disease.

There is no question but that abnormalities in lipid and lipoprotein metabolism are extremely important in the genesis or sequelae of a number of diseases of man. The procedures for the isolation and analysis of normal human serum lipoproteins by zonal ultracentrifugation can be extended to the identification and study of human hyperlipemias. We are convinced that these procedures when fully developed will become invaluable in the characterization and differential diagnosis of hyperlipemias in human disease. These procedures may be most appropriate for the study of metabolic diseases of man, atherosclerosis and other cardiovascular diseases, genetic abnormalities, endocrine disorders, and other situations in which alterations of the serum lipoproteins may be a prominent feature. The zonal procedures we have discussed will also be invaluable for the isolation of serum lipoproteins in experimental work with animals which is concerned with the origin and metabolism of the plasma lipids.

Ideally, a rotor with the capacity of a BXV and the ability to generate 150,000–200,000 g is required. If this were not feasible from the engineering viewpoint, then smaller-capacity high-speed rotors should be built. The BXIV-Ti rotor may be capable of exceeding its maximum rated speed, and this possibility should be evaluated thoroughly. We would suggest that a series of high-speed rotors be designed and prototypes manufactured. High-speed rotors (particularly if also of large volume capacity) would be invaluable in the study of structure and function of human serum lipoproteins.

<sup>1</sup> Work performed under UCCND Subcontract #2805.

<sup>2</sup> Abbreviations used: VLDL, very low density lipoprotein (e.g., density < 1.020); LDL, low density lipoprotein (density 1.020–1.063); HDL, high density lipoprotein (density 1.063–1.210).

## H. LIPID CLASS AND FATTY ACID COMPOSITION OF RAT LIVER CYTOPLASMIC MEMBRANES ISOLATED BY ZONAL CENTRIFUGATION

R. C. Pflieger      N. G. Anderson  
F. Snyder

Cytoplasmic membranes from normal rat liver were isolated by the zonal centrifugation technique noted previously. The membrane samples at an isopycnic concentration were then diluted, pelleted, and frozen to await lipid extraction.

Total membrane lipids were extracted twice by the procedure of Bligh and Dyer;<sup>1</sup> first from a 1 mM solution of NaHCO<sub>3</sub> in which the membranes were suspended and then from a 3% solution of NH<sub>4</sub>OH to assure complete extraction of the polyglycerol-phosphatides.<sup>2</sup> Neutral lipids were determined by the photodensitometric procedure of Privett.<sup>3</sup> Phospholipid phosphorus was determined by the Rouser procedure in the presence of silica gel.<sup>4</sup> Cytoplasmic membrane protein was assayed by the Lowry procedure.<sup>5</sup>

The ratio of cytoplasmic membrane lipid to protein was 0.59, whereas the phospholipid/protein ratio was 0.35 (Table 3.7). Unesterified cholesterol and total neutral lipids accounted for 21.2 and 27%, respectively, of the total lipids. This indicates that the combined values for esterified cholesterol, triglycerides and free fatty acids amount to only 5.8% of the total lipids (Table 3.8). However, Skipski *et al.*<sup>6</sup> reported the cholesterol and neutral lipid content as 13.6 and 34.6%, respectively, of the rat liver cytoplasmic membranes that they isolated by the Neville<sup>7</sup> procedure. The difference in percentages of the membrane lipids may be attributed to contamination of the Neville membrane preparation with mitochondria, as shown by Emmelot *et al.*<sup>8</sup>

Lecithin (phosphatidylcholine) accounted for 19.2% of the total lipids, 39.4% of the total lipid phosphorus, and 37.4% of the phospholipid phosphorus (Tables 3.8 and 3.9). These data and the other data in Table 3.9 indicate that essentially all of the total lipid phosphorus (P) is bound in phospholipids, which is the same conclusion that Emmelot *et al.*<sup>8</sup> decided upon from their work with rat-liver cytoplasmic membranes. The total lipid, protein and cholesterol to P ratios are shown in Table 3.7.

Phosphatidylethanolamine, phosphatidylserine, phosphatidylinositol, lysophosphatidylcholine, sphingomyelin and polyglycerolphosphatides (cardiolipin) were also present in the total lipid extract from the

**Table 3.7. Lipid, Phospholipid Phosphorus and Protein Values for Normal Rat Liver Plasma Membranes**

Protein (mg) / liver (g)	0.88 (0.62–1.23)
Total Lipid (mg) / liver (g)	0.39 (0.18–0.63)
Total Lipid (mg) / protein (mg)	0.59 (0.43–0.80)
Phospholipids (mg) / protein (mg)	0.37 (0.22–0.55)
Total Lipid (mg) / P (μmoles)	1.48 (0.87–2.11)
Protein (mg) / P (μmoles)	2.28 (1.28–3.08)
Cholesterol (mg) / P (μmoles)	0.74 (0.61–0.80)

**Table 3.8. Total Lipids from Normal Rat Liver Cytoplasmic Membranes**

Compounds	Percent of Total Lipid Extracted*
Total Neutral Lipids	27.0 (20.6–37.8)
Triglycerides	2.19 (0.74–3.24)
Free Fatty Acids	2.31 (1.02–3.38)
Cholesterol, Free	21.2 (17.5–27.1)
Cholesterol, Esterified	1.28 (0.39–2.43)
Total Polar Lipids	62.1 (51.7–69.4)
Lysophosphatidylcholine	1.15 (0.27–2.80)
Phosphatidylcholine	19.2 (16.3–25.3)
Phosphatidylethanolamine	9.96 (8.51–11.9)
Phosphatidylinositol + Phosphatidylserine	6.89 (5.02–8.34)
Sphingomyelin	8.01 (6.22–9.43)
Polyglycerolphosphatides	1.70 (1.20–2.46)
Unknown (contains no phosphorus)	11.9 (8.5–16.6)
Total Lipid Accounted for	91.1 (78.0–102)

\*Average values from 7 membrane preparations. Numbers in parentheses indicate the range.

rat-liver cytoplasmic membranes (Tables 3.8 and 3.9). An extremely polar unidentified component (<0.68% of the total lipid), containing 1.96% of the total phosphorus, remained at the origin of the thin-layer chromatogram [Silica gel HR; CHCl<sub>3</sub>:CH<sub>3</sub>OH:HAc:Saline (50:25:8:4, v/v/v/v)]. Another unidentified lipid extractable component, amounting to 11.9% of the total lipids, and more polar than lysolecithin but containing no phosphorus,<sup>4</sup> was also detected by thin-

**Table 3.9. Percent of Total Phosphorus in Various Fractions**

	Orig <sup>†</sup>	LL	Sphin	Lec	Ps + Pi	Cep	Card
Total Lipids*	1.96 (0.55-4.23) <sup>§</sup>	3.30 (0.91-3.73)	15.8 (14.4-17.4)	39.4 (32.0-47.0)	13.5 (10.6-16.2)	21.9 (19.1-25.6)	2.58 (1.52-3.59)
Phospholipids <sup>¶</sup>	3.66 (0.72-4.82)	4.21 (2.30-6.41)	15.7 (12.5-21.2)	37.4 (30.4-48.2)	13.1 (9.2-16.0)	21.5 (18.6-25.3)	3.23 (1.00-5.04)

\*96.6% (91.0-104%)P recovered.

<sup>¶</sup>109.2% (92.8-123%)P recovered.

<sup>†</sup>Orig (origin of chromatogram); LL (lysolecithin); Sphin (sphingomyelin); Lec (lecithin); Ps (phosphatidylserine); Pi (phosphatidylinositol); Cep (cephalin); Card (cardiolipinpolyglycerolphosphatides).

<sup>§</sup>Numbers in parentheses represent the range values from 7 samples. P determination according to Rouser, *et al.*, LIPIDS, 1, 85 (1966).

layer chromatography [Silica gel HR; CHCl<sub>3</sub>:CH<sub>3</sub>OH; 2M NH<sub>4</sub>OH (60:35:8, v/v/v)].

A continuation of this work will include the analysis by gas-liquid chromatography (GLC) of the fatty acid composition of the major phospholipid constituents found in the cytoplasmic membranes, as well as the GLC analysis of the free fatty acids. These data, together with the composition data herein presented, will complete the total lipid analysis of normal rat-liver cytoplasmic membranes.

## REFERENCES

- <sup>1</sup>E. G. Bligh and W. J. Dyer, *Canad. J. Biochem. Physiol.*, **39**, 911 (1959).
- <sup>2</sup>G. Rouser, G. Kritchevsky, D. Heller and E. Lieber, *J. Am. Oil Chemists' Soc.*, **40**, 425 (1963).
- <sup>3</sup>O. S. Privett, M. L. Blank, D. W. Codding and E. C. Nickell, *J. Am. Oil Chemists' Soc.*, **42**, 381 (1965).
- <sup>4</sup>G. Rouser, A. N. Siakotos and S. Fleischer, *Lipids*, **1**, 85 (1966).
- <sup>5</sup>O. H. Lowry, N. J. Rosebrough, A. L. Farr and R. J. Randall, *J. Biol. Chem.* **193**, 265 (1951).
- <sup>6</sup>V. P. Skipski, M. Barclay, F. M. Archibald, O. Terebus-Kekish, E. S. Reichman and J. J. Good, *Life Sci.* **4**, 1673 (1965).
- <sup>7</sup>D. M. Neville, Jr., *J. Biophys. Biochem. Cytol.* **8**, 413 (1960).
- <sup>8</sup>P. Emmelot, C. J. Bos, E. L. Benedetti and Ph. Rumke, *Biochim. Biophys. Acta* **90**, 126 (1964).

## I. ANALYTICAL DIFFERENTIAL CENTRIFUGATION IN ANGLE-HEAD ROTORS

Norman G. Anderson

Sedimentation in angle-head rotors has not been studied quantitatively. The object in using an angle-head centrifuge is almost invariably to separate a suspension into a pellet and a supernatant. Pickels'

theory of sedimentation in angle-head centrifuge tubes<sup>1</sup> is concerned chiefly with boundary movement; it neither predicts the fraction of particles in a given suspension sedimented as a function of integrated centrifugal force, nor agrees with experimental results obtained, nor takes Coriolis forces into consideration. It was concluded that the Pickels theory applied to relatively large particles (which were not studied), and only partially to the hemocyanin molecules examined.<sup>1-3</sup> It was also concluded that analytical ultracentrifuge data could not be used to predict accurately sedimentation in angle-head tubes, and that only a rough approximation of sedimentation coefficients could be obtained by angle-head centrifugation. Quantitative studies on particle sedimentation in inclined tubes and a theory accurately describing such sedimentation therefore do not appear to be available. How one of the older, more widely used, and simpler biophysical instruments actually functions has not been completely determined. In this paper, three questions are considered: (a) How can sedimentation be studied quantitatively in angle-head rotors? (b) Can reproducible results be obtained? (c) Can a theory be developed which agrees with the results?

The point is to study the distribution of particle mass between supernatant and pellet as a function of the time-force integral, and not to observe boundaries. Stated differently, we are interested in the rate of transport of particles across the plane which separates supernatant from pellet, and not, initially, with events occurring elsewhere in the tube.

In this paper a general method for studying angle-head centrifugation is described and applied to three classes of particles which differ greatly in size—red blood cells, polystyrene latex, and bovine serum al-

bumin (BSA). The work has been made possible by (a) the development of digital integrators for determining accurately the integral of  $\omega^2 dt$  during the centrifugation cycle,<sup>4</sup> (b) the availability of high-speed titanium rotors which allow particles as small as proteins to be sedimented in a reasonable period of time, and (c) the development of polycarbonate tubes which do not deform in high centrifugal fields.<sup>5</sup> The simple techniques described allow complex mixtures of particles to be characterized, provide data on which rational separation procedures may be based, and allow sedimentation coefficients of proteins (and possibly larger particles) to be approximated.

The particles separated in preparative centrifuges may have sedimentation coefficients which range over six orders of magnitude.<sup>6</sup> While zonal centrifuges<sup>4,7-9</sup> now allow high-resolution separations to be made over a very wide range of particle sizes, no *single* zonal centrifuge experiment can now achieve separations over more than a fraction of this range. Angle-head centrifugation is therefore often a necessary prelude to high-resolution zonal separations, especially where a minor component is to be concentrated and resolved. Methods for optimizing preparative separations are therefore of continuing interest.

### Theoretical Considerations

Although detailed theoretical studies on angle-head centrifugation are reserved for a later paper, two points should be stressed here. First, we are interested initially in how separations are actually made in practice; that is, in the separation of a suspension into only two fractions. The theoretical value we are most interested in predicting is the quantity  $\omega^2 t$  for complete sedimentation of a given particle species. Previous studies suggest that complete sedimentation may be approached asymptotically<sup>1-3</sup> and that complete sedimentation, at least of viruses, may not be obtained. If this is the case, then we must also be interested in developing methods for determining how the fractionation of multicomponent mixtures may be most efficiently achieved.

The second point concerns the circulation of fluid in tubes of circular cross-section inclined to the rotor axis during rotation. The simple theory of Pickels<sup>1</sup> assumes unconstrained convection in the tube due to concentration changes occurring at the outer and inner walls; no consideration is given to the fact that fluid moving from one radius to another must be accelerated or decelerated to conform to the tangential

velocity of each radius, *i.e.*, that the fluid is subject during movement to Coriolis forces.<sup>10</sup> However, accelerating and decelerating fluid elements have very complex flow patterns when they are not amenable to simple theoretical description. This is an additional reason why only the distribution of particles between supernatant and pellet is of interest initially, and why boundary phenomena are not examined here.

### Experimental Studies

In practice, a variety of centrifuge rotors are used to fractionate mixtures such as tissue extracts or homogenates. For this study, however, one rotor was employed so that data obtained with a wide range of particle sizes would be directly comparable.

**Centrifugal Procedures.**—A Spinco No. 50 titanium angle-head rotor was spun in either a Spinco L-2 centrifuge or in an experimental zonal centrifuge equipped with temperature control and with an integrator which indicates the integral of  $\omega^2 dt$  continuously in digital form.<sup>4</sup> To ensure that the tube geometry was constant, Oak Ridge-type polycarbonate tubes (obtained from International Equipment Company, Needham Heights, Massachusetts) with plastic closures<sup>5</sup> were used. These do not deform when centrifuged at high speeds.

For particles on the large end of the spectrum, it was not possible to measure the centrifugal field accurately with this rotor and integrator. Some data points were therefore obtained at  $1 \times g$  by mounting the tubes in a plastic block so that the tubes had the same angle with respect to the earth's gravitational field that the tubes have with respect to the centrifugal field in the rotor.

A 9-ml sample of each particle suspension was placed in each tube. After centrifugation, the tubes were rotated very slowly 180° while in place until the pellet was flat in the bottom of the tube. With a long-stem pasteur pipette, fluid was carefully removed along the upper wall. The end of the pipette was kept at, or just below, the surface (Figure 3.28). The recovered liquid was placed in a 10-ml graduated centrifuge tube to measure the volume removed. In this manner, 7 ml of the supernatant was removed, thus avoiding the problem of deciding how much of a loose pellet to remove. When a very dilute sample such as polystyrene latex was used, a small cotton plug was also used in some experiments to help keep sedimented material at the bottom of the tube.

For very long experiments (4 hr or more at 50,000 rpm), a digital integrator need not be used since the

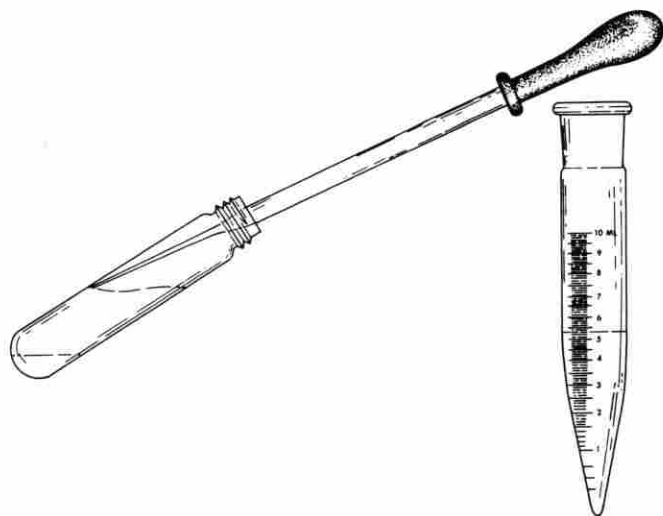


Fig. 3.28 Method used to remove fluid from angle-head tubes after they have been rotated *in situ* for 180°. See text for details.

acceleration and deceleration times are small in proportion to the total time of centrifugation. The average speed may be accurately calculated from the odometer, and 7 min added to the time at speed to compensate for centrifugation during acceleration and deceleration. All experiments were conducted with the temperature control set on 5°C. At 50,000 rpm the rotor temperature was 10–11°C.

**Calculations.**—Centrifugal treatment used for particle sedimentation has been expressed in a variety of ways including  $g$  min, speed and time with either  $R_{av}$ , or  $R_{min}$  and  $R_{max}$  specified, or simply time, speed, and the manufacturer's rotor number. We have chosen to use the integral of  $\omega^2 t$  because this value is used in further calculations of sedimentation rate and because the integrator used gives this number directly. Other numbers, such as  $g$  min are characteristic not only of the time-speed profile, but of the rotor used, and the amount of sample placed in each tube.

The values of  $\omega^2 t$  of interest range from  $10^5$  to  $10^{13}$ . To accommodate this range, data are plotted on a nine-cycle log plot as shown in Figure 3.29.

The radius of the menisci before and after removal of the 7 ml of supernatant are 4.88 and 6.8 cm respectively during rotation. The value of  $\omega^2 t$  equivalent to a given period of time at  $1 \times g$  was calculated two ways. From the equation

$$g = \frac{\omega^2 X_{av}}{980} = 1 \quad (1)$$

and by using the average radius,  $X_{av} = 5.84$  cm,  $\omega^2$  was found to be 167.8. The second method of calculation uses the equations

$$s = \frac{X_2 - X_1}{t \times 980} \quad (2)$$

which applies to tubes at rest, and

$$s = \frac{1}{\omega^2 t} \ln \frac{X_2}{X_1} \quad (3)$$

which applies to sedimentation in the centrifuge.

These may be equated if the same particle and geometry are used in both instances to give:

$$\omega^2 = \frac{980}{(X_2 - X_1)} = \ln \frac{X_2}{X_1} = 169.2 \quad (4)$$

Since the results agree within 1%, either method of calculation may be used; 1 hr at  $1 \times g$  with this geometry is therefore equivalent to  $\omega^2 t = 6.09 \times 10^5$ .

In the separation cells used in the analytical ultracentrifuge, the sedimentation coefficient may be determined by analyzing the solution remaining in the upper compartment.<sup>11–13</sup> These equations apply to ideal sedimentation in a sector-shaped compartment. The tubes used here have far from ideal geometry. Therefore, it has been considered of interest to ask: If the boundary-widening effect of diffusion is disregarded, when would all of a given particle species be expected to pass out of the volume being analyzed?

By using equation 3 and the values of  $X_1$  and  $X_2$  corresponding to the menisci before and after removal of 7 ml of supernatant, values of  $S_{complete,t}$  were calculated for 20°C in water and are included in Figure 3.29. The scale for  $S_{complete,20}$  was calculated for data taken at 5°C for red blood cells and polystyrene latex, and at 10°C for BSA. These values are useful in that they indicate how closely an experimental system which is subject to convective disturbances, agrees with theory. The sedimentation coefficient scale was aligned with the  $\omega^2 t$  scale in Figure 3.29 by solving equation 3 for a series of values of  $\omega^2 t$ .

**Sedimentation of Sheep Red Blood Cells.**—Sheep red blood cells were washed three times with the Veronal-buffered diluent (VBD) containing gelatin used for complement fixation studies.<sup>14</sup> A total of 1.1 ml of packed cells was added to 32 ml of gelatin-free VBD; 7 ml of this suspension plus an additional 2 ml of VBD were added to each 10-ml polycarbonate tube. The tubes were either left in the angle holder in the refrigerator for sedimentation at  $1 \times g$  or centrifuged briefly in the No. 50 rotor. Then 7 ml of super-

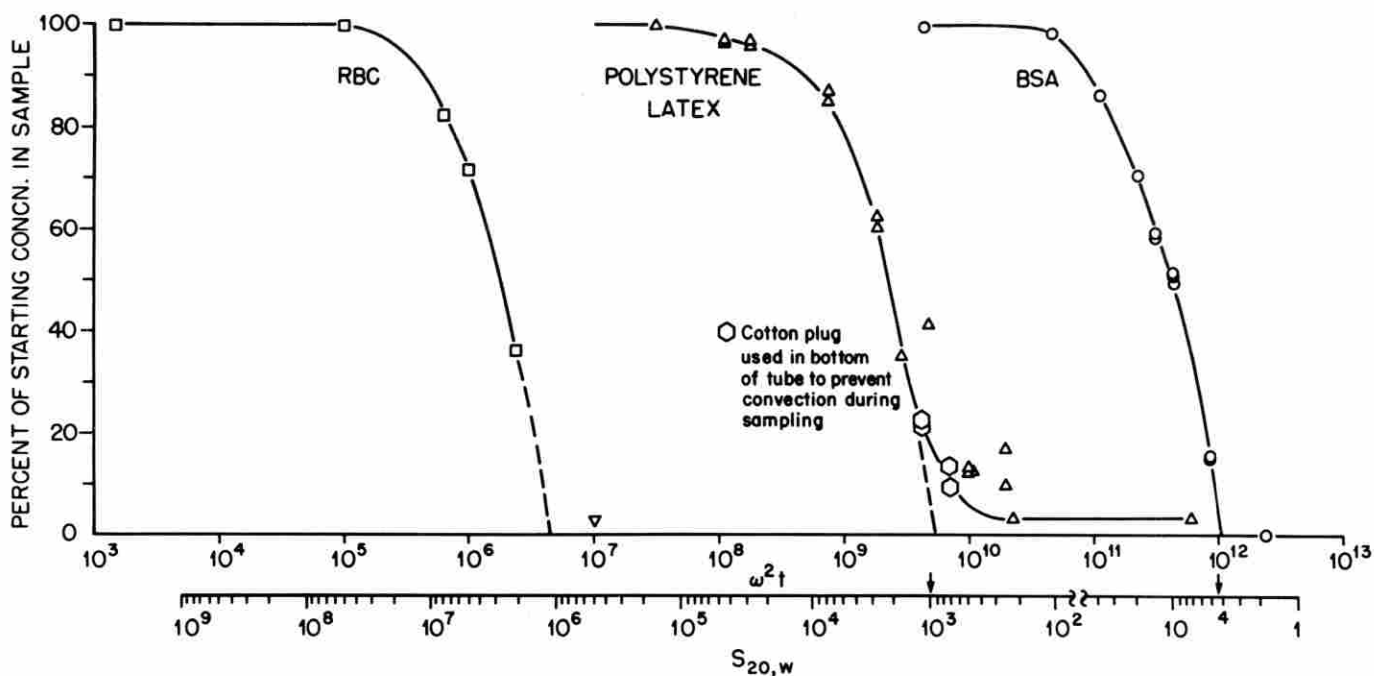


Fig. 3.29 Sedimentation of sheep red blood cells, polystyrene latex particles, and BSA. Points indicated by squares obtained at  $1 \times g$

natant were removed as described. A control tube was kept in the refrigerator and resuspended just before use. To effect complete hemolysis, 1 ml of each supernatant and of the control were added to 14 ml of buffered water<sup>14</sup> and read at 541 mμ in a 1-cm light path cells in a Beckman DB spectrophotometer. The results are shown in Figure 3.29. The small optical density observed at  $\omega^2 t = 10^7$  was due to a small amount of hemolysis. Results are given as the percent of the starting sample found in the 7 ml of supernatant.  $4 \times 10^6 \omega^2 t$  would probably effect complete sedimentation of red cells. The observed sedimentation coefficient is approximately  $10^6 S$  (calculated by extrapolating the curve to the base line, *i.e.*, to complete sedimentation of the particles out of the supernatant volume).

**Polystyrene Latex Sedimentation.**—Polystyrene latex beads (Dow Chemical Lot No. LS 055A) with a diameter of  $1.88 \mu$  (standard deviation  $0.0076 \mu$  in water) were diluted in distilled water and centrifuged to various values of  $\omega^2 t$  as indicated in Figure 3.29. The absorbance of the 7 ml of supernatant removed was read against distilled water, and plotted as percent of absorbance of the starting sample. Data obtained with and without a small cotton plug in the bottom of the tube to prevent convection during sample recovery are given. A small residual absorbance was observed

even after prolonged centrifugation. The slight skewness observed in the curve probably relates to both a small amount of aggregation and to particle heterogeneity. A sedimentation coefficient of approximately 1000 is inferred from the plot using the data obtained with cotton plugs. By using a density of 1.0525 for polystyrene,<sup>15</sup> a sedimentation coefficient of 1020 is calculated at 5°C in water for particles having a diameter of  $0.188 \mu$ .

**Sedimentation of BSA.**—A 1% solution of BSA in Veronal buffer<sup>13</sup> was centrifuged for periods up to 25 hr at 50,000 rpm. The absorbancies of the supernatants were read at 278 mμ with 1-cm light path cells after dilution with distilled water. Values are expressed as percent of the absorbance of the starting sample (Figure 3.29). The curve, if extrapolated to the base line, intersects it at approximately 4 S, which is in fair agreement with published values.<sup>16</sup>

It is of interest to see how closely the BSA data conformed to what would be expected theoretically in a separation cell used in the analytical ultracentrifuge. By using the equation (refs. 11–13):

$$s = -\frac{1}{2 \omega^2 t} \ln \left[ \frac{X_0^2}{X_p^2} + \frac{C_t}{C_0} \left( 1 - \frac{X_0^2}{X_p^2} \right) \right] \quad (5)$$

where  $X_0$  = radius of the meniscus,

$X_p$  = radius of the partition, or of the plane of the surface of the "pellet volume,"

$C_0$  = concentration of particles at the start of the run,

$C_t$  = concentration in supernatant at the conclusion of the run,

plots were made of  $\omega^2 t$  as a function of concentration of particles remaining in the 7 ml of supernatant volume. Two values for the sedimentation coefficient were used that corresponded to the sedimentation coefficient for BSA at 10°C and zero protein concentration, and to the sedimentation coefficient for the same temperature of the BSA solution used in the angle-head centrifuge studies reported here. As shown in Figure 3.30, the experimental points fall between the two calculated curves for the most part and are closer to the zero concentration curve.

The reproducibility of results is best indicated by considering the data for BSA. The results of two duplicate runs and one quadruplicate run are shown in Table 3.10 and indicate close agreement between different tubes run in the same rotor. The curve shown

**Table 3.10. Reproducibility of BSA Concentration Measurements**

$\omega^2 t$	Concentration in Supernatant Expressed (Percent Starting Concentration)
$3.07 \times 10^{11}$	58.1
	59.3
$4.22 \times 10^{11}$	51.4
	51.4
	51.1
	49.8
$8.61 \times 10^{11}$	15.2
	14.6

in Figure 3.30 indicates rather little scatter of points obtained in different experiments.

#### Discussion

An extremely simple and reproducible method has been developed for measuring and describing sedi-

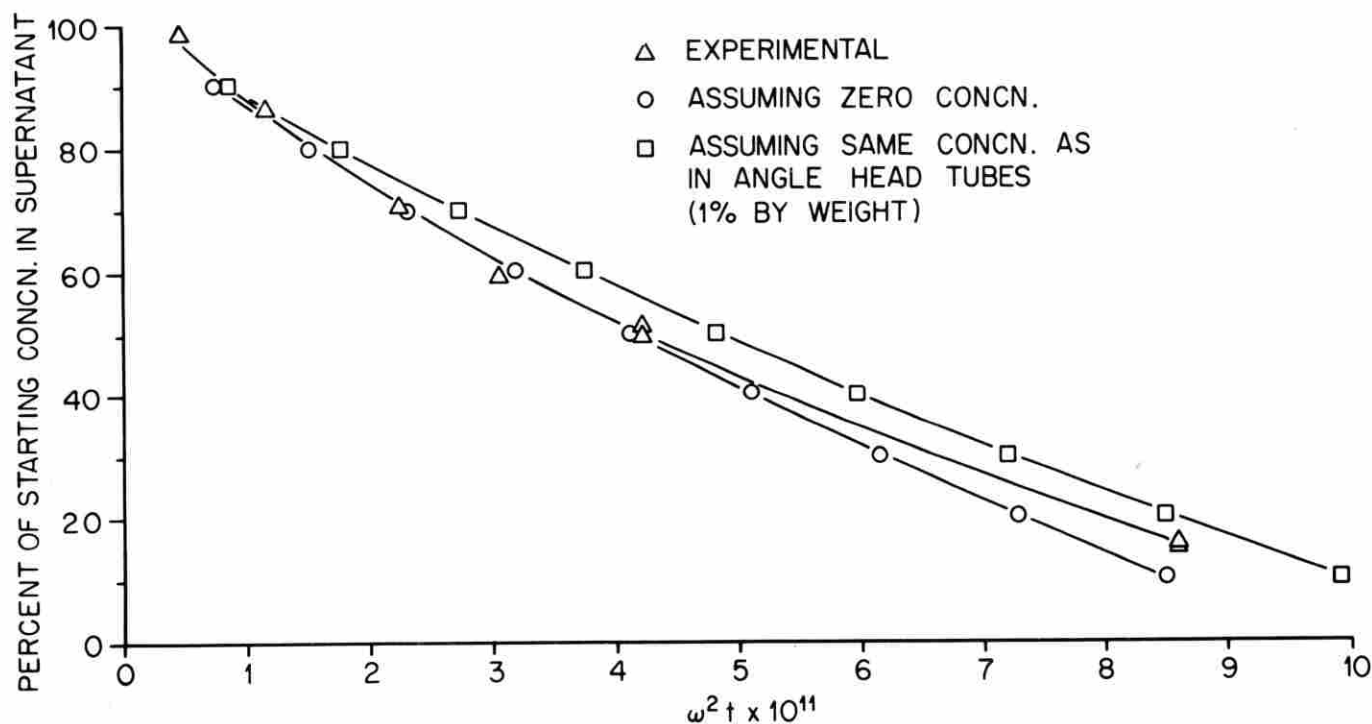


**Fig. 3.30** Plot of theoretical and observed concentration of protein in supernatant in Spinco No. 50 angle-head polycarbonate centrifuge tubes as a function of  $\omega^2 t$ . The experimental values agree more closely with the theoretical plot for zero protein concentration than for 1%.

mentation in angle-head centrifuges. The method is applicable over a very wide range of force-time values. The data obtained allow fractionation methods using centrifugation to be developed rationally. No indication has been found of anomalous nonreproducible sedimentation with the particle concentrations employed except with polystyrene latex. Insertion of a small cotton plug in the bottom of the centrifuge tube eliminates this problem. The method used measures only transport to an arbitrarily chosen pellet volume and is not concerned with the measuring boundaries or with observing convective flow in the tube.

With BSA, transport to the pellet volume occurs almost exactly as would be expected in a sector-shaped separation cell at zero protein concentration. Best agreement is observed when 50–70% of the protein has been sedimented. No evidence of an asymptotic approach to complete sedimentation was observed as would be expected if extensive convection occurred during centrifugation. It should be noted that somewhat different results would be obtained if an attempt were made to remove the entire supernatant solution since a small amount of pellet material will slide off the packed pellet during the interval between the time the rotor comes to rest and that when the tubes are rotated 180° in position.

The curve (Figure 3.29) based on observations with polystyrene latex does not suggest a homogeneous particle species, and indeed the suspension is not perfectly homogeneous. Does the curve obtained result from, and allow measurement of, heterogeneity? Sedimentation principles that apply to smaller more rapidly diffusing particles may not apply completely to particles in the size range of the polystyrene latex particle. Hence, a variety of particles in this size range should be more extensively studied. Note, however, that when the center portion of the latex sedimentation is extrapolated to zero concentration, the  $\omega^2 t$  value obtained agrees very well with the calculated value for the average latex particle.

Measurements of red blood cells illustrate the lower limits of the method used. Most points were obtained with the tubes subject to  $1 \times g$ . For reasons discussed below, sedimentation under these two conditions may not be strictly comparable, and a centrifugal system for precisely controlled studies below 1000 rpm is required.

This work suggests that the ordinary angle-head centrifuge is capable of yielding reproducible information on particle sedimentation over a very wide range of particle sizes. What is now required is a sys-

tematic study of the sedimentation of a variety of well-characterized particles over a range of concentrations, singly, and in mixtures under precisely controlled conditions.

Why did early studies yield results which have obscured the possibilities of this simple biophysical tool for so long? In the studies on which concepts of sedimentation in angle-head centrifuges have been based,<sup>1</sup> temperature could not be accurately controlled or measured during centrifugation. The results obtained were not reproducible, possibly because of thermal convection, and also because of variations in the deceleration schedule. The puzzling results obtained with yellow fever virus<sup>1, 2</sup> may be due to absorption of a few virus particles to the wall of the centrifuge tube, to entrapment of virus in lipid-rich particles which floated, or to stir back during deceleration.

The BSA results do not support the convective flow patterns proposed by Pickels. Rather they suggest that sedimentation occurs in an almost ideal fashion (in the sense that sedimentation in sector-shaped compartments is ideal). This can occur only if fluid translocation as proposed by Pickels<sup>1</sup> does not occur to an appreciable extent. In the Pickels theory, particle enrichment takes place at the outer wall, and depletion occurs at the inner wall. Enriched fluid, being denser, was thought to then flow directly to the bottom, whereas depleted fluid was thought to flow centripetally to the top of the tube. However, the tangential velocity increases by 40% as a fluid element moves from the meniscus to the pellet volume at the bottom along the outer wall. To be thus accelerated, the fluid element must move laterally until it is on a portion of the tube which slopes with respect to the circumferential path of rotation. The net effect of this will be to rotate the fluid mass in the tube in a direction which would, if the tube were quickly moved to a vertical orientation, be opposite to the direction of rotor rotation. This fluid rotation will, with fairly rapidly diffusing molecules, tend to keep the concentration identical at every point having the same radius. The net result to be expected is that the major mass transport will be that due to the sedimentation of particles through the fluid and not due to mass fluid movements. These considerations may not apply to a compacted sediment formed by large particles reaching the wall at any level. The particle size (or sedimentation velocity) at which this occurs remains to be determined. Since reproducible data points are obtained by the method used here, the magnitude of this latter effect may be evaluated.

Sedimentation in analytical ultracentrifuge tubes inclined so that the cell walls are at an angle to the radius is not a valid model for angle-head centrifugation, since Coriolis forces are directed *into* the impaction plane. In the angle-head centrifuge, in contrast, Coriolis forces are directed *along* the impaction plane and can produce fluid flow. As noted by Berman,<sup>10</sup> Coriolis forces have negligible effects on individual small particles, but appreciably alter the sedimentation path of particles the size of whole cells and larger. Fluid volumes having cellular dimensions cannot differ in particle content from the surrounding medium long enough to move an appreciable distance. To have an effect on centrifugation, larger volumes must be involved.

These studies are a continuation of earlier work in which the rotor speeds were accurately determined at intervals during acceleration and deceleration, and the square of the speed plotted against time to obtain a value proportional to  $\omega^2 t$  by simple integration.<sup>17</sup> A speed-recording device has also been described which recorded data for subsequent calculation of  $\omega^2 t$ .<sup>18</sup> The advantage of continuous digital integration is that the centrifugal procedures can be controlled to reach a certain predetermined value, and the value is indicated at once.

While these studies were initiated in an effort to devise better preconcentration steps for samples for subsequent zonal centrifugation, the technique is applicable to the solution of several other types of problems as well. By determining the enzyme activity, or virus or bacterial infectivity, information may be obtained on whether a single species of particle accounts for the activity. From the data obtained, both differential and zonal centrifugal experiments may be designed.

An additional advantage of the technique described is that information relative to the homogeneity or heterogeneity of particle species bearing a biochemical activity may be obtained in the original homogenization medium and therefore under more physiological conditions.

For vaccine purification with continuous-flow-with-banding rotors (for example, B-XIV, B-XVI, B-XXI, B-XXVI or K-II), the method may be used to determine the sedimentation characteristics of both the activity to be isolated and of contaminants which may be present. By using the equations developed by Berman,<sup>10</sup> cascaded centrifuge systems may also be used to remove contaminants which may float or sink with only a small loss in activity in low-speed stages,

and then the immunizing agent may be recovered in a higher-speed rotor.

In subsequent papers the numerous problems and possibilities raised by this study will be examined in greater detail.

### Summary

A simple method for studying sedimentation in angle-head centrifuges has been developed. This method (made possible by the use of the titanium rotor, polycarbonate tubes, and an electronic  $\omega^2 t$  integrator) is applicable to the study of particles having sedimentation coefficients ranging from 4 to  $10^6$  S. The range can be extended by including studies at  $1 \times g$ .

Sheep red blood cells, polystyrene latex spheres, and BSA were used as *test particles*. A 9-ml sample was used in each tube. At the end of a centrifuge cycle, the tubes were rotated *in situ* 180°, and then 7 ml of supernatant was carefully withdrawn. The remaining 2 ml were arbitrarily considered to be the pellet. When the concentration of particles remaining in the supernatant was plotted against the  $\omega^2 t$  (on a log scale), very similar curves were obtained with each test particle.

The transport of BSA to the pellet volume followed closely that predicted from the separation cell equation.

It is proposed that the Pickels theory of angle-head centrifugation must be revised to include the effect of Coriolis forces on fluid elements moving radially in the centrifuge tube.

The results obtained suggest that the angle-head centrifuge may be used as a precision biophysical instrument.

### REFERENCES

- <sup>1</sup> E. G. Pickels, *J. Gen. Physiol.* **26**, 341 (1943).
- <sup>2</sup> J. H. Bauer, and E. G. Pickels, *J. Exptl. Med.* **64**, 503 (1936).
- <sup>3</sup> T. P. Hughes, E. G. Pickels, and F. L. Horsfall, Jr., *J. Exptl. Med.* **67**, 941 (1938).
- <sup>4</sup> N. G. Anderson, H. P. Barringer, E. F. Babelay, C. E. Nunley, M. J. Bartkus, W. D. Fisher, and C. T. Rankin, Jr., (N. G. Anderson, ed.), *J. Natl. Cancer Inst. Monograph* **21**, 137 (1966).
- <sup>5</sup> N. Cho, H. P. Barringer, J. W. Amburgey, G. B. Cline, N. G. Anderson, L. L. McCauley, R. H. Stevens, and W. M. Swartout, (N. G. Anderson, ed.), *J. Natl. Cancer Inst. Monograph* **21**, 485 (1966).
- <sup>6</sup> N. G. Anderson, W. W. Harris, A. A. Barber, C. T. Rankin, Jr., and E. L. Candler, (N. G. Anderson, ed.), *J. Natl. Cancer Inst. Monograph* **21**, 253 (1966).
- <sup>7</sup> N. G. Anderson, *Bull. Am. Phys. Soc.* **1**, (Ser. II), 267 (1956).
- <sup>8</sup> N. G. Anderson, *J. Phys. Chem.* **66**, 1984 (1962).
- <sup>9</sup> N. G. Anderson, (N. G. Anderson, ed.), *J. Natl. Cancer Inst. Monograph* **21**, 9 (1966).

<sup>10</sup>A. S. Berman, (N. G. Anderson, ed.), *J. Natl. Cancer Inst. Monograph* **21**, 41 (1966).

<sup>11</sup>A. Tiselius, K. O. Pederson, and T. Svedberg, *Nature* **140**, 848 (1937).

<sup>12</sup>D. R. Waugh, and D. A. Yphantis, *J. Phys. Chem.* **57**, 312 (1953).

<sup>13</sup>D. A. Yphantis, in *Ultracentrifugal Analysis in Theory and Experiment*, (J. W. Williams, ed.), Academic Press, p. 227 (1963).

<sup>14</sup>H. L. Casey, *Public Health Monograph No. 74*, 1965.

<sup>15</sup>P. Y. Cheng, and H. K. Schachman, *J. Polymer Sci.* **16**, 19 (1955).

<sup>16</sup>K. O. Pederson, "The Ultracentrifuge" by T. Svedberg and K. O. Pederson, Oxford, p. 355 (1940).

<sup>17</sup>N. G. Anderson, "Physical Techniques in Biological Research, Vol. III, Cells and Tissues" (G. Oster and A. W. Pollister, eds.), New York, Academic Press Inc., p. 299 (1956).

<sup>18</sup>C. de Duve, J. Berthet, and H. Beaufay, *Progr. Biophys. Biophys. Chem.* **9**, 325 (1959).

## J. ZONAL SEPARATION OF HUMAN MACROGLOBULIN IN WARM DENSITY GRADIENTS

G. B. Cline

The usefulness of density gradient centrifugation as a separation technique for small particles and macromolecules is limited by the gravitational forces developed by zonal centrifuge rotors. Macromolecules are routinely sedimented in the Beckman Model E Analytical ultracentrifuge in gravitation fields of up to 250,000 X gravity. Lacking such gravitational forces in preparative centrifuges it has been necessary to spin for a longer period of time. When a density gradient is employed in a separation method, the problems of separation become even greater because of the increased density and viscosity. The lower size limit for efficient separation of useful amounts of material in swinging centrifuge tubes appears to be about 25 S. Analytical data may be obtained for much smaller particles, however. By using the larger capacity zonal centrifuge rotors, larger amounts of 18 S macroglobulin have been separated from other plasma proteins and cells. (See Section 3F of this report and ref. 1.) To achieve these separations however, 18 hr of centrifugation time is required. A method is described here which reduces an 18-hr separation to 3 to 6 hr. This method utilized sucrose density gradients at 30 to 35°C and has been applied to the large-scale separation of macroglobulin from other serum proteins in three different zonal centrifuge rotors. The higher temperature of the sucrose density gradients is compatible with the temperature-stability range of the serum protein while at the same time it reduces the viscosity of the sucrose to allow for more rapid sedimentation of the macroglobulin.

## Materials and Methods

The B-XVI is a continuous sample flow rotor which can be used for batch-type operation. The sucrose density gradients were built into the rotors while they were spinning at 2000 to 3000 rpm. The B-XV gradients were made by stacking 400 ml of 20% (w/w) over 450 ml of 25% sucrose. Twenty-five to 50 ml of human plasma or calf serum was used in addition to 800 ml of overlay solution. All components were prewarmed to 30°C before being introduced into the rotor. Gradients in the B-XVI rotor were made of 100 ml of buffer (Miller-Golder, pH 7.5), 50 ml of calf serum, 300 ml MG buffered 20% sucrose and 300 ml MG buffered 25% sucrose. The third rotor system, the K-II system, is described elsewhere in this report (Section 2A) and utilizes large volume gradients. Experiments were set up in the K-II rotor by loading 1350 ml of MG buffer as overlay, 250 ml human plasma, 1000 ml MG buffered 20% and 1000 ml MG buffered 25% sucrose.

The B-XV rotor was made of titanium alloy and was operated in a Spinco Model ZU centrifuge at an indicated temperature of 30°C for 4 to 6 hr at 28,000 rpm. The B-XVI rotor was made of an aluminum alloy and was operated at an indicated 30 degrees and 40,000 rpm. The K-II was preheated with water to 30°C and operated at 27,500 rpm for 5 hr.

Density gradients were unloaded from the rotors while they were spinning at 2500 rpm and the effluent stream monitored at 280 m $\mu$ . Confirmation of the presence of macroglobulin in the separated zone was obtained by Schlieren analysis in the Model E analytical ultracentrifuge.

## Results

Initial attempts were made to decrease the time required for the separation of macroglobulins from serum by using warm gradients in the B-XV zonal rotor. Figure 3.31 shows the absorbance profile at 280 m $\mu$  and sucrose density tracing of a 6-hr experiment with 25 ml of calf serum. The large zone centered in fraction 22 represents the starting zone and probably contains mostly albumin and other slowly sedimenting material. The broader and smaller zone centered in fraction 31 is purified macroglobulin as determined by Schlieren analysis in the Spinco Model E centrifuge. No attempt was made to determine concentration of macroglobulin in the zone.

Similar results were obtained in a macroglobulin separation from human plasma on a sucrose density gradient in the K-II zonal rotor. The gradient was

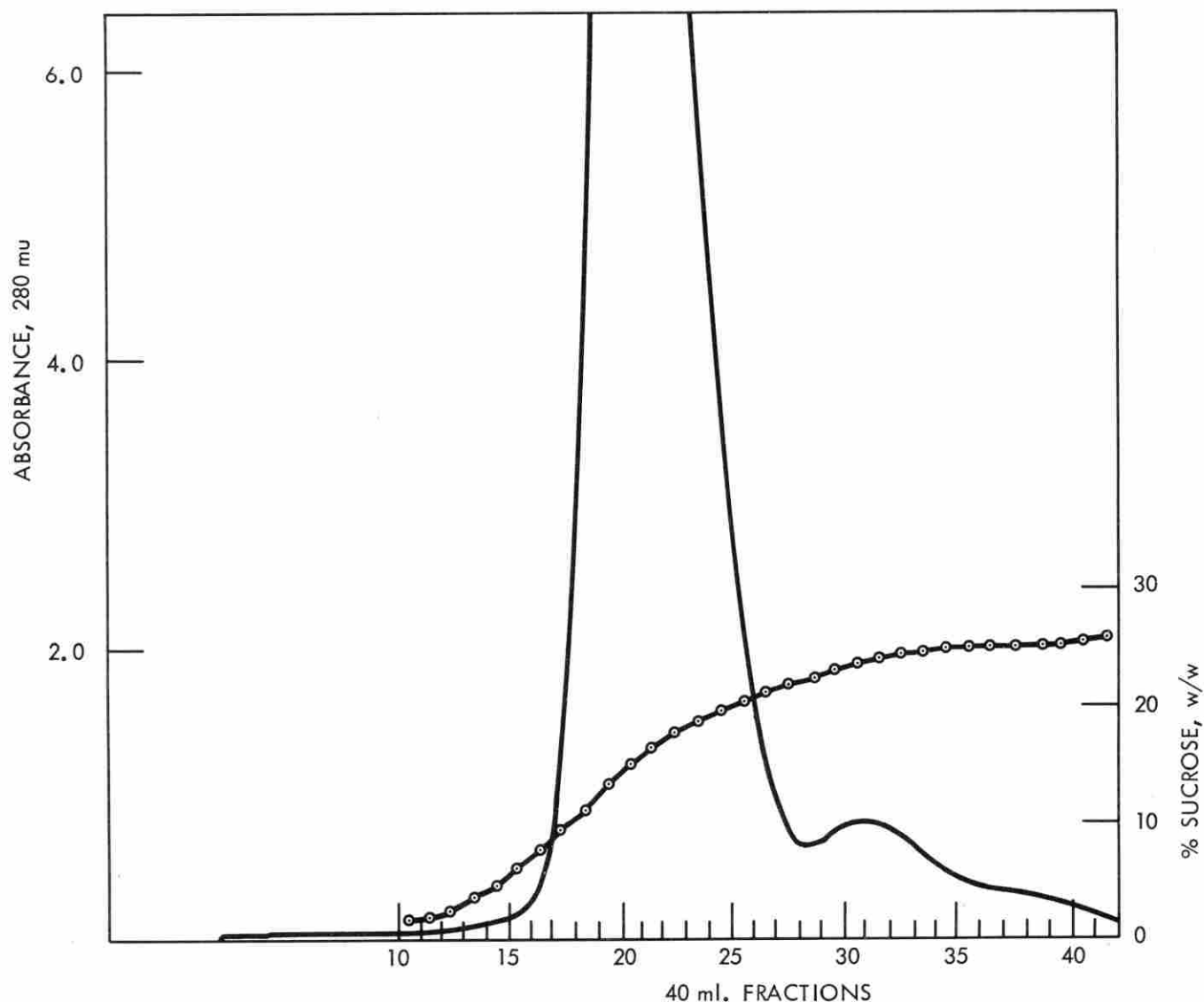


Fig. 3.31 Absorbance profile at 280  $m\mu$  and sucrose density tracing of a 6-hr experiment with 25 ml of calf serum.

prewarmed and was stacked into the rotor while the rotor was spinning at 2200 rpm. The sample was 250 ml of prewarmed plasma and this material was displaced from the core of the rotor with 1350 ml of MG buffer. The running time was 5 hr at 27,000 rpm at a final temperature of 28.5°C. The small zone centered in fraction 34 was macroglobulin as determined by Schlieren analysis. Similar separations of human macroglobulin have been achieved in the B-XVI rotor in 4 hr.

#### Discussion

The application of warm sucrose density gradients for the separation of blood proteins has a rational basis since blood proteins are not denatured at body temperatures. Use was made of this fact in designing this rapid technique for the isolation of usable quantities of macroglobulin from calf serum and human plasma.

While the results show that macroglobulin can be

separated from the remainder of calf serum in 6 hr in the B-XV zonal rotor using warm sucrose density gradients, a distinct advantage was found in using the B-XVI or K-II zonal rotor for such separations. The K-II zonal rotor separations not only utilized a large volume of starting sample (250 ml) but decreased the time required for separation to less than that for the B-XV. This decrease in time is made possible by the fact that the macroglobulin zone is sedimented a shorter distance through the gradient.

Temperature control of the density gradients is required for reproducible separations. Since the separation time is only a matter of hours, and the separation distance is short (in the B-XVI and K-II rotors), an additional hour of centrifuging can result in sedimenting the macroglobulin to the rotor wall. Warming of the rotor wall during centrifugation does not apparently set up thermal gradients within the liquid itself. Any warming at the rotor wall is undoubtedly uniform with the result that viscosity and density are decreased and sedimentation of the macroglobulin is therefore increased. Diffusion of the sample zone is not too great under these circumstances to give a workable separation method.

It is important to study the various parameters of this isolation method now that feasibility is demonstrated. As mentioned above, temperature control is required for reproducibility. Limited testing has been done on the shape of the density gradient. It has been found that a preformed gradient is not required. A two-step diffusion gradient gives results comparable to a gradient which was preformed with an elaborate gradient-forming device. It is important, in addition, to study the capacity of such gradients, since in practice the density of the sucrose immediately beneath the starting serum sample needs to be higher than the density of the serum. In these experiments, where densities are not adjusted, the starting sample seeks its own density in the gradient. This fact can be used to advantage in the loading procedures since little care is required to see that the sample is properly layered onto a gradient. The spreading of the starting sample zone with this technique will be compared experimentally with the spreading of the sample zone when using the conventional loading technique.

#### REFERENCE

- <sup>1</sup>W. D. Fisher, and R. E. Canning, *Natl. Cancer Inst. Monograph* 21, 403-412 (1966).

### K. A METHOD FOR ISOLATING NUCLEI USING SUCROSE-DEUTERIUM OXIDE GRADIENTS

L. H. Elrod

N. G. Anderson

The need for large amounts of pure nuclei has prompted the development of the following method for isolating nuclei from tissue homogenates by zonal centrifugation. Recent attempts to isopycally band some of the more dense subcellular particles have revealed the need for sucrose gradients that attain densities of 1.36 or higher. Our experience has shown that solutions greater than 66% w/w sucrose in water, as measured refractometrically, are too viscous to pump through the B-XIV and B-XV centrifuge systems where the gradient is built in a spinning rotor rather than in tubes. The viscosity of sucrose solutions in water increases very rapidly at high concentrations. For example the viscosity increases from 479.4 at 65% sucrose (w/w) to 620.3 centipoises at 66% at 5°C.<sup>1</sup>

Deuterium oxide (99.8%,  $\rho = 1.10754$  at 32°F) is now being used to build high-density gradients for banding particles.

For this work livers from male Sprague-Dawley rats (150-200 gm) were used to prepare the starting homogenate. The livers were perfused *in situ* using the technique described by N. G. Anderson<sup>2</sup> using Locke's solution as the perfusing fluid. Four to eight grams of tissue were then excised, freed of obvious fibrous material, and weighed in a beaker containing about 10 ml of cold homogenate suspending medium (8.5% sucrose in water  $1.5 \times 10^{-3}$  M CaCl<sub>2</sub> and made pH 7.6 with Tris acetate.) The tissue was then finely minced with scissors. About 50 ml more of the suspending medium was added to the minced liver before homogenization. Fifty up-and-down strokes in a Potter Elvehjem homogenizer with plastic pestle broke most of the cells without damaging the nuclei. Enough suspending medium was added to give a final concentration of 1% wet weight volume with a total volume of 400 to 800 ml. After dilution the homogenate was strained through four layers of cheesecloth. The homogenate tissue and solution were kept on ice throughout the preparation.

**Gradients:** Isolation of nuclei from the starting homogenate was made in a titanium B-XV zonal centrifuge rotor.<sup>1,3</sup> A 1200-ml gradient linear with volume was used, which ranged from 20% sucrose in water ( $\rho 1.085$  at 5°C) to 65% sucrose in deuterium oxide ( $\rho 1.368$  at 5°C). After the gradient was pumped

into the rotor the rotor was then filled with the 65% sucrose  $D_2O$  solution as cushion. All solutions in the gradient and cushion were  $5 \times 10^{-4} M$  with respect to  $CaCl_2$  and were made to pH 7.6 with Tris acetate.

**Sample loading:** A one hundred ml batch of the 1% homogenate was pushed into the rotor through the center line and allowed to sit on top of the gradient for two minutes at loading speed (3000 rpm). The sample zone was then pushed out by pumping in cushion solution until the effluent became clear (usually about 110 ml). This procedure was repeated as many times as was necessary to introduce all the starting homogenate into the rotor. After all the sample was loaded and pushed back out, the rotor was accelerated to 25,000 rpm for about 2 hr ( $50,000 w^2t$ ) to isopycally band the nuclei.

The gradient stream recovered after centrifugation was monitored by recording absorbance at  $260 m\mu$  using a Beckman DU spectrophotometer with a 0.2 cm path flowcell.<sup>4</sup> The stream was collected in 40 ml volumes, each of which was examined microscopically.

**Results:** 1240 ml (thirty-one cuts 40 ml each) of the rotor contents were recovered. Examination of the individual cuts by phase-contrast microscopy revealed the following:

- a. Cuts 1 through 28 contained cytoplasmic granules and some small membrane fragments.
- b. Cuts 19 through 25 contained whole cells, red blood cells (RBC), occasional broken cells, many membrane fragments and a few nuclei with granular cytoplasmic material attached.
- c. Cut 26 contained many RBCs, membrane fragments with granules and a few nuclei.
- d. Cut 27 contained more nuclei, fewer RBCs and fewer granules and membrane fragments.
- e. Cut 28 contained a greater number of nuclei and some small membrane fragments.
- f. Cuts 29 ( $\rho 1.353$ ) and 30 ( $\rho 1.364$ ) contained the nuclear peak with no observable contaminating material. There was no aggregation and the individual nuclei appeared to be intact and were morphologically indistinguishable from those in fresh starting homogenate.

### Discussion

The purpose of this investigation has been to develop a method of isolating nuclei, free of contaminating material, in quantities sufficient for biochemical and physiological studies. Using the method described here, it is possible to obtain a fraction containing nu-

clei that appear nongranular, unbroken, and show no obvious differences in size from those of cells *in vivo*. It is realized that optical observation is no guarantee that some nuclear constituents have not been lost.

The use of deuterium oxide as the solvent for sucrose solutions has enabled us to build gradients with sufficient density to isopycally band nuclei and other equally dense particles without encountering viscosities that are impossible to pump through the centrifuge systems. These gradients offer two advantages: first, the gradient solutions are less viscous at a given density, and secondly there is less sucrose in an isopycally banded sample harvested from the gradient.

The sample was prepared in 8.5% sucrose  $1.5 \times 10^{-3} M CaCl_2$  made to pH 7.6 with Tris acetate. Lower pH levels were tried as were higher and lower concentrations of  $CaCl_2$  but the above values proved best from the viewpoint of cell breakage and maintenance of nuclear integrity as observed optically.

The  $CaCl_2$  concentration of the gradient was reduced to  $5 \times 10^{-4} M$  when it was found that  $1.5 \times 10^{-3} M$ , as is used in the homogenizing medium, resulted in granular irregularly shaped nuclei.

Initial separations of nuclei were made using homogenate concentrations from 10% to 20% w/v. There were large aggregations of nuclei in the recovered fraction. These clumps contained much cellular debris that was trapped between the nuclei and in some cases, granular material appeared to be attached to the nuclei. It was found that dilute homogenates (1%) yield nuclear fractions with little or no clumping and free of contaminating material.

The batch method described in this paper for loading the centrifuge rotor was adopted for two reasons: Nuclei from the centripetal side of the sample must pass through the entire width of the sample zone. The width of a 100-ml sample zone is about 2.85 cm, while an 800-ml sample zone would have a width of about 6.33 cm. Any particle moving through a sample zone may come in contact with and aggregate with other particles. Thus a narrow sample zone would reduce the amount of particle contact and thus reduce contamination. Another advantage of using a narrow sample zone is that nuclei can move out of the sample zone into the gradient in a shorter time span. The shorter time allows fewer contaminating particles to move into the gradient with the nuclei.

These studies suggest that a low-speed, large-radius continuous-flow-with-banding rotor be designed which would allow nuclei to be continuously removed from a

sample stream and be sedimented into a D<sub>2</sub>O-sucrose gradient. After the completion of the continuous flow phase of the experiment, the rotor could be accelerated to very high speed for isopycnic banding. After deceleration to low speed it would be unloaded in a conventional manner.

#### REFERENCES

<sup>1</sup>E. J. Barber, *J. Natl. Cancer Inst. Monograph* **21**, 219 (1966).

<sup>2</sup>N. G. Anderson, *Exptl. Cell Res.* **8**, 91-100 (1955).

<sup>3</sup>N. G. Anderson, D. A. Waters, W. D. Fisher, G. B. Cline, C. E. Nunley, L. H. Elrod, and C. T. Rankin, Jr., *Analytical Techniques for Cell Fractions, V. Characteristics of the B-XIV and B-XV Zonal Centrifuge Rotors.* (In press).

<sup>4</sup>N. G. Anderson, H. P. Barringer, E. F. Babelay, C. E. Nunley, M. J. Bartkus, W. D. Fisher, and C. T. Rankin, Jr., *J. Natl. Cancer Inst. Monograph* **21**, 137 (1966).

## 4. Purification of Large Quantities of Influenza Virus

Experience has amply demonstrated that the development of centrifugal systems for vaccine purification should be carried out in close collaboration with groups producing vaccines, and that testing of new rotor systems should be done using materials identical to those used in vaccine production. Collaborative programs with interested pharmaceutical firms have therefore been arranged to test and evaluate centrifuges and other separations systems, and to define as clearly as possible the major problems which remain to be solved. The use of the B-IV, IX, XVI, and K-II rotors for influenza virus purification have been intensively evaluated in collaboration with Eli Lilly and Company over the past three years.

### PURIFICATION OF LARGE QUANTITIES OF INFLUENZA VIRUS BY DENSITY GRADIENT CENTRIFUGATION

C. B. Reimer <sup>1,2</sup>	R. M. van Frank <sup>1</sup>
R. S. Baker <sup>1</sup>	T. E. Newlin <sup>1</sup>
N. G. Anderson	G. B. Cline

By using a rate-zonal centrifugation followed by an isopycnic banding process, we demonstrated previously that commercial influenza virus vaccine could be purified an additional 10-fold, which permitted a separation of the protective antigens from most of the pyrogens usually found in such partially purified material.<sup>3</sup> In order to increase the amount of antigen processed with the zonal centrifuge, various ancillary procedures for concentrating and purifying the virus were also reported.<sup>4</sup> Subsequently, at the Oak Ridge National Laboratory, there has been a very rapid development of new continuous-flow zonal centrifuges which are generally useful because they permit the zonal centrifugation of much larger volumes of crude material than heretofore.<sup>5-12</sup> This paper reports some

of our current collaborative results insofar as influenza virus purification is concerned. Some new data is given which demonstrates the utility of the barium sulfate, absorption-elution technique,<sup>13-15</sup> when employed with zonal centrifugation.

### Materials and Methods

**Virus.** Influenza virus was produced by standard techniques<sup>16,17</sup> in the allantoic cavity of eleven-day-old embryonated chicken eggs. The strains used in this study were: A/PR-8, A<sub>1</sub>/Ann Arbor/1-57, A<sub>2</sub>/Taiwan/1-64, A<sub>2</sub>/Japan-170/62, B/Maryland/1-59, and B/Massachusetts/3-66.

**Barium sulfate absorption-elution.** Prior to zonal centrifugation, virus was concentrated 3.5X and partially purified by the barium sulfate, absorption-elution procedure,<sup>13-15</sup> as modified below:

Virus was absorbed from allantoic fluid (pH 7.8-8.0) in the cold room (0-3°C) by the addition of potassium oxalate and the amount of dry barium sulfate shown in Table 4.1. After stirring for 90 min and standing overnight, the barium sulfate with absorbed virus was harvested by centrifugation into the 4-liter bowl of a Sharples continuous-flow centrifuge at 7000 rev/min, with a flow rate of 50 to 80 liters/hr.

Virus was eluted by resuspending the barium sulfate into  $\frac{1}{7}$  the original volume of fluid having a composition shown in Table 4.1. The next day, the barium sulfate was removed from the resuspended virus at room temperature by centrifugation at  $800 \times g$  for 10 min in an International Centrifuge. The final eluate containing the partially purified virus was adjusted to pH 8.0 and diluted approximately 2-fold with pyrogen-free distilled water to a final specific gravity of  $1.050 \pm 0.005$ .

**Zonal Centrifugation.**—The batch type zonal rotors, B-IV<sup>5,18</sup> (Spinco Division, Beckman Industries, Palo Alto, California) and B-XV<sup>6</sup> (Oak Ridge National

**Table 4.1. Amounts of Dry Barium Sulfate Used to Adsorb Six Strains of Influenza Virus and the Composition of the Eluting Media to Remove the Virus from the Barium Sulfate**

Strain	ADSORPTION			ELUTION				
	Gms of BaSO <sub>4</sub> Added per liter Allantoic Fluid	Oxalate	Bone Gelatin	Na <sub>3</sub> Citrate	pH	NaCl	Tris	Tween 80
PR-8	40 gm	None	0.2%	0.25 M	7.2	None	None	None
Taiwan	50	0.16 M	0.2	0.25	7.2	1.0 M	0.4 M	0.16 M
AA	50	0.16	0.2	0.25	7.2	1.0	0.4	0.16
Jap 170	50	0.16	0.2	0.25	8.8	1.0	0.4	0.002
B Mass.	50	0.16	0.2	0.25	7.2	1.0	0.4	0.16
B Md.	60	0.16	0.2	0.25	7.2	1.0	0.4	None

Laboratory) were used in a modified Spinco Zonal Ultracentrifuge in a manner described in the literature.

The B-IX rotor used was an Oak Ridge developmental design.<sup>7,8,11,12</sup> During the course of this study numerous improvements of this type of rotor were evolved at Oak Ridge, culminating in the present B-XVI rotor. This development is not the concern of this paper.

The K-II centrifuge (Figure 4.1) used for these studies was a prototype air-driven centrifuge, designed and constructed at the Oak Ridge National Laboratory and the Oak Ridge Gaseous Diffusion Plant as a continuous-flow, isopycnic banding zonal centrifuge, suitable for large capacity production.<sup>9,10</sup> In general, the principles and manner of operating this centrifuge were identical to the other Oak Ridge continuous-flow zonal centrifuges. However, some important operational differences are noted here.

Reorienting gradient technique,<sup>5</sup> for initially loading the gradient and terminally unloading the fractions while the rotor was at rest was used exclusively. Initially, the rotor (3.6 liters) and associated tubing is filled with the lighter of the two solutions which was used to make the diffusion gradient. We used sucrose solutions, buffered with 0.01 M phosphate and 0.02% gelatin at pH 8.0, for our gradients. Sucrose concentration in the lighter of the two gradient solutions had been previously adjusted so that this solution was 0.005 units heavier than the specific gravity of the virus eluate (1.050) from the BaSO<sub>4</sub>.

After filling, the rotor was then accelerated from rest to 2000 rev/min, where the fluid flow was reversed several times to de-gas the system. The rotor was then brought to rest by means of the air brake. An appropri-

ate amount (usually about 1.8 liters) of the heavier of the two solutions used to form the diffusion gradient (60% sucrose, buffered the same as the lighter gradient solution) was then forced into the bottom of the rotor, displacing an equal volume of the lighter solution from the top. The lower rotor inlet line was clamped off and the rotor was smoothly accelerated to 2000 rev/min. The acceleration rates were: 120 rev/min<sup>2</sup> to 500 rev/min, 250 rev/min<sup>2</sup> to 2000 rev/min. At this speed, the gradient had become reoriented from a vertical to a centrifugal direction. Fluid flow inboard of the imprisoned gradient was then established, from the top to the bottom of the rotor, and maintained while the rotor was smoothly accelerated to 20,000 rev/min (400 rev/min<sup>2</sup> to 4000 rev/min, maximum acceleration rate to 20,000 rev/min). Virus sample flow was then started while the rotor was further accelerated at a rate manually governed to prevent high hydrostatic pressure (not above 15 psi) in the input line. This backpressure is due to the presence of two fluids which differ in density by 0.005 sp. gr. units in a large gravitational field of the 700-ml core-taper volume. Displacement of a dense fluid by a light one results in a backpressure in a continuous flow rotor where both fluid lines are brought back to the axis of rotation before leaving the rotor. Once 700 ml of gradient had been displaced by the lighter virus sample, rotor acceleration could proceed to the operational speed without development of hydrostatic backpressure in the input line.

Generally, the K-II centrifuge was operated at 27,000 rev/min,<sup>19</sup> using 75 cubic feet of filtered dry air per minute at 25 psi square inch. Acceptable clean-out of influenza virus occurred from the 1.050 specific gravity citrate solutions we employed when sample

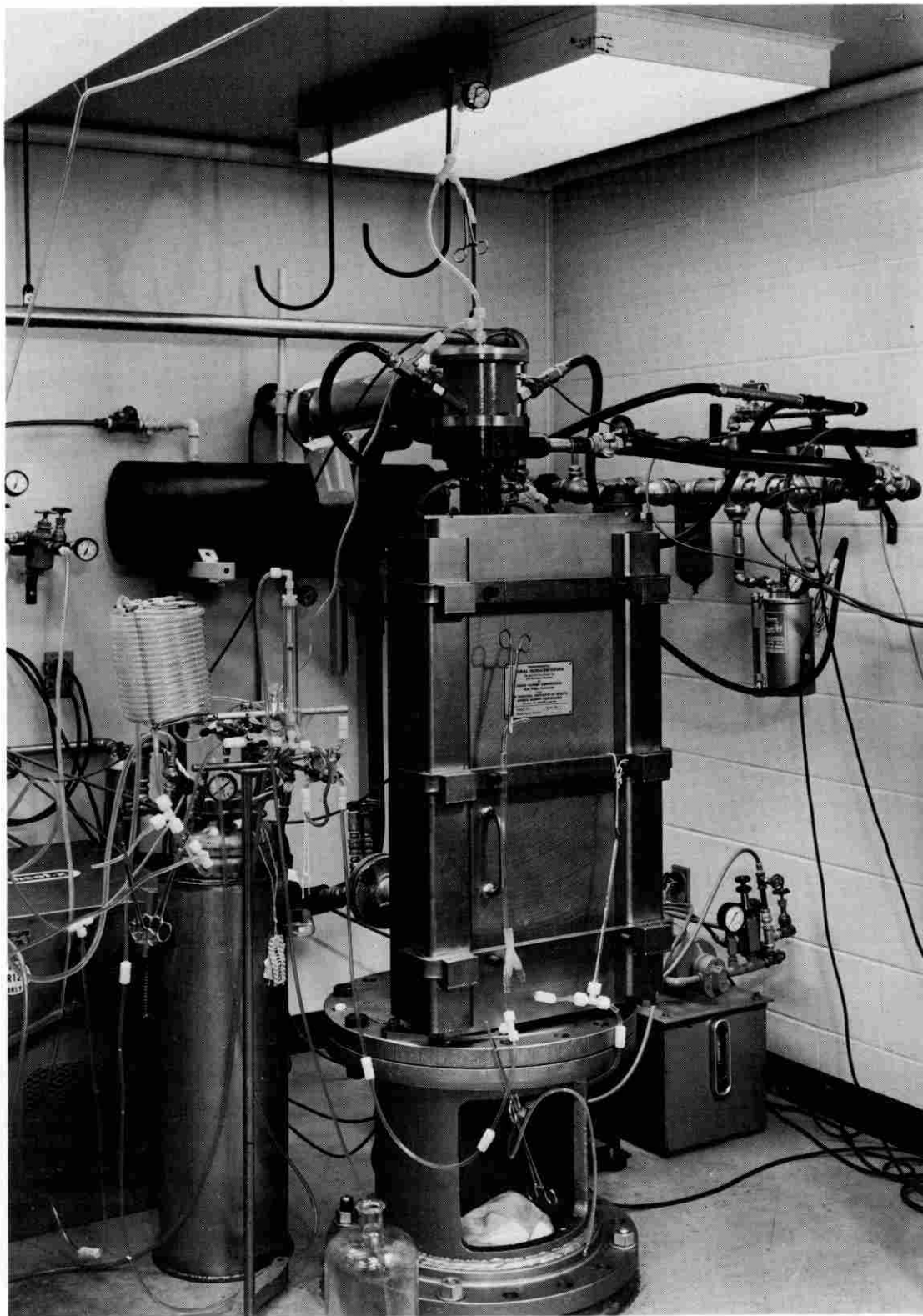


Fig. 4.1 K-II zonal centrifuge.

flow was adjusted between 4 and 5 liters/hr. This is equivalent to processing 14 to 18 liters of allantoic fluid per hour.

Upon termination of flow, sample remaining in the core-taper volume (700 ml) was displaced by a sucrose gradient solution 0.005 sp. gr. units lighter than the sample. Rotation was continued at full speed to allow virus to band an additional 30 min.

To unload, the rotor was allowed to coast to rest. The mass of the rotor is sufficiently large to insure even reorientation during deceleration. The fractions were collected from the bottom of the rotor by displacing the gradient with compressed air.

*Gradient shape* was determined by measuring the sucrose concentration refractometrically with a Bausch & Lomb Abbe refractometer.

*Optical density* between 250 and 350  $m\mu$  was determined for all fractions with a Cary 15 spectrophotometer.

*CCA assays* were performed as specified in references 16 and 17.

*Mouse protection* tests were performed as specified in references 16 and 17.

*Protein determinations* were made by the method of Lowry *et al.*<sup>20</sup>

*Hemagglutinin assays* were done using Microtiter equipment,<sup>21</sup> or alternatively, in plastic trays as follows: a 0.5-ml sample was serially diluted in 2-fold increments with buffered saline, and a washed chicken red cell suspension (0.7%) was added to each cup. After a 1-hr incubation period at room temperature, the trays were inclined at approximately 45°. The

endpoint was read as the dilution where the red cells remain in a button in the bottom of the cup for at least 15 sec without migrating down the wall.

*Immunodiffusion* was performed using the NIL-Saravis Apparatus of The National Instrument Laboratories Inc. with Millipore Celotrate membranes. At the end of a 72–90 hr incubation period and fixing and rinsing, the membrane was stained using Coomassie Brilliant Blue according to the method of Fazekas de St. Groth,<sup>22</sup> except the drying of the membrane is done at 37°C for 45 min. Rabbit antisera against chicken serum was obtained from Colorado Serum Company. The membrane was cleared using light paraffin oil, mounted between two 3¼ in. × 4 in. lantern slide cover glasses, sealed with Permout, bound together with tape, and photographed.

## Results

One hundred and five liters of allantoic fluid containing the Maryland B strain of influenza virus were processed through the B-IX rotor. Figure 4.2 shows the optical density and hemagglutinin profiles of fractions harvested from this continuous-flow isopycnic banding device. The crude egg harvest first had been cleared of gross debris in the Sharples Supercentrifuge with essentially all of the virus remaining in the flowing stream. This virus was then quantitatively captured in the B-IX rotor when it was spinning at 40,000 rpm with a flow rate of 8 liters/hr. In this case, the bulk of soluble impurity remained in the stream flowing through the B-IX rotor and was discarded. Calculated either from the hemagglutinin pattern test or from the standard chicken cell agglutinin test, two-thirds of the total virus originally present in the 105-liter pool of crude allantoic fluid was recovered in the sucrose gradient as a 200-ml band (with peak at buoyant density 1.187 g/ml). The HA titer at the peak was greater than 320,000 in comparison with an HA titer of 512 for the original allantoic fluid.

Eighty ml of this B-IX concentrate was further purified by a rate-zonal process in the B-IV rotor after first removing the sucrose with a G-25 Sephadex column. Figure 4.3 (top) shows the rate-zonal sedimentation profile for this B-IV centrifugation in comparison with the sedimentation profile for an identical B-IV rate zonal run made with a typical commercial 10X concentrate (bottom). Soluble impurities are found in the peak on the left, large particulate impurities in the peak on the right. The central peak, rising out of the microsomal background, contains the

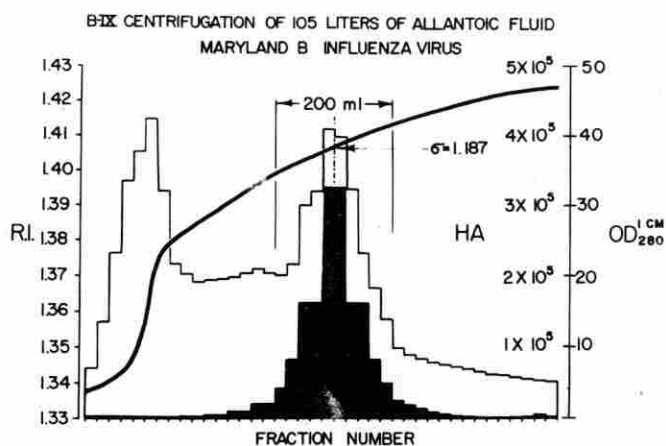


Fig. 4.2 Distribution of influenza virus (HA shaded area) and optical density in a sucrose gradient (refractive index) from a B-IX rotor. See test for details.

B-IV RATE-ZONAL PURIFICATION OF MARYLAND-B INFLUENZA VIRUS

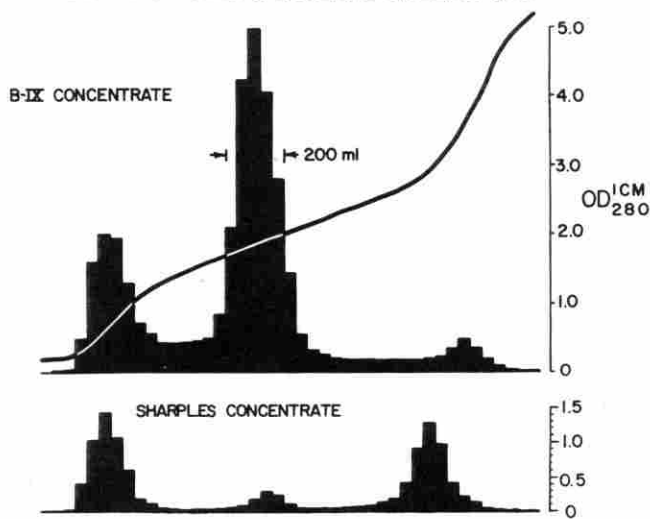


Fig. 4.3 Rate zonal sedimentation profiles for the B-IX concentrate of Figure 2, and a 10X Sharples commercial virus concentrate. The central peak contains the virus.

virus. The relative amplitude of the virus peak to the impurity peaks graphically demonstrates the greater purity of virus from the B-IX process. Dilutions of material taken from various peak regions of a similar rate-zonal centrifugation of 10X commercial concentrate were tested for pyrogenicity in rabbits. Table 4.2 shows that much of the pyrogen is present with the soluble macromolecular impurity, and was separable from the immunizing fraction by the rate-zonal technique. Based on the dilution giving approximately equal pyrogenicity the purified virus fraction was

one-tenth as pyrogenic as the commercial product from which it came. Very little pyrogen was associated with the large particulate impurity of this lot.

Virus from the B-IX purified concentrate and virus from the B-IV purified derivative was diluted, inactivated with formalin, and sterilized by filtration through HA millipore membranes. These vaccines passed all control testing necessary for vaccine production for human use. Table 4.3 gives a tabular comparison of the original crude allantoic fluid, B-IX and B-IV vaccines, and a standard 10X Sharples concentrate made from the same egg lot, as a control. Table 4.4 shows the results of a mouse potency test of these zonal purified vaccines, as performed under standard conditions. It is seen that both of these experimental monovalent Maryland B vaccines protected half the mice even when diluted 625-fold.

Essentially identical results were obtained for similar monovalent A<sub>2</sub>/Taiwan vaccines. However, difficulty often has been experienced with the B-IX rotor in attempting to routinely repeat these results with volumes of allantoic fluid as large as 100 liters. This is because large particulate impurity, present in variable amount in large volumes of allantoic fluid interfered with sedimentation by overloading the gradient or even plugging the small channels in the rotor or rotating seal to prevent steady-state flow or terminal unloading of the fractions. (Considerably less trouble from this cause was experienced with 100-liter volumes of tissue culture fluid in the B-IX rotor.)

This problem was largely solved by first absorbing the virus from allantoic fluid by BaSO<sub>4</sub>, followed by elution with citrate solutions. Figure 4.4 shows an

Table 4.2. Pyrogenicity of a Standard Commercial Monovalent Strain of PR-8 Influenza Virus: Fractionated in B-XV Rotor

Sample	Original	Soluble Impurities	Purified Virus Pool	Particulate Impurities
Volume (ml)	350	440	480	720
CCA/ml	1,940	148	716	<68
Total CCA	680K (100%)	65K (9.6%)	343K (50.4%)	<49K (<7.2%)
Protein mg/ml	0.644	0.164	0.040	0.088
Total Protein mg	225 (100%)	72 (32%)	19 (8.5%)	63 (28%)
Pyrogenicity*				
1:4 dilution	+1.02°C	+0.98°C	+0.92°C	+0.42°C
1:40 dilution	+0.90°C	+0.62°C	+0.39°C	+0.40°C
1:400 dilution	+0.38°C	+0.17°C	+0.05°C	-0.29°C

\*Mean temperature rise of three rabbits during first 3 hr.

**Table 4.3. A Comparison of Purity and Concentration of Several Experimental Vaccines**

	Original Allantoic Fluid	Sharples Purified	B-IX Purified	B-IV Purified
Volume Concentration Factor	1X	10X	525X	210X
Concentration: CCA units/ml	145	1,164	43,350	9,000
CCA Concentration Factor	1X	8X	300X	62X
Lowery Protein: mg/ml	10.5	0.64	6.1	1.1
Purity: CCA Units/ml Protein	13.8	1,820	4,250	8,500
Purification Factor	1X	132X	318X	618X

**Table 4.4. Mouse Protection Test, Purified Monovalent (Md. B) Influenza Vaccine**

Vaccine	Original Vaccine Concentration (CCA/ml)	LD <sub>50</sub> Challenge Dose	No. Mice Surviving/No. Mice Inoculated				
			Vaccine Dilution				
			1/5	1/25	1/125	1/625	1/3125
B-IX Purified	933	40	6/6	6/6	6/6	5/6	1/6
B-IV Purified	898	40	6/6	6/6	6/6	3/6	0/6
NIH Reference	200	40	6/6	6/6	2/6	1/6	0/6

(as Md. B)

analytical rate-zonal sedimentation profile obtained with the B-XV rotor, using influenza virus processed by this absorption-elution technique. In comparison with other ancillary procedures we have studied<sup>4</sup> this process appeared relatively more efficient for separat-

ing the virus from the large particulate impurities found in allantoic fluid. The relative inefficiency of the BaSO<sub>4</sub> process for removing soluble macromolecular impurities (Figure 4.4) suggested the complementary character of this process with a continuous-flow isopycnic banding centrifugation, which is very efficient for removing soluble macromolecular impurities but is invalidated by large particulate impurity, as already discussed.

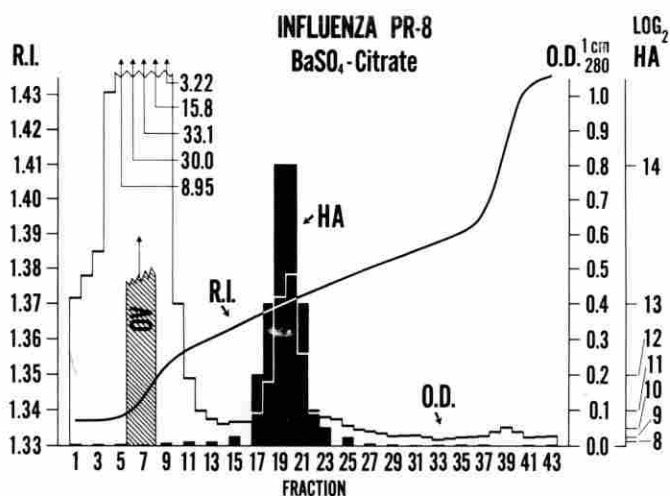


Fig. 4.4 Rate zonal sedimentation profile for influenza virus concentrated by the BaSO<sub>4</sub> adsorption-elution technique. Initial zone (O.V.) was 100 ml, O.D.<sub>280</sub><sup>1.0</sup> = 48.0, log<sub>2</sub> HA = 16.

Figure 4.5 shows the hemagglutinin and optical density profiles for six strains of influenza virus purified by the combined process: BaSO<sub>4</sub> adsorption-elution, followed by isopycnic banding in the K-II centrifuge. These are representative profiles from commercial production-sized lots, which utilized an average of 15,000 eggs each. These virus pools were diluted and further processed through formalin inactivation and bacteriological filters to make concentrated monovalent vaccines for further compounding to polyvalent vaccines. Table 4.5 lists some of the overall yield and purity data for twelve lots of monovalent vaccine. Table 4.6 gives a breakdown of the source of loss. Table 4.7 lists mouse potency data for a BaSO<sub>4</sub>-K-II polyvalent vaccine. After the A and B potency

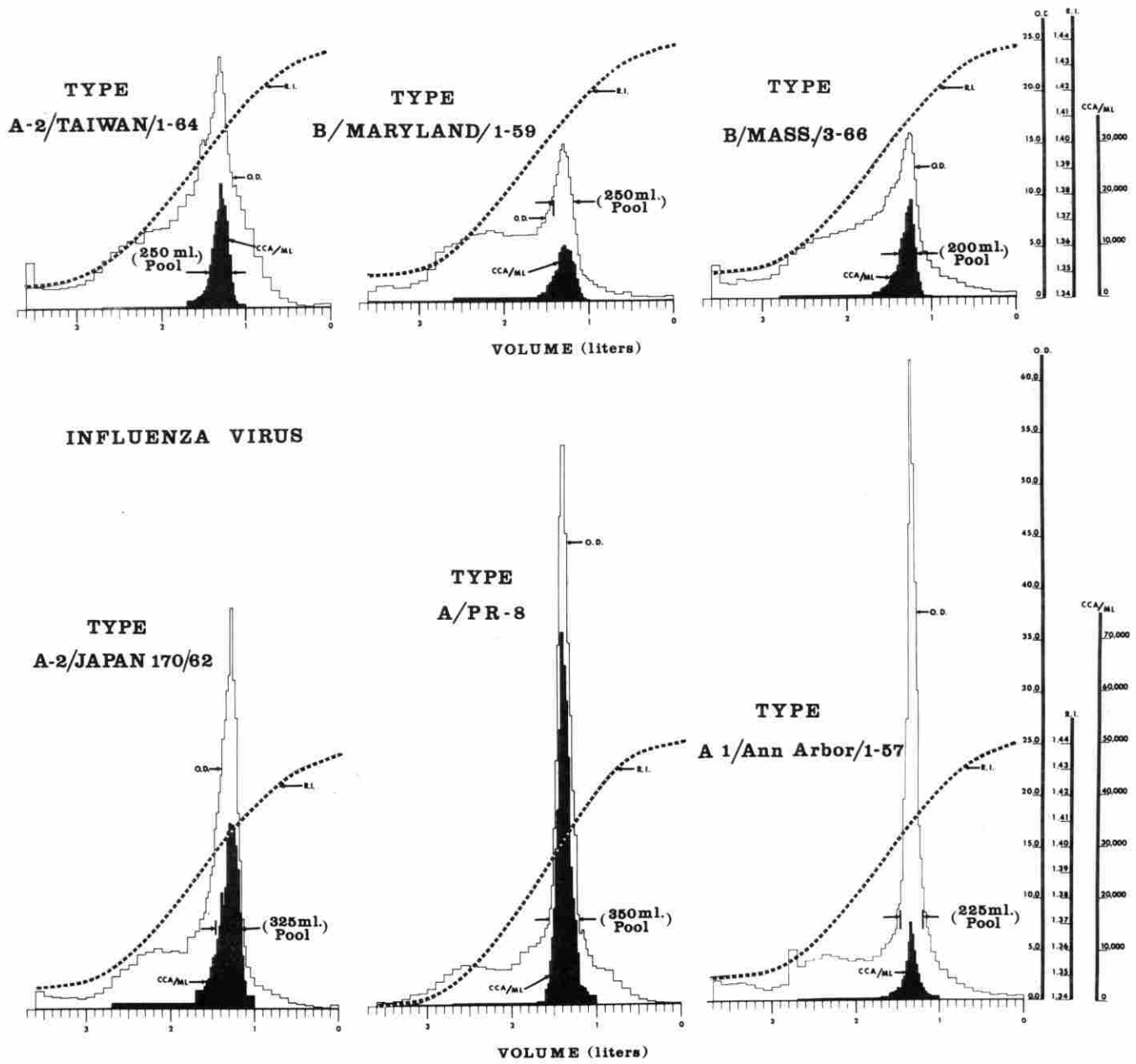


Fig. 4.5 Hemagglutinin and optical density profiles of influenza virus purified by the combined process: BaSO<sub>4</sub> absorption-elution, followed by isopycnic banding in the K-II zonal ultracentrifuge.

**Table 4.5. Influenza Virus Purification by Combined BaSO<sub>4</sub> Absorption-Elution, Followed by Isopycnic Banding in the K-II Centrifuge**

		INPUT			OUTPUT			
Strain	Lot No.	Volume of Allantoic Fluid (liters)	Virus Concentration (CCA/ml)	Total Input CCA × 10 <sup>6</sup>	Total Output CCA × 10 <sup>6</sup>	Over-all Over-all Yield (%)	No. of 100 CCA Doses Per Harvested Egg	Purity CCA/mg Prot.
Md. B	T-61160	89.5	159	14.2	3.70	26.0	4.0	22,300
	T-61164	93.0	128	11.9	4.12	34.6	4.2	18,020
	T-61166	152.0	62	9.44	3.18	33.7	2.1	8,820
Taiwan	T-61162	145.0	152	22.0	4.40	20.0	3.2	8,380
	T-61165	78.0	148	11.55	1.74	15.0	2.5	20,000
	T-61167	81.0	129	10.50	2.36	22.4	2.9	8,580
Ann Arbor	T-61163	150.8	200	30.2	2.60	8.6	1.9	15,770
	T-61168	103.7	132	13.7	2.56	18.7	2.7	8,580
	T-61171	95.0	193	18.3	2.12	11.6	2.4	8,480
PR-8	T-61161	56.7	323	18.3	7.29	39.8	11.9	10,500
	T-61169	144.0	200	25.6	15.90	62.0	13.6	13,400
	T-61170	99.3	314	31.2	13.30	42.7	13.7	8,680

**Table 4.6. Source of Loss, in Percent of Total CCA Originally Present in Allantoic Fluid (Minus Equals a Loss, Plus Equals a Gain)**

Strain	Over-all Average Yield of Product	Lost Un-absorbed to BaSO <sub>4</sub>	Lost Uneluted from BaSO <sub>4</sub>	Lost in K-II Effluent	Lost in K-II			
					Gradient, Outside of Virus Band	Lost During Inactivation & Filtration	Lost to Assay Sampling	Unaccounted For Loss
Md. B	31.4%	-15.7%	+6.3%	-29.8%	-16.8%	+0.8%	-10.0%	-3.4%
Taiwan	19.1	-25.2	-28.3	-22.7	-11.1	+2.5	-10.0	+13.9
AA	13.0	-11.2	-37.0	-28.4	-11.0	+3.4	-10.0	+7.2
PR-8	48.2	-20.2	-0.2	-17.1	-6.7	+4.2	-10.0	+2.4
Average	27.9%	-18.1%	-14.8%	-24.5%	-11.4%	+2.7%	-10.0%	+4.0

**Table 4.7. Mouse Potency Ratios for a BaSO<sub>4</sub>-K-II Purified Influenza Vaccine**

Strain	Conc. CCA/ml	Potency ratio: Exptl. vaccine/NIH Ref.			
		Test A	Test B	Test C	Test D
PR-8	165	11.03	5.71	9.87	8.67
AA	110	13.49	5.01	3.35	6.59
Md. B	300	8.69	8.65	5.70	25.12
Taiwan	225	2.56	2.95	1.70	3.35
Jap 170	300	1.00	1.29	1.14	3.40

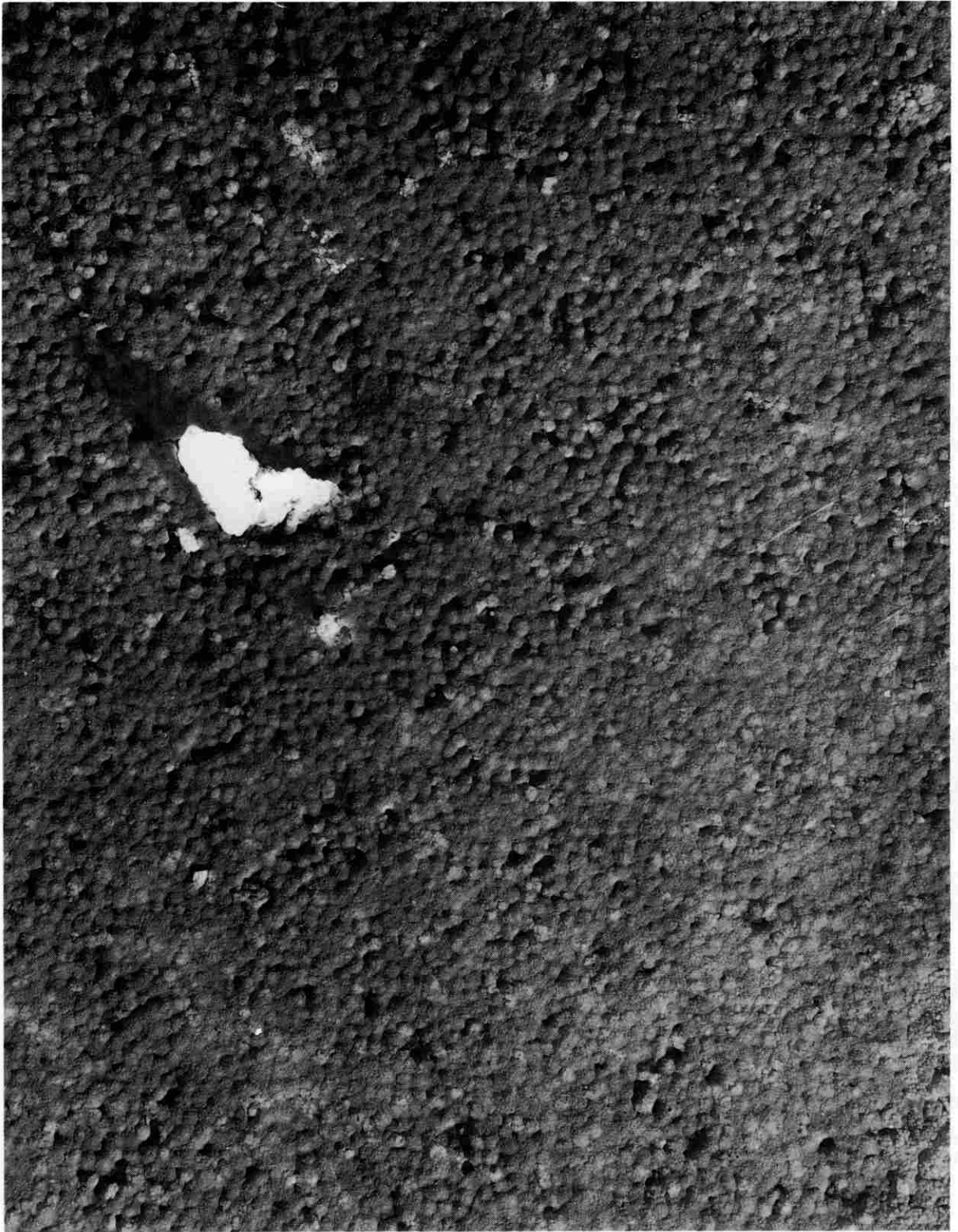
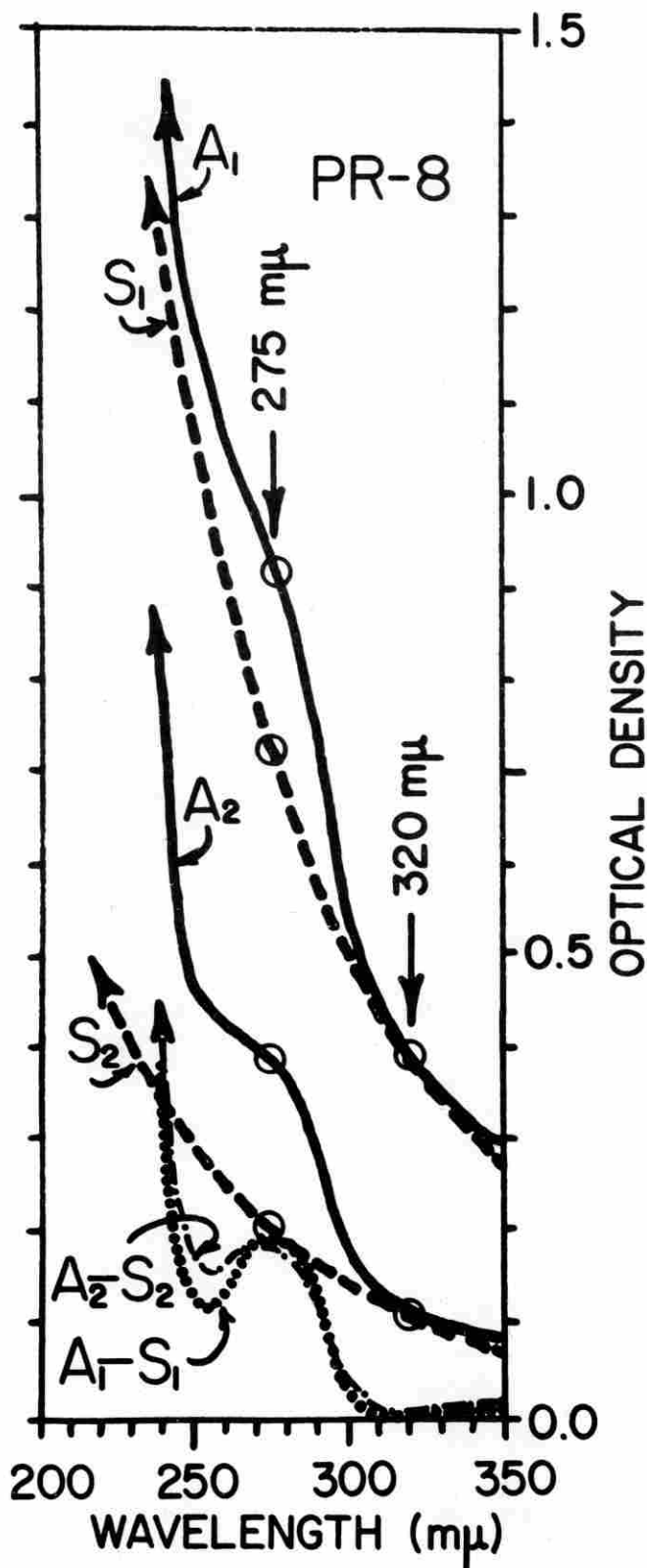


Fig. 4.6 Electron micrograph of a monovalent vaccine (Md-B) purified by the combined process. Magnification: 37,200 X.



tests were made the polyvalent vaccine was found to be inadvertently contaminated with a staphylococcus. It was then sterilized by HA Millipore filtration. The C and D tests show that potency was not lost by this process. Figure 4.6 is an electron micrograph made of an experimental monovalent vaccine made with the combined process.

Portions of K-II virus pools were further purified by a rate-zonal centrifugation in the B-XV rotor, as previously described. Figure 4.7 shows a typical ultraviolet spectral absorption curve for this more highly purified material, with and without  $\lambda^{-4}$  scatter correction. These rate-zonal purified virus pools, generally found in 25% sucrose, usually contained between 1000 and 2000 CCA units (50 to 100 micrograms of virus protein) per unit optical density (1.0, uncorrected) at 280  $m\mu$  in a 1 cm cell. Figure 4.8 shows an immuno-diffusion pattern obtained with rabbit anti-chicken serum in the center well and highly purified vaccine or commercial vaccine in the peripheral wells.

#### Discussion

Density gradient centrifugation, which customarily has been performed in swinging buckets with milliliter quantities of sample and centiliter amounts of gradient, has proved most useful in virology and other areas as an analytical (and small scale preparative) technique. The B-IV and B-XV batch type zonal rotors with total volumes of 1.7 liters, utilizing a deciliter or greater sample volume, extends the preparative possibility of zonal technique by 2 orders of magnitude. The continuous flow, isopycnic banding B-IX rotor (total volume 750 ml) permits optimal processing of liters or tens of liters of sample to add 2 and even

Fig. 4.7 Ultraviolet absorption spectra for purified influenza virus, A/PR-8. 1.0 cm cell against  $H_2O$  blank.

Curve  $A_1$ : Total absorbance of a rate-zonal purified pool after dilution 5-fold with distilled  $H_2O$ , final refractive index 1.3438.

Curve  $S_1$ : Theoretical absorbance due to an object which scatters inversely with the 4th power of the wavelength (Rayleigh scattering), assuming entire absorbance at 320  $m\mu$  due to scatter.

Curve  $A_2$ : Total absorbance of the same pool as in  $A_1$ , except that pool was diluted 5-fold with optically transparent 60% (w/w) sucrose, final refractive index 1.4245.

Curve  $S_2$ : Same as  $S_1$  except that  $S_2$  equals entire absorbance of  $A_2$  at 320  $m\mu$ .

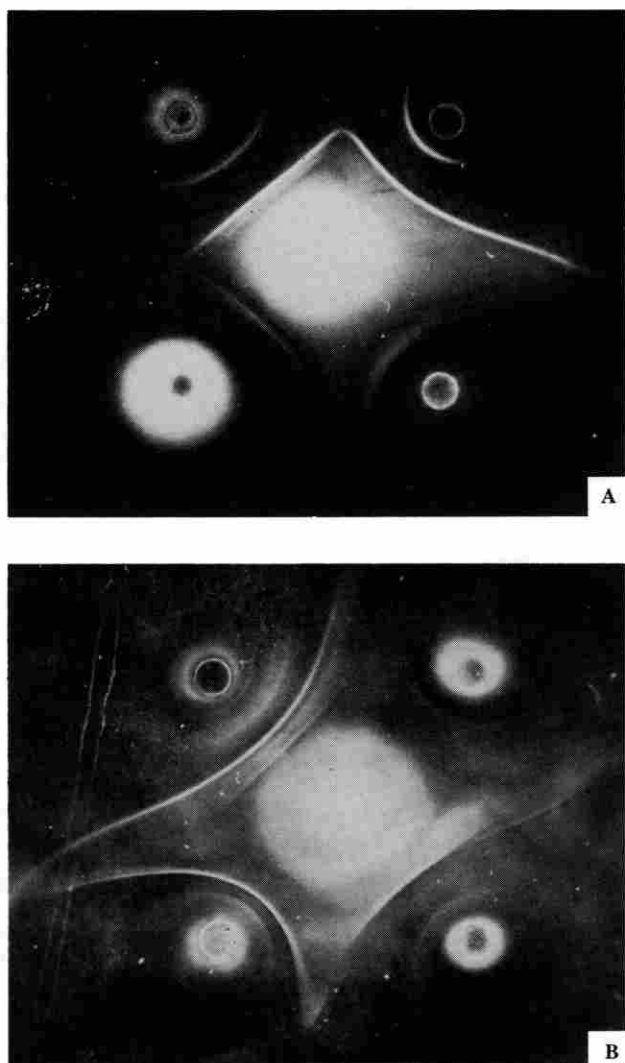


Fig. 4.8 Comparison of Commercial and Purified Influenza Vaccines by Immunodiffusion.

- A, upper left: commercial bivalent vaccine  
 A, upper right: commercial polyvalent vaccine  
 A, lower left: purified bivalent vaccine  
 A, lower right: purified polyvalent vaccine  
 B, upper right: purified trivalent vaccine  
 B, remaining peripheral wells: commercial poly-  
 valent vaccines from three different manufacturers.

In each case, the center well contains rabbit serum against chicken serum. The commercial vaccines contain a total of 600 CCA/ml; the purified bivalent and polyvalent vaccines, 1200 CCA/ml. The bivalent vaccines contained A<sub>2</sub>/Taiwan/1-64 and B/Maryland/1-59. The polyvalent vaccines had, in addition, A/PR-8 and A-1/Ann Arbor/1-57; and Figure 8b, A<sub>2</sub>/Japan 170/62. The purified trivalent vaccine had the 1967-68 "Bivalent" formula: A<sub>2</sub>/Taiwan/1-64, A<sub>2</sub>/Japan 170/62, and B/Massachusetts/3-66.

3 more orders of magnitude to the volumes conveniently processed in the batch type zonal rotors. When used sequentially with other purification procedures a single K-II centrifuge (volume 3.6 liters) has routinely processed more than 150-liter volumes of allantoic fluid per day.<sup>23</sup> Kilogram quantities of impurity have been rapidly separated from gram quantities of purified virus, which has been conveniently concentrated several hundredfold by the purification process.

We anticipate that some of the losses listed in Table 4.6 will be brought under better control. For example, the large sampling loss (10.0%) for these prototype runs can be diminished. Most of the virus lost in the K-II gradient (11.4%) was arbitrarily left there in the shoulders by selecting out a relatively narrow band centered on the virus peak. Some of the virus lost in the K-II effluent (24.5%) could have been captured by using a slower flow-rate, or faster rpm, or possibly by a more efficient rotor-core design. Likewise, with further study, one might anticipate improved yields (32.9% loss) from the BaSO<sub>4</sub> process.

The mouse potency ratios listed in Table 4.7 represent the factor by which a purified vaccine was diluted in excess of the NIH reference standard vaccine to confer equal protection (50% survival for challenged mice). A possible explanation for this enhanced potency in mice is that we underestimate the amount of antigen in these highly purified vaccines. This would happen if purified virus aggregated irreversibly causing an unequal distribution of the absolute number of virus particles during the serial dilutions used to measure the virus (CCA test). Mechanistically, an aggregate of many viruses may be no more efficient than a single virus for sticking together two red cells. We have direct electron microscopic evidence for some virus aggregation. Rational consequences of such an effect would be that:

1. Some yield loss of antigen as measured is only apparent and does not represent true loss.
2. The purity is underestimated.
3. Residual toxicity relates to a higher dose which may actually be given because we underestimate the amount of antigen present.

Alternatively, the mouse may respond more efficiently to a highly purified virus vaccine than it does to an impure material.

In Figure 4.7, it is seen that the total absorbancy of purified influenza virus at 275 m $\mu$  is due to two components. The major component, scatter, is variable depending on the refractive index of the suspending fluid. The minor component, best seen as a 275-m $\mu$

peak after scatter correction, is relatively independent of the refractive index of the suspending fluid. This component is probably due to the amino acids, tyrosin and tryptophan of the viral capsid protein. Clearly, light scattering must be taken into consideration if optical data are used as quantitative purity criteria in gradient separations of influenza virus.

The clinical evaluation of these vaccines, which is now in process, will be reported elsewhere (F. B. Peck, Jr. *et al.*, in preparation).

## REFERENCES

<sup>1</sup>Biological Research Division, Lilly Research Laboratories, Indianapolis, Indiana.

<sup>2</sup>Present address: National Communicable Disease Center, Atlanta, Georgia 30333.

<sup>3</sup>C. B. Reimer, R. S. Baker, T. E. Newlin, and M. L. Havens, *Science* **152**, 1379-1381 (1966).

<sup>4</sup>C. B. Reimer, R. S. Baker, T. E. Newlin, M. L. Havens, R. M. vanFrank, W. O. Storvick, and R. P. Miller, *J. Bacteriology* **92**, 1271-1272 (1966).

<sup>5</sup>N. G. Anderson, *J. Natl. Cancer Inst. Monograph* **21**, 9-40 (1966).

<sup>6</sup>N. G. Anderson, *Science* **154**, 103-112 (1966).

<sup>7</sup>N. G. Anderson, ORNL-3978 Special, Annual Report for period July 1, 1965 to June 30, 1966.

<sup>8</sup>N. G. Anderson, H. P. Barringer, J. W. Amburgey, Jr., C. B. Cline, C. E. Nunley, and A. S. Berman, *J. Natl. Cancer Inst. Monograph* **21**, 199-218 (1966).

<sup>9</sup>N. G. Anderson, and G. B. Cline, Semi-annual contract progress report to the National Institute of Allergy and Infectious Diseases. ORNL-4024. March 1 to July 1, 1966.

<sup>10</sup>N. G. Anderson, G. B. Cline, and W. W. Harris, Semi-annual contract progress report to the National Institute of Allergy and Infectious Diseases—NIAID Molecular Anatomy Program. September 1, 1966 to February 28, 1967.

<sup>11</sup>G. B. Cline, H. Coates, N. G. Anderson, R. M. Chanock, and W. W. Harris, *J. Bact.* (in press).

<sup>12</sup>I. Toplin, *J. Appl. Microbiol.* **15**, 582-589 (1967).

<sup>13</sup>J. Drescher, A. V. Hennessy, and F. M. Davenport, *J. Immunology* **89**, 794-804 (1962).

<sup>14</sup>M. Klembala, and I. Szekacs, *Nature* **205**, 828 (1965).

<sup>15</sup>H. Mizutani, *Nature* **198**, 109-110 (1963).

<sup>16</sup>Division of Biologics Standards, Minimum Requirements: Influenza Virus Vaccines, Types A and B.

<sup>17</sup>Division of Biologics Standards, Public Health Service Regulations. Title 42, Part 73.

<sup>18</sup>C. B. Reimer, J. E. Newlin, M. L. Havens, R. S. Baker, N. G. Anderson, G. B. Cline, H. P. Barringer, and C. E. Nunley, *J. Natl. Cancer Inst. Monograph* **21**, 375-388 (1966).

<sup>19</sup>The top operating speed of the K-II centrifuge with this type rotor will probably be about 30% higher, depending on adequate and complete evaluation of safety shielding. These studies are in progress. Presently the stream flows through a distance of 76 cm where the average force field is approximately  $37,500 \times g$ . At the proposed higher operating speed the G-force would be approximately 70% greater.

<sup>20</sup>O. H. Lowry, N. J. Rosebrough, A. L. Farr, and R. J. Randall, *J. Biol. Chem.* **193**, 265-275 (1951).

<sup>21</sup>J. L. Sever, *J. Immunol.* **88**, 320-329 (1962).

<sup>22</sup>S. Fazekas de St. Groth, R. G. Webster, and A. Datyner, *Biochem. Biophys. Acta* **71**, 377-391 (1963).

<sup>23</sup>To date 175 K-II runs have been made with only minor operating problems. This is approximately 1300 hr at 27,000 rev/min, using two instruments.

## 5. Electrophoretic Separations

### ELECTROPHORESIS IN LIQUID DENSITY GRADIENTS STABILIZED IN A CENTRIFUGAL FIELD

N. G. Anderson      A. Travaglini  
R. Jolley

#### Principles of Separation

Electrophoresis in a liquid density gradient has been widely used to separate proteins and other charged particles.<sup>1</sup> There are three limiting factors in electrophoresis of this type. The first is gradient capacity which limits the amount of sample which may be supported in a given zone on a gradient, the second is the length of the migration path which is limited by the limiting solution density available in aqueous systems, and the third factor is the rate of heat transfer out of the gradient which limits the distance between any point in gradient and a cooling surface. A variety of methods for maximizing the cooling surface area have been proposed. However, as the cooling area is increased, either by fluting the electrophoresis cell or by introducing cooling tubes internally along its length, the mixing produced by laminar flow during unloading is increased. Thus if a gradient is enlarged by placing it between two vertical cooling plates which are long in a horizontal direction, good cooling may be obtained, but considerable difficulty will be experienced in recovering the gradient. It should be noted that in a centrifugal field laminar mixing is minimized, and recovery of gradients stretched between thin plates is possible.

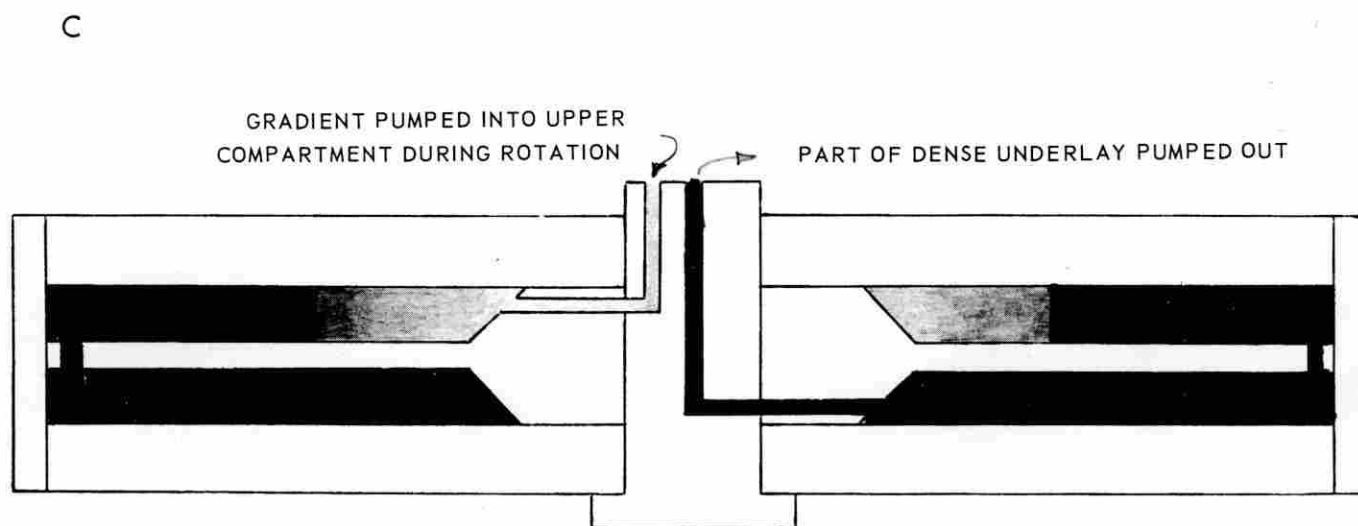
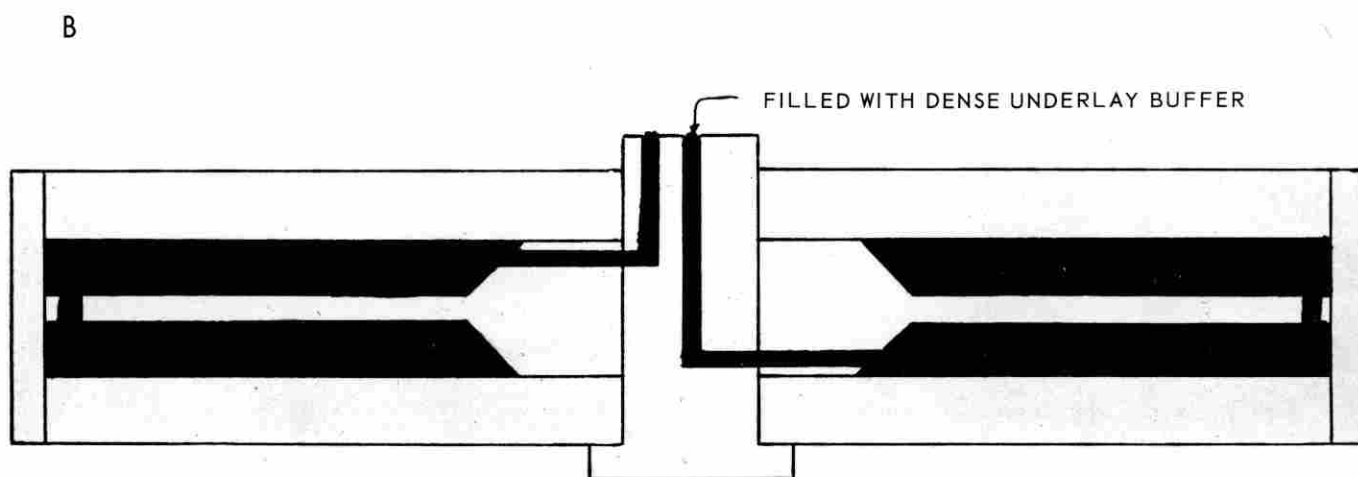
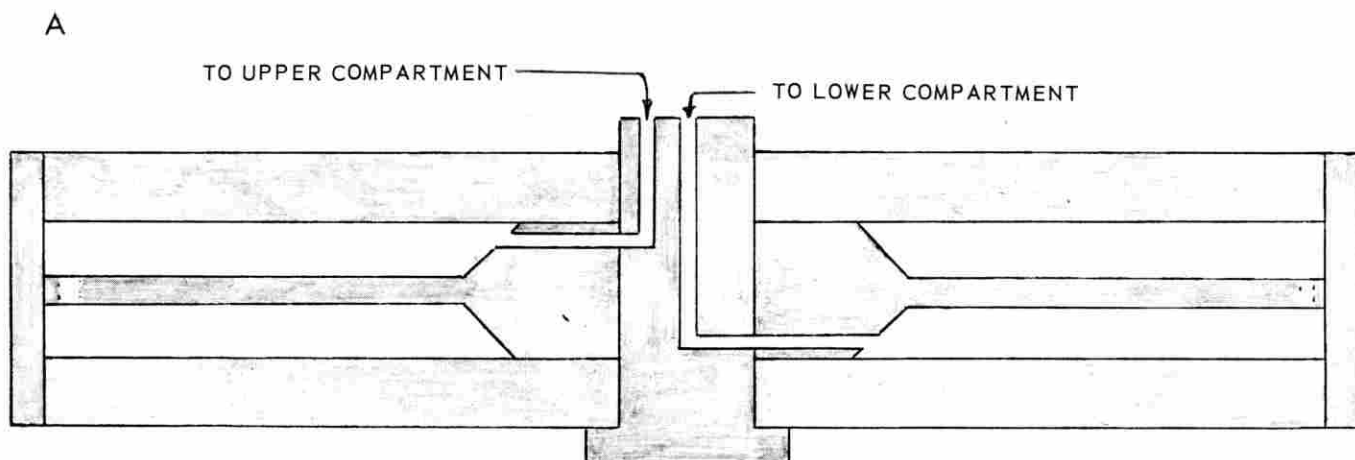
In electrophoresis in liquid gradients thermal convective disturbances cannot be avoided completely. Liquid in the center of the fluid column is slightly heated, decreases in density, and tends to rise level with liquid having less density when close to the cooling wall. Slight lateral movement causes cooling and a return to a lower density level. In many instances the

result is a series of convective disturbances which will result in <sup>hetero</sup>homogeneous levels or steps in a previously <sup>hetero</sup>homogeneous gradient. In a centrifugal field the driving force resulting from small density differences is markedly increased, and the width of a step produced in a gradient is therefore greatly decreased and the number of steps increased. Although some resolution may be lost by convection of this kind, it may not be serious if confined to extremely thin layers.

These considerations suggest that it would be interesting to explore the possibility of combining electrophoresis and centrifugation in such a manner as to stabilize a gradient between two discs normal to the centrifuge axis. The problems to be solved concern the methods for mounting the electrodes, the choice of buffers and gradient materials, and methods for loading and unloading the rotor.

#### Experimental Studies

For initial feasibility studies the simple design shown in Figure 5.1 is used. The stability requirements are similar to those previously described for the A-XII rotor. The chief innovation is the use of a center disc which divides the rotor chamber into an upper and a lower compartment. The lower compartment connects directly to the center line of the seal, while the upper chamber connects to the edge seal line. The upper and lower compartments connect at the outer edge of the rotor by means of a series of holes around the circumference of the center plate. Platinum elec- followed by the cathode buffer (150 ml). The gradient, sample, and anode buffer are now in position in the rotor. However the fluid extending into the metallic axis of the rotor would short circuit the current should electrophoresis be attempted at this point. Air pockets are formed in both the upper and lower chambers by forcing air into the upper chamber during rotation, thereby displacing out part of the solution in the lower



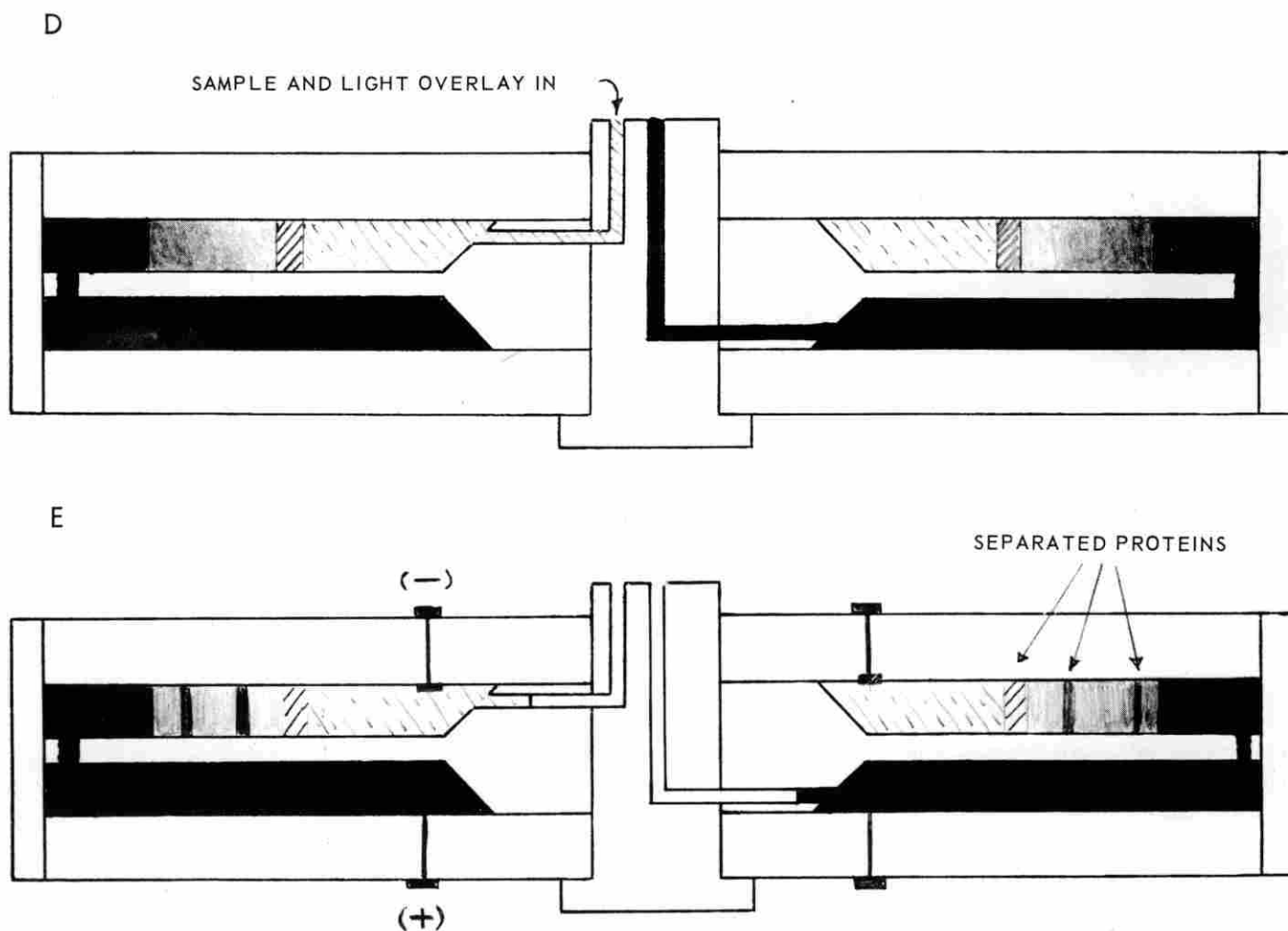


Fig. 5.1 Schematic diagram of loading and unloading of zonal centrifuge rotor for electrophoretic separations.

*Platinum electrodes*

rodes, concentric with the axis, are mounted in both the upper and lower chambers and connect with commutator rings as shown. The complete rotor is shown in Figure 5.2.

#### Operation of the Rotor

The problem is to set up suitable gradients and buffers in both the upper and the lower chambers, to introduce the sample at the right level, and to recover the gradient and separated zones at the end of the experiment.

Filling is begun by pumping in the underlay solution into the bottom chamber with the rotor at rest. When the lower chamber is full, (Figure 5.1b) the

underlay flows into the upper chamber through a series of holes around the outer edge of the dividing plate which also holds the septa. When the upper chamber is nearly full, the rotor is accelerated to 1000 rpm and filling is completed.

The direction of flow through the rotor is now reversed and the gradient is introduced into the center of the upper chamber, displacing an equal amount of the dense underlay from the lower chamber. The gradient (usually 250 ml) is stored in a vertical cylinder until ready for use, and is introduced into the rotor from the bottom of the cylinder (i.e. dense end of the gradient first).

When all of the liquid density gradient is in the rotor, the protein sample (20-30 ml) is pumped in so that it lies on top of the gradient. This in turn is

} (a)

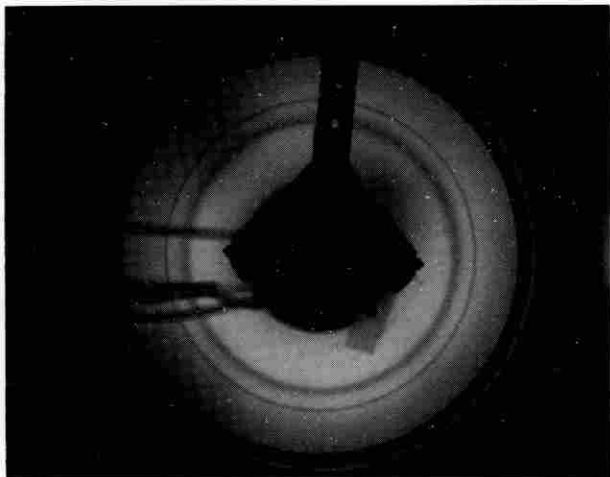


Fig. 5.2 Photograph of zonal electrophoresis rotor during rotation. Inner band is blue dyed dextran, outer band is bovine serum albumin stained with bromphenol blue.

chamber. When the pressure is released, the hydrostatic pressure due to centrifugal force equalizes in the upper and lower chambers, leaving the required centripetal air pocket.

For serum samples the current is kept at 450 ma throughout the experiment which takes approximately 1.75 hr using a 250-ml gradient. In this period of time the fastest-moving component has moved

through the gradient a radial distance of 1 to 1.25 in.

At the completion of the separation the rotor is unloaded by pumping in additional underlay solution through the bottom chamber line. The gradient flows through a recording spectrophotometer and is collected in 5- or 10-ml fractions.

The separation achieved using a sample consisting of blue stained dextran and bovine serum albumin dyed with bromphenol blue is shown in Figure 5.2.

### Conclusions

These studies demonstrate the feasibility of electrophoretic separations in centrifugally-stabilized liquid density gradients. The prototype instrument used in these studies was a modification of an existing instrument (the A-XII rotor) and has several deficiencies which will be corrected in subsequent designs in which the volume of the electrode buffer compartments are greatly increased, and the thickness of the upper and lower rotor end plates is decreased.

### REFERENCES

- <sup>1</sup>H. Svensson, Zonal density gradient electrophoresis, in *A Laboratory Manual of Analytical Methods in Protein Chemistry Including Polypeptides*. Vol. 1 (Ed. P. Alexander and R. J. Block), Pergamon Press London, pp. 193-244, 1960.

## 6. Chromatographic Separations Ultraviolet Absorbing Constituents of Urine

C. D. Scott

Over 400 molecular constituents of human urine have been reported.<sup>1-5</sup> These include inorganic compounds, organic acids, sugars, amino acids, purines and related compounds, hormones, vitamins, estrogens, proteins, enzymes, and many others. The quantitation of many of these constituents of urine represent a wealth of information that can be used to evaluate body function. This is particularly true of many of the organic chemicals of low molecular weight (less than 1000) and over 200 such constituents have been reported to have pathological significance.

An automatic, high-resolution analytical system is being developed to quantitatively determine many of the molecular constituents of low molecular weight in human urine. The present approach is to modify and expand the capabilities of an existing nucleotide analyzer<sup>6</sup> for this use. Initial results indicate that this concept is feasible; that is, a high-pressure, high-resolution modification of the nucleotide analyzer has resolved over 100 chromatographic peaks of UV-absorbing constituents from a 2-ml urine sample.<sup>7</sup>

For purposes of a logical presentation, the program can be divided into several specific areas of interest some of which are interconnected and can be carried out together while others must be carried out in consecutive order. These are: (1) operation of prototype systems; (2) a literature search for pathological urine constituents and analytical techniques; (3) urine-processing methods; (4) high-resolution separation systems; (5) development of detection and monitoring devices; (6) identification of the separated molecular constituents; and (7) data acquisition and analysis.

### Prototype Urine Analyzer

**Experimental System.**—The present prototype system for urine analysis is composed of a heated, high-

pressure, anion exchange column (typically 0.62 cm ID × 200 cm, filled with Dowex 1-X8 resin, and operating at 40°C) as the separations system and a recording ultraviolet (UV) spectrophotometer that operates alternately at two to four wavelengths as the detector. There are also provisions for volumetric measurement and collection of the column effluent.

The urine chromatogram, which shows the absorbance of the column effluent as a function of time, is developed by introducing a urine sample (0.5 to 2 ml) into the eluent stream at the top of the ion exchange column by use of high-pressure valves, and eluting it through the column with an ammonium acetate-acetic acid buffer solution ranging from 0.015 to 6 M, at a pH of 4.4 and a flow rate of 30 to 60 ml/hr. In the usual chromatogram, 80 to 100 peaks are resolved in about 48 hr. (See Figure 6.1.)

**Comparison between Pathological and Normal Urine.**—Several pathological urine samples have been run to determine if the system is capable of differentiating between normal and abnormal urine. Significant differences have been observed between normal samples and those from subjects with acute lymphocytic leukemia<sup>8</sup> and schizophrenia<sup>9</sup> (see Figure 6.1). The urine from four such leukemics showed a notable decrease in hippuric acid content as well as an increase in the ratio of uric acid to xanthine and hypoxanthine. The urine chromatograms from three schizophrenics had two very large unknown chromatographic peaks which we have not previously seen in normal urine.

### Literature Search

A literature survey on the pathological significance of organic compounds of low molecular weight present in human urine has been completed for the two-year

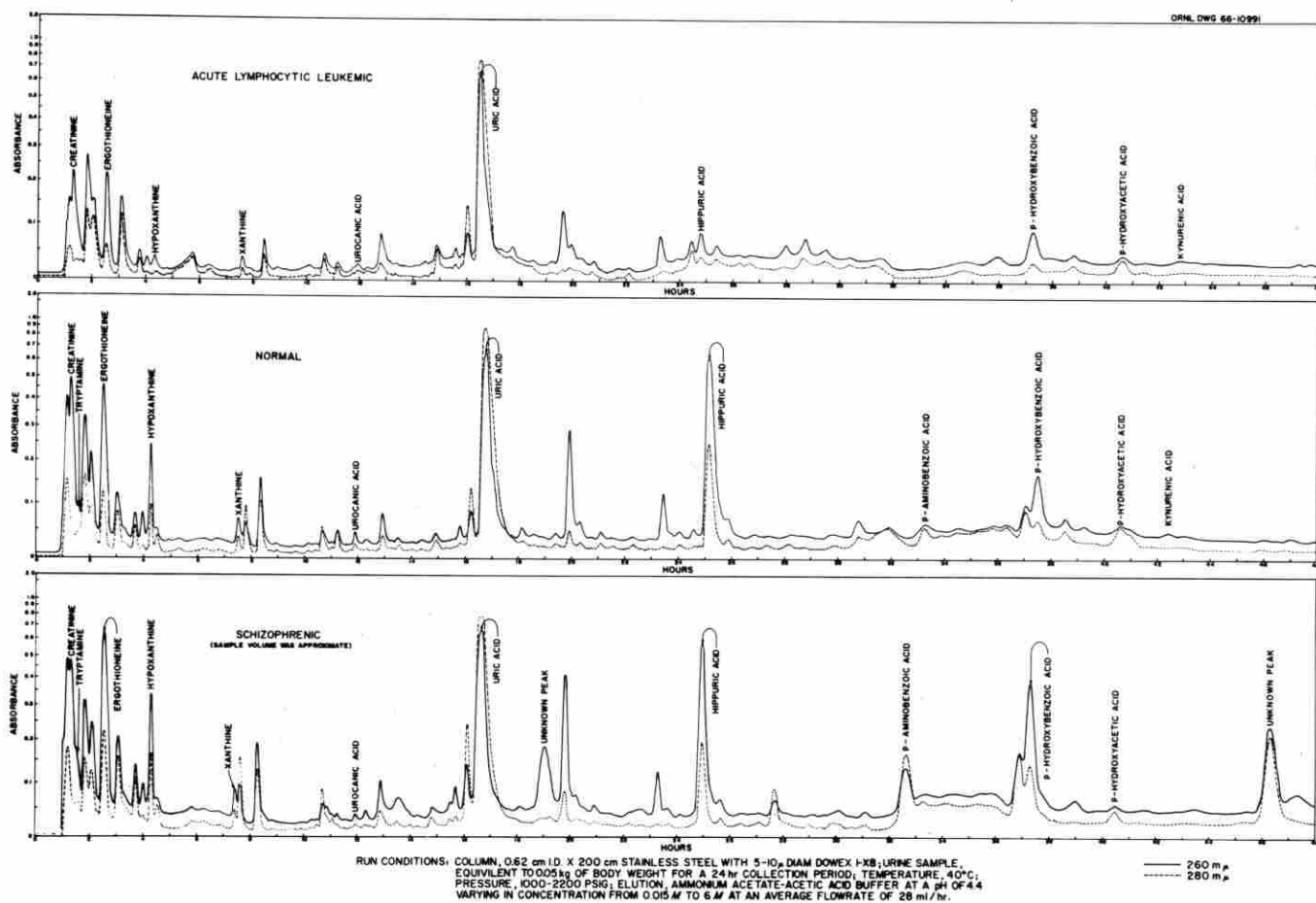


Fig. 6.1 Typical chromatograms from the urine analyzer showing reproducibility and the comparison between a normal chromatogram and those from a typical leukemic and a schizophrenic. Run conditions: column, 0.62 cm I.D.  $\times$  200 cm stainless steel with 5-10 $\mu$  diam dowex I-X8; urine sample, equivalent to 0.05 kg of body weight for a 24 hr collection period; temperature 40°C; pressure, 1000-2200 psig; elution, ammonium acetate-acetic acid buffer at a pH of 4.4 varying in concentration from 0.015M to 6M at an average flow rate of 28 ml/hr.

period 1964-1965 from *Chemical Abstracts* and *Biological Abstracts*. *Index Medicus* was also searched for 1965; however, it yielded only 20% as many literature citations as either of the other two for the same time period. Over 800 literature citations were found and this coupled with data from handbooks has resulted in mention of 312 urinary organic constituents of low molecular weight, over 200 of which are thought to be pathologically significant.

An automated bibliographic search was also made by the MEDLARS computer search facility at the National Library of Medicine. This search of literature for 1966 was not nearly as complete for urinary constituents as the manual searches have been.

### Urine Processing Methods

Until additional tests can be made, it has been assumed that quantitative evaluation of urinary components requires a sample from a composite of urine collection of at least 24 hr duration since many components vary as a function of the daily cycle. For example, diabetic urines characteristically show the highest glucose after meals, etc. It may be possible that a single sample, such as a first-morning specimen following a prescribed regimen of intake, can eventually be considered as acceptable for a screening test.

To prevent bacterial action and degradation by chemical reaction, prompt refrigeration of the urine

specimen during collection is desirable. If this is impractical, an antibacterial agent may be added to the collection vessel. Of those considered, formaldehyde appears to be the most useful. After collection, filtration through a membrane filter with pore size less than  $0.5\mu$  is sufficient to remove bacterial activity.

Urine specimens often contain a sediment which may be of considerable bulk. This occurs even in the absence of significant bacterial growth, and is apparently due to precipitation from decreased solubility at lower temperatures. In acid urines the precipitates consists of organic compounds such as uric acid, tyrosine, hippuric acid, etc., while alkaline precipitates are likely to be of inorganic nature. These can probably be put back into solution by heating to above  $37.5^{\circ}\text{C}$  in combination with dilution with distilled water. Our present operating procedure is to dilute with distilled water, to buffer the urine to the pH of the chromatographic system (pH of 4.4), and heat the urine sample to approximately  $40^{\circ}\text{C}$  prior to filtration. After processing, additional urine samples are frozen to  $-20^{\circ}\text{C}$ .

Compounds of high molecular weight, such as mucopolysaccharides and proteins, probably will not be eluted from the chromatographic column and may tend to foul the ion exchange resin. To circumvent this problem, pressure filtration of the urine sample through dialysis tubing is sufficient.

### Separations Systems

A large number of separation media have been evaluated by scouting tests for separation of the UV-absorbing constituents of urine. These included inorganic materials, activated charcoal, various organic anion and cation exchange resins, and a polyacrylamide gel (Table 6.1). Resolution was defined as the number of separate UV chromatographic peaks detected in the effluent. These scouting tests were made with a set of conditions which gave good results for a Dowex 1-type ion exchange resin; therefore, they may not have utilized the best conditions for each particular absorbant.

Organic ion exchange resins were the best separation media and Dowex 1 anion resin was the best of these. As reported earlier<sup>10</sup> resolution of the Dowex 1 resin is very dependent on particle size with  $5\text{--}10\mu$  resin giving 50% more chromatographic peaks than  $20\text{--}40\mu$  diameter resin.

The effect of cross-linkage of the polystyrene-base Dowex 1 anion exchange resin has also been investi-

gated. Cross-linkage is reported as the mole percent of pure divinylbenzene in the polymerization mixture. Low cross-linked resin (2-4%) gives better separation in the beginning of the chromatogram and the high cross-linked resin (10-12%) gives better separation in the latter part of the chromatogram. Medium cross-linked resin (8%) gives the best over-all results. Initial tests where several resins of different cross-linkage were used either mixed or in series and gave results inferior to any of the single resin tests. Additional tests will be made with both anion and cation exchange resins.

Although it is possible to operate a single ion exchange resin separations column with reasonable reproducibility, it is difficult to pack other columns with the same resin to get reproducibility between the two columns. If different batches of the same type of resin are used in two different columns, the results are frequently very different. Some of this difference can be attributed to a different particle size spectrum or varying amounts of cross-linkage; however some of the more fundamental properties of the resin such as the amount and type of porosity, type and quantity of active charges, are also probably important. In the future, an attempt will be made to more fully characterize the ion exchange resin which is used in an attempt to predict the behavior of different batches of the same type of resin.

### Detection Systems

The detection system used with the present model of the urine analyzer is a modified continuous-flow UV spectrophotometer which interrogates the column effluent stream alternately at two to four different wavelengths every 5 sec. A continuous-flow UV photometer using solid-state detectors and capable of automatic operation at two wavelengths is being developed for use as the column effluent detector. Such a detector will be less expensive and have a lower maintenance rate than the present modified spectrophotometer.

A continuous ratio refractometer with a sensitivity of  $10^{-7}$  refractive index units has been tested as the detector for the column effluent. It detected many of the same chromatographic peaks as the UV detector at the beginning of the chromatogram with much greater sensitivity; however, it was not usable during the latter part of the chromatogram. Apparently a large amount of material is eluted from the ion exchange column which blanks out refractive index differences.

**Table 6.1. Resolution of a Standard Urine Sample for UV-absorbing Constituents by Different Separations Media**

Material	Particle Size Range (microns)	Initial Operating Pressure (psig)	Total Number of Chromatographic Peaks	Comments
Biorad AG-1-X8, Anion Exchange Resin	10-20	370	68	All Biorad AG-1 resin is spherical
Biorad AG-1-X8, Anion Exchange Resin	20-40	220	53	
Biorad AG-1-X8, Anion Exchange Resin	40-60	170	41	
Biorad AG-1-X10, Anion Exchange Resin	20-50	240	50	
Biorad AG-1-X4, Anion Exchange Resin	20-50	140	44	
Biorad AG-1-X2, Anion Exchange Resin	20-50	250	37	Resin tended to compress with higher flow rates to give an increased pressure drop.
Biorad AG-1-X2, AG-1-X4, AG-X8, AG-X10 (An equal volumetric mixture of four)	20-50	290	35	Resin tended to compress with higher flow rates to give an increased pressure drop.
Bio-Rex 5, Anion Exchange Resin	40-70	120	24	(Copy above)
Amberlite CG-400, Anion Exchange Resin	10-20	2500	34	Ground resin of irregular shapes.
Amberlite IRA-900, Anion Exchange Resin	>100	800	32	This resin has very large pores and it compresses with high flow rates.
Biorad AG-50w-X8, Cation Exchange Resin	10-40	400	30	Some UV-absorbing material did not leave the column.
Bio Gel P-2, acrylamide gel	75-150	60	6	
Zehlon-H, Synthetic Zeolite	10-70	350	15	Ground material.
Activated Alumina	5-70	450	6	Ground material. Pressure became very high before end of run.
Activated Charcoal	20-70	100	14	Ground material. Some UV-absorbing material did not leave the column.
Silica Gel	20-70	140	7	Ground material.

Operating Conditions: Column, 0.62 cm ID × 150 cm stainless steel; elution system, three series-connected chambers containing 330 ml 0.015 M, 330 ml 3 M, 1000 ml 6 M acetic acid-sodium acetate solution buffered at pH 4.4; temperature, 40°C, average flow rate, 30-35 ml/hr.

Other detectors which are being considered are a continuous-flow fluorometer and a continuous-flow polarograph.

#### Identification of Separated Urinary Constituents

Urine constituents that are indicated by the chromatographic peaks are being tentatively identified by determining the position and the absorbance ratio at two or more different wavelengths, of the chromatographic peaks of known chemicals, and by comparing them with unknown peaks in the urine chromatogram. Standard mixtures of known chemicals are also being combined with urine samples to enlarge suspected chromatographic peaks. Chromatographic position and absorbance ratios give two independent means of comparison, both of which should be characteristic of specific urinary constituents or small groups of constituents. Fifteen urinary components, many of which have pathologic significance, have been tentatively identified in this manner. These are: creatinine, tryptamine, ergothioneine, hypoxanthine, xanthine, urocanic acid, uric acid, hippuric acid, p-aminobenzoic acid, p-hydroxybenzoic acid, p-hydroxyphenylacetic acid, kynurenic acid, vanillic acid, homovanillic acid, and salicylacetic acid.

A more definite identification is being made by isolating specific column eluate fractions associated with a chromatographic peak and by determining a sufficient number of its properties to achieve an identification. Several analytical methods are being investigated for use on these fractions.

**Thin-Layer Chromatography.**—Thin-layer chromatography will be useful in identification since the mobility in a thin-layer chromatogram should be rather specific for an individual compound or a small group of compounds and this specificity will be different from that in ion exchange chromatography. This chromatographic mobility is described as the partition  $R_f$  value and it is the ratio of the linear rate of movement of a solute zone to the linear rate of movement of the solvent front as measured in the thin layer of adsorbant.  $R_f$  values for 22 different urinary constituents that are present in urine in relatively large amounts have been determined for a solvent composed of a mixture of chloroform-methanol-acetic acid (75:20:5) on thin layers of unactivated silica gel (Table 6.2). These compounds were visualized on the developed chromatogram by either UV light or iodine vapor.

**Table 6.2. Relative Migration Rates of Some Urinary Compounds**

On Non-Activated Silica Gel	$R_f$ Value <sup>a</sup>
1. Arginine	0.06
2. Creatinine	0.06
3. Indican	0.11
4. Ergothionine	0.17
5. Cytosine	0.18
6. Tryptophan	0.30
7. Xanthine	0.43
8. 3-Methoxy-4-hydroxy-mandelic acid	0.44
9. Urocanic acid	0.45
10. Kynurenic acid	0.48
11. Maleuric acid	0.52
12. Adenine	0.58
13. Riboflavin	0.60
14. Hypoxanthine	0.71
15. Homovanillic acid	0.75
16. Hippuric acid	0.81
17. 5-Hydroxyindoleacetic acid	0.85
18. 3-Hydroxyanthranilic acid	0.89
19. Uric acid	0.92
20. p-Hydroxybenzoic acid	0.93
21. p-Hydroxyphenylacetic acid	0.94
22. p-Aminobenzoic acid	0.95

<sup>a</sup>Referred to the solvent front during development with  $\text{CHCl}_3/\text{CH}_3\text{OH}/\text{acetic acid}$  (75:20:5).

**UV Spectrophotometry.**—Since the present analytical systems use a UV spectrophotometer as a detector, comparison of the UV spectral properties of known urinary constituents with those of the components represented by the chromatographic peaks will be useful in the identification of peaks.

A large number of the organic compounds reported to be present in urine have been obtained from commercial sources and the UV spectra (220–340  $m\mu$ ) of standard buffered solutions (pH 4.4) have been made. The location of inflection points in the spectra as well as the general shape will be useful in identification. Table 6.3 gives a list of compounds that are thought to be present in urine in relatively high concentration with some of their spectral properties (maxima and minima). Five of the chromatographic peaks have been further identified in this manner. These are creatinine, hypoxanthine, xanthine, uric acid, and hippuric acid.

Table 6.3. Some Urinary Constituents<sup>a</sup> and Their UV Absorbance Characteristics

Wave Lengths: Absorbance Between 320-220 m $\mu$			Absorbance Ratios		
First Max. (m $\mu$ )	Minimum (m $\mu$ )	Second Max. (m $\mu$ )	Compound	$\frac{A_{280}}{A_{260}}$	$\frac{A_{290}}{A_{250}}$
	256		3-Methoxy-4-hydroxycinnamic acid (Ferulic acid)	2.32	2.32
234			L-Aspartic acid	0.5	0.1
237			Hippuric acid	0.235	0.005
238			Maleuric acid	0.183	0.043
240			Quinaldic acid	1.04	0.367
243	271		Anthranilic acid	0.392	0.173
244			Kynurenic acid	0.295	0.094
244			Thiamine (Vitamin B <sub>1</sub> )	0.417	0.121
245			Xanthurenic acid	0.568	0.099
249			Hypoxanthine	0.082	0.000
253			<i>p</i> -Hydroxybenzoic acid	0.236	0.024
253		235	Pyridoxamine	0.363	0.448
257			L-Phenylalanine	0	0
257			Ergothioneine	0.107	0.143
258	227		Uracil	0.142	0.012
259			Adenine	0.162	0.021
260	229		Ascorbic acid	0.492	0.193
261	237	222	Nicotinic acid	0.109	0.045
261	244	224	Nicotinamide	0.0906	0.0209
261	249		N'-Methylnicotinamide	0.0929	0.0144
263			Urocanic acid	0.590	0.301
263	233	220	Pseudouridine	0.425	0.113
264	237		FAD	0.575	0.915
266			Xanthine	0.577	0.144
266	239		Riboflavin	0.665	0.317
269	250	236	3-Hydroxykynurenine	0.687	0.229
270	236		Carbolic acid	0.674	0.026
272	240	233	<i>o</i> -Hydroxyphenylacetic acid	1.618	0.230
272	247	222	3,3'-Indolylacrylic acid	0.986	1.14
273	240		Cytosine	1.209	0.973
273	253	235	Pyridoxamine	0.363	0.448
274	244	235	Tyrosine	2.073	0.531
275	247		5-Hydroxyindoleacetic acid	1.55	1.97
275	249	236	<i>p</i> -Hydroxyphenylacetic acid	2.264	0.724
276	249	228	5-Hydroxytryptamine (Serotonin)	1.60	1.99
276	250	238	3,4,-Dimethoxyphenylethylamine	2.920	1.129
277	238		<i>p</i> -Cresol	3.027	2.153
277	265	220	Vitamin B <sub>12</sub> (cyanocobalamin)	1.08	0.670
278	238		Indican	1.410	1.556
278	249	227	Noradrenaline	3.88	2.84
279	235		Tryptamine	1.443	1.743
279	240		Tryptophan	1.447	1.667

Table 6.3. Continued

Wave Lengths: Absorbance Between 320-220 m $\mu$			Absorbance Ratios		
First Max. (m $\mu$ )	Minimum (m $\mu$ )	Second Max. (m $\mu$ )	Compound	$\frac{A_{280}}{A_{260}}$	$\frac{A_{290}}{A_{250}}$
279	250		Folic acid	1.61	1.96
279	250		Adrenaline	4.17	3.33
279	241	222	3-Indoleacetic acid	1.450	1.780
279	250	229	Methanephrine	3.88	2.47
279	253	237	Homovanillic acid	4.110	2.071
279	255	238	3-Methoxy-4-hydroxymandelic acid	2.82	1.09
280	235		<i>p</i> -Aminobenzoic acid	1.510	2.737
280	244	232	N-Acetyltryptophan	1.70	2.10
280	245	228	3,3'-Indolylactic acid	1.63	1.93
280	249	227	3-Hydroxytyramine (Dopamine)	4.62	4.69
281	259	221	Indole-3-carboxylic acid	1.63	1.10
283	254	236	Uric acid	2.900	2.813
290	231		Homogentisic acid	5.69	13.7
290	250	222	Pyridoxine	3.60	6.70
290	261	236	<i>m</i> -Hydroxybenzoic acid	2.835	1.444
290	279	256	Vanillic acid	0.476	0.558
295	271	228	3-Hydroxyanthranilic acid	0.645	0.530

<sup>a</sup>pH of all solutions examined is 4.4.

Changes in the shape of the UV spectral curve with varying pH have also been used by Cohn<sup>11</sup> and others to establish the identity of unknown biochemicals and this technique may also be useful in this program.

**Computer Resolution of Complex UV Spectra.**—A significant development in the field of radiochemical analyses has been use of computers to resolve the spectrum of a mixture of ten or more gamma-ray-emitting nuclides to determine the quantity of each nuclide present.<sup>12-14</sup> In this technique the spectra of individual components serve as a library in the linear least-squares resolution performed by a high-speed digital computer. This technique is being extended for use in the spectrum resolution of the UV spectra of aqueous mixtures of biochemicals. It may ultimately be a useful tool in the identification of unknown urinary compounds in the separation column effluent especially when the eluate fractions contain more than one compound.

At present the effects of the number of species present and their individual concentrations on the accuracy of this method of UV-spectrum resolution

are being studied. In studies on simulated spectra, each of which is composed of the summation of two bands having a Gaussian distribution about the wavelength of maximum absorption a spectrum composed of six to eight separate spectra can be resolved (that is, the concentrations of six to eight separate chemicals can be determined).

When the wavelength region of UV spectra taken on standard biochemicals in solution was extended from 220-340 m $\mu$  to 190-400 m $\mu$  sixteen of the seventeen materials tested showed structure in the wavelength region 190-220 m $\mu$  which has not been reported previously. For example, vanillic acid has two absorption maxima between 250-300 m $\mu$  and an additional two between 200-220 m $\mu$ . The presence of these additional maxima in the extended spectral range mean that more than the six to eight components can be resolved by the computer resolution technique.

Unfortunately, for this technique to be generally useful, one must have rather complete knowledge of all of the UV-absorbing urinary constituents or at

**Table 6.4. Reagents for Spot Tests**

<b>Reagent or Test (Pertinent compounds in parentheses)</b>	<b>Typical Compounds Giving a Positive Response (Examples in parentheses)</b>
Periodic acid ( $\text{KIO}_4 + \text{HNO}_3 + \text{AgNO}_3$ )	$\alpha$ -Hydroxyaldehydes, 1,2-glycols (Tartaric acid, maltose, glycerol, mannitol, galactose, glucose, ascorbic acid, benzoin, benzil)
Phosphomolybdic acid <sub>3-</sub> ( $\text{PO}_4 \cdot 12 \text{MoO}_3 + \text{excess NH}_3$ )	All compounds oxidizable by PMA (Phenols, ascorbic acid, uric acid, alloxantin)
Ehrlich diazo test (Diazotized sulfanilic acid)	Only phenols and aromatic amines that can couple (Phenols, anilines, tyrosine)
Colmant chlorination mixture ( $\text{HCl} + \text{KClO}_3$ )	Only aromatics that form chloranil (Tryptophan, salicylic acid, sulfamethazine, acetanilide, hydroxybenzaldehydes)
Thio-Michier's ketone <sup>a</sup>	Compounds that split off water or $\text{NH}_3$ when heated to 190°C (Urea, glycine, taurine, mucic acid, citric acid, tartaric acid)
Dimethyl oxalate ( $\text{Me}_2\text{C}_2\text{O}_4 + \text{thiobarbituric acid}$ )	Compounds that yield $\text{NH}_3$ on pyrolysis (Alanine, asparagine, nicotinamide, histidine, biuret, guanidines)
Hexamine (Hexamethylene tetramine)	Compounds that split off water at 180°C

<sup>a</sup>Heat to 190°C

least some knowledge of those constituents that can be present in a particular column eluate fraction for purposes of building up a spectra library. This information is not completely available and in generating it one must first solve the identification problem by another method. As a result the computer-resolving technique is not expected to be generally useful in the initial identification problem; however, it should have utility in analyzing the chromatogram after peak identification is completed, and in confirming analyses in pathological samples where a large increase in a given peak is observed. In this instance it is necessary to show that the incremental material is identical to that previously identified.

**Other Identification Methods.**—Many other techniques may be used to help identify the unknown chromatographic peaks.<sup>15</sup> Limited spot-testing may be conducted directly on the eluate fractions or concentrated portions of them. Table 6.4 gives a list of reagents and corresponding compounds known to yield a positive response.

For further collaborative identification other physical comparisons may be made. These may include melting-point determination after purification of the solute in the column eluate as well as various analytical instrumental methods such as x-ray powder diffraction, infrared spectroscopy, mass spectroscopy, and nuclear magnetic resonance spectroscopy.

#### **Data Acquisition**

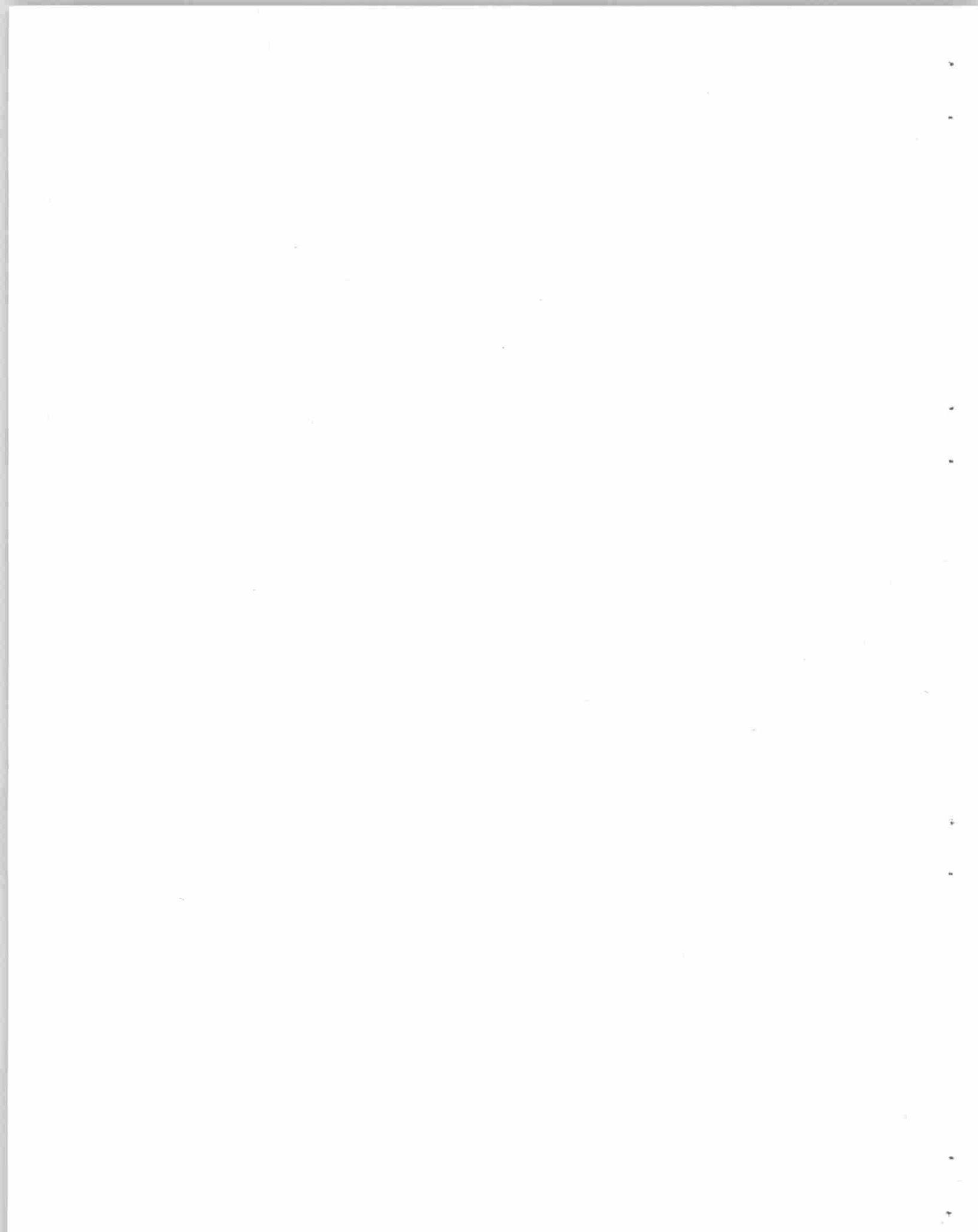
A data acquisition system for digitizing the output of the recording spectrophotometer monitoring the column effluent has been designed and it should be available by the fall of 1967. This system includes a digital voltmeter which digitized the analogue signal from the spectrophotometer, a paper tape punch and typewriter printer which record the digitized data, and the necessary control circuitry for proper operation.

After the data has been punched on paper tape it will be the input to a computer program which will

analyze the urine chromatogram to quantify the separated urinary constituents.

#### REFERENCES AND NOTES

- <sup>1</sup>P. L. Altman and D. S. Dittmer, *Blood and Other Body Fluids*, Federation of American Societies for Experimental Biology, Washington, D.C. (1961).
- <sup>2</sup>P. L. Altman and D. S. Dittmer, *Biology Data Book*, Federation of American Societies for Experimental Biology, Washington, D.C. (1964).
- <sup>3</sup>H. C. Damm (ed.), *Handbook of Clinical Laboratory Data*, The Chemical Rubber Co., Cleveland (1965).
- <sup>4</sup>C. Long (ed.), *Biochemists' Handbook*, E. and F. N. Spon, Ltd., London (1961).
- <sup>5</sup>S. A. McKee, "The Pathological Significance of Certain Organic Compounds in Human Urine." Cooperative Student Report for the Period September 1966–December 1966, ORNL-CF-66-12-34 (1966).
- <sup>6</sup>N. G. Anderson, J. G. Green, M. L. Barber, and F. C. Ladd, Sr., *Anal. Biochem.* **6**, 153 (1963).
- <sup>7</sup>C. D. Scott, J. E. Attrill, and N. G. Anderson, *Proc. Soc. Exp Biol. and Med.* (In Press).
- <sup>8</sup>Urine samples from subjects with leukemia were obtained from Dr. C. L. Edwards of the Medical Division of Oak Ridge Associated Universities, Oak Ridge, Tennessee.
- <sup>9</sup>Urine samples from subjects with schizophrenia were obtained from Dr. C. F. Mynatt of Eastern State Psychiatric Hospital, Knoxville, Tennessee.
- <sup>10</sup>Chem. Tech. Div. 1966 Annual Report.
- <sup>11</sup>W. E. Cohn, *J. Biol. Chem.* **235**, 1490 (1960).
- <sup>12</sup>E. Schonfeld, A. H. Kibbey, and W. Davis, Jr., *Nuclear Instruments and Methods* **45**, 1 (1966).
- <sup>13</sup>J. S. Eldridge and A. A. Brooks, *Nucleonics* **24**, (4), 54 (1966).
- <sup>14</sup>G. D. O'Kelley, Ed., "Applications of Computers to Nuclear and Radiochemistry," Proceedings of a Symposium, Gatlinburg, Tennessee, October 17–19, 1962, NAS-NS 3107 (Office of Technical Services, Dept. of Commerce).
- <sup>15</sup>K. S. Warren, "Identification of Urinary Constituents Separated by a High-Resolution Chromatographic System," ORNL-CF-67-2-22 (1967).



## 7. Automated Analytical Systems

### BASIC PROBLEMS

N. G. Anderson

#### Types of Systems

Automated analytical systems considered, and under development, for the MAN Program fall into two general classes. The first class of automated system (Class I) is termed a single-analysis multisample system and is used for analyzing large numbers of samples for a single substance. The discussion which follows is largely concerned with systems of this first class. The second class of system (Class II) is concerned with the analysis of complex mixtures and the quantitation of large numbers of components. Examples of such systems are the nucleotide analyzer and the carbohydrate analyzers discussed elsewhere in this report. The underlying concept is the use of a high-resolution separation system to resolve the mixture, and a sensor to detect and quantitate members of a class of substances. It is evident that if high enough resolution can be obtained, or if a pre-separation of compounds into discrete classes is used, then a sensor can be used which detects simply mass.

Analytical systems of this type are termed multi-component single-sample systems. As will be evident, hybrids of the two classes are possible in which many samples are analyzed for a large number of compounds.

For the analysis of samples from zonal centrifuges<sup>1-5</sup> sample-measuring methods are required which are insensitive to differences in viscosity and density of samples.

#### Principles of Single-Analysis Multi-Sample Systems

Systems of this first type may be further subdivided into two additional subgroups depending on whether

a number of procedures or steps are or can be carried out in unison or whether the samples and the analytical procedures are carried out sequentially for each sample. The Autotechnicon is the prime example of the second subgroup (Class IB) since a series of samples are introduced one at a time into a time-tube in which a series of reactions are being carried out continuously.<sup>3-6</sup> The samples flow *through* these reactions in sequence. The frequency of sample introduction is inversely proportional to the wavelength of the entire system, where wavelength is considered to be the distance between nonoverlapping samples (i.e., samples which do not interfere with each other).

Systems of the first subgroup (IA) carry out a series of reactions in parallel and all analyses can be completed at the same time. Here the prime example is the Micro-titre system for the assay of antigen, antibody, or complement-fixation titer. Dilutions are carried out simultaneously on a number of samples, and the end-points of all assays may be read simultaneously.

Certain basic differences between systems IA and IB should be stressed. The overall efficiency of systems based on either sequential or parallel single-analysis multi-sample systems depend on (a) the rate of sample acquisition, (b) the minimum result time, and (c) the maximum result time. This follows from the following. If all samples are acquired at once (i.e., if all the analyses for a working day are made available at one time), then the minimum result time will be the time elapsing until the first sample is analyzed, and the maximum result time will be the time required to finish the last analysis. However, if the samples are acquired at the same rate that they are, or can be, analyzed, then the minimum result time and the maximum result time can be the same. In practice, samples are almost never fed into an automated analyzer at the same rate as they are acquired. Rather they are separated into groups on trays and analyzed as a group. Until the

results for the group are available the data are not reduced and used. The maximum result time then becomes the average result time.

In parallel single-analysis multi-sample systems (IA), the time required to analyze a large number of samples may equal that required for one sample. For this reason it appeared of interest to explore them more thoroughly and see whether they offered any advantages over the systems presently in use.

#### Measurement and Transfer of Small Fluid Volumes

In wet analytical systems the ratio of the reactants must be kept constant to obtain accurate results. In on-stream devices (IB) this is done by controlling the flow rate of the reactants and the sample. The limiting factors have to do with mixing between consecutive samples, and the volume required to prevent such mixing.

In discrete-sample analysis (IA) the volumes are usually accurately controlled by using volumetric measuring devices<sup>7,8</sup> or by controlling the time of flow of a pump whose flow is accurately known. For the present purposes we desire methods for accurately measuring and quantitatively transferring small sample and reagent volumes. This is a classical problem in analytical chemistry and one which has not been previously solved for automated systems in a satisfactory manner.

Six problems plague transfer volume-measuring devices. The first is the problem of reproducibly defining the space to be filled. With syringes this means pulling the syringe to a predetermined mark. If a pipette is used, then a sensing device may be used to determine when the desired liquid level has been reached. For very small pipettes, capillary forces may be used to fill the pipette. The second problem is to ensure that air bubbles are not included in the measured liquid volume. In manual analysis this is done by visual inspection. In automated systems attempts are made to solve the problem by proper design. The third problem is the elimination of droplets adhering to the outside of the measuring device. Few satisfactory solutions to this problem with automated systems have been proposed.

The fourth problem is to quantitatively or at least reproducibly empty the transfer device. This again is visually inspected in manual methods. The fifth problem is cross-contamination of samples. Either multiple rinsing or use of disposable pipettes is required to eliminate this problem. The sixth and last problem is

that of making the measuring device independent of variations in the density, viscosity, or surface tension of solutions being measured.

It should be noted that the use of wet-chemistry analyses in space presents a series of additional problems since it has not been possible to design fluid measuring and handling systems which will function properly in a weightless environment.

#### Automated Volumetric Measurement

We do not believe that the problem of automating Type IA systems can be solved by merely attempting to mechanize devices originally developed for human hands. Rather we are interested in determining what the basic problems are and, if possible, solving these.

#### Fabrication Requirements for Disposable Volumetric Containers

Initially we shall assume that small single-use measuring devices offer an advantage over pipettes which must be washed. The first requirement is that all containers have identical volumes. Techniques for blow molding, drawing, or injection molding into molds which leave seams in the wall of the container must therefore be avoided. The conclusion is that the device must be fabricated in such a manner that it *need not be calibrated*. Automatic and semi-automatic methods for calibrating small-volume plastic pipettes have been built. However, this step is costly and subject to error.

It appears that the only form of container suitable for this purpose is one in which the measuring space is initially defined by a steel pin which can be reproducibly withdrawn from a molded piece of dimensionally stable plastic. The general shape, therefore, would be approximately that shown in Figure 7.1. The die design leaves no mold marks on the measuring or fluid-containing surfaces. The volumes considered here would range from 10–500 $\lambda$ . The tubes would therefore have rather small dimensions.

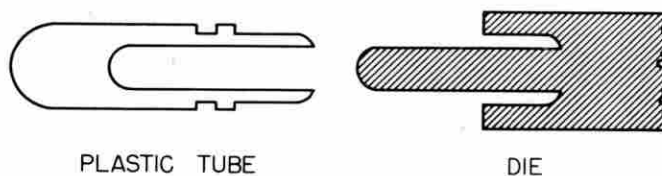


Fig. 7.1 Schematic drawing of measuring tube and die.

### Methods for Positive Filling

To ensure that no air bubbles interfere with volume measurements, the tubes are filled in a centrifugal field. A variety of methods may be employed for this purpose. When a single sample is required, the tube may be placed in a container as shown in Figure 7.2a surrounded by the sample liquid. When the sample cup is centrifuged, the air in the tubes is expelled and the entire tube volume fills with liquid. Even the smallest air bubbles are floated out in a field of several hundred  $\times$  g.

### Producing Flat Menisci

The continuation of centrifugation after excess fluid around the tube has been removed will, in the absence of wind effects, produce a very flat meniscus. In Figure 7.2 the excess sample volume may be removed manually or automatically by suction at rest, by merely tipping the cup at rest, or by opening a hole in the bottom of the cup either during rotation or at rest. The tubes are best held in a hollow-bowl centrifuge rotor which can be closed at the top to minimize the effects of windage.

After the tubes are filled they may be capped to prevent evaporation.

Where a flat meniscus at the end of a micro-tube is considered a disadvantage, a small slot may be made in the upper lip of the tube. In a centrifugal field, the solution level will be that of the bottom of the slot.

The techniques described are useful for filling both sample and reagent measuring tubes. By increasing the ratio of fluid column length to fluid column diameter, the rate of evaporation may be decreased.

The techniques are also applicable to a zero gravity environment, in which case centrifugal force must be used to remove excess fluid.

### Quantitative Transfer of Fluids

The measured volumes are quantitatively transferred using centrifugal force. For this purpose the tubes are inserted into a small plastic cuvette. When the cuvette is centrifuged the fluid is forced out of the measuring tube and into the chamber of the cuvette. By rapidly altering the speed of the centrifuge the small fluid volumes may be mixed. This technique is adapted to reactions in which a sample and one to three different reagents are mixed to yield a color which is then read. Where there is an incuba-

tion time between reagent additions, the centrifuge may be stopped, the tubes allowed to incubate, additional tubes inserted, and the centrifuge started again. When a precipitate forms which must be removed, the centrifugation step used to transfer reagents may be prolonged until the solution is clear.

By working with very small fluid volumes the problem of accidental loss is minimized since surface tension tends to prevent small droplets from forming. In addition, fluids tend to remain in the tubes in the absence of gravitational force.

### Cuvette Design

The cuvettes must be carefully designed to give optimal optical properties and an accurately known light path. Two types are being investigated. One is a reusable model with glass or quartz windows. The second is of plastic. The plastic windows cannot be assumed to have the optical properties of glass. The body of the cuvette is made of black plastic to prevent scattered light from being transmitted parallel to the light passing through the solution. The end windows may be either clear or translucent.

In most colorimeters or spectrophotometers the light rays must be approximately parallel as they pass through the sample. Deviated rays may not strike the photo cell. For the cuvettes described here a diffuse light source and the photosensitive surface are positioned close to the cuvette to minimize the effects of irregularities in the end windows.

We recognize that these techniques are *unhandy*. They are, however, well adapted to mechanization. In this they resemble binary counting devices, which taken singly are of little practical use, but which have unique properties when properly arrayed in large numbers.

### Experimental Studies

We wish to ask only whether the methods outlined will yield identical volumes and quantitative transfers.

For initial studies plastic components have been machined to reduce costs. Characteristics of molded tubes will be discussed in another paper.

The sequence of steps used experimentally is shown in Figure 7.2. After centrifugal filling the tubes were capped and weighed. They were then uncapped and inserted in the transfer vessels and centrifuged. The tubes were then removed from the transfer vessels, and the latter capped and weighed.

The radius from the centrifuge axis to the meniscus in the measuring tube (Figure 7.2d) was 11 cm, while the radius to the top of the transfer vessel was 18 cm. All centrifugal procedures were performed in the International PR-2 centrifuge at room temperature

(25°C). The centrifuge was accelerated rapidly to speed in each instance and turned off as soon as speed was reached. Tube-filling was done at 2000 rpm ( $490 \times g$  at top of measuring tube) while meniscus levelling was done at 2500 rpm ( $769 \times g$  meniscus).

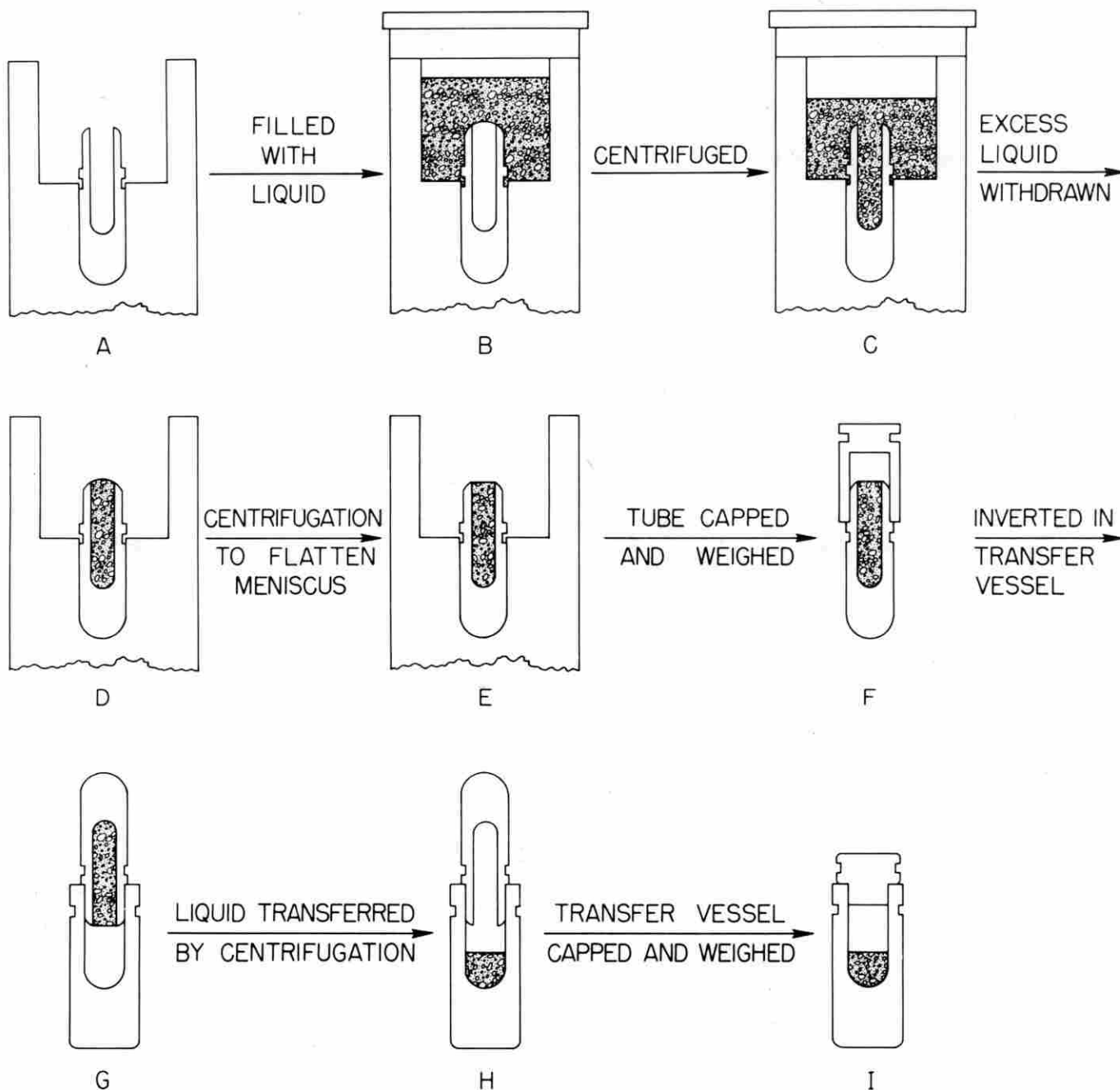


Fig. 7.2 Schematic diagram of procedures used to determine reproducibility of filling and transfer method.

Transfer was done at 2,000 rpm ( $805 \times g$  at top of transfer vessel).

Two sizes of measuring tubes having similar external dimensions were used. The chambers were  $\frac{5}{8}$  in. deep with diameters of  $\frac{1}{8}$  and  $\frac{1}{16}$  in. The tubes, transfer vessels, centrifuge cup adapters, and caps are shown in Figure 7.3. Kel-F and nylon measuring tubes were used, while all transfer vessels were of Kel-F.

Calculations show that the maximum height of a water droplet at  $770 \times g$  would be  $139 \mu$ . This is less than 1% of the height of the liquid column. Variations in meniscus curvature produced by differences in fluid density or surface tension would be therefore only a small fraction of 1% of the volume.

The results obtained with pure water in Kel-F and nylon tubes are shown in Table 7.1. Using three

different Kel-F tubes standard deviations of 0.6, 0.28, and 0.29% were observed. The nylon tube gave a standard deviation of 0.61%. Three smaller (circa  $30\lambda$ ) tubes gave standard deviations on replicate filling of 0.25, 0.15, and 0.19%, while the single nylon tube had a standard deviation of 0.61%. In general, nylon tubes have been inferior to Kel-F tubes.

In the centrifugal transfer studies the average losses in four series of experiments were 0.0, 0.2, and 0.2 mg for Kel-F and 0.8 for nylon using the large tubes. With the smaller tubes average losses were 0.2, 0.1, and 0.05 mg in three sets of experiments with Kel-F tubes, and 0.3 mg with a nylon measuring tube.

Additional experiments were performed with a 0.05% solution of sodium dodecyl sulfate and with 45.1% sucrose as shown in Table 7.2. The detergent

**Table 7.1. Weight of Distilled Water in Measuring Tubes and After Transfer to a Receiving Vessel**

Results with $1/8 \times 5/8$ in. Chamber			
Tube No.	Wt. of water in tube (mg)	Wt. of water in transfer vessel (mg)	Difference (mg)
1 Kel-F	122.0	122.3	+0.3
	120.4	120.4	0.0
	122.0	122.2	+0.2
	122.5	122.3	-0.2
	122.7	122.4	-0.3
	122.3	122.3	0.0
	Av = 122.0 SD = 0.75 mg (0.60%) V = 122.2 $\mu$ l	Av = 122.0 V = 122.2 $\mu$ l	Av loss = 0.0 mg
2 Kel-F	123.6	123.5	-0.1
	123.2	123.0	-0.2
	123.1	122.9	-0.2
	124.1	123.8	-0.3
	123.5	123.4	-0.1
	Av = 123.5 SD = 0.35 mg (0.28%) V = 123.7 $\mu$ l	Av = 123.3 V = 123.5 $\mu$ l	Av loss = 0.2 mg
3 Kel-F	121.3	120.9	-0.4
	120.9	121.1	+0.2
	121.0	120.6	-0.4
	121.5	121.4	-0.1
	121.7	121.2	-0.5
	Av = 121.3 SD = 0.35 mg (0.29%)	Av = 121.0	Av loss = 0.2 mg

**Table 7.1. (Continued)**

4 Nylon	$V = 121.5 \mu\text{l}$	$V = 121.3 \mu\text{l}$	
	125.0	123.8	-1.2
	124.4	123.6	-0.9
	124.3	123.6	-0.7
	126.1	125.8	-0.3
	<u>123.9</u>	<u>123.2</u>	<u>-0.7</u>
$Av = 124.7$	$Av = 124.0$	$Av \text{ loss} = 0.8 \text{ mg}$	
$SD = 0.77 \text{ mg (0.61\%)}$			
$V = 124.9 \mu\text{l}$	$V = 124.2 \mu\text{l}$		
<b>Results with 1/16 × 5/8 in. Chamber</b>			
5 Kel-F	32.2	32.0	-0.2
	32.0	31.8	-0.2
	32.1	31.8	-0.3
	32.0	31.9	-0.1
	<u>32.0</u>	<u>31.9</u>	<u>-0.1</u>
	$Av = 32.1$	$Av = 31.9$	$Av \text{ loss} = 0.2 \text{ mg}$
$SD = 0.08 \text{ mg (0.25\%)}$			
$V = 32.1 \mu\text{l}$	$V = 31.9 \mu\text{l}$		
6 Kel-F	32.2	32.1	-0.1
	32.2	32.2	0.0
	32.1	32.0	-0.1
	32.1	32.0	-0.1
	<u>32.2</u>	<u>32.2</u>	<u>0.0</u>
	$Av = 32.2$	$Av = 32.1$	$Av \text{ loss} = 0.1 \text{ mg}$
$SD = 0.049 \text{ mg (0.15\%)}$			
$V = 32.2 \mu\text{l}$	$V = 32.2 \mu\text{l}$		
7 Kel-F	31.7	31.7	0.0
	31.8	31.8	0.0
	31.9	31.8	-0.1
	31.8	31.7	-0.1
	<u>31.9</u>	<u>31.9</u>	<u>0.0</u>
	$Av = 31.8$	$Av = 31.9$	$Av \text{ loss} = 0.05 \text{ mg}$
$SD = 0.06 \text{ mg (0.19\%)}$			
$V = 31.9 \mu\text{l}$	$V = 32.0 \mu\text{l}$		
8 Nylon	31.5	30.8	-0.7
	31.4	31.0	-0.4
	31.1	30.8	-0.3
	31.0	30.9	-0.1
	<u>31.2</u>	<u>31.0</u>	<u>-0.2</u>
	$Av = 31.2$	$Av = 30.9$	$Av \text{ loss} = 0.3 \text{ mg}$
$SD = 0.19 \text{ mg (0.61\%)}$			
$V = 31.3 \mu\text{l}$	$V = 31.0 \mu\text{l}$		

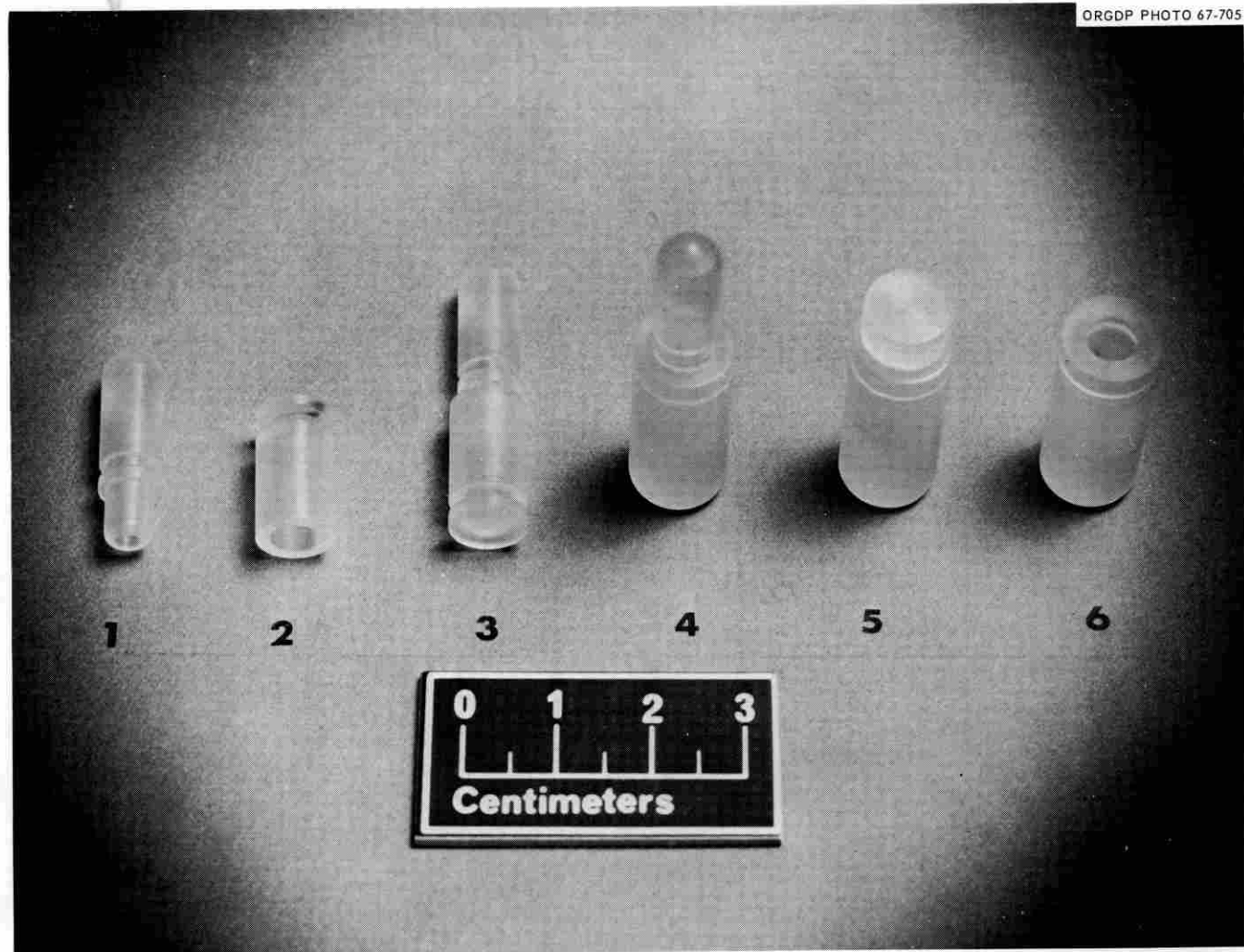


Fig. 7.3 Plastic measuring and transfer containers (1) large plastic measuring tube ( $\sim 120 \mu\text{l}$ ); (2) cap for measuring tube; (3) measuring tube with cap in place; (4) measuring tube inverted into transfer vessel; (5) transfer vessel with cap; and (6) transfer vessel without cap.

solution density was not appreciably different from water and yielded very similar results. With sucrose slightly more variation was seen than with water alone. Volumes are calculated using a density of 0.9981 for water and 1.2048<sup>9</sup> for 45.1% sucrose at 23.5°C. A summary of the results is shown in Table 7.3. It is evident that errors in measurement and loss in transfer have been kept within the desired range of 1%.

#### Discussion

A method for accurately measuring and quantitatively transferring small fluid volumes has been de-

veloped. All previously available methods working in the microliter range have been calibrated either to contain or to deliver a specified volume. The "to contain" pipettes must be rinsed several times to achieve quantitative transfer. Delivery pipettes are subject to rather large errors when solutions differing in density, viscosity, and surface tension are used. The method described here is independent of these factors over a rather wide range and is well adapted to automated manipulation. In addition to measuring volumes, the method is well adapted to micropycnometry. The plastic used must be inert, nonwetting, dimensionally stable, and should not take up moisture. A fluorinated hydrocarbon, Kel-F, has been found suitable for this

**Table 7.2. Measurement of Weight of Solutions in Kel-F Measuring Tubes and Weight of Solution after Transfer**

0.05% sodium lauryl sulfate			45.1% Sucrose w/w		
Tube No.	Wt. in measuring tube (mg)	Wt. in transfer vessel (mg)	Tube No.	Wt. in measuring tube (mg)	Wt. in transfer vessel (mg)
1	*	122.5	1	147.5	147.4
	122.0	122.0		147.2	147.1
	122.5	122.5		147.2	147.2
	122.0	122.0		Av = 147.3	Av = 147.23
	Av = 122.17	Av = 122.25		Volume = 122.3 $\mu$ l	Volume = 122.3 $\mu$ l
5	31.9	31.7	2	148.4	148.5
	31.9	31.8		147.9	147.9
	31.9	31.9		147.9	148.0
	31.9	31.5		Av = 148.07	Av = 148.13
	Av = 31.9	Av = 31.725		Volume = 122.9 $\mu$ l	Volume = 122.9 $\mu$ l
6	32.1	32.0	5	38.5	38.2
	32.0	32.0		38.2	38.2
	32.9	31.9		38.4	38.2
	32.1	31.8		Av = 38.37	Av = 38.2
	Av = 32.27	Av = 31.92		Volume = 31.8 $\mu$ l	Volume = 31.7 $\mu$ l
7	*	31.9	6	38.6	38.6
	31.7	31.7		38.5	38.5
	31.7	31.7		38.5	38.5
	31.9	31.7		Av = 38.53	Av = 38.53
	Av = 31.77	Av = 31.75		Volume = 32.0 $\mu$ l	Volume = 32.0 $\mu$ l
7	*	31.9	6	38.6	38.6
	31.7	31.7		38.5	38.5
	31.7	31.7		38.5	38.5
	31.9	31.7		Av = 38.53	Av = 38.53
	Av = 31.77	Av = 31.75		Volume = 32.0 $\mu$ l	Volume = 32.0 $\mu$ l

\*Transferred immediately without weighing.

purpose. Indication of water absorption by nylon renders this material unsatisfactory.

When centrifugal force is employed to fill simple plastic tubes, to level menisci, and to transfer fluids, the average error between consecutive measurements, and the loss on transfer is well below 1%. These errors may be largely due to errors in weighing since a balance sensitive to only 0.1 mg was used, to evaporation, and to the fact that the ratio between diameter and length of the measuring space was kept large to simplify fabrication.

In addition, no special precautions were taken to control temperature, and all components were manipulated by hand since we are interested in evaluating

the technique under the conditions in which it may be used. The errors observed are well below the 1% level required.

The ratio between the diameter and depth of the measuring tubes has not been examined. These ratios were 1:5 and 1:10 in the tubes tested. Additional work will be required before the optimal ratio is known.

It is evident that with higher centrifugal fields, and much smaller vessels, measurement and transfer below the microliter range should be possible, providing the problem of evaporation can be solved.

Surface tension tends to keep fluids loaded centrifugally from flowing out, even if inverted at 1 g. It appears therefore that this technique for measuring

### 7.3. Volumes in Microliters Calculated as Described in Text Averages from Experiments in Tables 7.1 and 7.2

Tube No.	H <sub>2</sub> O		SDS		40.1% Sucrose	
	Measured	Transferred	Measured	Transferred	Measured	Transferred
1	122.2	122.2	122.4	122.5	122.3	122.2
2	123.7	123.5	—	—	122.9	122.9
3	121.5	121.3	—	—	—	—
4*	124.9	124.2	—	—	—	—
5	32.1	31.9	32.0	31.9	31.8	31.7
6	32.2	32.2	32.3	32.0	32.0	32.0
7	31.9	32.0	31.8	31.8	—	—
8*	31.3	31.0	—	—	—	—

\*Measuring tubes of Nylon. All others made of Kel-F.

and transferring fluids may be useful in a weightless environment.

In subsequent papers the application of the measuring and transfer concepts presented here to both manual and automated analysis will be presented.

#### REFERENCES

- <sup>1</sup>N. G. Anderson, *J. Phys. Chem.* **66**, 1984-1989 (1962).
- <sup>2</sup>N. G. Anderson, *J. Natl. Cancer Inst. Monograph* **21**, 9-39 (1966).
- <sup>3</sup>H. Schuel, and N. G. Anderson, *J. Cell Biol.* **21**, 309-323 (1966).
- <sup>4</sup>H. Schuel, S. R. Tipton, and N. G. Anderson, *J. Cell Biol.* **22**, 317-326 (1964).
- <sup>5</sup>J. R. Corbett, *Fed. Proc.* **25**, 759 (1966).
- <sup>6</sup>L. T. Skeggs, *Am. J. Clin. Path.* **28**, 311 (1957).
- <sup>7</sup>P. O. Kirk, *Quantitative ultramicroanalysis*. John Wiley and Sons, Inc., New York (1950).
- <sup>8</sup>N. D. Cheronis, *Technique of Organic Chemistry*, Vol. VI. A. Weissberger, Ed., Interscience Publishers, Inc., New York (1954).
- <sup>9</sup>E. J. Barber, *J. Natl. Cancer Inst. Monograph* **21**, 219-239 (1966).

#### B. AN IMPROVED AUTOMATED SYSTEM FOR TOTAL PROTEIN ANALYSIS

L. H. Elrod

Total protein analyses in this laboratory have utilized the auto analyzer and Technicon Methodology Protein 1b which is a modification of the Lowry<sup>1</sup> technique. The Technicon method did not provide the sensitivity that was necessary.

The following changes have been made in the methodology:

1. Sample volume was increased 87.5% to 0.60 ml/min nominal delivery.

2. Copper reagent volume was increased 467.0% to 3.40 ml/min nominal flow. The concentration of the copper reagent was reduced by 50%; therefore the amount of copper was increased by 233.5%.

3. Buffer volume was reduced by 73.3% to 0.32 ml/min nominal flow. The buffer composition was changed by using Na<sub>2</sub>CO<sub>3</sub> instead of NaHCO<sub>3</sub>. The amount of NaOH was reduced by 28.89%.

4. The concentration of Folin Ciocaltau reagent was kept the same but the volume was reduced 80.0% to 0.32 ml/min nominal flow.

5. The Technicon sampler used in this system draws sample for a given period and then raises the sample line out of the sample cup. Air is drawn through the line until the beginning of the next sampling period.

A water line with the same delivery rate as the sample line has been added. This line is arranged so that while air is being drawn through the sample line distilled water is fed into the system. This modification was made necessary when increased sensitivity allowed the colorimeter to read changes in reagent concentration.

Figure 7.4 is a diagrammatic presentation of the modified system.

#### Reagents

1. **Copper.** 0.05% CuSO<sub>4</sub> · 5H<sub>2</sub>O dissolved in 0.10% sodium potassium tartrate. It is not necessary to make fresh copper reagent each day. We have kept reagent as long as 10 days with no loss in sensitivity.

2. **Buffer.** 80 grams per liter Na<sub>2</sub>CO<sub>3</sub>; 32 grams per liter NaOH, dissolve Na<sub>2</sub>CO<sub>3</sub> and NaOH in water, mix, and then bring to volume.

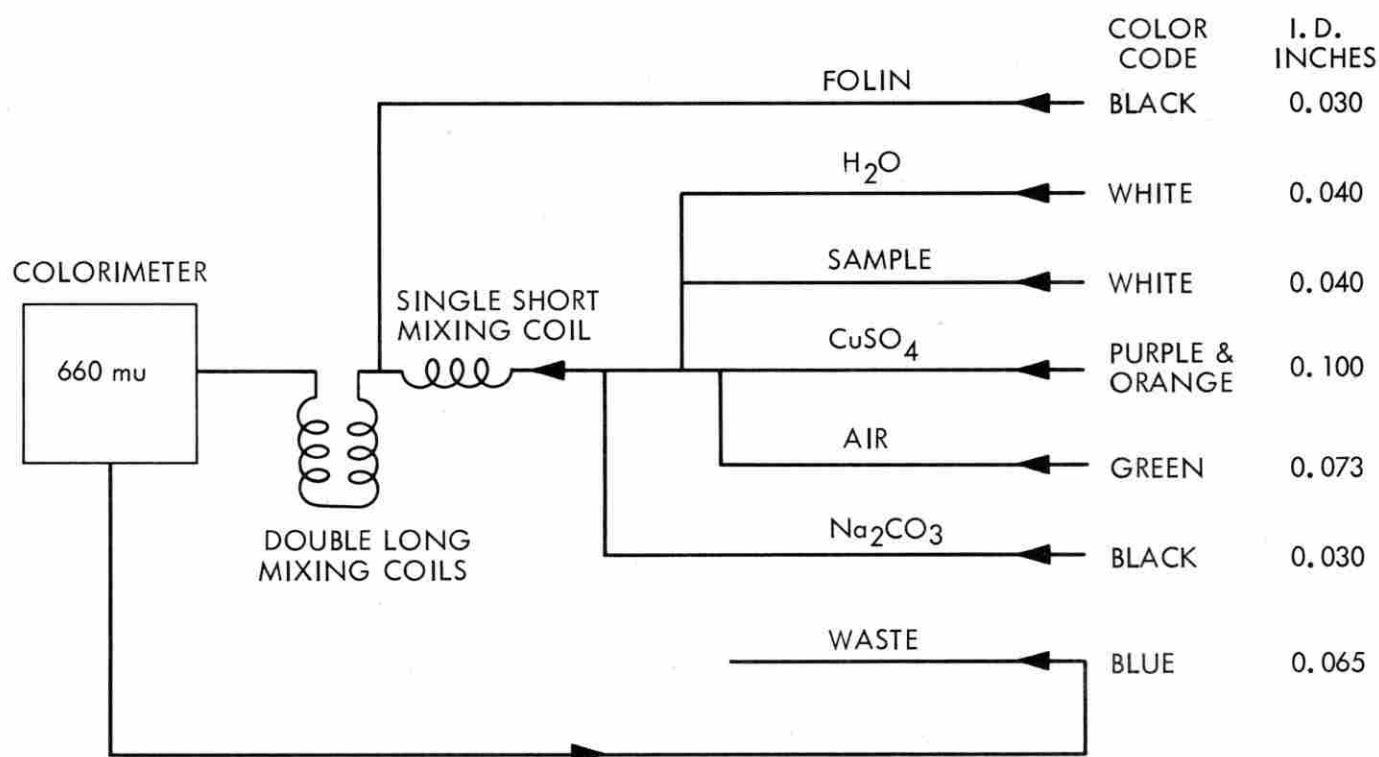


Fig. 7.4 Schematic Diagram of Protein Analyzer.

3. **Folin reagent.**<sup>2</sup> 1 part Folin and Ciocalteu phenol reagent plus 3 parts distilled water.

Standard samples of Bovine Serum albumin (Armour Pharmaceutical Co.) were made in distilled water to concentrations of 25, 50, 100, 250, 500, and 800  $\gamma$ /ml (1  $\gamma$  = 0.000001g/ml). Each standard was run several times under identical conditions using the same instruments and where possible the same reagents. The sample stream was monitored at 660  $m\mu$ .

Table 7.4 demonstrates the increased sensitivity of the modified method. Not only is there an overall increase in sensitivity but the greatest increase is in

the low-concentration range where it is most needed.

Further studies are being made to determine the effects of sucrose concentrations, various detergents, and buffers on the determination of total protein by using this method.

#### REFERENCES

<sup>1</sup>O. H. Lowry, N. J. Rosebrough, A. L. Farr, and R. J. Randall, *J. Biol. Chem.* **193**, 265 (1951).

<sup>2</sup>O. Folin and V. Ciocalteu, *J. Biol. Chem.* **73**, 627 (1927).

Table 7.4. Results

Conc.	Methodology Protein 1b			Modified Method				Modified Method % Increase		
	Peak Height ( $OD_{660}$ ) (Results with three experiments)	Aver.		Peak Height ( $OD_{660}$ ) (Results with three experiments)	Aver.	Diff.				
25 $\gamma$	0.020	0.022	0.020	.021	0.036	0.037	0.037	.037	.016	76.19
50 $\gamma$	0.044	0.045	0.043	.044	0.071	0.073	0.072	.072	.028	63.64
100 $\gamma$	0.081	0.083	0.083	.082	0.135	0.135	0.134	.135	.053	64.63
250 $\gamma$	0.199	0.200	0.197	.199	0.326	0.325	0.323	.325	.126	63.32
500 $\gamma$	0.365	0.369	0.367	.367	0.570	0.565	0.571	.569	.202	55.04
800 $\gamma$	0.552	0.550	0.549	.550	0.785	0.788	0.790	.789	.238	43.27

## 8. Electron Microscopy<sup>1,2</sup>

### A. ELECTRON PHASE CONTRAST IMAGES OF MYOGLOBIN

W.W. Harris, F.L. Ball, and N.G. Anderson

The achievement of near 2 Å resolution in defocused electron microscope images<sup>3</sup> creates the possibility of direct observation of molecular detail. Utilization of this level of resolution requires specimens approaching mono-molecular thicknesses for the scattered electrons to carry noise-free spatial information of the specimen. A consequence of this requirement is that the specimen may not be supported by the carbon-coated organic films generally used for electron microscopy because these films have resolvable structures which introduce interference. In addition, since the films are several hundred Angstroms thick, they raise the overall background of diffuse scattered electrons.

Elimination of specimen support has been achieved in several ways. Fernandez-Moran used fenestrated films<sup>4</sup> as well as asbestos fibers<sup>5</sup> while Heidenreich dispersed partially graphitized carbon black in CHCl<sub>3</sub> solutions of ethyl cellulose polymers and cast films on glass slides, removed them in water, and then blasted a drop of the solution onto bare copper screens with high-pressure air.<sup>6</sup> In this laboratory similar results have been obtained with graphite fibers. This report describes results obtained with a new, simple method for preparing unsupported films of some amino acids and several proteins.

We have prepared stable films of a variety of proteins and amino acids in the following way: A small drop of an aqueous solution of a purified protein fraction is placed on a bare 400 mesh copper grid which is clamped in tweezers. The drop diameter should be less than the diameter of the grid. The grid, held in the tweezers, and a microscope specimen

holder, are placed in a deep freeze at -65°F. After 10 min. the grid is inserted in the specimen holder and immediately pumped in the microscope. Film thickness can be varied by varying the concentration of the protein solution. Pure amino acids generally do not form thin films by this method, but one can usually find portions of thin films protruding from grid wires which give clear images with 80-kv electrons.

In exploratory examinations of carbon, amino acids, and plasma protein films using a modified Siemens Elmiskop IA,<sup>7</sup> the electron phase images were visually nearly indistinguishable and it was impossible to decide whether or not the amino acid or protein specimens had undergone extensive vacuum and radiation damage resulting in a carbonaceous skeleton. Resolution of this question depended, in part, on finding a protein for which the crystal structure was known. Myoglobin was chosen since the x-ray crystal structure and amino acid sequences are known.<sup>8</sup> The molecule is 45 × 35 × 25 Å, has a molecular weight of 17,800, encompasses 151 amino acids, and the unit cell consists of two molecules. The structure is compact with little internal water and so is not likely to be deformed by the microscope vacuum.

Phase images of unsupported myoglobin films differed distinctly from those of amino acids. The defocused image of glycine, Figure 8.1 (top), shows no systematic arrangement of electron scattering centers. The image at 11,000,000× consists of irregular bright spots varying from 2 to 7 Å in diameter. Some are isolated but the majority appear to be in continuous contact forming short rods or chains up to 20 Å in length. The separation between spots and chains averages 7 Å.

Myoglobin images differ from the glycine image both dimensionally and in apparent ordering. As seen in Figure 8.1 (center), the defocused myoglobin image is composed of white centers from 4 to 10 Å in

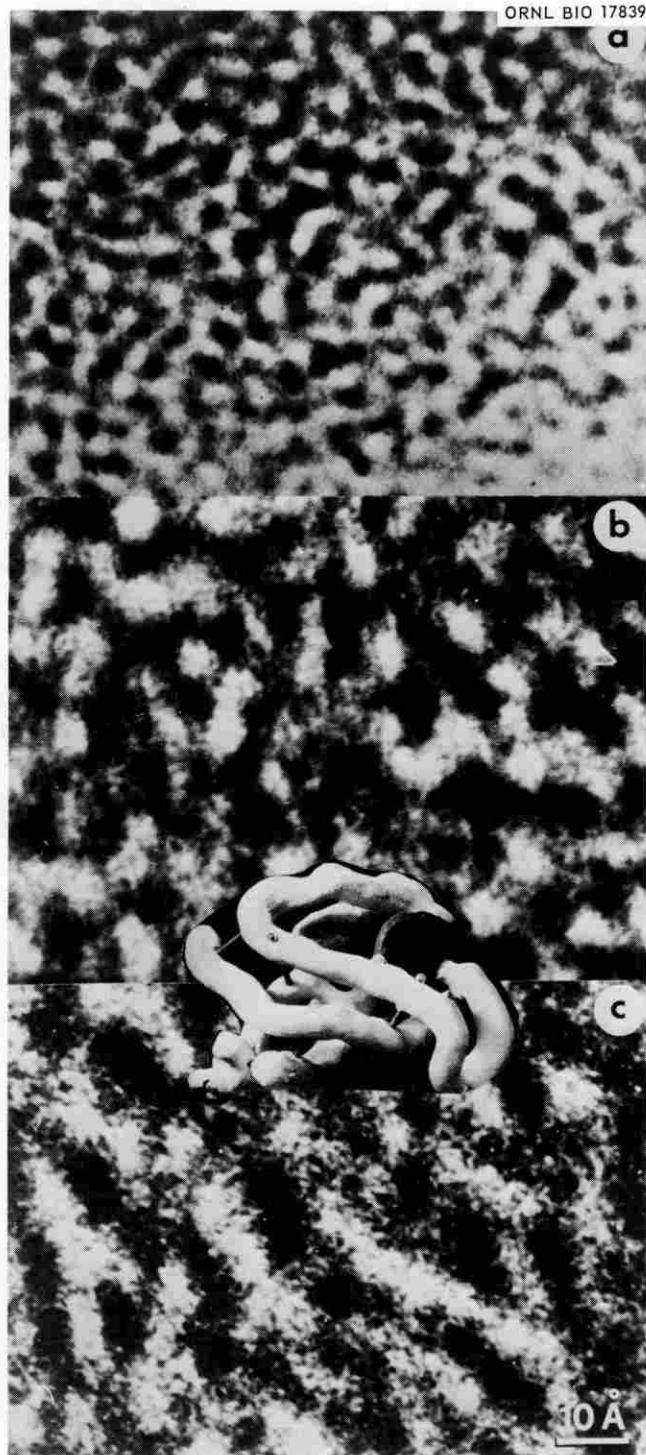


Fig. 8.1a Electron phase contrast image of portion of an unsupported glycine film. 11,000,000 $\times$ . b Electron phase contrast image of myoglobin film at 210 Å defocus. 11,000,000 $\times$ . Superimposed is a photograph of a model of the myoglobin molecule (ref. 10). c Out-of-register positive and negative print. 11,000,000 $\times$ .

diameter each of which is made up of bright spots measuring from 1.8 to 2.3 Å in diameter. The 4 to 10 Å spots are, on the average, in continuous contact, making tortuous paths within the image. These columns frequently form nearly closed loops. The calculated repeat distance for a defocus of 210 Å is 3.9 Å.<sup>9</sup>

The columnar arrays are more easily seen in Figure 8.1 (bottom), which is a print of a positive and negative slightly out of register. The average separation between columns is 14 Å and the continuous segments of the columns varies from 10 to 45 Å. Superposed on Figure 8.1 is a photocopy of Kendrew's<sup>10</sup> 6 Å model of the myoglobin molecule.

Defocussed phase or refraction contrast images afford high contrast but are less well understood than diffraction contrast images usually considered in electron microscopy of inorganic or stained organic substances. Therefore, though the myoglobin images show some patterns and dimensions which can be related to x-ray structure derived models, they are not expected to be direct images equivalent to ones obtained at focus. They are the resultant of recombination of electron rays scattered by layers of several, possibly twenty, molecules for these experiments, in such a way that the gross features of the total structure may possibly be revealed. Until a number of known undamaged structures are examined by electron phase contrast, great caution is needed in forming mental impressions of the structures producing the microscope images.

One-to-one correspondence between electron microscope observations and x-ray diffraction derived structures ought not to be expected of biological substances due to adverse environmental conditions of vacuum and to potentially damaging radiation. At present there is no really satisfactory way of estimating the degree to which a specimen degrades in the electron microscope. If the electron diffraction pattern shows no rapid change during observation and if the visible details in the image on the fluorescent screen survive during photographing, one assumes no significant damage has occurred. Recent studies of Kobayashi and Sakaoku<sup>11</sup> and of Bahr, Johnson, and Zeitler<sup>12</sup> and Reimer<sup>13</sup> emphasize the potential seriousness of this problem.

The initial objective of this present investigation has been to determine whether or not electron phase contrast images of selected amino acids, proteins, and ribosome fractions show reproducibly different images and, if so, then to choose specific ones for detailed study of the electron scattering and imaging

mechanisms occurring in the electron microscope. The primary question has been answered in that reproducibly different structures have been observed, the most distinctive of which is that of myoglobin. Experiments to substitute heavy metals and/or anions into the myoglobin crystal are now underway.

## NOTES AND REFERENCES

<sup>1</sup>Research supported by the Joint AEC-NIH Molecular Anatomy Program sponsored by the Atomic Energy Commission, the National Cancer Institute, the National Institute of General Medical Sciences, and the National Institute of Allergy and Infectious Diseases.

<sup>2</sup>Operated for the U.S. Atomic Energy Commission by the Nuclear Division of Union Carbide Corporation.

<sup>3</sup>R. D. Heidenreich, *Bell Telephone System Technical Journal*, **45**, 65 (1965).

<sup>4</sup>H. Fernandez-Moran, and J. B. Fincan, *Journal of Biophysical and Biochemical Cytology*, **3**, 729 (1957).

<sup>5</sup>H. Fernandez-Moran, International Conference on Electron Microscopy 6, Kyoto, Japan, 1966.

<sup>6</sup>R. D. Heidenreich, International Conference on Electron Microscopy 6, Kyoto, Japan, 1966.

<sup>7</sup>R. D. Heidenreich, *Bell Telephone System Technical Journal*, **45**, 65 (1965).

<sup>8</sup>J. C. Kendrew, *Science*, **139**, 1259.

<sup>9</sup>R. D. Heidenreich, *Fundamentals of Transmission Electron Microscopy*, New York: Interscience Publishers, (1964).

<sup>10</sup>J. C. Kendrew, *Scientific American*, **205**, 109.

<sup>11</sup>K. Kobayashi and K. Sakaoku, *Laboratory Investigation* 1097, **14**, No. 6, Part 2.

<sup>12</sup>G. F. Bahr, F. B. Johnson, and E. Zeitter, *Laboratory Investigation* 1115, **14**, No. 6, Part 2.

<sup>13</sup>L. Reimer, *Laboratory Investigation* 1080, **14**, No. 6, Part 2.

## B. PARTICLE COUNTING AND DETECTION

W. W. Harris

F. L. Ball

The limit of detection of viral particles with UV absorption is  $10^{10}$  particles per milliliter and that of the routinely employed electron microscopy technique is  $10^7$  to  $10^8$  particles per milliliter so that low titre virus preparations such as hepatitis serum must be concentrated severalfold if these physical methods are to be used.

The sensitivity of the electron microscope can be increased if all the particles in a given volume of sample can be sedimented onto one microscope grid and a study of this has been made using polio virus which titred  $4 \times 10^{12}$  by light scattering and  $6 \times 10^{11}$  by sedimentation.

The relation of Sharp<sup>1</sup> that the number  $N$  of particles per milliliter equals the number counted,  $N_c$ ,

times the magnification,  $M$ , squared divided by a constant,  $K$ , times the height of the liquid in the centrifuge tube times the picture area  $A$ ,

$$N = \frac{N_c M^2}{AhK}$$

has been used to establish the number of micrographs and the necessary magnification to detect  $10^5$  particles per milliliter.

The size of the particle sought and the resolution of the eye set the usable magnification. Thus, taking 0.1 mm as resolvable by a trained eye at 10 in. viewing distance and a particle diameter of 25 m $\mu$ , the diameter of polio virus, the minimum final magnification is 4000 $\times$ . Experiments with purified polio virus showed that the particles could be readily counted in Pt-Pd shadowed preparations using an electronic magnification of 3000 $\times$  and additional optical magnification from 6 $\times$  to 10 $\times$ . Substituting into the Sharp equation 3000 for  $M$ ,  $5 \times 10^5$  for  $N$ , 3 for  $N_c$ ,  $4 \times 0.09$  for  $hK$  (the parameters of an experimental SW39 centrifuge tube), and solving for  $A$  one obtains 150 cm<sup>2</sup> of picture area to find three particles, if uniformly sedimented. A picture area of 150 cm<sup>2</sup> can be obtained in the RCA microscope with two 3- $\frac{1}{4}$   $\times$  4 in. negatives or six 2  $\times$  2 in. negatives or with three 6.5  $\times$  9.0 cm negatives in a Siemens microscope.

In order to sediment all the particles in a given volume of fluid onto one 3.3-mm specimen support special centrifuge tubes were designed for the SW39 rotor. A variety of different geometries were evaluated. It was assumed that the ideal geometry would be that of an inverted cone with an opening below the constriction to prevent sedimentation in a ring. Experiments with this geometry shows this precaution not to be necessary. The tubes without the constriction gave better total particle recovery and were, therefore, used for initial counting. The tubes developed are shown in Figure 8.2.

Polio vaccine provided by C. Reimer of Eli Lilly and purified and concentrated by N. G. Anderson was used as a model system for evaluating the counting techniques. The particle titre by light scattering was  $4 \times 10^{12}$  and by sedimentation counting (Reimer) was  $6 \times 10^{11}$  in Tyrode buffer solution.

Initially, dilute phosphotungstic acid stain was added directly to the virus solution before pelleting onto the specimen grid. No satisfactory dilution was found for in-place staining for the reason that the purified virus suspensions always contained enough

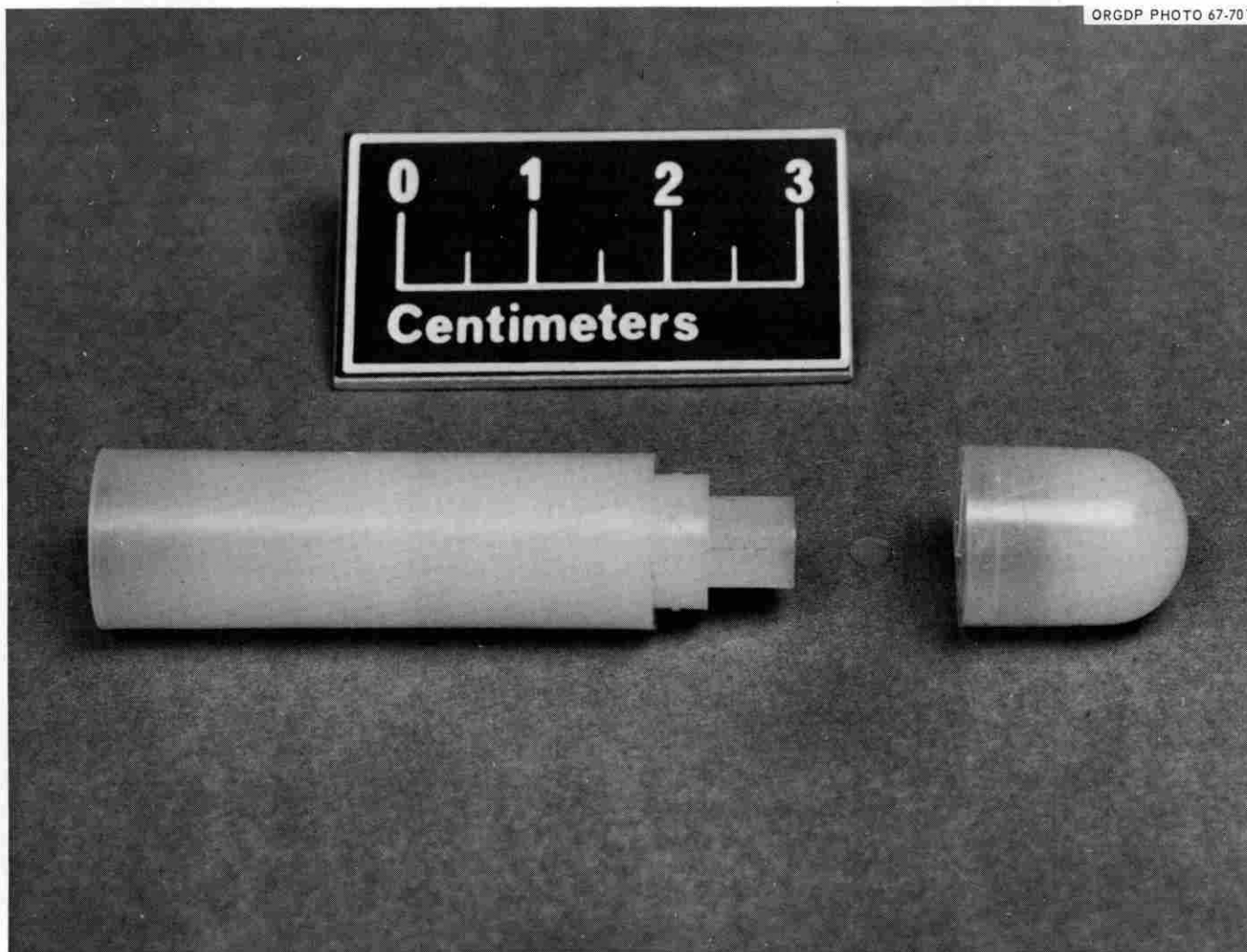


Fig. 8.2 Nylon tubes used to sediment virus particles onto electron microscope grids.

soluble protein to give a stain background which obscured the virus particles. Excessive proteinaceous background was also observed when phosphotungstic acid was used to stain the pelleted virus onto the specimen grid. The most usable preparations were obtained by shadowing the pelleted virus with Pt-Pd at a 4 to 1 shadow angle. This latter technique was used to test the counting procedure.

The preliminary counting dilutions of stock purified virus were made up to be  $6 \times 10^9$ ,  $6 \times 10^7$ ,  $6 \times 10^6$ , and  $6 \times 10^5$  particles per milliliter using Reimer's count of  $6 \times 10^{11}$ . After preliminary studies a series of dilutions of  $6 \times 10^5$  and  $6 \times 10^6$  particles per milliliter

was run in tubes of the geometry shown in Figure 8.2. Results are given in Table 8.1.

These data show a mean deviation of half an order of magnitude for the nominal  $6 \times 10^5$  dilution and four tenths of an order for the  $6 \times 10^6$  dilution. The variance at the 95% confidence interval for the  $6 \times 10^5$  dilution was  $\pm 1.5 \times 10^6$  or  $\pm 15 \times 10^5$  for  $6 \times 10^6$  dilution and  $\pm 2.5 \times 10^7$  for three values (Students'  $t$  factor for an  $n-1$  of 2 being 6.57).

The mean deviation of the values for the  $6 \times 10^5$  dilution is such that the limit of detection of this procedure can be  $6 \times 10^5$  particles if the original titre was  $4.4 \times 10^{12}$  particles or  $6 \times 10^4$  if the original titre

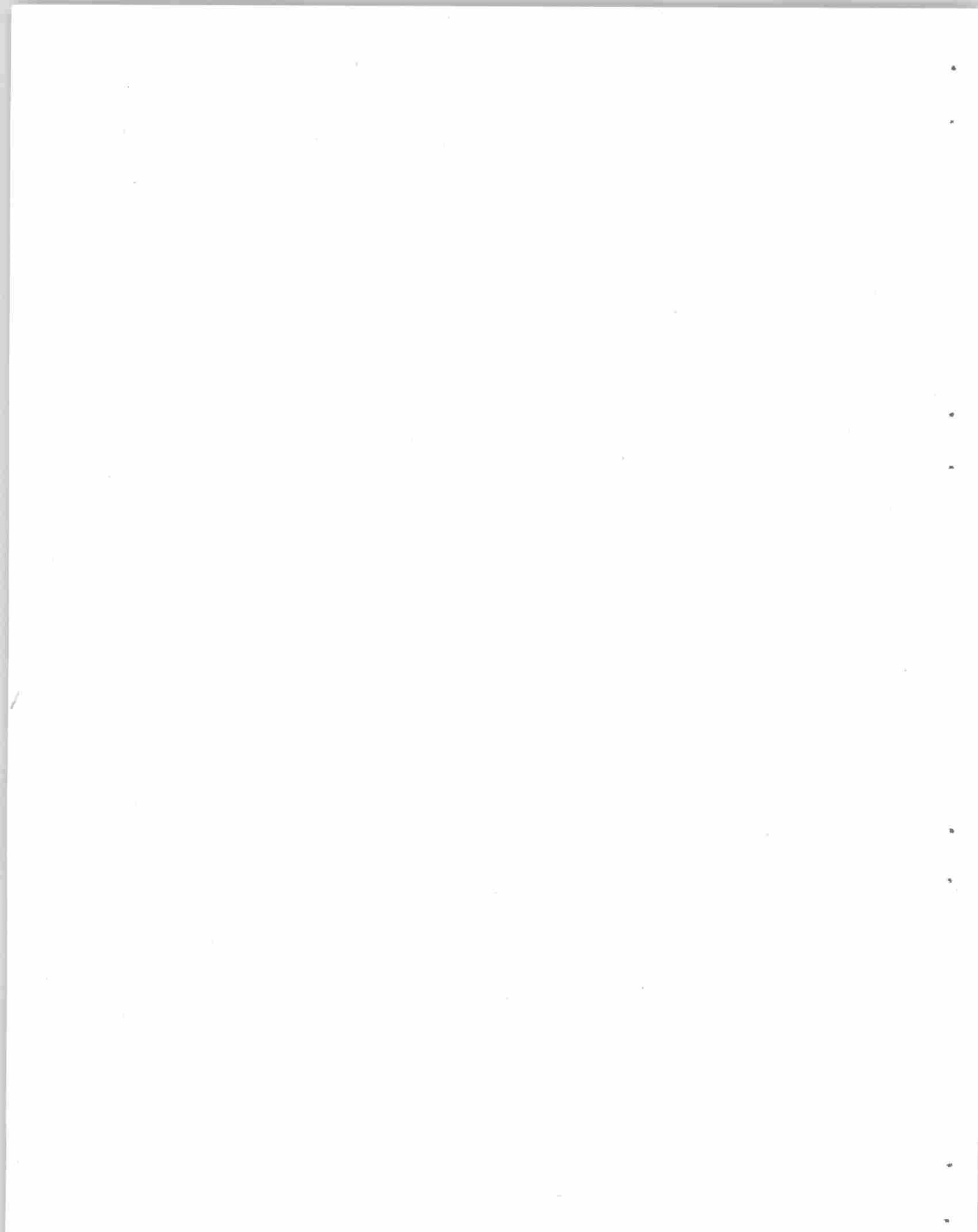
**Table 8.1. Statistical Study of Particle Counting Using Nylon Taper Tubes and Polio Virus.**

Dilution	Date of Run	Counted	Area	No./ml	Deviation
$6 \times 10^5$	10/17	2	130 cm <sup>2</sup>	$0.4 \times 10^6$	-0.8
$6 \times 10^5$	10/17	4	130 cm <sup>2</sup>	$0.9 \times 10^6$	-0.3
$6 \times 10^5$	10/14	5	130 cm <sup>2</sup>	$1.1 \times 10^6$	-0.1
$6 \times 10^5$	10/14	3	130 cm <sup>2</sup>	$0.66 \times 10^6$	-0.5
$6 \times 10^5$	10/14	11	130 cm <sup>2</sup>	$2.4 \times 10^6$	+1.2
$6 \times 10^5$	10/14	9	130 cm <sup>2</sup>	$2 \times 10^6$	+ .8
			Mean	$1.2 \times 10^6$	$\pm 0.6 \times 10^6$
$6 \times 10^6$	10/17	68	130 cm <sup>2</sup>	$1.5 \times 10^7$	0.1
$6 \times 10^6$	10/17	39	130 cm <sup>2</sup>	$0.8 \times 10^7$	0.6
$6 \times 10^6$	10/17	87	130 cm <sup>2</sup>	$2 \times 10^7$	0.6
			Mean	$1.4 \times 10^7$	$\pm 0.4 \times 10^7$

was  $6 \times 10^{11}$  particles per milliliter. In either event this sensitivity is expected to allow us to detect virus particles of polio size in plasma of particle titres of  $10^4$  per milliliter if preconcentration of one or two orders is accomplished in the centrifuge.

Thus far this has been a feasibility study involving particle counting theory, centrifuge tube design, and selection of materials of construction. Centrifuge

tubes of polycarbonate were difficult to fabricate and deteriorated with use either due to stresses developed in the centrifuge or to exposure to 0.N NH<sub>4</sub>Ac solutions. Preliminary experiments indicate that Nylon tubes such as in Figure 8.2 can be used, especially if they can be fabricated at a cost which will permit disposing of them after each run.



## 9. Tumor Immunology

### TUMOR IMMUNOLOGY STUDIES

J. H. Coggin

Efforts in this laboratory to prepare and characterize tumor cell antigens by physio-chemical separation have progressed to the stage where biological assay of cell fractions has become necessary. Therefore, several hamster test systems are currently being evaluated as potential assay models to screen cell fractions for immunogenic response. These systems include the evaluation of vaccine efficacy in the live tumor cell challenge assay and in the virus-newborn hamster system. The selection of a suitable tumor vaccine assay system will depend upon the specificity, reproducibility, and time-requirement of the test.

**Transplantation Immunity In The Adenovirus 31—Transformed Tumor Cell Challenge System.**—The live cell challenge assay has been effectively utilized to study vaccine effectiveness against the transplantation of polyoma, simian virus 40, adenovirus 7 and certain other oncogenic virus transformed-cell types in homologous hamster systems. Live cell challenge has proven to be a rapid, specific and reproducible means of assaying homologous tumor antigen and has compared favorably with results obtained using the virus-newborn system.

Adenovirus 31 transformed cells used in this laboratory are highly neoplastic on transplant into homologous hamsters. The following study was undertaken to determine if this tumor cell line could be used in a cell challenge assay system.

**Materials and Methods.**—Syrian golden hamsters were obtained from the Lakeview Hamster Colony. This strain of hamster is a random-bred line originating from three original animals and these hamsters are uniformly and completely histo-compatible with respect to transplantation antigens (homologous). Female hamsters between four and five weeks of age

were used for all experiments. Animals were housed four per box, given water and food *ad libitum* and bedded on San-I-Cel.

Adenovirus 31 transformed Syrian hamster muscle cells were obtained from Flow Laboratories, Rockville, Maryland, and were maintained by subcutaneous passage in young hamsters in the sub-scapular region. The tumor line is free of mycoplasma as well as bacterial and fungal contamination. Recent results have shown that as few as 100 live (trypan blue exclusion method) tumor cells are capable of producing a tumor on transplant in 4-week-old hamsters within a 50-day period.

Several vaccines were used initially to evaluate the adenovirus 31 cell challenge system. These included whole irradiated Adenovirus 31 (Adv. 31) tumor cells, disrupted Adv. 31 tumor cells, live Adenovirus 31 and placebo controls. Vaccines were prepared as follows:

Whole tumor was removed from young hamsters, rinsed thoroughly with 50-100 ml of Hanks's balanced salt solution (HBSS), trimmed free of connective tissue and hemorrhagic areas where present and minced into 3-4 mm. size pieces in a sterile Petri dish. The tissue mince was suspended in 30 ml of medium 199 containing no serum and placed in a 50 ml trypsinizing flask with a fluted bottom. A one inch-teflon-coated magnetic stir bar was added (too large to properly rotate in the flask) and the bar agitated with a magnetic stirrer. The bumping action of the stir bar effectively disaggregated the tissue into a uniform single-cell suspension after 15 minutes of operation. The resultant suspension was passed through a sterile stainless steel wire mesh and the cells collected in a 50 cc centrifuge tube. The cells were then pelleted at 1000 rpm for 10 mins in the PR-2 International Centrifuge at 4°C and resuspended in the desired volume of medium 199 containing no serum for treatment.

Irradiation was performed in plastic Petri dishes in 20-ml volume using the Maxitron X-ray unit operating at 20 m Amps, 250 KVP, at a distance of 18 cm from the top of the dish. A uniform dosage of 10,000 R was given to all irradiated cells. Following the irradiation procedure, the cells were diluted to the proper cell density (viable count as determined by the trypan blue exclusion test) and kept at 4°C until inoculated. An irradiated, 199 medium control was also included.

Disrupted cell vaccine was prepared by suspending the desired number of viable tumor cells in 20 mls of 199 medium and passing the suspension through a chilled French Pressure cell apparatus. The pressure (8000–9000 psi) was initially held for 3 mins prior to extrusion of the cells from the press under pressure and the material was collected in a chilled serum vial, diluted and immediately inoculated into hamsters.

radiation at 10,000 R as previously described, the cells were counted, diluted to the desired cell density and held at 4°C until inoculated into hamsters.

Adenovirus 31 was given on 2 occasions (first and third week) as vaccine against live adenovirus 31 cell challenge in one group of animals. Virus prepared in primary human embryonic kidney tissue (HEK) and having a titer of  $10^{6.5}$  TCID<sub>50</sub>/0.2 ml was given by the intraperitoneal route in 0.2 ml doses.

All other vaccines were administered in 1.0cc aliquots by the intraperitoneal route at weekly intervals until three doses had been given. Ten days after the third vaccination dose had been given, the animals were challenged with increasing numbers of live, washed Adenovirus 31 tumor cells by subcutaneous challenge in the right subscapular area. The following protocol was followed:

**Adv. 31A  
Cell Challenge Level\***

Experimental Groups	Vaccine**	Cell Challenge Level*			
		10 <sup>5</sup>	5 × 10 <sup>5</sup>	10 <sup>6</sup>	Not Challenged
		Number of Hamsters Inoculated			
Challenge Control	No Vaccine	12	12	12	12
Irradiated Cell	Adenovirus 31				
Vaccine (2.5 × 10 <sup>6</sup> cells/ml)	Tumor Cells (10,000 r)	12	12	12	8
Enhancement Control	Adv. 31 Tumor Brei				
(Debris from 2.5 × 10 <sup>6</sup> cells/ml)	French Pressure (8,000 psi)	8	8	8	8
Virus Control	Adenovirus 31	8	8	8	8
199 Control	199 (10,000 r)	4	4	4	4
Heterologous Cell	SV 40 Tumor Cells				
Control (2.5 × 10 <sup>6</sup> cells/ml)	(10,000 r)	8	8	8	8

\*Hamsters challenged 10 days post-third vaccine dose in the right subscapular area.

\*\*Vaccine administered weekly for three weeks ip. in 1.0 ml aliquots.

Results from this experiment are forthcoming.

Only cell debris was observed in these preparations.

An SV40 transformed-hamster cell line (F5-1) prepared in an isologous animal was also included as vaccine to serve as a heterologous control. These cells were cultured in 199 medium with 5% calf serum as an established cell line, harvested seven days after "seeding" by brief trypsinization, washed by centrifugation in HBSS, and resuspended for irradiation in 20 ml of 199 medium without calf serum. After ir-

radiation at 10,000 R as previously described, the cells were counted, diluted to the desired cell density and held at 4°C until inoculated into hamsters.

Future vaccines to be evaluated in the live cell challenge system will include plasma membranes from adenovirus 31 tumor cells, T Antigen preparation and other isolated and concentrated subcellular components.

**Adenovirus 31—Newborn Hamster System.**—We have observed that Adenovirus type 31 prepared in HEK cells will produce 95–100% tumor in hamsters in 60–65 days when inoculated into newborns at a

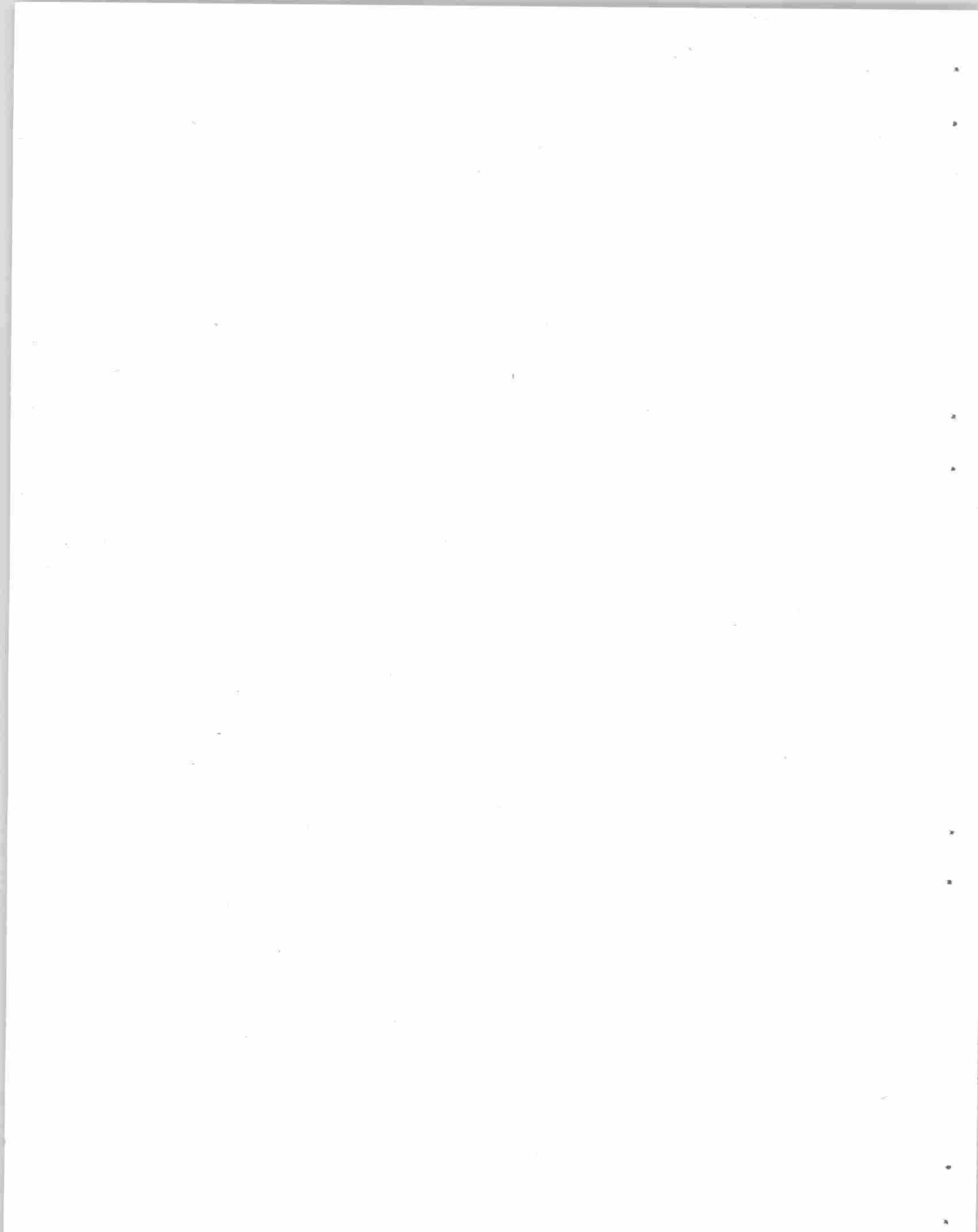
concentration of  $10^7$  TCID<sub>50</sub> within 24 hrs after birth. Tumor has been observed as early as 33 days after inoculation of virus. This system is being evaluated as a potential rapid assay of tumor vaccine. In preliminary results, the effect of a small dilution (5- to 10-fold) of the virus inoculum suggests that the incidence of tumors is greatly diminished and the time to tumor appearance is significantly prolonged. This may make it impractical to use the virus-newborn system for routine screening of tumor cell preparation. Efforts continue in an attempt to utilize this system for evaluating vaccine efficacy.

#### **Serologic Evaluation of Adenovirus 31 Induced Tumor Cell Antigen Obtained From *in vivo* and *in vitro* Transformed Cells**

A comparative investigation of CF antigen (T antigen) prepared from tumor cells obtained from cells transformed *in vivo* in the Syrian hamster and *in vitro*

in primary Syrian hamster tissue in culture is now underway.

Primary embryonic hamster lung, kidney and muscle tissue have been prepared and inoculated 5 days after culture "planting" with  $10^{6.5}$  TCID<sub>50</sub> of adenovirus 31A prepared in HEK cells. The cells are cultured in Eagle's Minimal Essential Medium containing 10% fetal calf serum, 2x vitamins and 0.5% lactalbumin hydrolysate. The infected cells are kept in a 5% CO<sub>2</sub> atmosphere and will be continually observed for signs of transformed foci among the normal cell population. After 16 days of observation no foci have been observed. When transformed cells appear, they will be cloned, cultured *in vitro*, checked for the presence of Adenovirus 31 by culture in HEK cells, typed for viral neoantigens and then be used to prepare CF antigen. This antigen will be compared with CF antigen prepared from the Flow Laboratories Adenovirus 31 cell line passaged routinely in hamsters and derived therefrom originally and used in all cell fractionation procedures to date in this laboratory.



INTERNAL DISTRIBUTION

1. S. I. Auerbach
2. R. Baldock
3. R. E. Biggers
4. A. L. Boch
5. D. S. Billington
6. C. J. Borkowski
7. G. E. Boyd
- 8-9. S. Sinichak
10. C. J. Collins
11. F. L. Culler
12. P. B. Dunaway
13. J. L. Fowler
14. J. H. Frye, Jr.
- 15-16. R. F. Hibbs (Y-12)
17. A. S. Householder
18. J. S. Johnson
19. W. H. Jordan
20. K. A. Kraus
21. M. T. Kelley
22. J. A. Lane
- 23-24. C. E. Larson
25. T. A. Lincoln
26. J. L. Liverman
27. R. S. Livingston
28. H. G. MacPherson
29. K. Z. Morgan
30. D. J. Nelson
31. J. S. Olson
- 32-33. R. B. Parker
34. M. E. Ramsey
35. R. M. Rush
36. C. D. Scott
37. M. J. Skinner
38. E. H. Taylor
39. A. M. Weinberg
40. G. C. Williams
41. H. I. Adler
- 42-61. N. G. Anderson
62. W. A. Arnold
63. M. A. Bender
64. S. F. Carson
65. E. H. Y. Chu
66. W. E. Cohn
67. C. C. Congdon
68. F. J. de Serres
69. D. G. Doherty
70. W. D. Fisher
- 71-73. C. J. Whitmire, Jr.
74. A. H. Haber
75. A. Hollaender
76. M. A. Kastenbaum
77. R. F. Kimball
78. S. P. Leibo
79. T. Makinodan
80. P. Mazur
81. G. D. Novelli
82. T. T. Odell, Jr.
83. A. P. Pfuderer
84. M. L. Randolph
85. W. L. Russell
86. R. B. Setlow
87. A. C. Upton
88. E. Volkin
89. R. C. von Borstel
90. T. Yamada
91. E. F. Babelay
92. F. L. Ball
93. E. J. Barber
94. J. C. Barton
95. H. A. Bernhardt
96. Barbara S. Bishop
97. H. D. Culpepper
98. J. T. Dalton
- 99-113. E. C. Evans
114. J. Farquharson
115. R. L. Farrar, Jr.
116. R. F. Gibson
117. W. W. Harris
- 118-120. W. L. Harwell
121. E. T. Henson
122. A. P. Huber
123. G. R. Jamieson
124. E. C. Johnson
125. R. G. Jordan
126. C. E. Nunley
127. R. H. Stevens
128. P. R. Vanstrum
129. D. A. Waters
130. C. W. Weber
131. S. J. Wheatley
132. W. J. Wilcox, Jr.
133. J. Breillatt

### INTERNAL DISTRIBUTION

- |      |                              |          |   |
|------|------------------------------|----------|---|
| 134. | D. H. Brown                  | 145.     | Curt Stern (consultant)                                   |
| 135. | R. E. Canning                | 146.     | C. E. Carter (consultant)                                 |
| 136. | E. L. Candler                | 147.     | Henry S. Kaplan (consultant)                              |
| 137. | P. C. F. Castellani, Jr.     | 148-149. | Biology Library   |
| 138. | L. H. Elrod, Jr.             | 150.     | Reactor Division Library                                  |
| 139. | J. W. Holleman               | 151-153. | Central Research Library                                  |
| 140. | C. T. Rankin, Jr.            | 154-155. | ORNL-Y-12 Technical Library<br>Document Reference Section |
| 141. | Elizabeth L. Rutenberg       | 156-199. | Laboratory Records Department                             |
| 142. | R. D. Hotchkiss (consultant) | 200.     | Laboratory Records, ORNL R.C.                             |
| 143. | E. R. Stadtman (consultant)  | 201.     | Laboratory Shift Supervisor                               |
| 144. | Herschel Roman (consultant)  |          |   |

### EXTERNAL DISTRIBUTION

- 202. AEC Patent Branch, Washington, D.C.
- 203. Peter Alexander, Chester Beatty Cancer Institute, London, England
- 204. G. A. Andrews, ORINS Medical Division, ORAU
- 205. Division of Technical Information Extension, Oak Ridge
- 206. C. Baker, National Cancer Institute, Bethesda, Maryland
- 207. F. Baronowski, AEC Production Division, Washington, D.C.
- 208. N. F. Barr, Atomic Energy Commission, Washington, D.C.
- 209. H. P. Barringer, Stellite Division, Union Carbide Corporation, Kokomo, Indiana
- 210. N. Berlin, National Cancer Institute, Bethesda, Maryland
- 211. A. S. Berman, Dept. of Eng., Univ. of Minnesota, Minneapolis, Minnesota
- 212. Biomedical Library, University of California, Center for the Health Sciences, Los Angeles, California
- 213. H. E. Bond, National Cancer Institute, Bethesda, Maryland
- 214-263. C. W. Boone, National Cancer Institute, Bethesda, Maryland
- 264. Myron Brakke, U.S. Department of Agriculture, Agriculture Research Service, Plant Physiol. Department, University of Nebraska, Lincoln 3, Nebraska
- 265. H. D. Bruner, Atomic Energy Commission, Washington, D.C.
- 266. W. R. Bryan, National Cancer Institute, Bethesda, Maryland
- 267. J. C. Bugher, Puerto Rico Nuclear Center, Rio Piedras, P.R.
- 268. W. W. Burr, Jr., Atomic Energy Commission, Washington, D.C.
- 269. R. M. Chanock, National Institute of Allergy and Infectious Diseases, Bethesda, Maryland
- 270. R. A. Charpie, Union Carbide Corporation, New York
- 271. M. A. Churchill, Chief, Stream Sanitation Staff, Edney Bldg., TVA, Chattanooga, Tennessee
- 272. W. D. Claus, Atomic Energy Commission, Washington, D.C.
- 273. G. B. Cline, University of Alabama Medical Center, 720 South 20th Street, Birmingham, Alabama
- 274. James Colbert, Office of the Surgeon General, National Institutes of Health, Bethesda, Maryland
- 275. B. T. Cole, Department of Zoology, University of South Carolina, Columbia, S.C.

276. Peter Dans, National Institute of Allergy and Infectious Diseases, Bethesda, Maryland
277. E. Dapper, U.S. Army Chemical Corps, Fort Detrick, Maryland
278. C. M. Davidson, Environmental Hygiene Branch, Edney Bldg., TVA, Chattanooga, Tennessee
279. D. J. Davis, NIAID (Director), Bethesda, Maryland
280. O. M. Derryberry, Director of Health and Safety, Edney Bldg., TVA, Chattanooga, Tennessee
281. Harold S. Diehl, Sr., Vice President for Research in Medical Affairs, American Cancer Society, 521 W. 57th St., New York 19, New York
282. C. L. Dunham, National Science Foundation, Washington, D.C.
283. K. M. Endicott, National Cancer Institute, Washington, D.C.
284. S. G. English, Assistant General Manager for Research and Development, AEC, Washington, D.C.
285. J. L. Fahey, National Cancer Institute, Bethesda, Maryland
286. E. Frei, M. D. Anderson Memorial Hospital, The Texas Medical Center, Houston, Texas
287. H. Friedericy, University of Virginia, Charlottesville, Virginia
288. F. E. Gartrell, Assistant Director of Health and Safety, Edney Bldg., TVA, Chattanooga, Tennessee
289. General Electric Company, Richland, Washington
290. H. Bentley Glass, State University of New York, Stony Brook, L.I., New York
291. Donald A. Glasser, Virus Lab., University of California, Berkeley 4, California
292. H. N. Glassman, U.S. Army Chemical Corps, Fort Detrick, Maryland
293. E. Grabowski, AEC Production Division, Washington, D.C.
294. S. T. Grey, Food and Drug Administration, Washington, D.C.
295. N. S. Hall, University of Tennessee, Knoxville, Tennessee
296. Fred J. Hodges, University of Michigan, Medical Center, Ann Arbor
297. E. C. Horn, Department of Zoology, Duke University, Durham, N.C.
298. J. G. Horsfall, Connecticut Agricultural Experiment Station, New Haven, Conn
299. R. D. Housewright, U.S. Army Chemical Corps, Fort Detrick, Maryland
300. R. J. Huebner, National Cancer Institute, Bethesda, Maryland
301. G. W. Irving, Jr., Agriculture Research Service, USDA, Washington, D.C.
302. H. P. Jenerick, National Institute of General Medical Sciences, Bethesda, Maryland
303. Irving S. Johnson, Eli Lilly Co., Indianapolis, Indiana
304. J. S. Kirby-Smith, Atomic Energy Commission, Washington, D.C.
305. R. M. Kniseley, ORINS Medical Division, ORAU
306. K. W. Kohn, National Cancer Institute, Bethesda, Maryland
307. P. Kotin, National Cancer Institute, Bethesda, Maryland
308. E. L. Kuff, National Cancer Institute, Bethesda, Maryland
309. W. T. Lammers, Davidson College, Davidson, North Carolina
310. A. D. Langmuir, Chief, Epidemiology Branch, Communicable Disease Center, Atlanta, Georgia
311. R. E. Learmouth, National Cancer Institute, Bethesda, Maryland
312. E. H. Lennette, Chief, Viral and Rickettsial Disease Laboratory, Department of Public Health, 2151 Berkeley Way, Berkeley, Cal.

313. R. F. Loeb, College of Physicians and Surgeons, Columbia University, New York
314. W. H. Magruder, National Cancer Institute, Bethesda, Maryland
315. W. G. Marley, UKAEA, Health and Safety Branch, Radiology Protection Division, Harwell, Didcott, Berks., England
316. W. E. McMahon, Atomic Energy Commission, ORO
317. R. G. Meader, National Cancer Institute, Bethesda, Maryland
318. J. L. Melnick, Department of Virology and Epidemiology, Baylor University, College of Medicine, Houston, Texas
319. Robert Melville, National Institute of General Medical Sciences, Bethesda, Maryland
320. G. R. Mider, National Cancer Institute, Bethesda, Maryland
321. Carl V. Moore, Washington University, St. Louis, Missouri
322. P. T. Mora, National Cancer Institute, Bethesda, Maryland
323. J. E. Moynihan, National Institutes of Health, Bethesda, Maryland  
New York Operations Office
- 324-423. John Overman, Assistant Director for Collaborative Research, National Institute of Allergy and Infectious Diseases, Bethesda, Maryland
424. W. G. Pollard, ORINS, ORAU
425. C. A. Price, Department of Plant Physiol., Rutgers, The State University, New Brunswick, N.J.
426. Wayne Range, AEC Public Relations Division, ORO
427. H. M. Roth, Research and Development Division, AEC, ORO
428. W. P. Rowe, National Institute of Allergy and Infectious Diseases, Bethesda, Maryland
429. Wayne Rundles, Medical School, Duke University, Durham, N.C.
430. A. B. Sabin, Children's Hospital Research Foundation, Cincinnati, Ohio
431. James A. Shannon, Director, National Institutes of Health, Bethesda, Maryland
432. D. G. Sharp, University of North Carolina, Department of Biophysics, Chapel Hill, North Carolina
433. Byron T. Shaw, Administrator, Agricultural Research Service, U.S. Department of Agriculture, Washington, D.C.
434. C. S. Shoup, Atomic Energy Commission, Oak Ridge, Tennessee
435. L. E. Slater, BIAC, American Institute of Biological Sciences, Washington, D.C.
436. R. G. Smith, Food and Drug Administration, Washington, D.C.
437. H. A. Sober, National Cancer Institute, Bethesda, Maryland
438. S. P. Spragg, Department of Chemistry, The University, Birmingham 15, England
439. W. M. Stanley, Virus Laboratory, University of California, Berkeley, Cal.
440. R. E. Stevenson, Union Carbide, New York
441. F. L. Stone, Director, National Institutes of General Medical Sciences, National Institutes of Health, Bethesda, Maryland
442. J. A. Swartout, Union Carbide Corporation, New York, N.Y.
443. S. R. Tipton, Department of Zoology, University of Tennessee, Knoxville, Tenn.
444. Arne Tiselius, University of Uppsala, Uppsala, Sweden
445. John Totter, Atomic Energy Commission, Washington, D.C.

446. Rodes Trautman, Plum Island Lab., USDA, Greenport, L.I., New York
447. UCLA Medical Research Laboratory, Los Angeles, California
448. Shields Warren, New England Deaconess Hospital, Boston, Massachusetts
449. A. G. Wedum, U.S. Army Chemical Corps, Fort Detrick, Maryland
450. J. White, National Cancer Institute, Bethesda, Maryland
451. H. G. Wood, Western Reserve University, Cleveland, Ohio
452. M. Zelle, Argonne National Laboratory, Argonne, Illinois
453. C. G. Zubrod, National Cancer Institute, Bethesda, Maryland